UNIVERSITÀ DEGLI STUDI DI PALERMO

Dottorato in Scienze Agrarie, Forestali e Ambientali
Dipartimento Scienze Agrarie e Forestali (SAF)
AGR/07

FUNCTIONAL GENOMIC APPROACHES TO ELUCIDATE BIOTIC AND ABIOTIC STRESS RESPONSES IN PLANTS

IL DOTTORE
VERONICA FILECCIA

IL COORDINATORE
PROF. VINCENZO BAGARELLO

IL TUTOR
DOTT. FEDERICO MARTINELLI

IL CO TUTOR
PROF. DARIO GIAMBALVO

CICLO XXIX
ANNO CONSEGUIMENTO TITOLO 2017

Whatever the mind of man can conceive and believe,
it can achieve

Napoleon Hill

INDEX

CHAPTER 1

INTRODUCTION

Plants, as sessile organisms, have developed different and sophisticated mechanisms to face adversity environmental conditions and biotic challenges, which affect their biological processes. Stress signals detected by plants are then transduced by a complex network of cell biological molecules that finally generate the observed phenotypic responses (Pandey et al., 2016). Nowadays the greatest challenge is to dissect this very complicated molecular systems in order to identify which points and steps play important roles in the final expression of phenotypic traits (i.e. plant biotic and abiotic responses).

Genomics is the discipline that deals with the structure, sequence, function and evolution of the genome. It investigates how the genetic information contained in DNA (deoxyribonucleic acid) is inherited and explains the phenotypic expression of traits in living organisms. Genomics mainly includes two sub-areas, a structural and functional. The structural genomics deals with the genetic and physical mapping and sequencing of genomes. Particularly it studies the size of the genome, the number and position of genes contained therein vary between living organisms and how they are associated together in the chromosomes. Structural genomics investigates the shapes of proteins and other biomolecules encoded by genes through experimental and computational methodologies. Structural genomics can help in revealing how transcription and translation are regulated through the study of promoter sequences and other DNA regulation regions and the computational and modeling analysis of the structure of transcription factors.

Functional genomics aims to understand the ways in which genes direct the development and functioning of cells and how their failure may affects the expression of key traits (i.e. plant environmental responses). It is a field of molecular biology that has tremendous technological progresses in the techniques used to study how biological molecules interact and function in cell system. Particularly it gain insight into the functions of genes, how they interact each other, their expression patterns, how their modulation affect the phenotype. The transfer of knowledge and discoveries obtained in organism models into crops is one of the main issues in plant functional genomics. The enormous quantity of data has to be compared and integrated into the breeding programs in order to identify which genes have to be selected in parents to obtain improved progenies.

Functional genomics measures expression levels of RNAs and protein on a global scale (genome-wide or system-wide) to understand the relationship between genotype and phenotype

investigating gene function, focusing on gene transcription, translation, epigenetic regulation and protein-protein interactions, and often involving high-throughput methods (**Fig. 1**).

Gene function can have a meaning at different livels, such as biochemical, cellular, developmental or adaptive role (e.g. its contribution to the fitness). (Bouchez and Höfte, 1998).

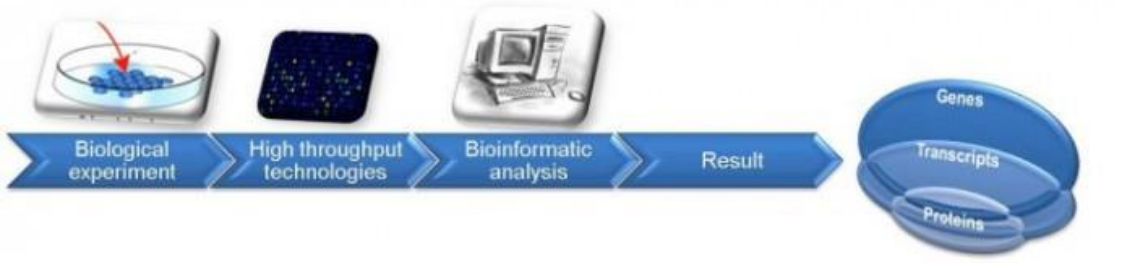

Fig. 1| Functional genomics integrates information from various molecular methodologies to understand how DNA sequence is translated into complex information in a cell (DNA → RNA → Proteins → biological process). From EMBL-EBI website (http://www.ebi.ac.uk/).

All the informations collected by specific techniques and processes that operate on genome wide analysis should facilitate the development of plants more resistent to abiotic and biotic stress (Al-Khayri et al., 2016; Campos-De Quiroz, 2002).

Thanks to the development of bioengineering methodologies occurred mainly in the last 30 years, several biomolecular disciplines have been promoted that have the "-omics" suffix, such as genomics, metabolomics. The complex of molecular regulatory networks modulating plant stress adaptation, resistance and tolerance may be deeply understood through different "omics" approaches (Chawla et al., 2011). **Fig. 2** shows the four main tecnologies of the “omics” science: transcriptomics, proteomics, metabolomics and phenomics that allow gain insights into the understanding of plant system biology.

The identification of key genes, proteins and metabolites associated with a stress response allows improving presymptomatic diagnosis of diseases and disorders (Dandekar et al., 2010).

In detail, transcriptomics includes structural and functional analyses of coding and non-coding RNA or transcriptome. This is mainly obtained by two different highthrouput methodologies: microarrays and next generation sequencing.

In a cell, the proteome is defined as the complete set of its proteins. Proteomics is a branch of functional genomics that studies the proteins at both level, structure and function,

with the purpose to elucidate what role is played by the protein in the cell (ISAAA, 2006). Proteomics deals with protein and post-translational protein modification along with their regulatory pathway.

Metabolomics is another "omic" large scale analysis aiming at investigating the metabolic networks occurring in cells and living organisms (Gupta et al., 2013) by the analysis of all small molecules in a biological system (Fiehn, 2001).

At last, phenomics analyze many phenotipic traits at the same time allowing to determine how, in a organism, these traits are translated by the informations present in a gene or in a whole genome (NSF, 2011).

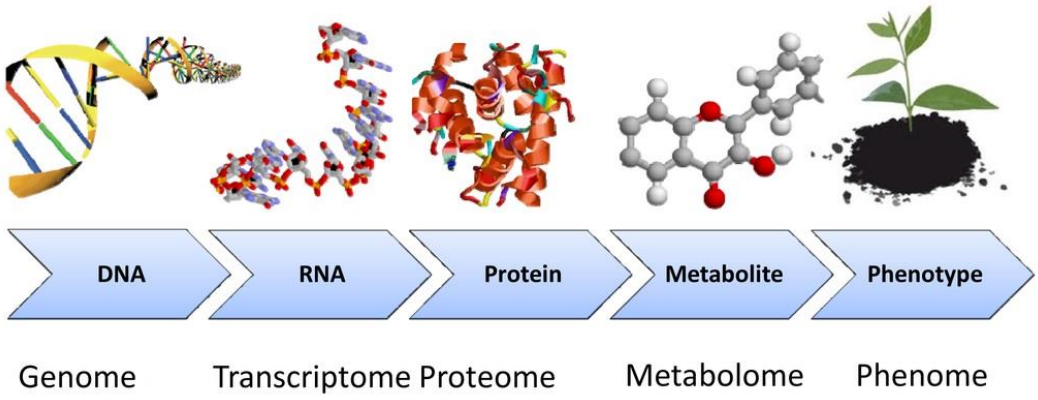

Fig. 2| Schematic diagram explaining the complexity of cellular function from DNA to phenotype (modified from Arbona et al., 2013).

These "omic" technologies provide a large amount of data that are difficult to interprete and render meaningful. The development of potent computational methods and the progress of bioinformatics have allowed analyzing large-scale heterogenous dataset and integrating them to understand key points of metabolic regulations occurring in cells (Bieda, 2012; Kohl et al., 2014; Schumacher et al., 2014).

The increased knowledge on function of all plant genes affects many aspects of the stages necessary to gain plant improvement (Somerville and Somerville, 1999).

TRANSCRIPTOMICS

Transcriptomics deals with the large-scale analysis of transcripts at whole organism, organ, tissues and cell level at a particular development stage and under specific environmental conditions. Two are the main methodologies used in transcriptomic analysis: microarrays and next-generation sequencing.

Microarrays technology converts the information from raw sequence data into an extensive understanding of gene function. The advantage of microarray-based expression analysis is the simultaneous monitoring of a large number of different genes using a small amount of biological sample material (Holtorf et al., 2002). The accumulation of microarray data from many different experiments creates the opportunity to assign functional informations to unknown genes based on the concept that if the gene has a similar sequence and trend of expression to a known one; the two genes should play the same role in the cell and have the same annotation. (Somerville and Somerville, 1999). Exploiting the gene expression similarity in response to different stimuli or conditions, it is possible to use known function of genes to assign functions to many unknown genes of the cluster (Chu et al., 1998; Eisen et al., 1998). Microarray technology has been used to characterize some plant biotic responses (Albrecht and Bowman, 2008). However, microarrays lack the range and sensitivity of qRT-PCR and the relationships between expressed genes and symptom development are unknown. Microarray analysis is also limited to those genes present on the microarray, a subset of the studied plant genome. It is a transcriptomic technology that allows providing detailed information on a genome- wide scale thorugh the analysis of thousands of genes at the same time. It is a technique that is characterized by a high speed of analysis and comprehensiveness (Brandl and Anderson, 2015). The analysis consists in comparing the gene expression of different cells, development stages, environmental conditions at a specific time and linked to a particular phenotype or by determining the co-expression known genes (Mingzhu et al., 2015). DNA microarray is a solid surface (chip or slide) composed by attached fixed single DNA molecules that after exposion to a dye-labelled nucleic acid target forms a duplex. Signals analysed by a scannering are analyzed using specific bioinformatics softwares. Two types of microarrays are present: one is made by automated robotic spotting or by the other through in situ synthesis. Spotted microarrays are obtained using PCR products or oligonucleotide molecules that are directly spotted on glass slides. The DNA molecules present into the chip are named probes. Their attachment on the solid support takes place though two types of bonds: 1) covalent through the aliphatic amine group added to the 5-end of cDNA, 2) non-covalent by electrostatic attraction between amine groups and phosphate of the DNA structure. Microarray chip can be divided in

two cDNA or oligonucleotide microarrays. In the first type, cDNAs are linked to more than one position in amino-labelled slides while oligonucleotide microarrays are characterized by shorter DNA molecules binded with covalent bond using the amine group added during their production. In in situ microarray, these oligo probes are synthesized directly, base by base thorugh the typical bond between the phosphate linked to the 5'-OH of the nucleotide and the '3-OH of the previous one. The accuracy and analitical efficiency of oligo microarrays depend on the specific sequence and length, Cyanine dyes are usually employed to label the target RNA through direct and indirect labelling methodologies. The accuracy of hybridization between the probe and target is a critical step and depends on many factors. Scanning with excitation wave-lengths of the two dyes is performed by a laser scanner via the determination of fluorescence signals in accordance with their concentration. Through the analysis of signal intensity the expression of genes is determined. The comprehension of a large quantity of gene expression data is a very important step for the practical use of this technique. During the recent 20 years, many bioinformtic softwares have been created for data processing, quality filtering and functional mining (i.e. microarray Suite5 and Robust Multi Array Average (RMA). The networks between genes can allow us to dissect gene regulatory networks in plants coping with the changing environment. Microarray-based research have been particularly developed with the creation of new chip methodologies. Many types of gene chips have been formulated with the increase of genomic sequences that have been characterized, analyzing oligonucleotide, DNA methylation, single nucleotide polymorphisms and miRNAs. Oligonucleotide microarray is the most widely used to investigate the gene expression at the genomic and transcriptomic level, technology for almost all model plants and important crops, such as wheat, barley, apple, citrus.

Next-Generation Sequencing (NGS) is a revolutionary transcriptomic technology developed in the recent 10 years. It detects rare, splice variants or unknown transcripts that are not present in microarrays (Martinelli et al., 2012). This technique allows in isolating genes of interest and to quantife their expression in more accurate way than microarrays (Garq and Jain, 2013). Indeed, NGS Sequencing produces a more detailed picture of the transcriptome at a particular developmental and environmental stage.

There are different NGS technologies such as 454 sequencing (used in 454 Genome Sequencers, Roche Applied Science, Basel), Illumina technology and the SOLiD platform (Applied Biosystems; Foster City, CA, USA) (Shendure and Hanlee, 2008). While these platforms rather differ in array generation mode, they are analogous workflows concept that consist on cDNA preparation, DNA random fragmentation, library preparation and PCR-based amplification with in vitro ligation of appropriate adapters (Shendure and Hanlee, 2008). 454

technology provides longer reads at higher accuracy and greater throughput than Illimina and SOLiD machines. For this reason it is frequently used for de novo assembly and sequencing of novel organisms. The technology is characterized by the use of DNA coated beads and Emulsion PCR. Although base calling is more than 90% a constraint consists on the presence of INDELs that induces errors and need high work in data processing. Illumina platform employs the sequencing by synthesis approach. It is the most commonly used platform. The system uses a sequencing technology and novel reversible terminator chemistry optimized to achieve unprecedented levels of cost effectiveness and throughput. It has the advantage of generating superior reads. Illumina platform consists on MiSeq and HiSeq machines able to generate over 2000Gb per run. Call base accuracy is more than 99% and the quality filtering can reduce it more.Data processing is less complex than 454 technology.

SOLiD platform employs the Sequencing By Ligation (SBL) approach. It consists in the processing of two slides at a time, and providing data of high quality. The library preparation obtained with an emulsion PCR as 454 prior to sequencing, is highly labour and time consuming. The new next-generation sequencing technologies are still more powerful because they allow to reduce bias (i.e. due to PCR procedure) and perform more accurate studies at both structural and functional level. The Single Molecule Sequencing (SMS) technology allows reading of a sequence at very fast rates and thus reduces costs of analysis. This technology is being developed by a diverse number of platforms. Pacific Biosciences created a single single molecule sequencing technology based on flourescence detection that analyzes nucleotides marked with diverse colors. New improvement are quickly obtained in detecting the activity of polymerase enzyme forming the DNA strand in sequence by synthesis approach. LightSpeed Genomics is creating a new detection system using electron microscopy in analyse the signals.

A general assumption is that the transcriptomic response to any particular environmental factor is represented in the complexity of the RNA population, including both coding (mRNA) and noncoding (small RNA) sequences. Rapid and specific induction of messenger and small RNAs is a potential early biomarker to characterize a particular response (i.e. biotic stress responses). This complexity can now be analyzed to an unprecedented depth using new DNA sequencing methods which reveal very rare mRNA, splice variants, allelic variants, and SNPs. Analysis of the deep transcriptome using network theory will help define gene regulatory networks and identify key genes modulating consistent parts of the regulatory networks.

Table 1 shows a comparison between microarray and RNA-seq. From this table is evident that RNA-seq need a low quantity of material compared to microarray. It has also the capacity to distinguish allelic expression and known splice forms, and the ability to discover new genes.

Table 1| Microarray vs. RNA-seq. Pros and cons of these two transcriptomics tecnlogies. (modified from Bauer et al., 2014).

	Microarray	RNA-seq
Principle	Hybridization	Cloning & sequencing
Required amount of RNA	High	Low
Resolution	Several to 100 bp	Single base
Distinguish Allelic expression?	Limited	Yes
Distinguish splice forms?	Limited	Yes
Discover new genes?	No	Yes
Strandedness?	No	Yes
Dynamic range	Few hundred-fold	> 8000-fold
Reproducibility	Yes	Yes
Re-analyzable data	No	Yes
Cost	Medium	High (due to computation)

PROTEOMICS

Much of the cell physiology is determined by gene products (particularly proteins) rather than by nucleic acid. Proteomics is the branch of functional genomics that investigates proteins at lage extent, their sequence and functional actuality. Many of the key expression regulation mechanisms occur at post-transcriptional, translational and post-translational stage and needed the use of proteomics to identify genes play a key role in a important phenotypic response. A proteomic analysis characterizes the full protein present in a particular organism, organ, tissue or cell (Witzel et al., 2015). The term proteome represents the protein complex expressed by a genome. Proteome has a dynamic meaning on contrast of the static concept of the genome. The expression products of the genome can vary greatly in response to external and internal factors. Therefore a genome corresponds to a multiplicity of proteomes whose until now are not easy to be definable. Proteomics, therefore, can be defined as the study, in their complexity, of proteomes. As genomics, two proteomic sub-areas can be considered. The first is structural proteomics that refers to specific objectives dealing with ultimately and purely structural aspects. The second is functional proteomics that deals with the elucidation of protein functions and roles in the cells. The typical workflow of quantitative proteomic approaches deal with protein and peptide labeling mixed by stable isotopes followed by combined sample

processing and mass spectrometer analysis. The comparison of ion signal intensities or peak areas of isotope- encoded peptide pairs allows a quantitative analysis of protein expression.

There are three principal areas in which proteomics can be differentiated: first, proteins identification on large-scale by connecting structural informations; second, identification of proteins post-translational modifications and finally, identification of protein-protein interactions by using mass spectrometry, the yeast two-hybrid system or other molecular genetic techniques (Pandey and Mann, 2000).

Furthermore, different high-throughput techniques have been developed to identify and study proteins function such as mass spectrometry analysis of nuclear pore (Rout et al., 2000) or spliceosome (Neubauer et al., 1998).

Some techniques have been developed to allow the differential expression analysis of proteins and the most accurate are based on Isotopic Labeling. Among these, the iTRAQ (Isobaric Tag for Relative and Absolute Quantitation) technology labels the primary amines of peptides through the use of isobaric reagents allowing by tandem mass spectrometry (MS/MS or MS^2) to identify quantitative changes in the proteome (Vélez-Bermúdez et al., 2016). This technique consists essentially in these different steps **(Fig. 3)**: cell lysis to extract proteins, enzymatic digestion using normally trypsin, peptides labeling with different iTRAQ reagents, combination of them into a mixture and analysis by LC-MS/MS for identification and quantification (www.creative-proteomics.com).

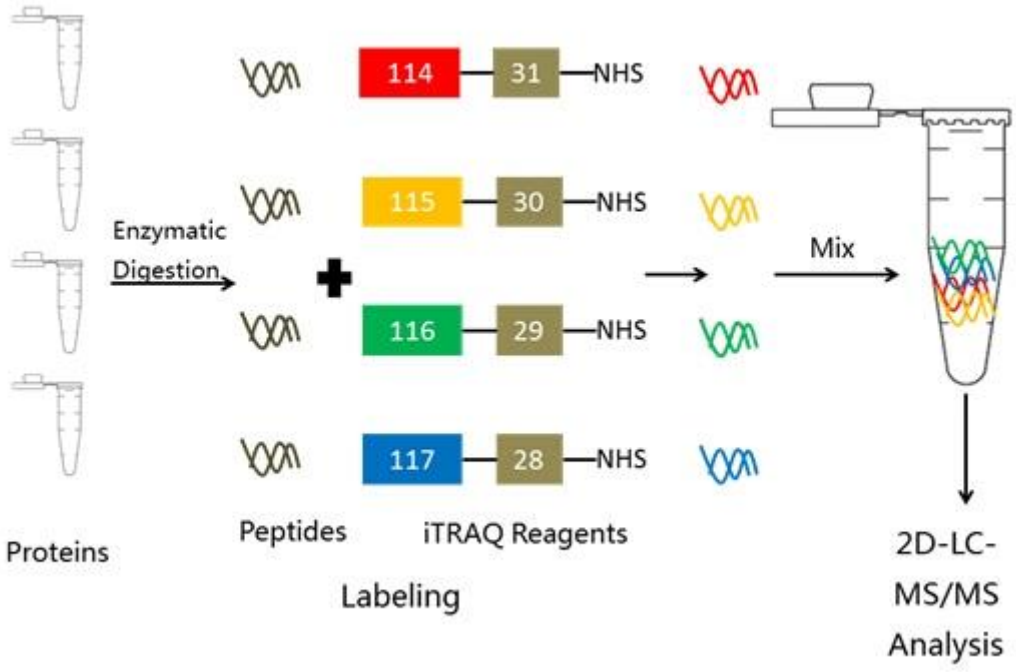

Fig. 3| Different steps of iTRAQ workflow: proteins extraction, enzymatic digestion, labeling and LC-MS/MS analysis (from www.creative-proteomics.com/services/itraq-based-proteomics-analysis.htm).

The iTRAQ technology also exploits an N-hydroxysuccinimide ester derivative to modify primary amino molecules by binding a carbonyl group and a reporter molecule (based on N-methylpiperazine) to proteolytic peptides. Differentially labeled peptides are shown as single peaks in mass spectrometer scans decreasing the probability of peak overlapping. Using four different iTRAQ reagents, comparative analysis of four samples is possible in single MS run. A drawback of iTRAQ approaches consists on enzymatic digestion of proteins before labeling, increasing sample complexity. ITRAQ approaches is proposed to be an applicable approach to obtain quantitative infor-mation for those peptides that are subjected to MS/MS analyses.

METABOLOMICS

Metabolomics is concerned with the metabolism, identifying the amounts of different metabolites as well as the activity of enzymes at cell, tissue, organ, organism level. The metabolomic approach is based on the analysis of global metabolites in a cell or biological fluid, not guided by a priori hypothesis. This allows characterize the metabolic profile of a given

condition and allows identify which metabolites or pattern of metabolites may be useful in discriminating between different study groups. Through the analysis of spectroscopic data and multivariate statistical analysis tools it is possible to extrapolate the relevant metabolic data in the characterization of specific physiological and stress conditions in living organisms such as plants. Furthermore, this approach needs low amounts of biological sample, rendering it applicable to multiple biological samples. Metabolomics is a complementary science to the most developed functional genomics sciences, proteomics and transcriptomics. Compared to these other omics sciences, metabolomics should allow producing even more directly practical information, since changes regarding transcriptome and proteome not always reflected in an equally direct changes in the biochemical phenotype (metabolome). Metabolomics is one of the most important new omics sciences to contribute to the study of systems biology. In the context of already decoded crop genomes metabolomics may play a central role for the gene-function studies in plants. Most of metabolomes of plants, are not well accurately defined. A number of unidentified compounds, which are the product of metabolic pathways, have unknown functions. Two hundred thusands of diverse metabolites are estimated to be in plants. The metabolites vary from inorganic species to carbohydrates and lipids and secondary metabolites. The chemical diversity and complexity of the metabolome is so high that there is no single analytical technique that can address the complete metabolome.

Since the analytical nature of the metabolomic analysis it is "inherently" incomplete, the analysis of only a small fraction of the metabolome in which most of the metabolites are not detected is a limiting factor. Taking into account that the analysis of the whole of metabolites present system is not possible at the moment, the use of at least the metabolite profiling approach, consisting in a simultaneous analysis of several hundreds of metabolites is an essential tool for the study of systems biology.

Metabolites influence the phenotype much more directly than the transcripts or proteins, and the metabolome changes are often more amplified than transcriptome or proteome. The metabolomic analysis is extremely valuable in estimating the effects of environmental or agronomic factors on the composition of the products (Martinelli et al., 2012).

Metabolite profiles are typically measured by using techniques such as gas chromatography plus mass spectrometry (GC/MS) and high performance liquid chromatography (HPLC). Also, the combination of GC and HPLC with time-of-flight (TOF) mass spectrometers and nuclear magnetic resonance (NMR) spectroscopy-based techniques have been applied for biochemical profiling applications (Glassbrook and Ryals, 2001; Bligny and Douce, 2001; Raamsdonk et al., 2001).

Therefore, metabolomics can improve plants metabolic engineering because enable to better understand plant biochemical networks and their regulation by characterizing low-molecular-weight chemicals (Holtorf et al., 2002).

PHENOMICS

The important ability of an organism, especially sessile organisms (plants), to change its phenotype in response to environmental changing is called "phenotypic plasticity" (Großkinsky et al., 2015). Phenomics is then a functional genomics technology that studies how genetic, environment and their interaction influence the phenotype of an organism using a large scale approach. The improvement of the accuracy and celerity of phenotypic estimation is the principal objective of phenotyping. Second aim is to decrease costs and labor through automation, remote sensing, and improving data integration (Cobb et al., 2013).

To investigate plant growth and development, automated-imaging and software solutions have been used recently for several high-throughput phenotyping studies (Cobb et al., 2013).

Particularly, digital imaging is an innovative non-destructive technology that is used in plant to control all morphological changes basing on leaf area index (LAI), tillering and compactness parameters (Neilson et al., 2015). Recently, new imaging technique has been created to examine photosynthetic responses to abiotic stresses such as drought in plants, called pulse-modulated chlorofyll fluorescence imaging (Jansen et al., 2009).

L-systems is, instead, a set of mathematical approaches used to develop 3D models that mimic the development of the plant organs and which is particularly effective in the case of cereals (Prusinkiewicz et al., 1996; 2002).

Two important abiotic stresses are drought and salinity that produce stomatal closure due to the the osmotic effect caused by the root's ability to uptake water from the soil (Munns and Tester, 2008). Therefore, to select genotypes able to cop with this problem in presence of osmotic stress, infrared thermography (IR) has been used in wheat and barley seedling (Sirault et al., 2009)

Phenomics have allowed to closely link genetics and physiology to reveal the molecular mechanisms of regulation of a wide range of important metabolic processes and pathways (Furbank and Tester, 2011).

ABIOTIC AND BIOTIC STRESS

Plants are exposed to abiotic or biotic stresses, or a combination of these, which are a major cause of economic loss and instability of agricultural production. Plants sense and respond to these stresses through the development of a series of molecular mechanisms that depart from the perception of an environmental change condition. The signal is then transduced by molecular cascades that amplify it, to determine a final response. The understanding of these molecular mechanisms is fundamental to obtaining varieties which ensure production stability even in unfavorable environmental conditions. Most of the signaling molecules are proteins such as G-protein, kinases, phosphatases, transcription factors, transporters and receptors (Yamaguchi-Shinozaki and Shinozaki 2006; Pareek et al. 2010; Pandey 2012, 2013).

Among signal transduction components, ROS (Reactive Oxygen Species) are crucial molecules involved in abiotic stress responses and in the defense against pathogens (Jalmi and Sinha 2015) while calmodulin and calmodulin-like proteins (Ca2+ sensors) have, especially, a role in the regulation of abiotic stress responses (Zeng et al. 2015; Virdi et al. 2015).

It is well known that transcription factors (TFs) regulating stress responses in plants. For example, NACs and WRKYs are involved in plant development and biotic and abiotic stresses responses (Shao et al. 2015). In cotton Yan et al. (2015) have identified a WRKY gene that has a different functional role, it regulates in a negative way drought tolerance and positively the resistance to *R. solani* pathogen. A peculiar class of plants transcription factors is called HD-Zip. Many of the genes in this class are probably involved in the regulation of development of the plant in relation to environmental conditions and responses to stress.

Also phytohormones, chemical molecules, are involved in plant development and stress responses. Among these, jasmonic acid (JA) has a functional role in regulation of abiotic stress responses such as salinity and drought (Riemann et al. 2015) while ABA modulates both abiotic and biotic responses by two different pathways, the ABA-independent and the ABA-dependent cascades.

Different functional genomic approaches allow identify those genes involved in signaling cascades and understand the function of these genes in response to certain stimuli, through the use of high-throughput techniques it is possible to greatly understand how the stress signal transduction pathways are modulated by the environmental stress. Expression genomics, mutant analysis, microarrays, RNA-seq and proteomics are usually used to identify stress responsive genes and their mechanism. The greater understanding of regulatory networks involved in the adaptation of the plants to the environmental conditions provides knowledge

and tools for the genetic improvement with the aim of increasing stress tolerance but also implementing the nutrient content.

The results of these approaches will determine new ways of using biotechnology to develop and improve food and agricultural products in terms of quality, yield and environmental impact. In this thesis several omic techniques were employed to gain insight into the gene regulatory networks modulating plant molecular responses to environmental stresses. The integration of different platforms is the real weak point of this kind of analysis. Due to the costs of their analysis per single sample, it is difficult to include all omic tools in a single study and this reduces the possibility to determine which key players (genes, miRNAs, proteins, metabolites) modulate the phenotypic expression of a particular plant trait.

REFERENCES

Al-Khayri JM, Jain SM, Johnson DV (2016) Advances in Plant Breeding Strategies: Agronomic, Abiotic and Biotic Stress Traits. Eds Springer.

Albrecht U, Bowman KD (2008) Gene expression in *Citrus sinensis* (L.) Osbeck following infection with the bacterial pathogen *Candidatus* Liberibacter asiaticus causing Huanglongbing in Florida. Plant Sci 175:291-306. doi: http://dx.doi.org/10.1016/j.plantsci.2008.05.001

Arbona V, Manzi M, de Ollas C, Gómez-Cadenas A (2013) Metabolomics as a Tool to Investigate Abiotic Stress Tolerance in Plants. Int J Mol Sci 14:4885-4911. doi: 10.3390/ijms14034885

Bauer MA, Chavan SS, Peterson EA, Heuck CJ, Johann JDJ (2014) Leveraging the new with the old: providing a framework for the integration of historic microarray studies with next generation sequencing. BMC Bioinformatics 15:S3. doi: 10.1186/1471-2105-15-S11-S3

Bieda M (2012). Kepler for 'Omics Bioinformatics. Procedia Comput Sci 9:1635–1638. doi: 10.1016/j.procs.2012.04.180

Bligny R, Douce R (2001) NMR and plant metabolism. Curr Opin Plant Biol 4:191-196.

Bouchez D, Höfte H (1998) Functional Genomics in Plant. Plant Physiol 118:725-732.

Brandl J, Andersen MR (2015). Current state of genome-scale modeling in filamentous fungi. Biotechnol Lett 37:1131–1139. http://doi.org/10.1007/s10529-015-1782-8

Campos-De Quiroz H (2002) Plant genomics: an overview. Biol Res 35:385-399. http://dx.doi.org/10.4067/S0716-97602002000300013

Chawla K, Barah P, Kuiper M, Bones AM (2011) Systems biology: a promising tool to study abiotic stress responses. Omics and Plant Abiotic Stress Tolerance 163-172.

Chu S, DeRisi J, Eisen M, Mulholland J, Botstein D, Brown PO, Herskowitz I (1998) The transcriptional program of sporulation in budding yeast. Science 282:699-705.

Cobb JN, DeClerck G, Greenberg A, Clark R, McCouch S (2013) Next-generation phenotyping: requirements and strategies for enhancing our understanding of genotype–phenotype relationships and its relevance to crop improvement. Theor Appl Genet 126:867–887. doi: 10.1007/s00122-013-2066-0

Dandekar AM, Martinelli F, Davis CE, et al (2010) Analysis of Early Host Responses for Asymptomatic Disease Detection and Management of Specialty Crops. Crit Rev Immunol 30:277-89.

Eisen MB, Spellman PT, Brown PO, Botstein D (1998) Cluster analysis and display of genome-wide expression patterns. Proc Natl Acad Sci USA 95:14863-8.

Fiehn O (2001) Combining genomics, metabolome analysis, and biochemical modelling to understand metabolic networks. Comp Funct Genomics 2:155–168. doi: 10.1002/cfg.82.

Furbank RT, Tester M (2011) Phenomics--technologies to relieve the phenotyping bottleneck. Trends Plant Sci 16:635-44. doi: 10.1016/j.tplants.2011.09.005

Garq R, Jain M (2013) RNA-Seq for transcriptome analysis in non-model plants. Methods Mol Biol 1069:43-58. doi: 10.1007/978-1-62703-613-9_4

Glassbrook N, Ryals J (2001) A systematic approach to biochemical profiling. Curr Opin Plant Biol 4:186-190.

Großkinsky DK, Svensgaard J, Christensen S, Roitsch T (2015) Plant phenomics and the need for physiological phenotyping across scales to narrow the genotype-to-phenotype knowledge gap. J Exp Bot 66:5429-40.doi:10.1093/jxb/erv345

Gupta B, Sengupta A, Saha J, Gupta K (2013) Plant Abiotic Stress: "Omics" Approach. J Plant Biochem Physiol 1:e108. doi: 10.4172/2329-9029.1000e108

Holtorf H, Guitton MC, Reski R (2002) Plant functional genomics. Naturwissenschaften 89:235-249. doi:10.1007/s00114-002-0321-3

ISAAA International Service for the acquisition of agri-biotechapplications (2006) "Omics sciences: Genomics, Proteomics, and Metabolomics. www.isaaas.org. Access on 2016, 17th November.

Jalmi SK, Sinha AK (2015) ROS mediated MAPK signaling in abiotic and biotic stress-striking similarities and differences. Front Plant Sci 6:769. doi: 10.3389/fpls.2015.00769

Jansen M, Gilmer F, Biskup B, Nagel KA et al (2009) Simultaneous measurement of leaf growth and chlorophyll fluorescence via GROWSCREEN FLUORO allows detection of stress tolerance in Arabidopsis thaliana and other rosette plants. Funct Plant Biol 36:902–914.

Kohl M, Megger DA, Trippler M, Meckel H, Ahrens M, Bracht T et al (2014) A practical data processing workflow for multi-OMICS projects. Biochim Biophys Acta 1844:52–62. doi: 10.1016/j.bbapap.2013.02.029

Martinelli F, Basile B, Morelli G et al (2012) Effects of irrigation on fruit ripening behavior and metabolic changes in olive. Scientia Horticulturae 144(6):201-207.

Mingzhu M, Chen A, Wang Z et al (2015) Plant microarray for gene expression profiling and their application. J Agr Technol 11:93–105.

Munns R, Tester M (2008) Mechanisms of salinity tolerance. Annu Rev Plant Biol 59:651–681.

Neilson EH, Edwards AM, Blomstedt CK, Berger B, Lindberg Møller B, Gleadow RM (2015) Utilization of a high-throughput shoot imaging system to examine the dynamic phenotypic responses of a C4 cereal crop plant to nitrogen and water deficiency over time. J Exp Bot 66:1817-32. doi: 10.1093/jxb/eru526

Neubauer G, King A, Rappsilber J, Calvio C, Watson M, Ajuh P, Sleeman J, Lamond A, Mann M (1998) Mass spectrometry and EST-database searching allows characterization of the multi-protein spliceosome complex. Nat Genet 20:46-50.

NSF (2011) Phenomics: Genotype to Phenotype. A report of the Phenomics workshop sponsored by the USDA and NSF. http://www.nsf.gov/bio/pubs/reports/phenomics_workshop_report.pdf

Pandey A, Mann M (2000) Proteomics to study genes and genomes. Nature 405:837-846.

Pandey GK (2012) Stress Mediated Signaling in Plants I and II. Plant Stress, Vol. 6 and 7, Special Issue. Miki Cho: Global Science Books.

Pandey GK (2013) Stress Mediated Signaling in Plants I and II. Plant Stress, Vol. 6 and 7, Special Issue. Miki Cho: Global Science Books.

Pandey GK, Pandey A, Prasad M, Böhmer M (2016) Editorial: Abiotic Stress Signaling in Plants: Functional Genomic Intervention. Front Plant Sci 7:681. doi: 10.3389/fpls.2016.00681

Pareek A, Sopory SK, Bohnert HJ, Govindjee (2010) Abiotic Stress Adaptation in Plants: Physiological, Molecular and Genomic Foundation. Dordrecht: Springer Business media.

Prusinkiewicz P, Hanan J, Hammel M, Mech R (1996) L-systems: from the theory to visual models of plants. In 2nd CSIRO Symposium on Computational Challenges in Life Sciences (Michalewicz, M.T., ed.), CSIRO Publishing.

Prusinkiewicz P, Mündermann L, Karwowski R, Lane B (2002) The use of positional information in the modeling of plants. SIGGRAPH'01, 289–300. doi: 10.1145/383259.383291

Raamsdonk LM, Teusink B, Broadhurst D et al (2001) A functional genomics strategy that uses metabolome data to reveal the phenotype of silent mutations. Nat Biotechnol 19:45-50. doi: 10.1038/83496

Riemann M, Dhakarey R, Hazman M, Miro B, Kohli A, Nick P (2015) Exploring Jasmonates in the Hormonal Network of Drought and Salinity Responses. Front Plant Sci 6:1077. doi: 10.3389/fpls.2015.01077

Rout MP, Aitchison JD, Suprapto A, Hjertaas K, Zhao Y, et al (2000) The yeast nuclear pore complex: composition, architecture, and transport mechanism. J Cell Biol 148: 635–651.

Schumacher A, Rujan T, Hoefkens J (2014) A collaborative approach to develop a multi-omics data analytics platform for translational research. Appl Transl Genomics 3:105–108. doi: 10.1016/j.atg.2014.09.010

Shao H, Wang H, Tang X (2015) NAC transcription factors in plant multiple abiotic stress responses: progress and prospects. Front Plant Sci 6:902. doi: 10.3389/fpls.2015.00902

Shendure J, Hanlee J (2008) Next-generation DNA sequencing. Nat Biotechnol 26:1135-1145. doi:10.1038/nbt1486

Sirault XRR, James RA, Furbank RT (2009) A new screening method for osmotic component of salinity tolerance in cereals using infrared thermography. Funct Plant Biol 36:970–977

Somerville C, Somerville S (1999) Plant Functional Genomics. Science 285:380-3.

Vélez-Bermúdez IC, Wen TN, Lan P, Schmidt W (2016) Isobaric Tag for Relative and Absolute Quantitation (iTRAQ)-Based Protein Profiling in Plants. Methods Mol Biol 1450:213-221. doi: 10.1007/978-1-4939-3759-2_17

Virdi AS, Singh S, Singh P (2015) Abiotic stress responses in plants: roles of calmodulin-regulated proteins. Front Plant Sci 6:809. doi: 10.3389/fpls.2015.00809

Witzel K, Neugart S, Ruppel S, Schreiner M, Wiesner M, Baldermann S (2015) Recent progress in the use of “omics” technologies in brassicaceous vegetables. Front Plant Sci 6:244. doi: 10.3389/fpls.2015.00244

Yamaguchi-Shinozaki K, Shinozaki K (2006) Transcriptional regulatory networks in cellular responses and tolerance to dehydration and cold stresses. Annu Rev Plant Biol 57:781–803.

Yan Y, Jia H, Wang F, Wang C, Liu S, Guo X (2015) Overexpression of GhWRKY27a reduces tolerance to drought stress and resistance to Rhizoctonia solani infection in transgenic Nicotiana benthamiana. Front Physiol 6:265. http://doi.org/10.3389/fphys.2015.00265

Zeng H, Xu L, Singh A, Wang H, Du L, Poovaiah BW (2015) Involvement of calmodulin and calmodulin-like proteins in plant responses to abiotic stresses. Front Plant Sci 6:600. doi: 10.3389/fpls.2015.00600

CHAPTER 2

AIM OF THIS WORK

The objective of my PhD thesis is to use innovative functional genomics techniques, to gain insight into the molecular mechanisms of regulation of crop responses to abiotic and biotic stress.

Particularly the following specific subjects in plant stress biology were addressed.

Biotic stress responses:

1. Large-scale analysis of the gene regulatory networks of *Phoenix canariensis* (Chabaud) in response to the attacks of *Rhynchophorus ferrugineus* (Olivier) (Chapter 3);
2. Microarray analisys in grapevine to elucidate early responses and recovery mechanisms to "stolbur" infection (Chapter 4).
3. Molecular responses to small regulating molecules against Huanglongbing disease in *Citrus* (Chapter 5)
4. Proteomic responses of two *Citrus* genotypes with variabletolerance to HLB, in order to identify proteins playing a key role in the diverse phenotypic sensitivity to the disease (Chapter 6).

Abiotic stress responses in durum wheat:

1. Annotation and characterization of miRNAs and their targets in response to drought stress, mycorrhizal inoculations and the combination of the two treatments (Chapter 7);
2. Analyze the agronomic and key molecular responses to salt stress and mycorrhizal inoculation (cv. Anco Marzio) (Chapter 8).

CHAPTER 3

TRANSCRIPTOME ANALYSIS OF *Phoenix canariensis* CHABAUD IN RESPONSE TO *Rhynchophorus ferrugineus* OLIVIER ATTACKS[1]

Antonio Giovino[1], Edoardo Bertolini[2], Veronica Fileccia[3,4], Mohamad Al Hassan[5], Massimo Labra[6] and Federico Martinelli[3, 4*]

[1]Unità di Ricerca per il Recupero e la Valorizzazione delle Specie Floricole Mediterranee, Consiglio per la Ricerca in Agricoltura e l'Analisi dell'Economia Agraria, Palermo, Italy, [2]Istituto di Scienze della Vita, Scuola Superiore Sant'Anna, Pisa, Italy, [3]Dipartimento di Scienze Agrarie e Forestali, Università degli Studi di Palermo, Palermo, Italy, [4]Istituto Euromediterraneo di Scienza e Tecnologia, Palermo,I taly, [5]Universitat Politècnica de València, Instituto de Biología Moleculary Celular de Plantas, Consejo Superior de Investigaciones Científicas (CSIC), Ciudad Politécnica de la Investigación (CPI), Valencia, Spain, [6]Dipartimento di Biotecnologie e Bioscienze, Università degli Studi di Milano Bicocca, Milano, Italy

Background: Red Palm Weevil (RPW, Rhynchophorus ferrugineus Olivier) threatens most palm species worldwide. Untilnow, no studies have analyzed the gene regulatory networks of Phoenix canariensis (Chabaud) in response to RPW attacks. The aim of this study was to fill this knowledge gap. Providing this basic knowledge is very important to improve its management.

Results: A deep transcriptome analysis was performed on fully expanded leaves of healthy non-infested trees and attacked trees at two symptom stages (middle and late infestation). A total of 54 genes were significantly regulated during middle stage. Pathway enrichment analysis showed that phenylpropanoid-related pathways were induced at this stage. More than 3300 genes were affected during late stage of attacks. Higher transcript abundances were observed for lipid fatty acid metabolism (fatty acid and glycerolipids), tryptophan metabolism, phenylpropanoid metabolism. Key RPW-modulated genes involved in innate response mediated by hormone cross talk were observed belonging to auxin, jasmonate and salicylic acid (SA) pathways. Among transcription factors, some WRKYs were clearly induced. qRT-PCR validation confirmed the upregulation of key genes chosen as validation of transcriptomic analysis.

Conclusion: A subset of these genes may be further analyzed in future studies to confirm their specificity to be induced by RPW infestations.

[1] Published to Frontiers in Plant Science, 2015, 6:817. doi: 10.3389/fpls.2015.00817

1_INTRODUCTION

Rhynchophorus ferrugineus Olivier (commonly known as the Red Palm Weevil, RPW) is considered the worst pest threat for palm species worldwide. More than 30 palm species are attacked by this insect, including *Phoenix canariensis* Chabaud, *P. dactylifera* L. and *Cocos nucifera* L. (Ju *et al.*, 2011). RPW was first reported in tropical Asia and then spread worldwide, reaching several Middle Eastern countries, Africa and the Mediterranean basin in the 1980s (Faleiro, 2006). In Europe, including Spain, especially the Canary Islands, and Southern Italy, RPW inflicted great economic damage in areas where palm distinguishes the scenic beauty of the public and private gardens of the cities and countryside. In the United States a species of RPW has been identified (Rugman-Jones *et al.*, 2013). RPW belongs to the Curculionidae family of Coleoptera. The damage caused to palm is due to the large larvae that make large tunnels within soft and terminal plant tissues. The larvae can achieve a size of 5 cm, and different generations can be present in the same infected tree. Adults may deposit approximately 200 eggs at the base of leaves or in wound tissues, and larvae migrate within all parts of trees, including the roots, destroying all the plant organs and structures (Gutierrez *et al*., 2010). A major issue in the management of pest attacks is the late detection of infestations. Usually, symptoms are only visible when the larvae have reached the latest developmental stage and when plant organs are already compromised (Ju *et al*., 2011). Indeed, at this point, it is too late to save the infected trees. The symptoms of infestation include a gnawing sound caused by larvae feeding inside infested trees, chewed plant material at the external entrances of tunnels generating particular smells, the presence of empty pupal and dead adult bodies close to infested palms, the breaking of the palm crown and trunk (Faleiro, 2006) and the asymmetry of the palm crown. These symptoms are not visible prior to 5-6 months of infestation, when any prophylaxis is useless (Failero, 2006). The evaluation of the signs of larval mines and chewed material at the leaf bases is the typical way to detect signs of early infestation. However, early infestations can be difficult to detect in adult palms because actively growing portions are usually at the top of the plants. Therefore, a wide range of physical, chemical and biological methodologies are under development to detect the insect inside the palms as soon as infestations occur. Computer-assisted tomography shows interesting results for the inspection of the granary weevil in wheat (Haff and Slaughter, 2004). However, these methods are expensive and difficult to be applied in infected palms where the whole tree needs to be inspected. Indeed, these methods may not be used for the large-scale scouting of infestations. The analysis of volatiles that are emitted by the fermentation processes of infested trees was also addressed by means of trained dogs that recognized the characteristic odors of plants that were attacked by RPW (Nakash *et al*., 2000).

However, the low selectivity and reliability due to the presence of several volatiles that are unrelated to the RPW infection limit the use of such methods (Mielle and Marquis, 1999). Bioacoustic sensors could represent an alternative system for early detection (Gutierrez *et al.*, 2010). However, this detection is still expensive and requires trained technical staff to discriminate the RPW noise from others. Moreover, these methods are not very effective at early feeding phases. Until now, no large-scale analyses of palm responses to RPW attacks have been conducted. Transcriptomics represent a powerful tool not only to elucidate the physiological effects of RPW attacks on infected palms but also to the identify biomarkers that are usable to improve detection when symptoms are still unclear. In addition, transcriptomics is essential to develop therapeutics based on gene biotechnology. Next-Generation Sequencing (NGS) has revolutionized transcriptomic studies because this technology can detect rare and unknown transcripts and splice variants that are not present in microarrays, offering a more detailed and profound analysis of the transcriptome. The power of this method is fully exploitable when extensive genomic information is available for the organism under investigation. In plants, RNA-seq has proven effective in studying the transcriptomic profile after pathogenic infections (Martinelli *et al*., 2012, 2013; Chen *et al*., 2014; Zhang *et al*., 2014) and in identifying possible targets for their early detection (Tremblay *et al*., 2013).

Recent studies have been published on the genomic analysis of *P. dactylifera* L. A genome assembly was performed for Khalas, an elite cultivar (Al-Dous *et al*., 2011). The assembled sequence was approximately 380 Mb spanning mostly gene-rich regions (90% of genes were covered) and including >25,000 gene models. Another genome sequence of date palm is available (Al-Mssallem *et al*., 2013).

The aim of this study was to gain insight into gene regulatory networks of responses to RPW attack in *Phoenix canariensis*. This research will allow us to (1) clarify the gene regulation mechanisms of leaf metabolism in response to RPW attacks at different stage of infestations and (2) identify possible host biomarkers that may confirm RPW typical symptomatology.

2_MATERIALS AND METHODS

2.1_Plant Material and Experimental Design

This study was performed on *Phoenix canariensis* Chabaud. We selected 15-20-year-old trees with a diameter of 70-90 cm. Analyzed leaves were 4-5m long with 80-100 segments on each side of the spine. The plants were field-grown in a former cultivation of approximately 2 ha, located in Trabia (Palermo, Italy). These plants were genetically different although they have a similar genetic background since they were derived from the same mother plant. No specific permissions were required for these locations and activities. The field studies did not involve endangered or protected species. These are the GPS coordinates of the area where plants were analyzed: 38°00′00″N 13°39′00″E; 38°00′00″N 13°39′00″E.

The plants were arranged on the sides of the private driveway. The trees were divided into three groups: Healthy unattacked trees (He); stage 1 (the middle stage of infection – S1) and stage 2 (plants with late symptoms – S2). The pathogen presence was visually confirmed. No plants were available at very early stage of infection. Although trees at S1 showed symptoms, analyzed leaves were green and did not show any symptoms such as the healthy ones.

The He category was composed of palm trees with no symptoms of Red Palm Weevil attacks and no signs of other common diseases or pathogen attacks (**Fig. 1**). The sampled individuals showed fully expanded leaves without any sign of gnawing. To exclude sampling errors (i.e., sampling asymptomatic infested plants instead of healthy uninfected plants), we monitored the sampled He trees for the following 90 days from sampling. This period was defined based on the timing needed to show early symptoms of infestations (Ju *et al.*, 2011).

The S1 category represents trees that showed anomalous behavior of the canopy with the beginning of characteristic retracted asymmetry of the crown. Individuals showed fully expanded leaves without any sign of gnawing at the sampling time; however, after 30-40 days, some of the leaves showed a flattened and nibbled vegetative apex. Moreover, after 50 days, some larvae were detected in the S1 individuals. The S2 category included trees with loss of leaves for subsidence of foliar rachis. In these trees, most of the leaves showed the typical recline induced by RPW. Foliar desiccation was much more apparent than in S1. While analyzed leaves of S1 looked green as the healthy ones, S2 leaves showed evident yellowing.

Each of the three conditions was analyzed in duplicate; thus, a total of six samples (biological replicates) were analyzed by deep sequencing. Each biological replicate was composed of 10-15 leaf portions of three distinct trees. The leaf portions were collected from

the middle of the palm leaves at the same time during the day. The samples were immediately frozen in liquid nitrogen and stored at – 80 °C.

Fig. 1| Palm trees of the three analyzed categories: (A) healthy (He); (B) stage S1 (middle stage of infestation); (C) stage S2 (intense level of infestation)

2.2_Analysis of the Plant Health Status

The rhizosphere was analyzed to identify any other pathogenic organisms in addition to RPW. The soil samples were collected from all four plant sides at a depth of 30 cm (500 g per plant). The pathogens were isolated through different traditional techniques. Substrates of the soil, roots and bark were prepared for both generic and selective pathogen isolation. The soil samples were repeatedly mixed, and 10 g was taken, dissolved in 100 ml of sterile distilled water and agitated for 15 min. A 1 ml aliquot of the suspension was inoculated in Petri dishes with cultured generic potato dextrose agar (PDA). The root and bark tissues were previously superficially sterilized and immersed in an aqueous solution of sodium hypochlorite at 10% for 3-5 min, rinsed in sterile distilled water and dried. The tissue fragments were placed on the

culture substrates PDA, corn meal agar (CMA) plus streptomycin (20-30 mg/L) and PARPNH substrate-selective culture. All the plates were dark-incubated at 24 ± 1 °C. The developed fungal colonies were grown in purity and characterized based on both macroscopic (morphology, color, and speed of growth of the colony) and microscopic features (fruiting bodies, spores, and conidia). The genera and species were identified based on dichotomous recognized keys. All the analyzed palms were tested for the presence of common bacterial and fungal pathogens (i.e., Penicillium sp., Alternaria sp., Mortierella sp., Aspergillus sp.). None of these common pathogens were present.

2.3_RNA Extraction

The total RNA from each biological replicate was isolated using a rapid RNA extraction method that was developed by Gambino *et al*. (2008). The RNA concentrations were determined using a NanoDrop ND-1000 spectrophotometer (NanoDrop Technologies, Wilmington, DE). The RNA quality and purity were assessed by an Agilent Bioanalyzer (Folsom, CA).

2.4_RNA-seq Analysis

The RNA samples were processed using the TruSeq RNA-seq sample prep kit from Illumina (Illumina, Inc., CA, USA). Briefly, the poly-A containing mRNA molecules were purified using poly-T oligo-attached magnetic beads and fragmented into small pieces using divalent cations at an elevated temperature. The cDNA was synthesized by reverse transcription, and standard blunt-ending plus add 'A' was performed. Then, Illumina TruSeq adapters with indexes were ligated to the ends of the cDNA fragments. After the ligation reaction and separation of the unligated adapters, the samples were amplified by PCR to selectively enrich those cDNA fragments in the library with adapter molecules at both ends. The six samples (RNA pools of 10-15 leaves of three individual plants) were loaded into one lane of an Illumina flow cell, and clusters were created by Illumina cBot. The clusters were sequenced at ultra-high throughput on the Illumina HiSeq 2000 (Illumina Inc.). One lane in 6-plex was run, obtaining between approximately 21.1 and 29.8 million single reads per sample, each 50 bp long. The data were produced on an IGA Technology Services Srl (Udine, Italy) Illumina platform. All the sequenced reads were compared to the Date Palm Genome Draft Sequence Version 3.0 (http://qatar-weill.cornell.edu/). The gene prediction from the Date Palm Genome Draft Sequence Version 3.0 (file PDK30-mrna.fsa.gz downloaded from http://qatar-weill.cornell.edu/) was used. The Software CLC Genomic Workbench 5.5.1 (CLC Bio,

Denmark) was used for reads trimming and alignment on the reference. The reads were quality trimmed using the modified-Mott trimming algorithm (parameter: trim using quality score = 0.05). The alignment on a reference parameters were set-up in CLC Genomics Workbench as following: Mismatch cost = 2; Insertion cost = 3; Deletion cost = 3; Length fraction = 0.9; Similarity fraction = 0.95. BLASTx was used to determine the date palm gene predictions of the putative orthologous *Arabidopsis thaliana* genes ($e < 10^{-4}$). DESeq 2 package from Bioconductor in the R statistical software suite (Love *et al.*, 2014) was used to estimate the euclidean sample distance and the expression level of transcripts among different conditions. DEseq program performs normalization, variance estimation and differential expression of the raw read counts and works best with experiments with replicates. The log2-fold ratio and adjusted p-values (FDR) based on the t-distribution for each gene for the two pairwise comparisons (He-S1 and He-S2) were calculated. Genes with a log2-fold ratio > 1 or < -1 and with an adjusted p-value (FDR) below 0.1 were considered differentially expressed. RNA-seq and details of the samples were submitted on Sequence Read Archive (NCBI) (SAMN04031658).

2.5_Functional Categorization of the Predicted RPW-regulated Transcripts

The sequenced transcripts were mapped to the Date Palm Genome Draft Sequence Version 3.0 and used as a reference genome. For each of the palm genes, the gene length, unique and total gene reads, annotation and RPKM expression values were obtained. The closest *Arabidopsis* putative orthologs were determined for each gene to allow the use of functional genomics tools. The integrated data-mining approach used different web tools, such as MapMan, PageMan, PathExpress and Cytoscape to dissect the transcriptome responses and decipher the gene regulatory networks. A list of predicted transcripts that were differentially expressed at a significant level ($p < 0.05$ and an absolute value of log2-fold change > 1 or < -1) was obtained for each of the two pairwise comparisons (S1 vs. He and S2 vs. He). These input data files were used for all the data mining tools.

The functions of the differentially expressed genes (as *Arabidopsis* putative orthologs) were visualized using the MapMan web-tool (Thimm *et al.*, 2004; http://mapman.gabipd.org/web/guest/mapman) through the Ath_AGI_isoform_model_Tair10_Aug2012.m02 mapping file that was downloaded from the MapMan server. The PageMan visualization tool was used for GSEA analysis using the Wilcoxon test (no correction and ORA cutoff = 1.0). A pathway enrichment analysis was

performed using PathExpress (Goffard and Weiller, 2007) using the *Arabidopsis* putative orthologs of the differentially expressed palm transcripts.

2.6_RT-PCR Validation

Nine genes were chosen for qRT-PCR validation of RNA-seq data. Four biological replicates were considered for each of three conditions (Healthy, S1 and S2). Each replicate was a pool of 10-15 mature leaves from the same plant. The four chosen plants belonged to those used for RNA-seq analysis: two belongs to the first replicate and the other two belonged to the second replicate of deep sequencing analysis. Primers were designed basing on each target sequence using Primer Express software (Applied Biosystems, Foster City, CA, Table S1). RNA was extracted as previously described. Retrotranscription was performed following the Quantitect Reverse Transcription Kit (Qiagen) instructions. A standard curve was generated for each gene. Amplifications used 25 ng cDNA in a 15 µL final volume were performed on a Biorad iQ5 PCR system (Biorad) using standard amplification conditions: 10 min at 95°C; 40 cycles of 15 s at 95°C; and 1 min at 60°C. All PCR reactions were performed in duplicate (technical replicates). Fluorescent signals were collected during the annealing step and C_T values extracted with an auto calculated threshold followed by baseline subtraction. *18S* (AF206991.1) was used as an endogenous reference and $\Delta\Delta C_T$ was calculated by subtracting the average of *18S* from the average C_T of the gene of interest. The reference gene was tested on the 12 analyzed samples and any significant changes of expression were observed between the three samples categories.

3_RESULTS

3.1_Illumina RNA Sequencing

RNA-seq was used to evaluate palm responses to RPW attack by comparing the expression profiles of healthy trees (He) with infected trees during the middle and late stages of infection (S1 and S2). The genome sequence of *Phoenix dactylifera* was used as referred genome for sequence annotation (Al-Dous *et al.*, 2011). This allowed obtain a list of palm genes correspondent to the assembled sequences. Then we identified the correspondent *Arabidopsis* ortholog to each of these genes. We obtained a total of 21.3-29.8 million raw reads for the six palm samples (**Table 1**). Of them 21.1-29.5 were trimmed. A total of approximately 8.6-12.3

million 50-nt single-end reads from each cDNA library were uniquely mapped to the genome published by Al-Dous *et al*. (2011). Unique mapped reads were approximately 40.6-41.6 % of the corresponding total trimmed reads per sample. Multiple mapped reads were approximately 1.1 % and they were discarded from the analysis.

The gene expression data of the two pairwise comparisons (S1 vs. He and S2 vs. He) were provided in Table S2, S3. **Fig. 2** showed a Venn diagram of up- and down-regulated genes by RPW in both pairwise comparisons. A total of 44 genes were upregulated, and 10 were downregulated in S1 vs. He comparison. Most of them were reported in **Table 2**. A total of 3373 genes were differentially expressed in S2 vs. He comparison (approximately 13.5 % of the predicted genes in the genome reference); 1938 were upregulated and 1435 were downregulated. A dendrogram was constructed based on the overall transcriptome analysis of the six analyzed samples (**Fig. 3**). As expected He and S1 were grouped together while S2 showed to be clearly distinguished by the other two sample categories. Volcano plots were performed for both S1/He and S2/He comparisons (**Fig. 4**). In the S1/He comparison, although many genes have a log fold ratio higher than 1, they had a non significant FDR. In the S2/He comparison a considerable portions of the analyzed genes were significantly regulated. These genes were mainly those that presented a higher fold ratio.

Table 1| Number of raw reads, trimmed raw reads, mapped reads (unique), mapped reads (multiple).

Sample	Healthy 1	Healthy 2	Stage 1-1	Stage 1-2	Stage 2-1	Stage 2-2
Raw reads	21,333,300	25,657,081	22,350,317	29,707,097	29,781,177	26,491,474
Trimmed raw reads	21,139,613	25,438,175	22,142,923	29,456,600	29,527,217	26,123,111
Mapped reads (unique)	8,591,083	10,460,021	9,023,479	12,174,309	12,291,541	10,860,082
% of mapped reads (unique)	40.64	41.12	40.75	41.33	41.63	41.57
Mapped reads (multiple)	227,933	268,690	233,928	337,254	337,657	297,427
% of mapped reads (multiple)	1.08	1.06	1.06	1.14	1.14	1.14

Percentages of mapped reads (unique or multiple) were calculated from trimmed raw reads.

Table 2| List of the main differentially regulated genes during stage 1 (FDR < 0.1).

Annotation	AGI	Log_2 fold ratio
REDOX PATHWAYS		
Peroxidase superfamily protein	AT1G05260.1	-4.0
Peroxidase superfamily protein	AT1G68850.1	2.4
(2OG) and Fe(II)-dependent oxygenase protein	AT5G05600.1	3.0
(2OG) and Fe(II)-dependent oxygenase protein	AT4G10490.1	1.7
LARGE ENZYME FAMILIES		
GDSL-like Lipase/Acylhydrolase protein	AT1G74460.1	2.6
Glutathione S-transferase TAU 18	AT1G10360.1	2.0
Cytochrome P450 superfamily protein	AT5G07990.1	-3.9
Cytochrome P450 family 94 C polypeptide 1	AT2G27690.1	3.4
SIGNAL PERCEPTION AND SIGNALING		
Protein kinase superfamily protein	AT1G18670.1	1.6
Calcium-dependent protein kinase 16	AT2G17890.1	1.5
Protein of unknown function (DUF604)	AT2G37730.1	-3.3
Protein of unknown function (DUF616)	AT1G53040.1	1.6
Calcium-dependent protein kinase 28	AT5G66210.2	2.0
TRANSCRIPTION FACTORS		
WRKY40	AT1G80840.1	2.8
WRKY51	AT5G64810.1	2.7
NAC domain containing protein 32	AT1G77450.1	1.8
PROTEIN MODIFICATIONS		
RING/U-box superfamily protein	AT1G78420.1	-7.6
RING/U-box superfamily protein	AT1G53820.1	3.1
RING/U-box superfamily protein	AT2G18650.1	-4.1
U-box domain-containing protein kinase protein	AT2G45910.1	1.6
SECONDARY METABOLISM		
Cinnamate-4-hydroxylase	AT2G30490.1	3.0

Laccase 7	AT3G09220.1	2.9
Laccase 12	AT5G05390.1	2.3
Chalcone and stilbene synthase protein	AT5G13930.1	1.8
Leucoanthocyanidin dioxygenase	AT4G22880.1	-3.6
DEFENSE RESPONSES		
Disease resistance family protein / LRR protein	AT2G34930.1	1.7
Pathogenesis-related thaumatin protein	AT2G17860.1	1.8
Lipid-transfer protein/seed storage 2S albumin	AT3G22600.1	2.5
CELL WALL MODIFICATIONS		
Xyloglucan endotransglycosylase 6	AT4G25810.1	2.1
Beta-1 3-glucanase 5	AT5G20340.1	2.1
D-arabinono-1 4-lactone oxidase family protein	AT2G46740.1	3.4
Pectin lyase-like superfamily protein	AT3G62110.1	-3.7
HORMONE-RELATED		
Ethylene response factor 110	AT5G50080.1	1.2
Auxin amidohydrolase	AT1G51760.1	3.4
OTHERS		
Nitrate transporter 1.5	AT1G32450.1	1.3
LOB domain-containing protein 1	AT1G07900.1	2.2
Amino acid permease 3	AT1G77380.1	1.8
Formin homology5	AT5G54650.1	1.5
HXXXD-type acyl-transferase protein	AT5G41040.1	2.4
Alpha/beta-Hydrolases superfamily protein	AT2G39420.1	3.4
P-loop nucleoside triphosphate hydrolases protein	AT3G45080.1	-2.7
Glutamate receptor 2.8	AT2G29110.1	1.5
Glutamate receptor 2.7	AT2G29120.1	1.8
Di-glucose binding protein Kinesin motor domain	AT2G22610.1	-3.1
Integrase-type DNA-binding protein	AT4G36920.1	-1.9
Glycosyl hydrolase superfamily protein	AT4G16260.1	2.1

The Log FD (Fold Ratio) was indicated. The complete list with the palm gene ID and Arabidopsis putative orthologs is available in the supplemental material (Table S2).

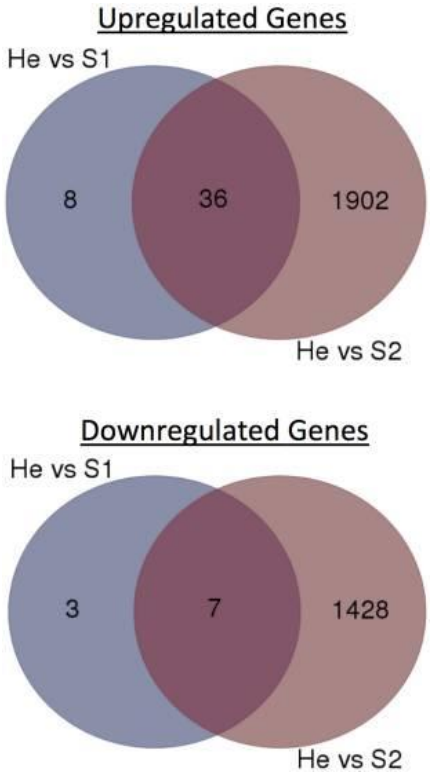

Fig. 2| Venn diagrams of RPW-regulated genes at He vs. S1 and He vs. S2 comaprisons. Numbers of up- or down-regulated genes were shown.

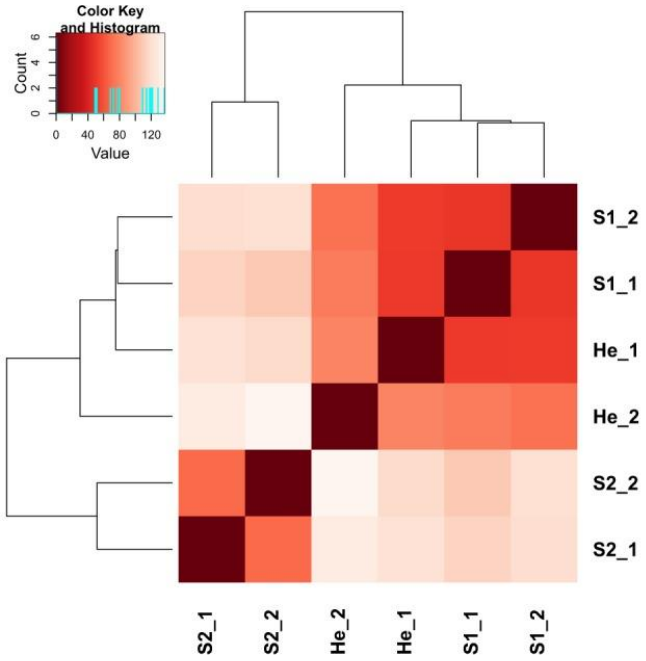

Fig. 3| A dendogram based on mapped read counts was constructed for the six analyzed samples belonging to Healthy (He), Stage 1 (S1) - middle stage of infestation, Stage 2 (S2) - intense level of infestation.

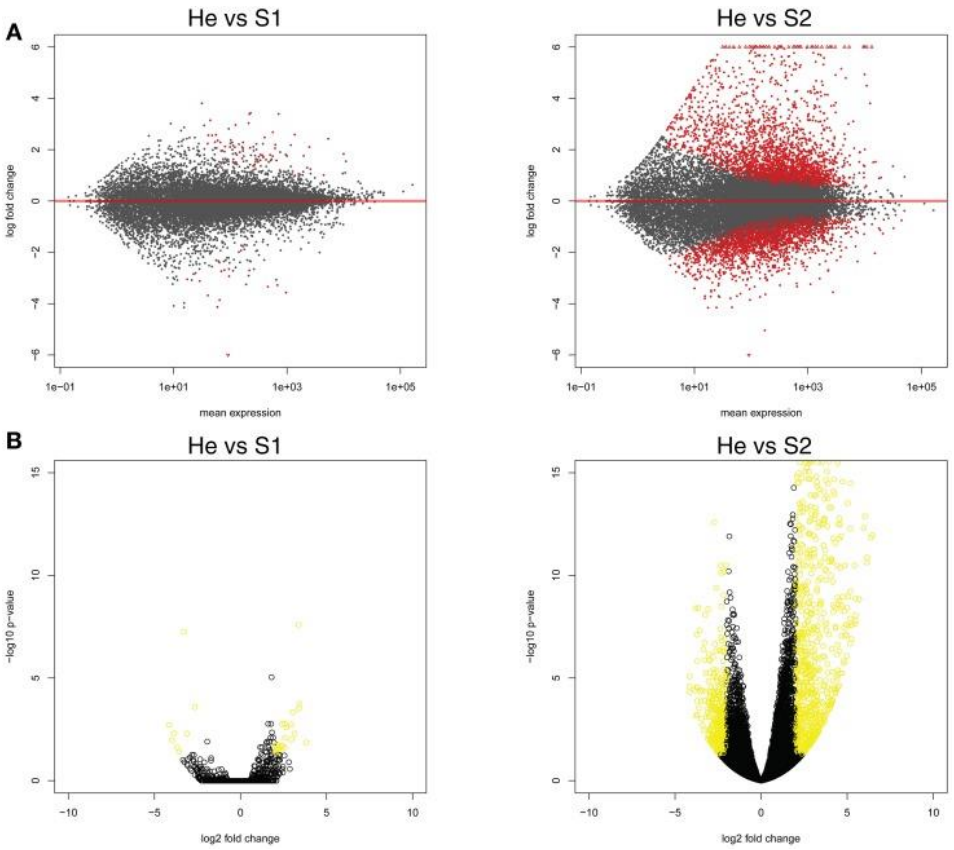

Fig. 4| (A) Expression changes for each analyzed palm gene in the two pairwise comparisons (He vs. S1 and He vs. S2). In abscissa axis mean expression and in ordinate axis log fold changes were shown. (B) Volcano plots for both He/S1 and He/S2 comparisons were shown. In abscissa axis log_2 fold change while in ordinate axis log_{10} *p*-value were shown for each identified gene.

3.2_Metabolomic Pathway and Gene Set Enrichment Analysis

The metabolic pathway enrichment analysis indicated that at stage S1 of infestation, phenylalanine metabolism, phenylpropanoid biosynthesis, flavonoid biosynthesis and xenobiotic metabolism mediated by citochrome P450 were significantly upregulated by RPW attacks (**Table 3**). In contrast, flavone and flavonol biosynthesis were significantly repressed at S1. At S2, RPW significantly induced lipid-related pathways such as fatty acid, sphingolipid, glycerolipid metabolism. In contrast RPW repressed starch and sucrose metabolism and inositol-related pathways.

Key primary metabolism pathways were influenced by RPW at S2, such as the sucrose (upregulated) and callose metabolism (downregulated) (**Fig. 5**). Interestingly key players in transcription regulation of biotic stress responses were upregulated such as WRKYs. Genes encoding receptor kinases (including leucine rich repeat III) and cell organization-related proteins were repressed.

Table 3| PathExpress analysis of the up and downregulated genes in each of the two pairwise comparisons.

S1 vs. He	**P-values**
UPREGULATED	
Phenylalanine metabolism	$4.1*10^{-3}$
Phenylpropanoid biosynthesis	$5.1*10^{-3}$
Flavonoid biosynthesis	$7.9*10^{-3}$
Metabolism of xenobiotics by citochrome P450	$2.6*10^{-2}$
DOWNREGULATED	
Flavone and flavonol biosynthesis	$1.3*10^{-2}$
S2 vs. He	**P-values**
UPREGULATED	
Fatty acid metabolism	$3.3*10^{-4}$
Sphingolipid metabolism	$3.6*10^{-2}$
Glycerolipid metabolism	$3.7*10^{-2}$
Tryptophan metabolism	0.05
Alkaloid biosynthesis	0.05
DOWNREGULATED	
Starch and sucrose metabolism	$2.1*10^{-3}$
Phosphatidylinositol signaling system	$3.6*10^{-3}$
Inositol phosphate metabolism	$9.3*10^{-3}$
Glycosaminoglycan degradation	0.04

Pathways with P < 0.05 (no corrections) were affected by the RPW attacks. He, Healthy; S1, stage 1; S2, stage 2.

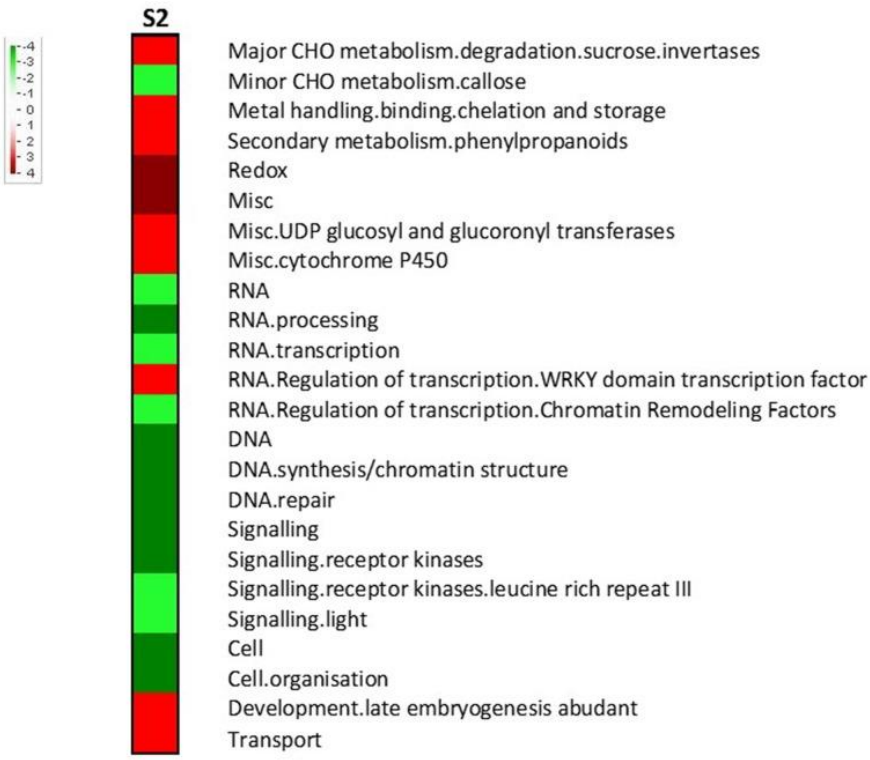

Fig. 5| Gene set enrichment analysis of the transcriptomic changes during stage 2 (S2). Pageman web-tool was used. Wilcoxon test with ORA cut off = 1 was used. A scale bar between -4 and 4 was chosen. Increased intensity of red and green respectively represented higher level of upregulation and downregulation.

3.3_Secondary Metabolism, Transcription Factors, Signaling, Redox

At S1, some genes involved in phenylpropanoids were upregulated (**Table 2**). At S2, a high number of genes belonging to secondary metabolism were induced. Some phenylpropanoid genes were strongly activated during the late stage S2 such as *O-methyltransferasefamily protein 1* and *2, 3-coumarate-CoAligase, ferulic acid 5-hydroxylase 1, cinnamoyl-CoA reductase*.

A list of differentially regulated genes at S2 encoded transcription factors was provided (Table S4). Regarding signal perception and transduction signaling, different classes of receptor kinases showed different trends of expression (Table S4). At S1, genes encoding a specific category of signal receptors DUF were differentially regulated: *DUF616* was slightly enhanced and *DUF604* was repressed (-3.3). At S2, most of the genes of DUF26 protein kinases and LRK10-like (serine/threonine protein kinases) were more abundant while leucine-rich repeat III, VI, and XII were mostly repressed. In addition, post-translational modifications seemed to be positively affected. The transcript abundance of genes of large enzyme families (thioredoxin-

related and cytochrome-related) that are involved in redox was severely affected by RPW attack.

3.4_Hormone-related Pathways

At S1, *Auxin amidohydrolase* and *ethylene response factor 110* were slightly higher in abundance. At S2, significant transcriptional changes were observed for a group of genes that are involved in auxin signal transduction (*PIN2* and *PIN4*) (Table S4). ABA-related pathways were affected as demonstrated by the induction of *HVA22J* and two *GRAM-domain-containing proteins*. In contrast, the expressions of *ABA1* and *AREB3* were lower at S2 compared to He. In general hormone-related pathways were drastically affected by RPW at S2. Two *ACC oxidases* that are involved in ethylene biosynthesis were upregulated. Two cytokinin receptors were significantly repressed, *HK2* and *HK3*. Some significant increases in transcript abundance were observed for genes that were involved in jasmonate synthesis (*allene oxide synthase* and *OPR2*) and salicylic acid-mediated response (glucosyltransferases).

3.5_Biotic Stress Responses

Defense-related pathways were activated at S1 as shown by the upregulation of genes encoding a *pathogenesis-related thaumatin protein* and a *disease resistance/LRR protein*. An overview of the transcriptomic changes involved in biotic stress pathways at stage 2 was provided (**Fig. 6**). Extensive induction of genes encoding enzymes involved in redox state and peroxidases was observed in response to RPW at both disease stages. Two peroxidase genes were differentially regulated at S1: one was induced (Log FD = 2.4) and the other was repressed (Log FD = -4.0). Key genes encoding antioxidant enzymes were slightly upregulated at S1 (**Table 2**).

As far as it concerns, cell wall modification genes were upregulated at S1. Two laccase genes were induced at both S1 and S2. At S2, five genes involved in cell wall restructuring and encoding five *beta-1,3,- glucan hydrolases* were enhanced.

Pathogenesis-related (PR) proteins were mostly repressed although three disease-resistance family proteins were upregulated at late symptomatic stage. At S1, two WRKYs were upregulated. At S2, several WRKY genes were clearly enhanced, such as *WRKY9, WRKY14, WRKY40, WRKY47, WRKY28, WRKY72, WRKY75* and *WRKY51*. In contrast, WRKY2 was downregulated.

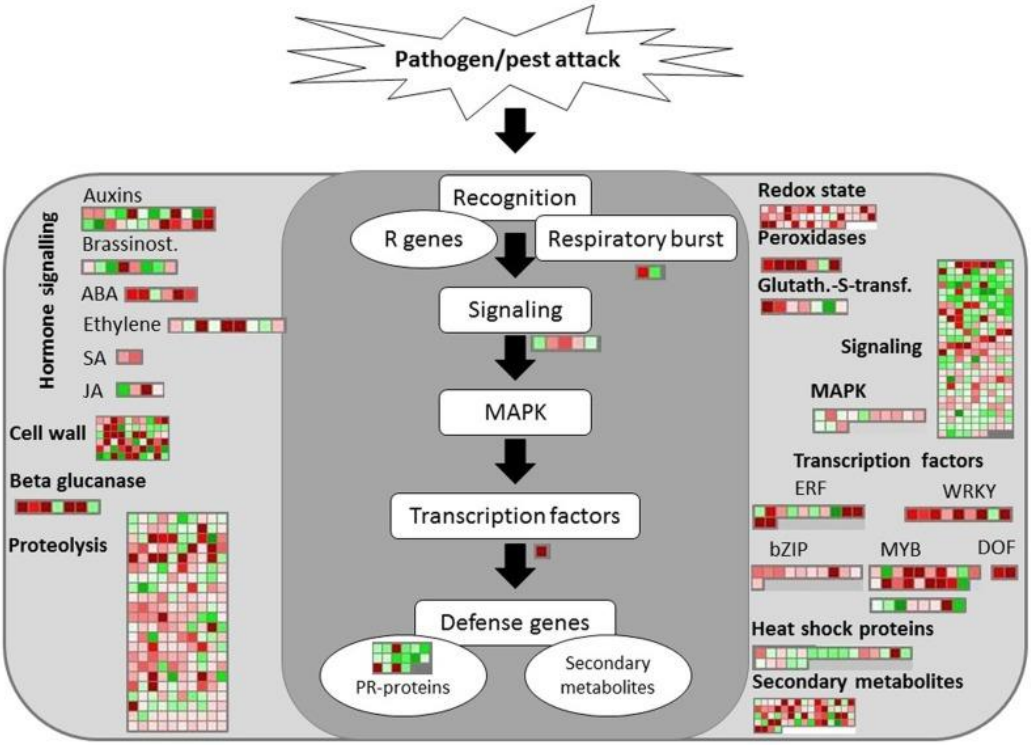

Fig. 6| Transcriptomic changes involved in biotic stress responses at stage S2. The same scale bar used for the other figures was shown. Negative values represented repressed genes (green) at S2 in comparison to He and positive values (red) represented upregulated genes.

3.6_qRT-PCR Analysis

qRT-PCR were performed to validate expression trend of nine RPW-regulated genes (**Table 4**). Statistical differences of 15 of the 18 pairwise comparisons of gene expressions observed by RNA-seq were confirmed by qRT-PCR analysis. *Alpha-amylase* and *invertase* belonged to sugar and starch metabolism. RNA-seq analysis showed that both these two genes were not regulated at stage S1 while they were induced at stage S2. qRT-PCR confirmed data on S2 but showed that they were also significantly induced at S1. *UDP-glycosyltransferase* was confirmed to be induced at S2 while *UDP-glucose-SA glycosyltransferase* was enhanced at both S1 and S2. *Laccase7*, involved in secondary metabolism, was upregulated at S1. *Auxin amidohydrolase* was upregulated at both stages of infestation. *WRKY72* and *WRKY75* were confirmed to be higher in abundance at S2.

Table 4| qRT-PCR analysis of 9 chosen genes.

Date Palm ID	Description	ANOVA (RNA-seq)		ANOVA (qRT-PCR)	
		He vs. S1	He vs. S2	He vs. S1	He vs. S2
PDK_30s654931g003	Alpha-Amylase	n.s.	6.4 (*)	1.5 (*)	4.9 (*)
PDK_30s705371g005	UDP-Glycosyltransf.	n.s.	5.6 (*)	n.s.	80.9 (*)
PDK_30s888011g002	Laccase 7	2.9 (*)	n.s.	0.37 (*)	n.s.
PDK_30s835131g001	WRKY 75	n.s.	7.5 (*)	n.s.	4.3 (*)
PDK_30s883821g030	UDP-glucose-SA glycosyltransf.	n.s.	1,5 (*)	2.4 (*)	3.2 (*)
PDK_30s936891g001	WRKY 40	2.8 (*)	2,7 (*)	9.2 (*)	1.4 (*)
PDK_30s1151561g006	Invertase	n.s.	3,0 (*)	0.8 (*)	1.4 (*)
PDK_30s1173851g004	Auxin amidohydrolase	3.4 (*)	1.7 (*)	10.1 (*)	1.2 (*)
PDK_30s1138471g004	WRKY 72	n.s.	3.3 (*)	n.s.	0.7 (*)

*Statistical analysis using ANOVA ($P < 0.05$) was shown: * means significant, n.s. means not significant. Log_2 fold ratio were indicated.*

3.7_Protein-protein network analysis

A protein-protein interaction network (PPI) was generated between the proteins that are encoded by RPW-regulated genes and their predicted interactions at stage S2 (Appendix S7). Only pairwise interactions among the RPW-regulated genes and their partners reduced the network complexity. The network was highly complex, and more than 2000 pairwise interactions were detected. Some important hub proteins that are encoded by a RPW-regulated genes were identified (Appendix S7). Around 20 proteins (with more than 50 pairwise interactions) are responsible for most of the changes at predictive protein-protein interaction level in the gene regulatory network in response to RPW attacks.

4_DISCUSSION

In this work, we addressed the lack of knowledge on transcriptomic responses to RPW attacks. Plant secondary metabolites are well-known compounds involved in plant-insect interactions (Becerra, 2007). Phenylpropanoid genes were strongly affected by RPW attacks. This evidence highlight that palms are activating counteracting responses to RPW from the middle stage of infection. We observed that BACT3 and IIL1 genes and other genes (*allinase* and *TAR2*) involved in the biosynthesis of sulfur-containing compounds were enhanced. These compounds have well-known defensive properties. Plants have been engineered to produce a cyanogenic glycoside, obtaining enhanced resistance to Phyllotreta nemorum in *Arabidopsis* (Tattersall et al., 2001). These genes were not induced at S1 implying that palm responses to RPW attacks are activated too late and in an inefficient manner. Genes encoding *strictosidine synthases* were clearly enhanced only in response to RPW during the late stage. These genes are involved in alkaloid metabolism, a pathway that is generally stimulated in defense against insect herbivory. Flavonoids are known to be important compounds playing a key role in plant-insect interactions (Treutter, 2006). We observed an unclear pattern of expression of some members of this pathways. *Flavanone isomerase* was repressed while *chalcone synthase* was induced. Taken together all these data related to secondary metabolism let us to conclude that *Phoenix canariensis* did not trigger appropriate defenses to promptly counterbalance RPW attacks.

This is might be due to two factors: (1) the RPW-induced genes involved in phenylpropanoids are induced only at late stage when plants are already compromised, (2) it is possible that the genes playing a major roles in the transcriptional regulation of secondary metabolism were not sufficiently enhanced at middle stage of infection (S1).

Other key genes involved in volatile biosynthesis were differentially regulated. The emission of plant volatiles may represent a direct defensive benefit by precluding oviposition (De Moraes et al., 2001) or attracting predators (Kessler and Baldwin, 2001). The important transcript changes that were observed in volatile pathways confirmed that infestations may lead to drastic changes in the volatile profiles detectable by biological methods (Nakash et al., 2000). Novel methods based on detection of induced volatile organic compounds have been recently proposed and should be applied to detect RPW attacks (Dandekar et al., 2010; Martinelli et al., 2015).

Fig. 7 summarized a global view of the main changes that were detected in leaf metabolism considering both analyzed symptom stages. We identified some RPW-induced genes encoding receptor kinases belonging to receptor kinase VIII, DUF26 protein kinases,

RLK10-like, and S-locus glycoprotein-like categories. LRR receptor like serine/threonine-protein kinase, S-locus receptor kinase, and TIR-NBS-LRR resistance proteins have been previously found to be upregulated by aphid attacks (Coppola et al., 2013). Interestingly LRR III and LRR XII were mostly repressed. It is possible that the repression of some of these classes might be involved in a delay or complete lack of signal perception of RPW attacks and consequently in inadequate immune responses to RPW infestations. However, the size and complexity of these gene families make it extremely difficult to understand which family could be involved in susceptible reactions to RPW.

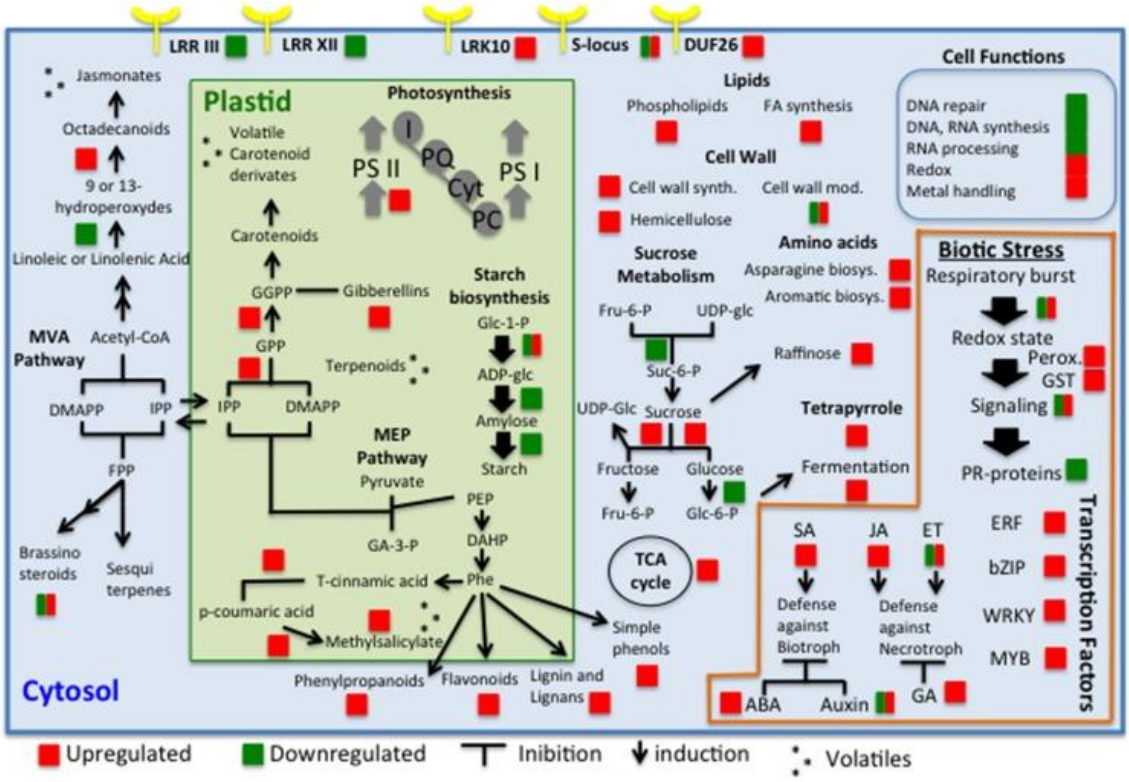

Fig. 7| Global view of the transcriptomic changes in palm leaves in response to RPW attacks. The genes, pathways, and cell functions that were differentially expressed are indicated with a square (red for upregulated and green for downregulated).

Plant-induced defense responses are modulated by a network of interconnecting hormone crosstalk in which salicylic acid (SA), jasmonic acid (JA), and ethylene (ET) play pivotal roles (Glazebrook, 2001). Jasmonic-related genes were induced by RPW attacks at S2. The synthesis of jasmonic acid (JA) and its precursors and derivatives (collectively termed jasmonates) occurs when plant are wounded. Jasmonates play a central role in regulating defense responses to herbivores (Heil and Ton, 2008). It is expected that a trauma caused by

chewing insects or mechanical damage results in the rapid accumulation of JA at the site of wounding. Previous data have demonstrated that the repression of JA responses induce susceptibility to herbivorous insects (Kessler et al., 2004). Here, we observed the upregulation of two key genes (*AOS* and *OPR2*) that are involved in JA biosynthesis during S2. Interestingly, jasmonic-related genes were not upregulated during the middle stage (S1), although their roles in herbivore attack have been demonstrated. This evidence is another clue that demonstrates the inefficient response of *Phoenix canariensis* to RPW infestations. Although crosstalk between defense signaling pathways presents a powerful regulatory instrument, it may also represent a weakness. Here, we observed that a *UDP-glucosyltransferase* that is involved in the conversion of SA to methyl-salicylate was induced during S2. qRT-PCR showed that this gene was significantly upregulated at both stages. It is well known that systemic acquired resistance-against biotroph attacks is antagonist to JA-mediated responses to necrotrophs such as insects. It is possible that the induction of *salicylic acid methyl transferase* would benefit the insect by regulating negatively jasmonic acid-mediated responses. However, previous transcriptomic studies highlight the upregulation of SA-related genes in response to aphid attacks while the effect on JA-related genes showed a more complex regulation (Coppola et al., 2013). The differences in hormonal plant responses may be due to their diverse type of insect feeding. ABA is connected to the SA-JA-ET network, stimulating JA biosynthesis and antagonizing the onset of SA-dependent defenses. Here, we report that RPW induced genes that are involved in ABA metabolism and response (*HVA22J, C3HC4-type ring finger*, two *GRAM-domain-containing proteins*). The antagonistic effect of auxin on SA signaling has been documented (Pieterse et al., 2009).

PR proteins were associated with the induction of both locally and systemically induced resistance to pathogens (Van Loon, 1997). Here, we showed that PR genes were differentially regulated by RPW infestations. The majority of PR genes were downregulated implying again a probably weak and inefficacious response to RPW invasion. WRKY proteins are a well-known family of transcription factors involved in biotic stress responses and comprise more than 70 members in *Arabidopsis* (Rushton et al., 2010). Induction of WRKY members have been observed in longitudinal studies of *Macrosyphum euphorbiae* aphid attacks (Coppola et al., 2013). Upregulation of some members of this family was observed mainly at S2. However, *WRKY40* and *WRKY51* were enhanced also at S1 and might be considered candidate host biomarkers for RPW infestations. *WRKY40* gene has been linked to response to the aphid B. brassicae attack (Kusnierczyk et al., 2008). A total of 8 WRKY members were significantly enhanced by RPW at stage S2. This important evidence indicates that palms activate a transcription induction of defense responses to RPW larvae feeding although these responses

are too late. *WRKY51* transcript was the most abundant (log FD = 7.7). Gao et al. (2011) showed that *WRKY51* plays a key role in stimulating SA-mediated responses and inhibiting JA-inducible defenses, resulting in enhanced resistance to biotrophs but increased susceptibility to necrotrophs. Basing on these data, we may speculate that the induction of this gene as observed in RPW-attacked trees may have negative effects on host plant.

Laccases are enzymes leading to the polymerization of monolignol precursors of lignin.

The activation of these genes at middle stage of infestation confirmed that attacked palms responded to RPW invasion. A large number of *peroxidase* genes were induced at stage S2. Two of them were differentially regulated also at stage S1. These transcript changes were expected since peroxidases are well-known to be involved in ROS-detoxifying reactions, in the modulation of the redox and Ca2+ homeostasis as well as the regulation of defense-related genes (Kawano, 2003). Peroxidases act against biotic attacks in a passive way building up stronger walls or actively producing ROS against pathogens (Moura et al., 2010). When the attacking organism overcomes lignin barriers, peroxidases may be important to isolate the intruder. The evidence that these genes were induced at S1 is a clue that palmare activating defense responses against pathogen colonization.

The ability to rapidly identify RPW infestations is of particular interest because it would allow to rapidly activate the management practices against RPW. In addition, the qRT- PCR analysis of RPW-regulated genes might help in speeding up detection of infestations. Genes upregulated at S1, involved in biotic stress responses, may be further analyzed to check their specificity for RPW attacks such as WRKY40 and WRKY51. A panel of genes may be analyzed in response to abiotic stresses and other typical biotic attacks to check their level of reliability in improving RPW management.

Some possible short-term therapeutic approaches might be proposed. A first approach could focus on boosting JA-mediated defense responses by applying molecules, such as methyl jasmonate, JA, and linolenic acid, which would most likely shift the hormone crosstalk to JA, penalizing SA and allowing trees to localize efforts to pathways that might impair the larvae feeding aptitude. Another possible strategy could be the over-expression of genes playing a key role in the production of compounds that are repellant or not attractive to larvae or adults. Because auxin-responsive genes are antagonists of SA, a worthwhile experiment would be to test the effects of auxin inhibitor compounds on an attacked tree. It is possibly worthwhile to test the combination of sucrose with agents that stimulate xenobiotic responses through ROS signaling induction as previously suggested (Sulmon et al., 2006). Although an effective RPW management is still absent, the data presented in this work may lead to novel methods of

detection of infestations and offer an essential contribution to save palms from RPW attacks, especially in designated World Heritage areas.

SUPPLEMENTARY MATERIAL

The Supplementary Material for this article can be found online at: http://journal.frontiersin.org/article/10.3389/fpls.2015.00817

5_REFERENCES

Al-Dous, E. K., George, B., Al-Mahmoud, M. E., Al-Jaber, M. Y., Wang, H., Salameh, Y. M., et al. (2011). De novo genome sequencing and comparative genomics of date palm (*Phoenix dactylifera*). *Nat. Biotechnol.* 29, 521-527. doi: 10.1038/nbt.1860

Al-Mssallem, I. S., Hu, S., Zhang, X., Lin, Q., Liu, W., Tan, J., et al. (2013). Genome sequence of the date palm *Phoenix dactylifera* L. *Nat Commun*. 4:2274. doi: 10.1038/ncomms3274

Becerra, J. X. (2007). The impact of herbivore-plant coevolution on plant community structure. *Proc. Natl. Acad. Sci. U.S.A.* 104, 7483-7488. doi: 10.1073/pnas.0608253104

Chen, X. R., Zhang, B. Y., Xing, Y.P., Li, Q. Y., Li, Y. P., Tong, Y. H., et al. (2014). Transcriptomic analysis of the phytopathogenic oomycete Phytophthora cactorum provides insights into infection-related effectors. *BMC Genomics* 15:980. doi: 10.1186/1471-2164-15-980

Coppola, V., Coppola, M., Rocco, M., Digilio, M. C., D'Ambrosio, C., Renzone, G., et al. (2013). Transcriptomic and proteomic analysis of a compatible tomato-aphid interaction reveals a predominant salicylic acid-dependent plant response. *BMC Genomics* 14:515. doi: 10.1186/1471-2164-14-515

Dandekar, A. M., Martinelli, F., Davis, C. E., Bhushan, A., Zhao, W., Fiehn, O., et al. (2010). Analysis of Early Host Responses for Asymptomatic Disease Detection and Management of Specialty Crops. *Crit. Rev. Immunol*. 30, 277-289. doi: 10.1615/CritRevImmunol.v30.i3.50

De Moraes, C. M., Mescher, M. C., and Tumlinson, J. H. (2001). Caterpillar-induced nocturnal plant volatiles repel conspecific females. *Nature* 410, 577-580. doi: 10.1038/35069058

Faleiro, J. (2006). A review of the issues and management of the red palm weevil *Rhynchophorus ferrugineus* (Coleoptera: Rhynchophoridae) in coconut and date palm during the last one hundred years. *Int. J. Trop. Insect Sci.* 26, 135-154. doi: 10.1079/IJT2006113

Gambino, G., Perrone, I., and Gribaudo, I. (2008). A rapid and effective method for RNA extraction from different tissues of grapevine and other woody plants. *Phytochem. Anal*. 19, 520–525. doi: 10.1002/pca.1078

Gao, Q. M., Venugopal, S., Navarre, D., and Kachroo, A. (2011). Low Oleic Acid-Derived Repression of Jasmonic Acid-Inducible Defense Responses Requires the WRKY50 and WRKY51 Proteins. *Plant Physiol*. 155, 464-476. doi: 10.1104/pp.110.166876

Glazebrook, J. (2001). Genes controlling expression of defense responses in *Arabidopsis* - 2001 status. *Curr. Opin. Plant Biol*. 4, 301-308. doi: 10.1016/S1369-5266(00)00177-1

Goffard, N., and Weiller, G. (2007). PathExpress: a web-based tool to identify relevant pathways in gene expression data. *Nucleic Acids Res*. 35, 176-181. doi: 10.1093/nar/gkm261

Gutierrez, A., Ruiz, V., Moltó, E., Tapia, G., and Téllez, M. M. (2010). Development of a bioacoustic sensor for the early detection of Red Palm Weevil (*Rhynchophorus ferrugineus* Olivier). *Crop Prot*. 29, 671-676. doi: 10.1016/j.cropro.2010.02.001

Haff, R. P., and Slaughter, D. C. (2004). Real-time X-ray inspection of wheat for infestation by the granary weevil, *Sitophilus granarius* (L). *Trans. Am. Soc. Agric. Eng.*. 47, 531−537. doi: 10.13031/2013.16022

Heil, M., and Ton, J. (2008). Long-distance signalling in plant defence. *Trends Plant Sci*. 13, 264-272. doi: 10.1016/j.tplants.2008.03.005

Ju, R. T., Wang, F., Wan, F. H., and Li, B. (2011). Effect of host plants on development and reproduction of *Rhynchophorus ferrugineus* (Olivier) (Coleoptera: Curculionidae). *J Pest. Sci*. 84, 33-39. doi: 10.1007/s10340-010- 0323-4

Kawano, T. (2003). Roles of the reactive oxygen species-generating peroxidase reactions in plant defense and growth induction. *Plant Cell Rep*. 21, 829-837. doi: 10.1007/s00299-003-0591-z

Kessler, A., and Baldwin, I. T. (2001). Defensive function of herbivore-induced plant volatile emissions in nature. *Science* 291, 2141-2144. doi: 10.1126/science.291.5511.2141

Kessler, A., Halitschke, R., and Baldwin, I. T. (2004). Silencing the Jasmonate Cascade: Induced Plant Defenses and Insect Populations. *Science* 305, 665-668. doi: 10.1126/science.1096931

Kusnierczyk, A., Winge, P., Jorstad, T. S., Troczynska, J., Rossiter, J. T., and Bones, A. M. (2008). Towards global understanding of plant defence against aphids - timing and dynamics of early Arabidopsis defence responses to cabbage aphid (*Brevicoryne brassicae*) attack. *Plant Cell Environ*. 31, 1097-1115. doi: 10.1111/j.1365-3040.2008.01823.x

Love, M. I., Huber, W., and Anders, S. (2014). Moderated estimation of fold change and dispersion for RNA-seq data with DESeq 2. *Genome Biol.* 15, 550. doi: 10.1101/002832

Martinelli, F., Reagan, R. L., Uratsu, S. L., Phu, M. L., Albrecht, U., Zhao, W., et al. (2013). Gene regulatory networks elucidating huanglongbing disease mechanisms. *PLoS ONE* 8:e74256. doi: 10.1371/journal.pone. 0074256

Martinelli, F., Scalenghe, R., Davino, S. W., Panno, S., Suderi, G., Ruisi, P., et al. (2015). Advanced methods of plant disease detection. A Review. *Agron. Sustain. Dev.* 35, 1-25. doi: 10.1007/s13593-014-0246-1

Martinelli, F., Uratsu, S. L., Albrecht, U., Reagan, R. L., Phu, M. L., Britton, M., et al. (2012). Transcriptome profiling of citrus fruit response to huanglongbing disease. *PLoS ONE* 7:e38039. doi:10.1371/journal.pone. 0038039

Mielle, P., and Marquis, F. (1999). An alternative way to improve the sensitivity of electronic olfactometers. *Sens. Actuators B Chem*. 58, 526-535. doi: 10.1016/S0925-4005(99)00158-6

Moura, J. C., Bonine, C. A., de Oliverira Fernandes Viana, J., Dornelas, M. C., and Mazzafera, P. (2010). Abiotic and biotic stresses and changes in the lignin contentand composition in plants. *J. Integr. Plant Biol.* 52, 360–376. doi: 10.1111/j.1744-7909.2010.00892.x

Nakash, J., Osem, Y., and Kehat, M. (2000). A suggestion to use dogs for detecting red palm weevil (*Rhynchophorus ferrugineus*) infestation in date palms in Israel. *Phytoparasitica* 28, 153-155. doi: 10.1007/BF02981745

Pieterse, C. M. J., Leon-Reyes, A., Van der Ent, S., and Van Wees, S. C. M. (2009). Networking by small-molecule hormones in plant immunity. *Nat. Chem. Biol.* 5, 308-316. doi: 10.1038/nchembio.164

Rugman-Jones, P. F., Hoddle, C. D., Hoddle, M. S., and Stouthamer, R. S. (2013). The lesser of two weevils: molecular-genetics of pest palm weevil populations confirm Rhynchophorus vulneratus (Panzer 1798) as a valid species distinct from R. ferrugineus (Olivier 1790), and reveal the global extent of both. *PLoS ONE* 8:e78379. doi:10.1371/journal.pone.0078379

Rushton, P. J., Somssich, I. E., Ringler, P., and Shen, Q. J. (2010). WRKY transcription factors. *Trends Plant Sci*. 15, 247-258. doi: 10.1016/j.tplants.2010.02.006

Sulmon, C., Gouesbet, G., El Amrani, A., and Couee, I. (2006). Sugar-induced tolerance to the herbicide atrazine in *Arabidopsis* seedlings involves activation of oxidative and xenobiotic stress responses. *Plant Cell Rep*. 25, 489-498. doi: 10.1007/s00299-005-0062-9

Tattersall, D. B., Bak, S., Jones, P. R., Olsen, C. E., Nielsen, J. K., Hansen, M. L., et al. (2001). Resistance to an herbivore through engineered cyanogenic glucoside synthesis. *Science* 293, 1826-1828. doi: 10.1126/science.1062249

Thimm, O., Blasing, O., Gibon, Y., Nagel, A., Meyer, S., Krüger, P., et al. (2004). MAPMAN: a user-driven tool to display genomics data sets onto diagrams of metabolic pathways and other biological processes. *Plant J*. 37, 914-939. doi: 10.1111/j.1365-313X.2004.02016.x

Tremblay, A., Hosseini, P., Li, S., Alkharouf, N. W., and Matthews, B. F. (2013). Analysis of Phakopsora pachyrhizi transcript abundance in critical pathways at four time-points during infection of a susceptible soybean cultivar using deep sequencing. *Bmc Genomics* 14:614. doi: 10.1186/1471-2164-14-614

Treutter, D. (2006). Significance of flavonoids in plant resistance: a review. *Environ. Chem. Lett*. 4, 147-157. doi: 10.1007/s10311-006-0068-8

Van Loon, L. C. (1997). Induced resistance in plants and the role of pathogenesis-related proteins. *Eur. J. Plant Pathol*. 103, 753-765. doi: 10.1023/A:1008638109140

Zhang, H., Yang, Y., Wang, C., Liu, M., Li, H., Fu, Y., et al. (2014). Large-scale transcriptome comparison reveals distinct gene activations in wheat responding to stripe rust and powdery mildew. *BMC Genomics* 15:898. doi: 10.1186/1471-2164-15-898

CHAPTER 4

A MICROARRAY ANALYSIS HIGHLIGHTS THE ROLE OF TETRAPYRROLE PATHWAYS IN GRAPEVINE RESPONSES TO "STOLBUR" PHYTOPLASMA, PHLOEM VIRUS INFECTIONS AND RECOVERED STATUS[2]

Federico Punelli[a], Mohamad Al Hassan[d], Veronica Fileccia[b,c], Paolo Uva[e], Graziella Pasquini[a], Federico Martinelli[b,c*]

[a] Consiglio per la Ricerca e la Sperimentazione in Agricoltura - Centro di Patologia Vegetale, Via C.G. Bertero 22, 00159, Rome, Italy
[b] Dipartimento di Scienze Agrarie e Forestali, Università di Palermo, Viale delle Scienze, Ed. 4, 90128, Palermo, Italy.
[c] I.E.ME.S.T. via Emerico Amari, 123, 90139, Palermo, Italy
[d] Universitat Politècnica de València, Instituto de Biología Molecular y Celular de Plantas (UPV-CSIC), CPI, edificio 8E, Camino de Vera s/n, 46022 Valencia, Spain
[e] CRS4, Loc. Piscina Manna, Ed. 1, 09010, Pula (CA), Italy.

*corresponding author: Tel: +393318039998; Email: federico.martinelli@unipa.it

After providing a picture of the global transcriptomic changes of grapevine responses to "stolbur" phytoplasma, the recovery status and the molecular responses to phytoplasma and virus co-presence were analyzed. NimbleGen® *Vitis vinifera* genome arrays were used. Lower transcript abundance of the genes involved in photosynthesis, trehalose, phospholipids was observed in response to the presence of "stolbur" phytoplasma. The expression of genes involved in tetrapyrrole increased. The recovered plants showed that the transcripts involved in ATP synthesis and amino acid metabolism, secondary metabolism and biotic stress-related pathways increased. Recovery was associated with tetrapyrrole pathway repression. Co-infection with viruses induced the genes involved in the hormone categories (cytokinin, gibberellin, salicylic acid and jasmonates).

[2] Published to Frontiers in Plant Science, 2015, 6:817. doi: 10.3389/fpls.2015.00817

1_INTRODUCTION

Vitis vinifera is severely affected by "grapevine yellows" (GY) disease, a syndrome associated with the different phytoplasmas related with diseases that are associated with several agricultural crops. They are wall-less prokaryotes belonging to *Mollicutes*, and they survive in phloem plant tissues and insects **[1]**. The main grapevine phytoplasma diseases are "flavescence dorée" (FD - groups 16SrV-C and 16SrV-D) and "stolbur" (STOL - group 16SrXII-A), the phytoplasma involved in "bois noir" disease (BN) **[2]**. FD is a quarantine pathogen that is restricted to a number of European grape-producing countries, whereas "bois noir" is distributed worldwide and causes serious epidemics in several susceptible grapevine varieties.

The symptoms of the two phytoplasma diseases are very similar and depend on grape varieties, environmental conditions and agronomic practices. Symptoms may appear on the whole plant or are limited to a sector or cane. They consist in downwardly rolled leaves with yellowing in the white-berried varieties, and a purple-reddish coloring in the red-berried varieties. Discolorations may affect some sectors or the whole blade, which becomes thicker and brittle. Internodes may shorten or new leaves are produced in summer months. Berries may ripen unevenly and be dry **[3]**.

Vineyard management against "bois noir" vector *Hyalesthes obsoletus* Signoret is not effective because this insect spends most of its life cycle on the wild plants that grow around vineyards. Different strategies have been followed; e.g. the specific elimination of the host wild plants, infected grapevine eradication and using healthy propagation material.

In some phytoplasma-infected plant hosts, recovery implies the complete remission of symptoms in previously symptomatic plants. This phenomenon is linked with the disappearance of phytoplasmas from the crowns on infected trees. Cytochemical analyses have shown that recovery is associated with biochemical changes in the phloem **[4]**. Recovery has been reported in several grapevine varieties affected by FD and/or BN in different viticultural regions, and depends on environmental conditions, grape varieties, rootstocks, and agronomic practices. It can be induced when grapevines are subjected to abiotic stress, such as uprooting plant followed by immediate transplanting, partial uprooting or plant pulling, and also by pruning or pollarding **[4]**. Although recovered plants show overproduced hydrogen peroxide in phloem tissue **[5]**, the physiological causes of the recovery process have still not been elucidated. "Stolbur" infection negatively regulates key primary pathways, such as photosynthesis, carbohydrate and lipid metabolism **[6,7]**. It also induces the genes involved in defense mechanisms, represses cell wall degradation and alters the balance of growth regulators **[8-10]**. The physiological response of grape plants to phytoplasma infection can be strongly modified by co-infection with one viruses

or more. Viral infections are very common in all grape varieties, and can either induce specific symptoms or correlate with a latent infection state. Some of the commonest viruses that affect grape plants are phloem-limited, which therefore make plant responses to phytoplasma infection more complex and significantly influence host/pathogen interactions.

This paper presents a picture of the global transcriptomic changes for grapevine leaf responses to "stolbur" infection before and after symptoms appear, and in the recovery status and with the co-presence of the phloem virus.

2_MATERIALS AND METHODS

2.1_Plant material and experimental design

The analysis was performed on the grapevine cultivar Montepulciano. Analyzed plants were located in a vineyard in Giulianello (province of Latina, Latium, central Italy; GPS coordinates: 41.683, 12.867), and showed typical yellows symptoms for 4 sequential years (**Fig. 1**).

For monitoring year 1, two vineyard rows (128 plants) were analyzed by nested-PCR to verify presence of phytoplasma, as described in the literature **[11,12]**. Absence of "flavescence dorée" (FD) was observed in all the samples. Serological tests (ELISA) were also performed to detect phloem viruses: *Arabis mosaic virus* - ArMV; *Grapevine Leafroll-associated Virus* type 1, 2 and 3 -GRLaV-1, GLRaV-2, GLRaV-3; *Grapevine virus A* - GVA; *Grapevine virus B* - GVB; *Grapevine Fleck virus* - GFkV; and *Grapevine Fanleaf virus* - GFLV.

During year 1, four symptomatic plants, solely infected by the "stolbur" phytoplasma, were uprooted and replanted to induce recovery **[4]**. They were classified as recovered because they had never shown any symptoms, and "stolbur" phytoplasma was never detected during a 4-years period. The plant material analyzed here was collected between the end of August and September and was divided into the following plant categories: healthy (He; no phytoplasma and viruses - three replicates); asymptomatic plants infected only by "stolbur" (Phy AS - two replicates); symptomatic plants infected only by "stolbur" (Phy SY - two replicates); symptomatic plants co-infected by "stolbur and GLRaV-3 and GVA viruses (Phy plus virus - two replicates); recovered plants (Re - two replicates). Each replicate comprised six medial leaves from two branches of three plants. The petioles and leaf midribs of each sample were frozen in liquid nitrogen and maintained at -20°C.

Fig. 1| Symptoms on "bois noir"-infected 'Montepulciano' plants. Leaves show reddish discoloration and downwardly rolled margins.

2.2_Microarray and functional analyses

RNA was extracted with the RNeasy Plant mini kit (Qiagen Inc., Valencia, CA). NimbleGen® *V. vinifera* genome array (Roche NimbleGen® Inc., Madison, WI, USA) was used for the microarray analysis. All the procedures for labeling and microarray hybridizations were performed following the NimbleGen® Inc. kit instructions. To retrieve additional functional annotations, probesets were associated with their homologous *Arabidopsis thaliana* genes. Robust Multiarray Average (RMA) data were analyzed with an additional normalization step (cubic spline) to remove the batch effect, such as the non-linear bias between duplicated arrays from different batches. Microarray data were submitted to NCBI's Gene Expression Omnibus (GEO), under the accession number GSE52540.

Functional classifications were based on those found in the MapMan software **[13]**. Differentially expressed genes were viewed using a mapping file constructed for the *Vitis* genome sequence **[14]**. Differentially regulated genes ($\log_2 > 1$ and $\log_2 < -1$; p-value < 0.05) in each pairwise comparison were shown in a different color based on a gradient legend of green (down-regulated) and red (up-regulated). The Pageman analysis was run with the list of the differentially regulated genes with a Wilcoxon test (ORA cut-off value = 1).

2.3_Array validation

Quantitative SYBRGreen real-time PCR (qRTPCR) was performed to validate the expression profiles obtained by the NimbleGen® Chip *V. vinifera* genome array. Five genes were selected from the panel of the differentially expressed genes in the pair-wise comparison: Phy/He SY and Re/He. The housekeeping gene used to normalize gene expression was V. vinifera actin (AF369524). The primers for each assayed gene were designed using the Primer3 software (http://primer3.sourceforge.net/). The Welch two-sample t-test was employed to compare the relative expression ratios of the infected and healthy samples (p-value < 0.05). RNAs were extracted from three replicates from each experimental conditions using the RNeasy Plant mini kit (Qiagen Inc., Valencia, CA). Amplifications were performed with 20 ng/µl of RNA extracted by the SensiMixTM one-step kit with ROX (Bioline - UK) according to the manufacturer's instructions. The primer sequences are provided in Table S1. The C_t value of each gene was normalized with actin to obtain the ΔC_t value.

3_RESULTS AND DISCUSSION

3.1_Grapevine responses to "stolbur" phytoplasma infection

3.1.1_Gene set enrichment analysis

Phytoplasmas-repressed photosynthesis were shown by the inhibition of the light reactions of Photosystem II, light harvesting complex II, Photosynthesis II and ATP synthase (**Fig. 2**). The mevalonate pathway, terpenoid and simple phenol gene set categories were significantly induced while lignin biosynthesis was repressed. The S-locus glycoprotein-like kinases were significantly induction.

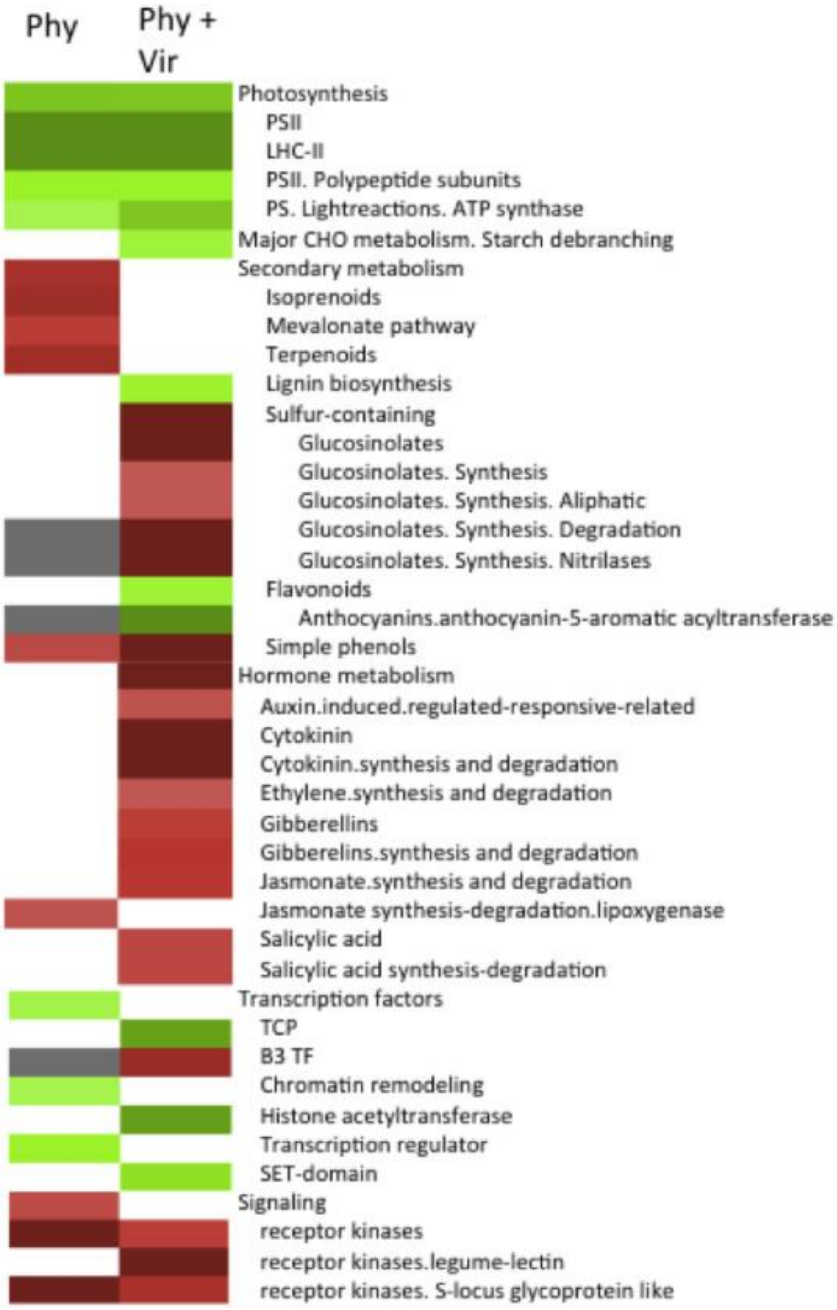

Fig. 2| The Pageman gene set enrichment analysis of leaf transcriptomic changes in response to phytoplasma infection (asymptomatic and symptomatic stages) and co-infection with viruses.

3.1.2_Primary metabolism

The MapMan software was used to identify which gene was regulated by "stolbur" on the significantly regulated pathways shown by the gene set enrichment analysis. Some key genes involved in aromatic amino acid synthesis and degradation were affected by presence, such as tryptophan synthase, prephenate dehydrogenases and 3-hydroxyisobutyrate dehydrogenase. The tetrapyrrole pathway was generally induced by the presence of "stolbur" (**Fig. 3**).

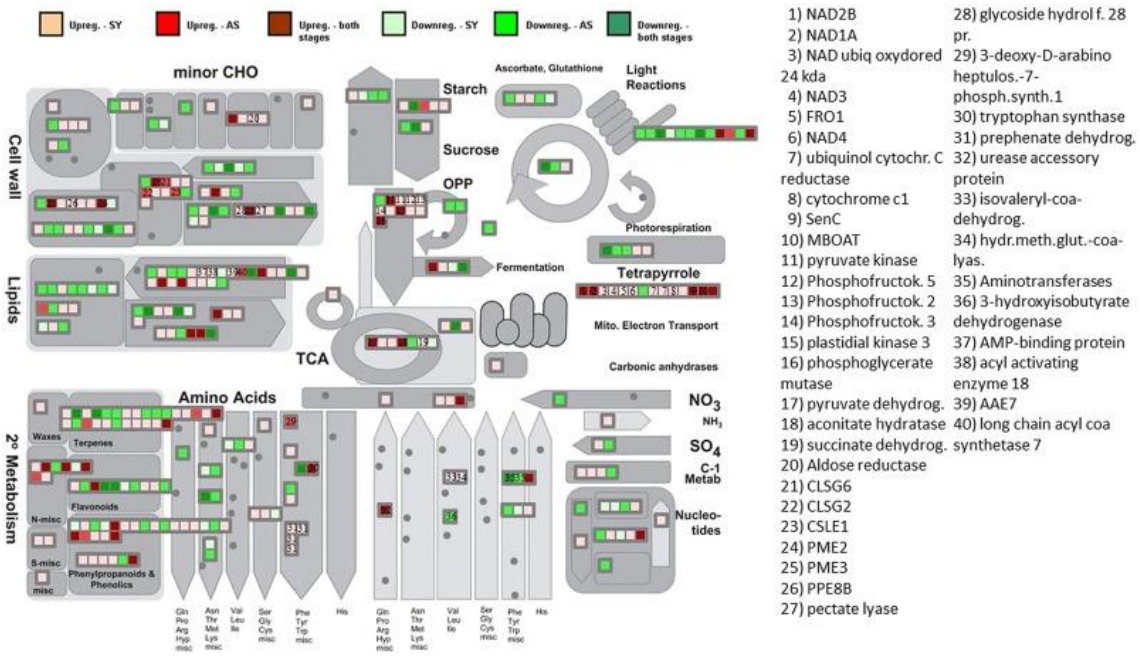

Fig. 3| Metabolism overview of the transcriptomic changes in response to "stolbur" phytoplasma presence in different disease stages. The phytoplasma-regulated genes were divided into five different categories: up-regulated or down-regulated in symptomatic leaves, up-regulated or down-regulated in asymptomatic leaves or regulated in both stages.

The transcript abundance of the genes involved in light reactions generally reduced (Fig. S1 A). These data agree with previous studies, which have emphasized the strong negative correlation between the repression of light reactions and pathogen infection **[5]**. In addition, the downregulation of ATP synthase protein I-related confirmed the data found in previous works **[8]**. The transcripts for starch synthase 2 and ADP-glucose pyrophosphorylase 1 decreased in the "stolbur"-infected grapevines. The genes involved in starch metabolism transcripts generally increased (beta-amylase 1, alpha-gluca phosphorylase 2) (Fig. S1 B). The transcript abundance of the sugar and starch metabolism genes generally coincided with the modified levels of sugars in the infected mature leaves **[15,16]**; these altered genes have been linked with responses to phloem-limited pathogens **[17,18]**. Studies on transgenic plants with altered carbohydrate accumulation have emphasized the importance of sugars for inducing defense responses against biotic stresses **[19]**. Phytoplasma has been shown to drastically alter the translocation of carbohydrates and amino acids **[20]**, which could affect photosynthesis, as regulated by a feedback mechanism: chlorosis occurs when carbohydrates levels increased. This has been hypothesized by Albertazzi et al. **[8]** via a mechanism of inhibition of several Calvin-cycle enzymes. The redistribution of carbohydrate reserves might be linked to the up-regulation of genes by converting sucrose and starch into fructose and glucose. A study **[9]** on cv. 'Chardonnay' has highlighted the role of sugar metabolism changes in relation to their

importance for phytoplasma nutrition. Albertazzi et al. **[8]** confirmed these findings by observing the up-regulation of vacuolar invertase, sucrose synthase and alpha amylase in infected samples. One piece of contrasting evidence provided herein, compared with previous studies, was invertase repression. This enzyme plays an important role in the regulation of stress responses, in addition to the possible extracellular signal for pathogen infection **[16]**. Invertase regulation depends on pathogen type **[21]**. However, it is hard to make comparisons because each member of this large family is finely modulated by different environmental signals and developmental stages. Raffinose metabolism was affected by phytoplasma infection, as shown by the induction of phosphofructokinase 2, 3 and 5, pyruvate kinase 3 and phosphoglycerate mutase (only in the symptomatic stage) (Fig. S1 C). The glycolitic and TCA pathways were slightly affected by the disease, as shown by the up-regulation of key genes, such as pyruvate kinase, phosphofructokinases, aconitate hydratase and succinate dehydrogenase. Two genes implicated in glycolysis were repressed in the infected Chardonnay plants: nonphosphorylating glyceraldehyde-3-phosphate dehydrogenase and fructose-bisphosphate aldolase **[9]**.

3.1.3_Secondary metabolism

The secondary metabolism (Fig. S2) was severely affected by "stolbur" in both asymptomatic and symptomatic stages. Some important terpene synthases and the genes involved in phenylpropanoids were enhanced. The genes involved in the shikimate pathway, such as laccase 14, laccase17, L-ascorbate oxidase, were up-regulated. Some key genes were repressed, such as cycloartenol synthase 1, beta-amyrin synthase 1, dihydroflavonol-4-reductase, and cinnamoyl-CoA reductase.

3.1.4_Transcription factors, protein modifications, signaling, redox and hormone-related pathways

Fig. 4 highlights how "stolbur" affected hormone biosynthesis, transcription, protein modifications, signaling and redox pathways. A complex and interconnected network between sugar, hormones, and environmental factors has been shown in plants **[22]**.

The majority of auxin-related genes were induced in the asymptomatic stage. ABA-related and brassinosteroid genes were induced, e.g. benzodiazepine receptor, HVA22 and DWF1. Most ethylene-related genes were up-regulated in the asymptomatic stage. ACS8 was also induced. Ethylene signaling appeared to be a key metabolic pathway in "stolbur" responses. Its role in hormone crosstalk is 2-fold in biotic stress responses is. EIN2 synergistically acts with salicylic acid responses by activating ROS. ERF1 is linked with the

up-regulation of jasmonic acid signaling **[23]**. ERF1 up-regulation suggested that jasmonic acid signaling is stimulated by phytoplasma infection. This is corroborated by the induction of some key JA-related genes in jasmonate (JA) synthesis such as lox3, allene oxide synthase and allene oxide cyclase 4. Taken together, these findings are intriguing since phytoplasma should not be the target of a jasmonic acid response if we consider its biotrophic nature. Although S-adenosyl methionine-dependent methyl transferase, involved in salicylic acid biosynthesis, was more abundant in the asymptomatic stage, the up-regulation of the jasmonic acid-related genes may negatively counterbalance this effect.

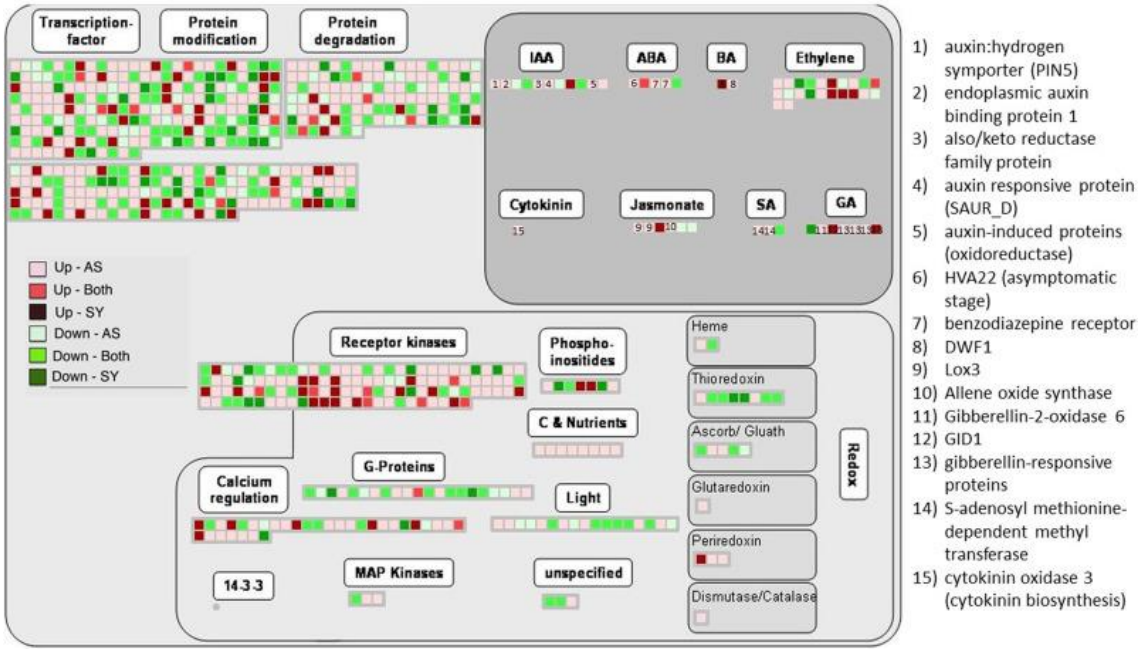

Fig. 4| "Stolbur" induced transcriptional reprogramming on transcription, protein-related, signaling, redox and hormone-related pathways.

3.1.5_Biotic stress-related responses and signaling

The majority of genes related to stress responses were boosted in the asymptomatic stage (Fig. S3). Key heat shock proteins were induced in the asymptomatic stage; e.g. HSP81-4, DNAJ, HSA32, HSP70-1 and TMS1. Some were repressed in both disease stages. The expressions of the genes involved in oxygen binding, thioredoxin, ascorbate/galactose, glutaredoxin, peroxiredoxin and dismutase/catalase were affected by presence of phytoplasma. Marker transcript abundance was observed for WRKY11 and WRKY23 (in the asymptomatic

stage), WRKY40 and WRKY7 (in the symptomatic stage), and WRKY48 (in both stages). The most affected category of receptor-like kinases was that which corresponded to S-locus glycoprotein like proteins: ATP binding/kinase, S-locus lectin protein kinases and PR5K.

3.2_Recovery from "stolbur" infection

Recovered plants were analyzed when they presented no symptom, which was why the induction of defense responses was much lower.

Compared to the control healthy status, the Pageman analysis showed that recovery status was associated with the induction of several secondary metabolism categories such as terpenoids, phenylpropanoids, lipid biosynthesis, sulfur-containing compounds (glucosinolates), flavonoids and simple phenols (**Fig. 5**). Polyamine biosynthesis and metabolism (particularly arginine decarboxylase) were significantly induced compared to the control. Some categories of transcription factors were inhibited only in the recovered grapevines. Regarding signaling, leucine-rich repeat proteins (III and XI) were repressed, while S-glycoprotein-like proteins and kinases were up-regulated.

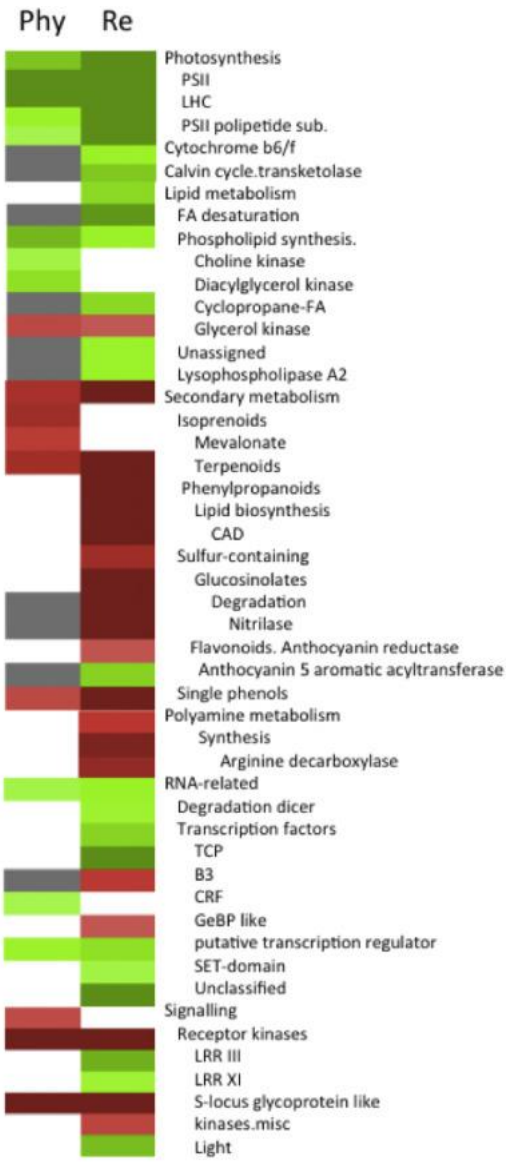

Fig. 5| The transcriptomic gene set enrichment analysis of the differentially regulated phytoplasma-infected (asymptomatic and symptomatic) and recovered plants compared to healthy leaves.

In metabolism terms, the recovered plants showed fewer genes to be involved in photosynthesis and amino acid biosynthesis and metabolism. Particularly in the primary metabolism (**Fig. 6**), very few important up-regulated genes were involved in starch and sucrose metabolism (alpha-amylase, hexokinase-like 3), in glycolysis (phosphofructokinase, phosphoglycerate/biphosphoglycerate mutase) and in tetrapyrrole (NDB2, NAD4).

Given the importance of cell wall modifications in plant-microbe interactions, the down-regulation of cellulose synthase, xyloglucan transferase, expansin B17, pectate lyases and polygalacturonases was noteworthy. Callose was synthesized in different plant organs and in response to environmental stress. Cellulose and callose production may require sucrose

synthase activity. Evidence that Susy2 was repressed in the recovered meant the presence of the pathogen in the phloem should be less aboundant.

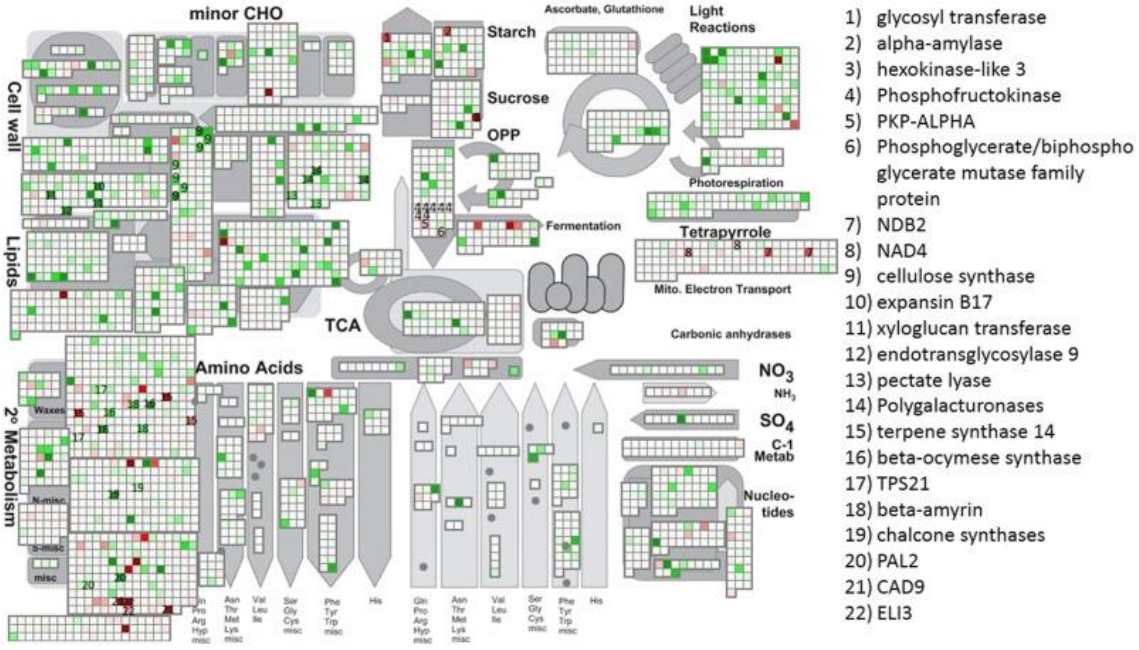

Fig. 6| Primary metabolism overview of recovered status. Up-regulated genes are in red, while down-regulated genes are in green on a log-fold ratio scale. (For interpretation of the references to color in this figure legend, the reader is referred to the web version of this article).

Some key important changes were observed in terpenoids, flavonoids and phenylpropanoids (Table S2). The up-regulation of the secondary metabolism genes could allow plants to be less susceptible to further infection. The roles suggested for phenylpropanoid compounds in plant defenses have been traditionally based on biological activities *in vitro*, and on correlations between accumulation rates and reduced susceptibility *in vivo*. Yet as plant defense responses are multicomponent, it is not easy to define which components are both necessary and sufficient to confer protection.

Regarding the hormone pathways (Table S3), two ethylene genes were highly induced (2OGFe(II) oxydase, AP2 domain TF) as well as a GRAM-domain contacting protein (the abscissic acid pathway), IPT5 (cytokinins). Many down-regulated genes belonged to ABA, auxins and jasmonic acid and ethylene responses (Table S3). Clearly the entire picture of hormone crosstalk differed completely from the infected status where all these pathways

(except ABA) were substantially induced. As expected, the genes that encode the transcription factors induced in infected plants, were strongly repressed (Table S4).

Regarding the biotic stress related pathways, it is noteworthy that very few key genes, such as HSC70, terpene synthase 14 (TPS14), a protein kinase family protein (Fig. S4) were up-regulated by recovered. The recovered plants showed repression of oxidases, glucosidases, glutathione-S-transferase compared to the infected plants. Regarding signaling reception, receptor kinases-S-locus glycoproteins seemed to be more involved in signal transduction. This evidence was confirmed by the down-regulation of these genes in the recovered plants. Transcription factors, such as WRKYs, AP2-EREBP, MYB, bHLH, were clearly induced in the asymptomatic infected plants, but were mainly down-regulated at the recovered status when healthy behavior returned. In conclusion, we speculate that recovery was gained mainly through the induction of those genes involved in the secondary metabolism.

3.3_Transcriptomic changes in response to co-infection with GLRaV-3 and GVA viruses

The transcriptome analysis of the plants co-infected by viruses (GLRaV-3 and GVA) and phytoplasma enabled us to identify common and different transcriptional responses. Comparing with solely the “stolbur” phytoplasma infection, the gene set enrichment analysis showed that presence of viral infections reduced the transcript abundance of the genes involved in starch debranching. Glucosinolates were induced in secondary metabolism terms, while flavonoids were generally repressed. Viruses induced extensive transcriptional reprogramming in hormonal crosstalk, as highlighted by the induction of the pathways involved in auxin, cytokinin, ethylene, gibberellins and salicylic acid. Moreover, a different signaling mechanisms was shown through the activation of lectin receptor kinases.

The phytoplasma and viruses co-infection induced more of the genes involved in tetrapyrrole than solely phytoplasma infections. Tetrapyrroles are important molecules in plant processes like photosynthesis and respiration **[24]**. As it remains whether the strenght of these genes could be a potential danger for grapevine plants, further research is needed.

Viruses and phytoplasma co-infections caused a significant induction of protein amino acid phosphorylation and oxidative stresses, alteretions in the specific genes involved in cell wall modifications, up-regulated pathogenesis-related pathways and reduced lipid metabolism and transport (**Fig. 7**). Presence of viruses (GLRaV-3 and GVA) up-regulated other genes involved in sucrose degradation, amino acid synthesis, glucosinolate synthesis and degradation, and tetrapyrrole. Some key genes were down-regulated, such as those involved in starch metabolism (starch synthase 2, alpha-amylase, starch synthase 3) and light reactions (PSII

center core and subunits, NADPH dehydrogenase). The data suggest that sugars play a role in not only the repression of photosynthetic genes **[25]**, but also in the induction of defense responses. Sheen **[23]** suggested the common mechanism of sugar sensing in the repression of photosynthetic genes and the activation of stress-related genes. The results obtained for the co-infected plants agreed with the data obtained for the plants solely by phytoplasma. However it is noteworthy that the key players in the glycolytic pathway and raffinose were up-regulated only when viruses were present.

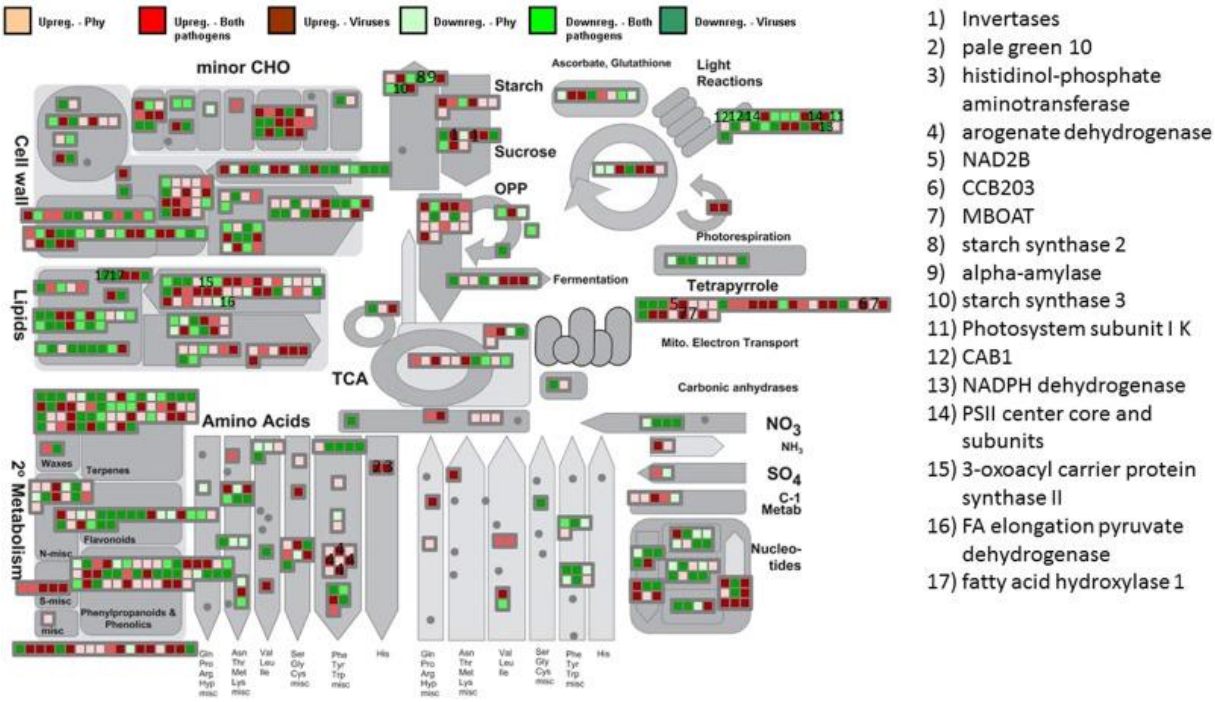

Fig. 7| Metabolism overview of the transcriptomic responses to "stolbur" phytoplasma (Phy), viruses and "stolbur" + viruses (both pathogens). The differentially regulated genes were divided into six different categories: up-regulated or down-regulated in response to only "stolbur" phytoplasma infections, up-regulated or down-regulated in response to only virus infections, up-regulated or down-regulated in the co-infections of both phytoplasma and viruses.

Regarding the hormone-related pathways, the co-presence of phytoplasma and viruses induced a larger number of genes related to cytokinin, gibberellin and salicylic acid (**Fig. 8**). Several key ethylene responsive genes were highly induced, such as flavonol synthase and ethylene response 2. Some other key genes were up-regulated: auxin-responsive protein (SAUR_C), PIN7 (auxins), abscissic acid responsive proteins, LOX3 (jasmonic acid) and 2OG Fe (II)-oxygenase.

Some key genes encoding transcription factors were induced only by viruses, e.g. a few MYB factors and WRKYs (WRKY75, WRKY7, WRKY49 - Table S5; Fig. S5). WRKY70 was down-regulated by the virus and phytoplasma co-presence. The effect of the down-regulation of WRKY70 in response to phytoplasma and viruses needs further investigation. It was most interest that some MYB genes were repressed. MYB proteins play a transcriptional regulation role in different pathways of the primary and secondary metabolism, or in cell development and the cell cycle, environmental stress responses, hormone biosynthesis and signaling **[26]**.

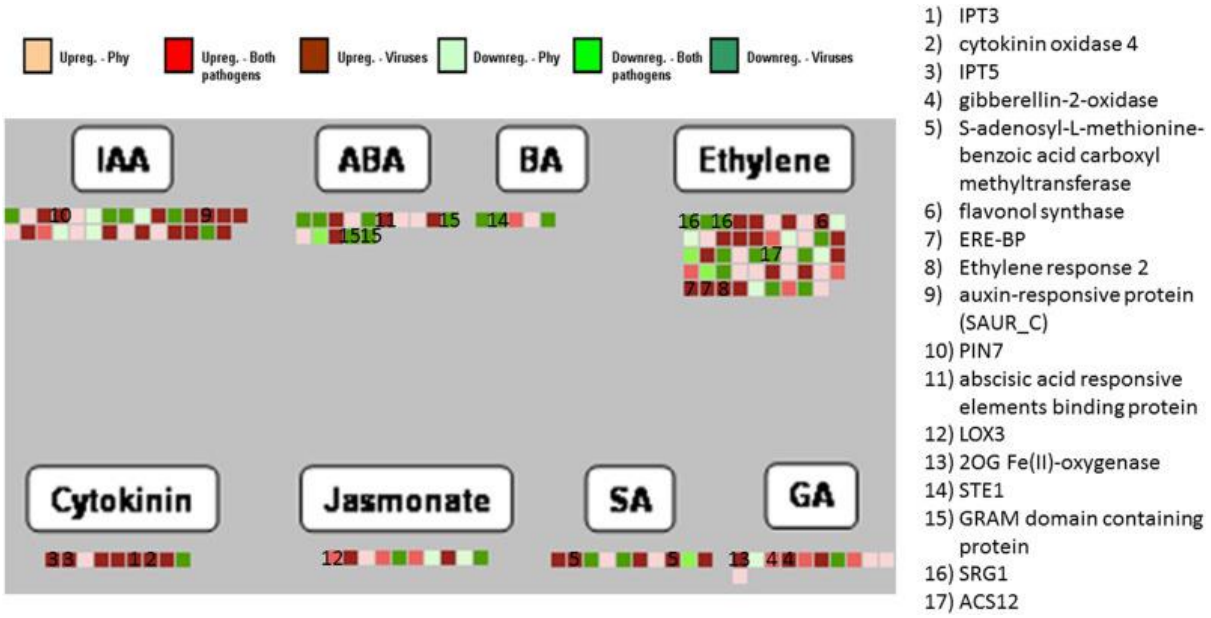

Fig. 8| Hormone-related genes that were differentially regulated by solely phytoplasma infections, by phytoplasma and GLRaV-3 and GVA viruses and by phytoplasma and virus coinfection.

3.4_qRT-validation of the microarray data

Five genes were chosen for the qRT-PCR analysis to validate the microarray data. Three genes were up-regulated in the infected and recovered samples compared to the uninfected ones: Photosystem I P-Subunit (PSI-P), Glutamyl-tRNA reductase 1 chloroplastic like (LOC100259052), and probable galactinol-sucrose galactosyltransferase 2-like (LOC100245094) (Fig. S5). Two genes were repressed in the infected and recovered samples compared to the uninfected ones: a plasma membrane-associated protein-like (XM003631860) and a polygalacturonase (AY043233). The expression trend of all five genes was consistent with the transcript abundance observed in the microarray data.

4_CONCLUSIONS

This study provides an overall picture of the main metabolism changes in grapevine in response to phytoplasma infection and in the co-presence with two grapevine viruses. The transcriptome of the recovered plants was characterized. Interestingly, the recovered plants shoewed that the transcripts involved in ATP synthesis and amino acid metabolism increased. The gene set enrichment analysis results highlight that the secondary metabolism (phenylpropanoids, isoprenoids, glucosinolates, flavonoids) was clearly induced. Higher levels of the secondary metabolism genes are very important for grapevine resistance to "stolbur" phytoplasmas. In agreement with the data observed for other diseases caused by phloem-restricted pathogens, a determinant role in symptom appearance and, consequently, in plant decline is played by imbalances in molecular transport through the phloem system, which then cause sink-source disorders. Although the complexity of the gene regulatory networks behind this phenomenon requires further studied, this work identified important players in this network, such as the genes involved in tetrapyrrole pathways, which can contribute to develop early disease diagnostics and new control strategies **[27]**. These findings will help to uncover disease mechanisms, and to facilitate the development of early diagnostic tools and short-term control strategies **[28]**.

Future studies conducted under controlled conditions are necessary to complement these field approaches, to reduce environmental variability and to focus on specific factors.

SUPPLEMENTARY DATA

Supplementary data related to this article can be found at http://dx.doi.org/10.1016/j.pmpp.2016.01.001.

5_REFERENCES

[1] Prince J.P., Davis R.E., Wolf T.K., Lee I.M., Mogen B.D., Dally E.L., et al. (1993). Molecular detection of diverse mycoplasmalike organisms (MLOs) associated with grapevine yellows and their classification with aster yellows, X-disease, and elm yellows MLOs. *Phytopathology* 83: 1130–1137.

[2] Martini M., Murari E., Mori N., Bertaccini A. (1999). Identification and epidemic distribution of two Flavescence doré e-related phytoplasmas in Veneto (Italy). *Plant Dis.* 83: 925–930.

[3] Battle A., Angels Martinez M., Lavina A. (2000). Occurrence, distribution and epidemiology of Grapevine Yellows in Spain. *Eur. J. Plant Pathol.* 106: 811–816.

[4] Romanazzi G., Musetti R., Marzachì C., Casati P. (2009). Induction of resistance in the control of phytoplasma diseases. *Petria* 19: 113-129.

[5] Musetti R., Marabottini R., Badiani M., Martini M., Sanità Di Toppi L., Borselli S., Borgo M., Osler R. (2007). On the role of H2O2 in the recovery of grapevine (*Vitis vinifera* cv. Prosecco) from Flavescence dorée disease. *Funct. Plant Biol.* 34: 750-758.

[6] Bertamini M., Nedunchezhian N., Tomasi F., Grando M.S. (2002b). Phytoplasma [Stolbur-subgroup (Bois Noir-BN)] infection inhibits photosynthetic pigments, ribulose-1,5-bisphosphate carboxylase and photosynthetic activities in field grown grapevine (*Vitis vinifera* L. cv. Chardonnay) leaves. *Physiol. Mol. Plant Pathol.* 61: 357-366.

[7] Rusjan H., Halbwirth K., Skvarc S.A., Mikulic-Petkovsek M. (2013). Biochemical alterations in primary and secondary metabolism of grapevine variety ‘Chardonnay’ (*Vitis vinifera* L.) infected by ‘bois noir’. 3th European Bois Noir Workshop, Barcelona, 20-21 March.

[8] Albertazzi G., Milc J., Caffagni A., Francia E., Roncaglia E., Ferrari F., Tagliafico E., Stefani E., Pecchioni N. (2009). Gene expression in grapevine cultivars in response to Bois Noir phytoplasma infection. *Plant Sci.* 176: 792-804.

[9] Hren M., Nikolić P., Rotter A., Blejec A., Terrier N., Ravnikar M., Dermastia M., Gruden K. (2009). 'Bois noir' phytoplasma induces significant reprogramming of the leaf transcriptome in the field grown grapevine. *BMC Genomics* 10: 460-476.

[10] Endeshaw S.T., Murolo S., Romanizzi G., Neri D. (2012). Effects of Bois noir on carbon assimilation, transpiration, stomatal conductance of leaves and yield of grapevine (*Vitis vinifera*) cv. Chardonnay. *Physiol. Plant.* 145: 286-295.

[11] Lee I.M., Gundersen D.E., Hammond R., Davis R.E. (1994). Use of mycoplasmalike organism (MLO) group-specific oligonucleotide primers for nested-PCR assays to detect mixed-MLO infections in a single host plant. *Phytopathology* 84: 559-566.

[12] Schneider B., Marcone C., Kampmann M., Ragozzino A., Lederer W., Cousin M.T., Seemüller E. (1997). Characterization and classification of phytoplasma from wild and cultivated plants by RFLP and sequence analysis of ribosomal DNA. *Eur. J. Plant Pathol.* 103: 675-686.

[13] Thimm O., Bläsing O., Gibon Y., Nagel A., Meyer S., Krüger P., Selbig J., Müller L.A., Rhee S.Y., Stitt M. (2004). MAPMAN: a user-driven tool to display genomics data sets onto diagrams of metabolic pathways and other biological processes. *Plant J.* 37: 914-939.

[14] Jaillon O., Aury J.M., Noel B., Policriti A., Clepet C., Casagrande A., Choisne N., Aubourg S., Vitulo N., Jubin C., et al. (2007). The grapevine genome sequence suggests ancestral hexaploidization in major angiosperm phyla. *Nature* 449: 463-467.

[15] Herbers K., Takahata Y., Melzer M., Mock H.P., Hajirezaei M., Sonnewald U. (2000). Regulation of carbohydrate partitioning during the interaction of potato virus Y with tobacco. *Mol. Plant Pathol.* 1: 51-59.

[16] Machenaud J., Henri R., Dieuaide-Noubhani M., Pracros P., Renaudin J., Eveillard S. (2007). Gene expression and enzymatic activity of invertases and sucrose synthase in *Spiroplasma citri* or *Stolbur phytoplasma* infected plants. *B. Insectol.* 60: 219-220.

[17] Martinelli F., Reagan R.L., Uratsu S., Phu M.L., Albrecht U., Zhao W., Davis C., Bowman K.D., Dandekar A.M. (2013) Gene regulatory networks elucidating Huanglongbing disease mechanisms. *Plos One* 8: e74256.

[18] Martinelli F., Ibanez A.M., Reagan L.R., Davino S., Dandekar A.M. (2015). Stress responses in citrus peel: comparative analysis of host responses to Huanglongbing disease and puffing disorder. *Sci. Hortic.* 192: 409e420.

[19] Stitt M., Sonnewald U. (1995). Regulation of metabolism in transgenic plants. *Annu. Rev. Plant. Physiol. Plant. Mol. Biol.* 46: 341-368.

[20] Lepka P., Stitt M., Moll E., Seemüller E. (1999). Effect of phytoplasmal infection on concentration and translocation of carbohydrates and amino acids in periwinkle and tobacco. *Physiol. Mol. Plant. Physiol.* 55: 59-68.

[21] Eveland A.L., Jackson D.P. (2012). Sugars, signalling, and plant development. *J. Exp. Bot.* 63: 3367-3377.

[22] Pieterse C.M.J., Leon-Reyes A., Van der Ent S., Van Wees S.C.M. (2009). Networking by small-olecule hormones in plant immunity. *Nat. Chem. Biol.* 5: 308-316.

[23] Hart C.M., Fischer B., Neuhaus J.M., Meins F.J. (1992). Regulated inactivation of homologous gene expression in transgenic *Nicotiana sylvestris* plants containing a defense-related tobacco chitinase gene. *Mol. Gen. Genet.* 235: 179–188.

[24] Tanaka R., Tanaka A. (2007). Tetrapyrrole biosynthesis in higher plants. *Annu. Rev. Plant Biol.* 58: 321-346.

[25] Sheen J. (1990). Metabolic repression of transcription in higher plants. *Plant Cell* 2: 1027-1038.

[26] Dubos C., Stracke R., Grotewold E., Weisshaar B., Martin C., Lepiniec L. (2010). MYB transcription factors in *Arabidopsis*. *Trends Plant Sci.* 15: 573-581.

[27] Martinelli F., Scalenghe R., Giovino A., Pasquale M., Aksenov A.A., Pasamontes A., Peirano D.J., Davis C.E., Dandekar A.M. (2016). Proposal of a Citrus translational genomic approach for early and infield detection of Flavescence dorée in Vitis. *Plant Biosyst.* http://dx.doi.org/10.1080/11263504.2014.908976 (in press).

[28] Martinelli F., Scalenghe R., Davino S.W., Panno S., Suderi G., Ruisi P., Villa P., Stroppiana D., Boschetti M., Goulart L.R., Davis C.E., Dandekar A.M. (2015). Advanced methods of plant disease detection. A Review. *Agron. Sustain. Dev.* 35: 1-25.

CHAPTER 5

MOLECULAR RESPONSES TO SMALL REGULATING MOLECULES AGAINST HUANGLONGBING DISEASE[3]

Federico Martinelli[1,2], David Dolan[3], Veronica Fileccia[1,2], Russell L. Reagan[3], My Phu[3], Timothy M. Spann[4], Thomas G. McCollum[5], Abhaya M. Dandekar[3*]

[1]Dipartimento di Scienze Agrarie e Forestali, Palermo, Italy, [2]Euro-Mediterranean Institute of Science and Technology (IEMEST), Palermo, Italy, [3]Department of Plant Sciences, University of California, Davis, California, United States of America, [4]California Avocado Commission, Irvine, California, United States of America, [5]United States Department of Agriculture-The Agricultural Research Service, U.S. Horticultural Research Laboratory, Fort Pierce, Florida, United States of America

*Corresponding author: Email: amdandekar@ucdavis.edu

Huanglongbing (HLB; citrus greening) is the most devastating disease of citrus worldwide. No cure is yet available for this disease and infected trees generally decline after several months. Disease management depends on early detection of symptoms and chemical control of insect vectors. In this work, different combinations of organic compounds were tested for the ability to modulate citrus molecular responses to HLB disease beneficially. Three small-molecule regulating compounds were tested: 1) L-arginine, 2) 6-benzyl-adenine combined with gibberellins, and 3) sucrose combined with atrazine. Each treatment contained K-phite mineral solution and was tested at two different concentrations. Two trials were conducted: one in the greenhouse and the other in the orchard. In the greenhouse study, responses of 42 key genes involved in sugar and starch metabolism, hormone-related pathways, biotic stress responses, and secondary metabolism in treated and untreated mature leaves were analyzed. TGA5 was significantly induced by arginine. Benzyladenine and gibberellins enhanced two important genes involved in biotic stress responses: WRKY54 and WRKY59. Sucrose combined with atrazine mainly upregulated key genes involved in carbohydrate metabolism such as sucrose-phosphate synthase, sucrose synthase, starch synthase, and α-amylase. Atrazine also affected expression of some key genes involved in systemic acquired resistance such as EDS1, TGA6, WRKY33, and MYC2. Several treatments upregulated HSP82, which might help protect protein folding and integrity. A subset of key genes was chosen as biomarkers for molecular responses to treatments under field conditions. GPT2 was downregulated by all small-molecule treatments. Arginine-induced genes involved in systemic acquired resistance included PR1, WRKY70, and EDS1. These molecular data encourage long-term application of treatments that combine these regulating molecules in field trials.

[3] Published to PLoS ONE, 2016, 11(7):e0159610. doi: 10.1371/journal.pone.0159610

1_INTRODUCTION

Plant pests and diseases threaten agricultural systems. Huanglongbing (HLB) disease endangers the citrus industry and citrus cultivation worldwide **[1]**. Neither genetic resistance nor short- or long-term therapeutic strategies to mitigate HLB has been found. Huanglongbing disease is associated with three *Candidatus liberibacter* (C. Las) species: *asiaticus, americanus,* and *africanus*. C. Las is a member of the alpha subdivision of the proteobacteria based on ribosomal region sequence data **[2]**. Symptoms have been extensively described and all citrus species are susceptible to HLB to varying degrees **[3,4]**.

Microarray analysis identified key genes and pathways affected by HLB at the transcriptomic level in mature, symptomatic leaves **[5,6]**. RNA-seq was applied to describe molecular responses in fruit with different degrees of HLB symptoms **[7]**. This allowed a comprehensive analysis of gene regulatory networks on source and sink tissues at different developmental stages **[8,9]**. Effects of C. Las infection on key genes involved in sugar and starch metabolism, disrupting source-sink relationships, was a key cause of the metabolic dysfunction. Fruits of infected plants remained immature and photosynthesizing while mature leaves became yellow and accumulated starch **[9]**. Protein expression has been linked to the nutritional condition of grapefruit plants before and after symptom appearance. C. Las-upregulated proteins were involved in redox reactions, cell wall modification, and biotic stress responses **[10]**. Isobaric tags for relative and absolute quantitation (iTRAQ) identified which pathways are affected post-transcriptionally by pathogen infections **[11]**. A predictive proteome analysis of C. Las has been conducted **[12]**. Because no toxins or other pathogenic substances were clearly identified in the genome **[13]**, the pathogenetic mechanisms of HLB disease are still unclear, nor is it clear whether the HLB-associated changes in sugar and starch metabolism are a cause or an effect of the disease **[9]**.

Current management procedures consist mainly of visual scouting for symptoms, PCR-based detection of the pathogen, and insecticides for vector control **[14]**. Although application of insecticides can reduce disease spread, the disease can spread with only a few infected psyllids in the orchard. Early disease detection and psyllid control are critical practices in areas where neither disease nor vector has yet been discovered **[1]**. At present, no chemical compounds have been tested to beneficially modulate Citrus host responses and eventually extend the life and production of HLB-infected trees, reducing high economic costs due to lost production. Research has focused only on testing compounds targeting the pathogen. A combination of two antibiotics (penicillin and streptomycin) applied by either root soaking or foliar spray decreased C. Las titer in infected plants **[15]**. Antimicrobial compounds have been

delivered through graft-based chemotherapy **[16]**. Nanoemulsion formulations were evaluated for their ability to increase permeability of antimicrobial molecules with success dependent on the citrus cultivar and degree of HLB symptoms **[17]**. Small-molecule inhibitors designed by molecular docking were significantly effective in inhibiting SecA ATPase in vitro **[18]**. Extensive use of antibiotics in open fields is not desirable due to environmental and human health concerns. Host-based treatments that modulate key genes involved in metabolic HLB syndrome are highly desirable. Data on citrus molecular responses to HLB can now be exploited to design small-molecule combinations to ameliorate the devastating symptoms. The aim of this study was to determine if small molecules are effective in modulating expression of key HLB-regulated or innate response genes after three to six days of treatment.

2_MATERIALS AND METHODS

2.1_Plant material

Greenhouse trial. In 2011, Valencia orange scions on Kuharske Carrizo rootstocks were grown in one-gallon plastic nursery containers and kept in the greenhouse under natural light at 17 to 25°C. Graft inoculations were performed using a standard inverted "T" budding technique with C. Las-infected budwood tested as described **[19]**. Starting three months after budding, each plant was tested monthly using quantitative RT-PCR for C. Las species as described **[19]**. Each control or treatment was represented by nine to 10 trees. The control consisted of trees sprayed with distilled water. The first treatment consisted of a Silwet (0.12%), DKP3XTRA (32.5 mL/20 L) and LK-phite spray (2 mL/20 L). The other six spray treatments were composed of three different small-molecule combinations at two different concentrations each: 1) L-arginine at 1 mM or 0.5 mM, 2) 120 μM 6-benzyl adenine in combination with 15 or 30 μM gibberellin, and 3) 80 mM sucrose combined with the herbicide atrazine (2 μM or 1 μM). All seven treatments contained the surfactant Silwet and LK-phite at the same concentration used for the first treatment. Phenotypes were evaluated to determine any phytotoxic effects of these sprays. All treatments were sprayed on the citrus foliage; the volume sprayed per tree was enough to wet both upper and lower leaf surfaces just to the point of runoff. Gene expression analyses were conducted on RNA extracted three days following treatment. Three biological replicates of nine mature leaves harvested from three trees (three leaves per tree) were analyzed for each treatment. Collected leaves were immediately frozen in liquid nitrogen and kept at -80°C until

RNA was extracted. Forty-two host genes were analyzed in mature symptomatic leaves of treated and untreated trees.

Field trial. The same treatments were applied during the field experiments, which were conducted in a commercial citrus orchard in Indian Ricer County, FL, composed of Valencia orange scions on Swingle rootstocks. The study was conducted on private land and the owner of the land gave permission to conduct the study on the site of our experiments. We also confirm that the field studies did not involve endangered or protected species. Twenty-four trees of medium height, 12 trees per row, were selected. These trees were mildly HLB-symptomatic and confirmed infected by C. Las through the same qPCR assay used for the greenhouse trial. The experimental design was a completely randomized blocks. There were eight treatments with three single-tree replicates. Samples were collected at three and six days following treatment. Each replicate was a pool of 10 mature symptomatic leaves per tree.

RNA extraction and qRT-PCR analysis. Total RNA was extracted from mature, fully-expanded leaves of plants grown in the greenhouse or orchard using the Rneasy Plant RNA Isolation kit (Qiagen Inc., Germany). The RNA concentration and purity were assessed by Nanodrop (Thermo Fischer Scientific Inc., MA, USA). RNA was stored at −80°C until analyzed. For each target gene, PCR primers were designed using Primer Express software (Applied Biosystems, Foster City, CA; S1 Table). DNase treatment and cDNA synthesis were completed following a combined protocol based on the Quantitect Reverse Transcription Kit (Qiagen Inc., Germany). A standard curve determined the linearity of amplicon quantity vs. initial cDNA quantity for each gene. Five µL cDNA at five ng/µL was diluted to a 12-µL final volume using Sybr Green Master Mix (Bio Rad Laboratories, Hercules, CA, USA). Amplifications were performed using standard conditions: 2 min at 50°C, 10 min at 95°C, 40 cycles of 15 s at 95°C, and 60 s at 60°C. Fluorescent signals were collected during the annealing temperature and ΔCT was calculated. Elongation factor 1 alpha (EF-1a, accession AY498567) was used as reference gene. $\Delta\Delta C_T$ was determined by subtracting the average EF-1a C_T from the average C_T of the studied gene **[9]**.

2.2_Phenotypic measurements

Four phenotypic parameters for all treated and untreated trees were measured in the field: trunk diameter (mm), trunk height (m), width drill (m), and width row (m). These measurements were taken on 5/21/2014 and 6/28/2014 during the vegetative season.

2.3_Statistical analysis

All statistical analyses of gene expression and phenotypic data were performed using SAS II (2008) SAS/STAT software (SAS Institute). Gene expression and phenotypic data were analyzed using ANOVA and a post-hoc test to identify significant differences among treatments. Principal component analysis (PCA) was used to reduce the dimensionality of the gene expression data. Data analysis was performed to alleviate possible bias caused by the collected material for each class or by other confounding factors. Principal component analysis was applied to the ratio matrix of gene expression data to examine the contribution of each target parameter to the separation of the sample classes. A biplot was constructed based on the first two principal components.

3_RESULTS

Gene expression analyses were conducted in the greenhouse and orchard. First, in greenhouse-grown plants, we quantified transcript abundance of 42 genes selected for their link with for being strongly up- or down-regulated by HLB syndrome **[7,9]** or for having a well-known role in plant responses to pathogen attacks **[20]**. Second, we selected a subset of five particularly representative genes to be analyzed in field-grown trees, to which we added an additional two genes previously linked with HLB syndrome in published data **[5,9]**. The presence of leaf drop or discoloration and other morphological features of trees were measured to check whether these treatments had deleterious effects on important vegetative parameters.

At advanced stages, HLB blocks sugar transport out of leaves, leading to starch accumulation in leaves, reduced photosynthesis and disrupted source-sink relationships **[9]**. Anatomical analysis showed that HLB caused phloem disruption, increased sucrose, and plugged sieve pores **[6]**. The disease also negatively modifies JA-SA crosstalk, leading to an ineffective innate immune response **[7,9]**. The three small-molecule treatments were selected for the potential to beneficially modulate these negative HLB-regulated responses. The combination of atrazine and sucrose upregulates genes associated with reactive-oxygen-species (ROS) defense mechanisms and sucrose metabolism **[21,22]**. We postulated that this treatment might upregulate genes that reduce sucrose and starch accumulation. Because L-arginine is the precursor of nitric oxide, which is involved in the SAR response and upregulates genes involved in secondary metabolism **[23]**, we designed a second treatment consisting of two concentrations

of L-arginine to induce upregulation of genes for secondary metabolic pathways such as phenols and terpenoids. Gibberellins boost systemic acquired resistance **[20]**, favoring the resistance response against biotrophs such as C. Las **[20]**. Benzyladenine downregulates hexose transport in leaves, based on data deposited in the Genevestigator database. Indeed, we postulated that the combination of gybberellins and L-benzyladenine should have two synergistic effecs: 1) it should beneficially induce genes involved in the innate response against C. Las such as WRKYs, MYC2 and salycilic acid methyl transferase, and 2) it should repress the expression of GPT2 in symptomatic leaves, mitigating the deleterious HLB-driven upregulation **[9]**.

3.1_Greenhouse trial

Atrazine combined with sucrose treatment. The transcript abundance of genes related to carbohydrate metabolism varied significantly in response to atrazine combined with sucrose (**Table 1**).

The *sucrose synthase* (Susy) and starch synthase transcripts were more abundant in 1 μM atrazine-treated plants. *Sucrose-phosphate-synthase* and *water dikinase starch degradation* (GWD) gene were upregulated by 2 μM atrazine + sucrose. Taken together, these findings highlight that activation of *sucrose synthase* should counter the accumulation of sucrose in symptomatic leaves, while the upregulation of *GWD* should promote degradation of accumulated starch.

Defense responses and hormone-related genes were affected by atrazine + sucrose treatments. *WRKY33* was upregulated by 1 μM atrazine + sucrose (**Table 2**).

A *zinc ion binding transcription factor*, *heat shock protein 82* (HSP82) and *ERF1* were strongly induced by 2 μM atrazine (**Tables 2** and **3**).

JIN1 was induced by 1 μM atrazine + sucrose (**Table 4**).

Salicylic acid methyl transferase and *12-oxophytodienoate reductase 1-like* were upregulated by 2 μM atrazine + sucrose.

Table 1| Relative transcript abundance of genes involved in carbohydrate metabolism.

Genes	Untreated	Control K-phite	1 μM Atrazine + sucrose	2 μM Atrazine + sucrose	120 μM BA + 30 μM GA	120 μM BA + 15 μM GA	1 mM Arginine	0.5 mM Arginine
Starch metabolism								
Alpha- amylase	0.470 b	4.950 ab	3.320 ab	4.860 ab	87.140 a	5.210 ab	8.520 ab	3.880 ab
Water dikinase starch degrad.	0.317 d	0.087 d	0.063 d	1.096 a	0.185 d	0.732 b	0.635 bc	0.364 cd
GPT2	0.569 a	0.012 b	0.219 b	0.171 b	0.025 b	0.107 b	0.243 b	0.119 b
Starch synthase	0.672 b	2.429 ab	4.256 a	1.886 ab	0.792 b	2.870 ab	2.016 ab	3.029 ab
Sucrose metabolism								
Invertase	0.839 a	0.766 a	0.351 a	0.274 a	0.296 a	0.851 a	0.758 a	0.611 a
Sugar signaling	0.546 a	2.116 a	0.937 a	2.769 a	7.359 a	1.763 a	1.750 a	3.209 a
Susy	2.310 b	4.218 ab	5.573 a	2.131 b	2.795 b	3.412 ab	4.296 ab	2.022 b
Sps	0.729 b	2.023 b	5.700 b	13.486 a	1.031 b	3.393 b	2.637 b	5.966 b

Means of three replicates were indicated. Letters means significant differences using ANOVA (P < = 0.05) and post-hoc test.

doi:10.1371/journal.pone.0159610.t001

Gibberellin and benzyl-adenine treatment. GA + BA treatments were tested to determine their effects on key genes involved in plant innate immune responses and carbohydrate metabolism. Among carbohydrate metabolism genes, alpha-amylase was significantly induced by 120 μM gibberellins combined with 30 μM benzyl-adenine (**Table 1**). Among innate immune response genes, *WRKY54* was upregulated in response to 120 μM gibberellins + 15 μM benzyl-adenine while *WRKY59* was enhanced by 120 μM gibberellins + 30 μM benzyl-adenine (**Table 2**). *Sulfotransferase 1* was enhanced by both gibberellin and benzyl-adenine treatments. *MYC2* was upregulated by benzyladenine + gibberellin.

Among the secondary metabolism and stress response genes, 120 μM gibberellins + 15 μM benzyl-adenine enhanced expression of *HSP82* and two genes encoding *pectate lyases* involved in cell wall metabolism (**Table 3**). *β-amyrin* was enhanced by 30 μM gibberellins combined with benzyl-adenine.

BA + GA treatments induced *SA methyl transferase* (**Table 4**). BA + GA partially induced HLB-related changes to SA-mediated defense response, but *EDS1* was not altered by the treatment, so the plant probably still can't downregulate jasmonic antagonistic signaling. *Ka02* involved in cytokinin metabolism was higher in response to 15 μM than to 30 μM benzyl-adenine.

Arginine treatment and K-phite treatments. 0.5 mM L-arginine upregulated *HSP21* and *terpene synthase3* (**Table 3**). Arginine treatments did not alter the expression of *terpene synthase14* and *terpene synthase21*, so the treated plant is still unable produce important terpene compounds. *TGA5* and *HSP82* were enhanced by 1 mM L-arginine. K-phite treatment

repressed *glucose-phosphate-transporter 2* (*GPT2*). This downregulation may have a beneficial effect since this gene allows glucose import into the chloroplast and starch accumulation.

K-phite significantly induced *HSP21*, a chaperone involved in functional protein stability.

Table 2| Relative transcript abundance of genes involved in plant innate immune responses.

Genes	Untreated	Control K-phite	1 μM Atrazine + sucrose	2 μM Atrazine + sucrose	120 μM BA + 30 μM GA	120 μM BA + 15 μM GA	1 mM Arginine	0.5 mM Arginine
RAD51 D	0.197 b	0.175 b	0.690 ab	1.878 a	0.335 b	0.350 b	0.272 b	1.362 ab
BZIP45	5.781 ab	7.650 ab	10.216 ab	11.644 ab	13.370 a	5.197 a	8.997 ab	4.983 ab
TGA5	2.391 b	3.107 ab	4.370 ab	3.366 ab	2.203 b	3.026 ab	6.010 a	2.201 b
RGA1	3.537 a	4.092 a	5.953 a	5.301 a	5.540 a	4.968 a	3.562 a	13.320 a
WRKY33	1.752 b	1.099 b	6.372 a	2.891 b	2.425 b	1.128 b	1.510 b	1.074 b
WRKY48	8.133 ab	4.783 b	6.387 ab	13.873 a	10.300 ab	3.918 b	3.405 b	1.928 b
WRKY54	1.701 a	4.708 a	4.753 a	6.452 a	3.576 a	6.850 a	2.723 a	1.808 a
EDS1	1.491 a	1.905 a	11.022 a	9.360 a	6.914 a	8.289 a	6.561 a	4.319 a
ERF1	7.064 b	6.616 b	17.691 ab	29.435 a	18.566 ab	9.641 b	5.636 b	11.654 b
MYC2	5.369 cd	3.872 d	10.282 abcd	6.505 bcd	17.029 ab	18.585 a	4.134 d	6.320 bcd
PR1	0.053 b	0.229 ab	0.078 b	0.970 ab	0.454 ab	0.119 ab	0.832 ab	2.27 ab
SR1	1.670 a	2.690 a	6.680 a	4.720 a	46.630 a	5.590 a	6.950 a	5.210 a
WRKY59	1.376 b	1.653 b	1.709 b	2.632 b	8.332 a	1.366b	2.996 ab	1.035 b

Means of three replicates were indicated. Letters means significant differences using ANOVA (P < = 0.05) and post-hoc test.

doi:10.1371/journal.pone.0159610.t002

Table 3| Relative transcript abundance of genes involved in stress responses and secondary metabolism.

Genes	Untreated	Control K-phite	1 μM Atrazine + sucrose	2 μM Atrazine + sucrose	120 μM BA + 30 μM GA	120 μM BA + 15 μM GA	1 mM Arginine	0.5 mM Arginine
Stress-related and cell wall								
HSP21	23.350 c	308.390 a	24.110 c	106.950 bc	27.670 c	83.290 bc	97.860 bc	288.346 a
HSP82	1.688 c	5.208 ab	0.729 c	5.585 a	3.364 abc	5.448 ab	4.332 ab	0.920 c
ABC Transporter	2.189 de	1.110 de	0.537 e	15.798 b	6.580 cd	24.822 a	9.245 c	1.229 de
ATPtranslocase2	0.022 a	0.052 a	0.032 a	11.499 a	0.012 a	0.148 a	0.125 a	0.029 a
Sulfotransfer. 1	0.298 c	0.008 c	0.6987 c	0.6015 c	2.678 b	6.932 a	0.483 c	0.136 c
NNLTP	0.022 a	0.052 a	0.032 a	11.499 a	0.012 a	0.148 a	0.125 a	0.029 a
PSBW	2.394 c	3.178 c	8.020 b	6.470 bc	2.287 c	6.226 bc	2.539 c	12.839 a
Pectate lyase 5	0.427 b	0.242 b	0.169 b	0.919 ab	0.231 b	4.233 a	0.817 ab	0.589 ab
Secondary metabolism								
Terpene synthase 14	0.198 b	0.184 b	0.402 b	0.112 b	0.101 b	0.345 b	0.051 b	1.944 a
Terpene synthase 21	3.472 a	1.309 a	1.026 a	5.870 a	4.891 a	1.849 a	1.543 a	6.564 a
Terpene synthase 3	0.76 a	0.53 a	4.92 a	38.40 a	0.64 a	1.37 a	0.32 a	0.19 a
B-Amyrin	1.457 b	2.300 ab	2.178 b	3.504 ab	22.614 a	9.651 ab	3.253 ab	6.649 ab

Means of three replicates were indicated. Letters means significant differences using ANOVA (P < = 0.05) and post-hoc test.

doi:10.1371/journal.pone.0159610.t003

Table 4| Relative transcript abundance of genes involved in hormone-related pathways.

Genes	Untreated	Control K-phite	1 μM Atrazine + sucrose	2 μM Atrazine + sucrose	120 μM BA + 30 μM GA	120 μM BA + 15 μM GA	1 mM Arginine	0.5 mM Arginine
Gibberellins								
GA2-oxidase	0.395 a	0.676 a	0.556 a	5.276 a	2.718 a	1.752 a	0.199 a	1.379 a
Gibberelin-2-oxygenase	0.765 a	0.357 a	0.793 a	1.367 a	2.629 a	3.965 a	1.158 a	0.487 a
Auxins and Benzyl-adenine								
GH3.1	0.077 b	0.021 b	0.135 b	0.511 a	0.048 b	0.070 b	0.118 b	0.255 ab
Ka02	2.837 ab	3.661 a	2.532 ab	3.608 a	0.139 b	4.164 a	0.929 ab	2.794 ab
Jasmonic acid								
12-oxophytodi. reductase 1-like	0.444 b	0.290 b	0.322 b	1.986 a	0.174 b	1.063 ab	1.964 a	0.732 ab
Salicylic acid methyl transferase								
SA-methyl transferase	0.033 b	0.015 b	0.052 b	0.277 a	0.314 a	0.091 a	0.360 a	0.434 b
Ethylene								
ACS-1	3.960 a	3.580 a	5.039 a	6.202 a	2.025 a	1.723 a	4.595 a	4.247 a

Means of three replicates were indicated. Letters means significant differences using ANOVA (P < = 0.05) and post-hoc test.

doi:10.1371/journal.pone.0159610.t004

Principal component analysis. Two principal component analyses were conducted to independently assess two gene subsets: 1) genes involved in sucrose and starch metabolism (PCA-1; **Fig. 1**) and 2) genes involved in hormone-related proteins and biotic stress responses (PCA-2; **Fig. 2**).

In PCA-1, the first two principle components explained 47 and 28% of data variability, respectively. The 2 μM atrazine + sucrose treatment separated from the rest of the treatments. *SPS* greatly contributed to this separation. 120 μM BA + 30 μM GA was also highly discriminated from the rest of the treatments. The other treatments were not distinct from the untreated controls.

PC 1 and PC 2 of PCA-2 (**Fig. 2**) explained 36 and 17% of data variability, respectively. The 1 mM L-arginine treatment was not distinct from untreated conditions, but the 2 μM atrazine + sucrose treatment was highly distant. *GA2-oxidase*, *zinc ion binding*, and *cysteine-histine rich domain C1* gene contributed significantly to the separation of 2 μM atrazine + sucrose treatment. *WRKY33* highly contributed to the separation of the 1 μM atrazine + sucrose treatment.

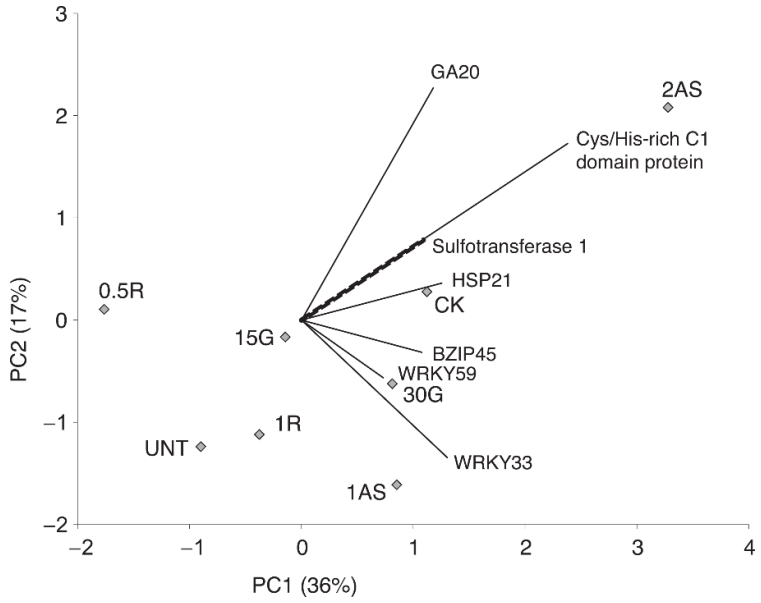

Fig. 1| Overall analysis of HLB-regulated changes in carbohydrate metabolism. Principal component analysis of treated and untreated Citrus categories in relation to genes involved in sucrose and starch pathways. UNT = Untreated with hormones (Control), CK = treated with K-phite, 30G = 30 µM gibberellin, 15G = 15 µM gibberellin, 1R = 1 mM L-arginine, 0.5R = 0.5 mM L-arginine, 2AS = sucrose combined with 2 µM atrazine, 1AS = sucrose combined with 2 µM atrazine. SPS = sucrose-phosphate-synthase.

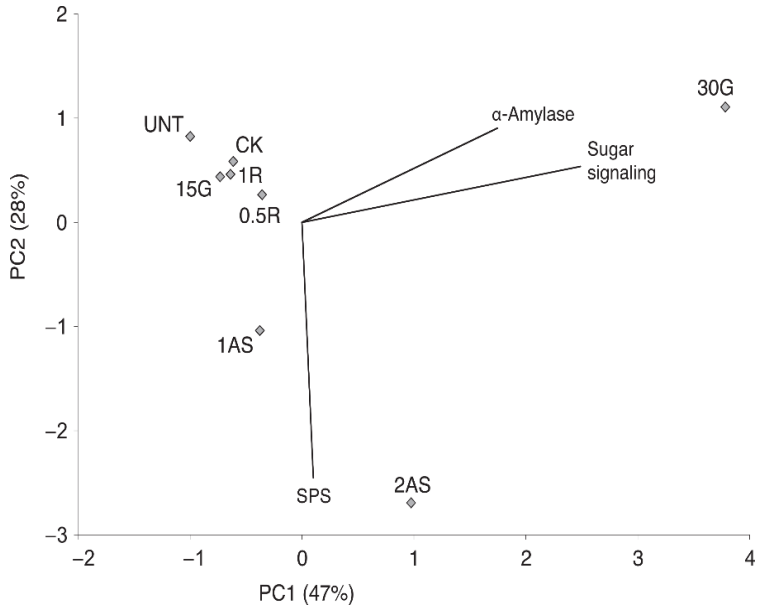

Fig. 2| Overall analysis of HLB-regulated changes in biotic stress response. Principal component analysis of treated and untreated Citrus categories in relation to genes involved in biotic stress responses. UNT = Untreated with hormones (Control), CK = treated with K-phite, 30G = 30 µM gibberellin, 15G = 15 µM gibberellin, 1R = 1 mM L-arginine, 0.5R = 0.5 mM L-arginine, 2AS = sucrose combined with 2 µM atrazine, 1AS = sucrose combined with 2 µM atrazine. GA20 = Ga2-oxidase, HSP21 = Heat shock protein 21.

3.2_Field trial

Small-molecule regulating treatments investigated in the greenhouse were also applied to HLB-symptomatic trees in a young orchard where disease symptoms were frequently present. The aim of this trial was to determine whether the same treatments used in the greenhouse could modulate the expression of key host genes at three and six days after their application. Seven key genes were selected to monitor the transcriptomic regulation of the treatments for two reasons: 1) previous data found them highly characteristic of an HLB-induced response **[7,9]** and 2) they play a key role in innate immune responses. A gibberellin responsive gene was used as a marker to determine the efficacy of GA + BA treatments to modulate gene expression under field conditions. *GPT2* is a key HLB-regulated gene involved in glucose import into the chloroplast and is linked to the increased accumulation of starch in symptomatic leaves. The other genes were involved in plant defense and hormonal-mediated innate responses. *WRKY70* and *EDS1* are key points of regulation of JA-SA crosstalk. *PR1* upregulation is a beneficial against C. Las since this gene is involved in the systemic acquired resistance response. *WRKY48* and *WRKY54* were induced by HLB in previous studies **[7,9]**.

At three days after treatment, 1 μM atrazine + sucrose induced the gibberellin-responsive protein and *PR1* and repressed *WRKY48* (**Fig 3**).

In addition, 30 μM GA + 120 μM BA induced *WRKY48* and *WRKY54*. This finding may have positive effects on infected Citrus since the two genes are involved in salicylic acid-mediated responses against biotrophs. 0.5 mM L-Arginine upregulated *WRKY48* and *EDS1*. *WRKY70* was enhanced by 1 mM arginine and 15 μM GA combined with 120 μM BA.

At six days following treatment, some important changes in expression of the seven host biomarkers were observed. 1 μM atrazine upregulated *PR1*. 2 μM atrazine and 0.5 mM L-arginine repressed *WRKY48*. A general inhibition of *GPT2* was observed in all treated trees at both three and six days after treatment. This repression was particularly evident in leaves sprayed with gibberellins + benzyladenine.

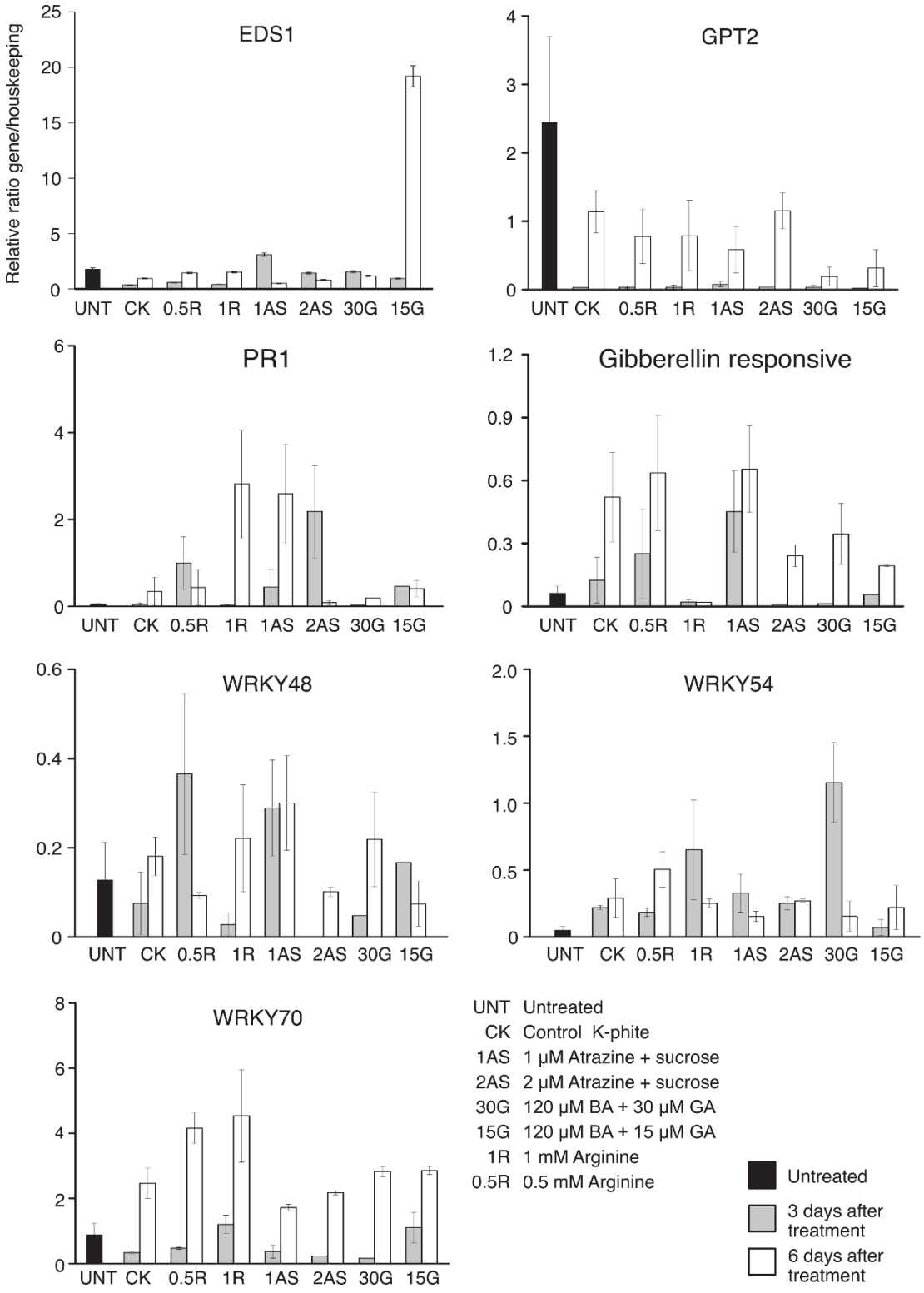

Fig. 3| Expression of seven host genes in response to spray treatments in field conditions. Relative expression of each gene and treatment was shown as average of three biological replicates. Standard deviations were indicated.

Phenotypic measurements and pathogen qPCR detection. No obvious symptoms of a harmful spray as leaf drop or discoloration was observed in treated trees. The tree trunk diameter, height, width drill, and width row of the treated trees grown under field conditions were measured in May and June 2014 (**Table 5**).

The aim of this analysis was to determine whether treatments were detrimental to tree growth or had undesirable phenotypic effects. No significant phenotypic differences were observed among untreated and treated trees except width row, which was significantly lower in untreated trees than in trees treated with 30 μM GA + 120 μM BA. There were no visible discolorations or other signs of plant distress from the spraying. No set of trees had visibly different vegetative vigor.

The quantification of pathogen titer was performed after three months from treatments as previously indicated to check if it was not changed in response to treatments.

Table 5| Phenotypic measurements in response to the seven treatments and control (untreated).

1st Measurement (5.21.14)	Untreated	120 μM BA + 30 μM GA	120 GA + 15 μM BA	1 μM Atrazine	2 μM Atrazine	.12% Siluet K-Phite +	0.5 mM L-Arginine	1.0 mM L-Arginine
Trunk Diameter (mm)	90.770 a	91.537 a	82.280 a	96.097 a	88.197 a	83.827 a	96.427 a	98.747 a
Tree Height (m)	2.9533 ab	3.0000 ab	2.5533 b	3.1667 ab	3.1900 ab	2.8133 ab	3.2567 ab	3.3200 a
Width Drill (m)	2.4167 a	2.7400 a	2.4733 a	2.7000 a	2.6767 a	2.4433 a	2.7467 a	2.6233 a
Width Row (m)	2.4767 a	2.7667 a	2.4400 a	2.7400 a	2.5267 a	2.5533 a	2.7400 a	2.6800 a
2nd Measurement (6.28.13)	Untreated	120 μM BA + 30 μM GA	120 GA + 15 μM BA	1 μM Atrazine	2 μM Atrazine	.12% Siluet K-Phite +	0.5 mM L-Arginine	1.0 mM L-Arginine
Trunk Diameter (mm)	70.940 a	77.427 a	70.503 a	80.813 a	75.207 a	72.513 a	82.293 a	83.617 a
Tree Height (m)	2.5500 abc	2.6833 ab	2.3533 bc	2.7067 ab	2.6733 abc	2.3100 c	2.7267 a	2.7700 a
Width Drill (m)	2.1767 a	2.5400 a	2.3133 a	2.4233 a	2.4000 a	2.4200 a	2.6533 a	2.4400 a
Width Row (m)	2.0700 c	2.6167 ab	2.2733 bc	2.4900 abc	2.3033 abc	2.2667 bc	2.7267 a	2.4267 abc

Means of three replicates were indicated. Letters means significant differences using ANOVA (P < = 0.05) and post-hoc test.

doi:10.1371/journal.pone.0159610.t005

4_DISCUSSION

Our objective was to test the ability of six combinations of small-molecule compounds to modulate expression of key genes involved in HLB syndrome and innate immune responses shortly after treatment. We did not pretend to reduce pathogen titers or cure the plants with only one treatment. Before performing a long-term study, we wanted to evaluate the ability of the treatments to modulate expression of a subset of key genes that are altered during HLB syndrome. As we expected pathogen titers did not significantly differ among treated and

control trees. A long-term study will reveal if repetitive and continuous applications will reduce pathogen concentrations and symptom severity.

Treatments were designed based on previously proposed hypotheses. Sucrose-induced protection against atrazine effects was linked to upregulation of reactive oxygen species (ROS) defence and repair mechanisms **[21]**.

Nitric oxide (NO) is produced by l-arginine. Treatment with arginine provoked resistance against *Botrytis cinerea* in tomato at three to six days after treatment. Endogenous NO concentrations correlated positively with induction of key enzymes involved in biotic stress responses such as phenylalanine ammonia-lyase, chitinase, β-1,3-glucanase and polyphenoloxidase **[23]**.

Gibberellins regulate plant growth by modulating degradation of growth-repressing DELLA proteins that promote susceptibility to biotrophic pathogens and resistance to necrotrophic pathogens **[24]**. This is accomplished by modulating the relative strength of the SA and JA signaling pathways **[24]**. Through regulation of DELLA stability, gibberellins affect the SA-JA-ET network and plant immune response. Genevestigator showed that benzyl-adenine downregulated the glucose-phosphate transporter in *Arabidopsis*. Since this gene is induced by HLB metabolic syndrome **[5,9]**, benzyl-adenine treatments might help mitigate the negative effects of HLB on leaf metabolism. In combination, the two hormones may beneficially modulate key HLB-regulated genes involved in carbohydrate metabolism **[7,9]**.

K-phite mineral solution was also tested, alone or in combination with the three small molecule compounds. This treatment was considered because of contrasting published reports on the effects of nutrient solutions such as K-phite **[25]**. Mineral solutions increased the concentrations of important N, Mn, Zn and B ions in leaves and long-term application reduced pathogen titer, leaf size, and leaf weight **[25]**. Although enhanced nutritional solutions composed of essential micronutrients did not improve fruit production and quality of C. Las-infected trees **[26]**, others results support the hypothesis that the pathogen severely affects nutrient patterns **[27]**. In addition, foliar nutrition and soil conditioners helped reduce economic and production losses due to HLB **[28,29]**.

To determine how the treatments affected the metabolism of infected trees, 42 genes were selected from previously published Citrus transcriptome data **[7,9]**. These genes fell into three subsets involved in: 1) carbohydrate metabolism and signaling, 2) innate immune responses, including key players in JA-SA signaling, crosstalk and induced responses, or 3) other genes involved in biotic stress responses such as those involved in hormone-related pathways, secondary metabolism and stress-preventing factors. From these biomarkers, we

chose seven representative biomarkers to be followed under field conditions in response to the same treatments. Treated plants were tested for the presence of C. Las using qPCR and showed clear HLB symptoms.

QRT-PCR analyses were conducted at three to six days after treatment. As expected, we observed no significant changes in pathogen titer. Repeated applications of treatments (at least weekly) should eventually affect the titer. Since we only treated infected trees once, an analysis of pathogen titer after treaments was outside the scope of this study. Long-term studies on the effects of repeated applications of these treatments should test pathogen titer using qPCR.

4.1_Atrazine combined with sucrose

The first small-molecule treatment tested was the combination of sucrose and the herbicide atrazine. Atrazine is a well-known photosystem II inhibitor that affects plant gene expression, seedling physiology, and potentiality impairs protein translation and the ROS defense mechanism **[30]**. However, in combination with sucrose, atrazine induces xenobiotic and ROS signaling. In addition, this treatment upregulated important classes of antioxidant enzymes **[21,22]**. These findings were consistent with our unpublished findings that *glutathione-S-transferases* are upregulated in more tolerant Citrus genotypes.

Here we observed that atrazine combined with sucrose drastically affected some key genes responsible for HLB-induced carbohydrate changes. Increased sucrose concentrations have been found in in C. Las-infected leaves **[6,11]**. 1 μM atrazine + sucrose enhanced sucrose synthase while 2 μM atrazine + sucrose upregulated the water dikinase starch degradation gene and sucrose-phosphate-synthase. Atrazine upregulated *alpha-amylase*, which was repressed in mature HLB-infected Citrus leaves **[9]** but upregulated in infected Citrus stems **[31]**. Taken together, these findings lead us to speculate that atrazine + sucrose might help sucrose degradation by activating *sucrose synthase*. In addition, upregulation of *alpha-amylase* may increase starch degradation in HLB-infected plants where its accumulation is advanced.

Atrazine (1 μM) combined with sucrose upregulated *WRKY33*. *Brassica napus* plants overexpressing *BnWRKY33* had increased resistance to *Sclerotinia sclerotiorum* infection **[32]**. This effect was mediated by SA **[32]**. *WRKY33* upregulation allowed resistance to the necrotroph *Botrytis cinerea* in *Arabidopsis* **[33]**. Loss of *WRKY33* function induces salicylic acid (SA)-mediated responses, increases salicylic acid and represses jasmonic acid (JA)-mediated responses **[34]**.

Overall, our results support the hypothesis that this treatment could beneficially modulate key HLB-regulated genes associated with the well-known HLB carbohydrate metabolic syndrome **[9]**. The changes to expression of some key genes involved in sugar and starch metabolism could beneficially modulate the metabolic responses of HLB disease in photosynthesizing Citrus leaves, restoring a more normal source-sink relationship and potentially inhibiting the characteristic and deleterious syndrome in the fruit.

4.2_Gibberelllins combined with benzyl adenine treatments

A mixture of gibberellin (GA3) and 6-benzyladenine (BA) was tested to modulate jasmonic acid-salicylic acid (JA-SA) crosstalk in favor of responses to biotrophs such as C. Las. Our hypothesis was that gibberellin treatments may activate SAR responses through positive regulation of hormone-mediated crosstalk regulating biotic stress responses **[19]**. Some key genes in hormone-related pathways and JA-SA crosstalk were chosen as indicators of treatment effects.

MYC2 was significantly induced by both 15 and 30 μM gibberellin treatments. *MYC2* is a transcription factor composed of a basic helix-loop-helix (bHLH) domain that activates and represses specific JA-responsive gene expression in *Arabidopsis* **[35]**. *MYC2* also induced responses to abiotic stress mediated by abscissic acid in *Arabidopsis* **[36]** and suppressed salicylic acid-mediated responses in *Arabidopsis* **[37]**. Upregulation of *WRKY54* in gibberellin-treated field trees is also interesting because this gene is a positive regulator of resistance against *Erwinia amylovora*, the agent of fire blight in the Rosaceae family.

The plant immune regulator *EDS1* (Enhanced Disease Susceptibility1) plays a fundamental role in resistance mechanisms to biotrophs and hemi-biotrophs **[38,39]**. This role is due to the formation of complexes with *PAD4* and *SAD101* in both cytoplasm and nucleus **[40]**. The 15 μM GA + BA treatment enhanced EDS1 at six days after treatment in the field. The increase in *EDS1* transcripts after application of these small molecules could help activate SAR response against pathogen infections. Mutant screening showed that upregulation of *EDS1* induces non-host resistance against *E. amylovora* in *Arabidopsis* by activating *WRKY46* and *WRKY54* genes **[41]**.

Our hypothesis was partially confirmed. GA + BA may beneficially increase innate responses by inducing *EDS1* and *MYC2*. Although long-term field trials are required, we speculate that continuous application of this small molecule mixture could stimulate improved SA-JA crosstalk.

4.3_L-arginine treatments

The third small-molecule treatment was composed of L-arginine, used in two concentrations. L-arginine positively regulates key genes involved in innate immune responses **[23]**. L-arginine may act on nitric oxide and directly upregulate key genes in salicylic acid signaling. Increased endogenous NO concentrations after L-arginine treatment in pre-harvest tomatoes correlated positively with increased defensive enzyme activity and postharvest disease resistance **[15]**. *PR1*, *WRKY70* and *WRKY54* were upregulated by1 mM L-arginine under field conditions. WRKY transcription factors are important regulators of responses to abiotic and biotic stresses. *WRKY54* and *WRKY70* play a key role in a regulatory network that affects leaf senescence by interacting with another WRKY factor **[42]**. In our field trial, arginine induced some key important gene regulation that should benefit SAR responses.

4.4_Common effects among treatments

Glucose accumulation induced by C. Las infection is transported to the plastid by hexose transporters **[5,9,43]**. GPT2 is a key player in HLB-mediated starch accumulation in leaves because this gene mediates glucose import into the chloroplast in infected leaves **[5,9]**. *GPT2* was significantly repressed by all spray applications at both three and six days after treatment under field conditions. This inhibition may reduce the amount of glucose carried into the plastid and thus starch accumulation, with consequent improvement of disrupted source-sink relationships.

Gene expression changes observed in this work corroborated the hypothesis that these spray treatments may help stimulate systemic acquired resistance responses by activating key genes involved in innate responses (**Fig. 4**).

PR gene induction is mediated through interaction with TGA transcription factors **[15]**. The observed upregulation of *TGA5* and *TGA6* by L-arginine and 2 μM atrazine + sucrose, respectively, might help stimulate defense responses against C. Las infection.

Arginine and atrazine sprays upregulated the *PR1* gene under field conditions. PR1 protein is the hallmark of the defense response induction mediated by salicylic acid through systemic acquired resistance **[44]**. Molecular action of this protein against pathogens is still unclear, although antifungal properties have been attributed to it **[45]**. *PR1* also interacted with fungal toxin activities, mediating necrosis in sensitive wheat **[31]**. This gene was not activated in response to C. Las infections in orchard trees **[9]**.

Interestingly, all three treatments upregulated *HSP82*. Previous data on C. Las-infected citrus leaves and fruits showed that C. Las caused a significant repression of genes encoding chaperones **[7-9]**. Modified expression of these genes plays a key role in general stress conditions **[46,47]**. A link between reduced HSP protein amount and HLB symptoms was also confirmed by analysis **[10]**.

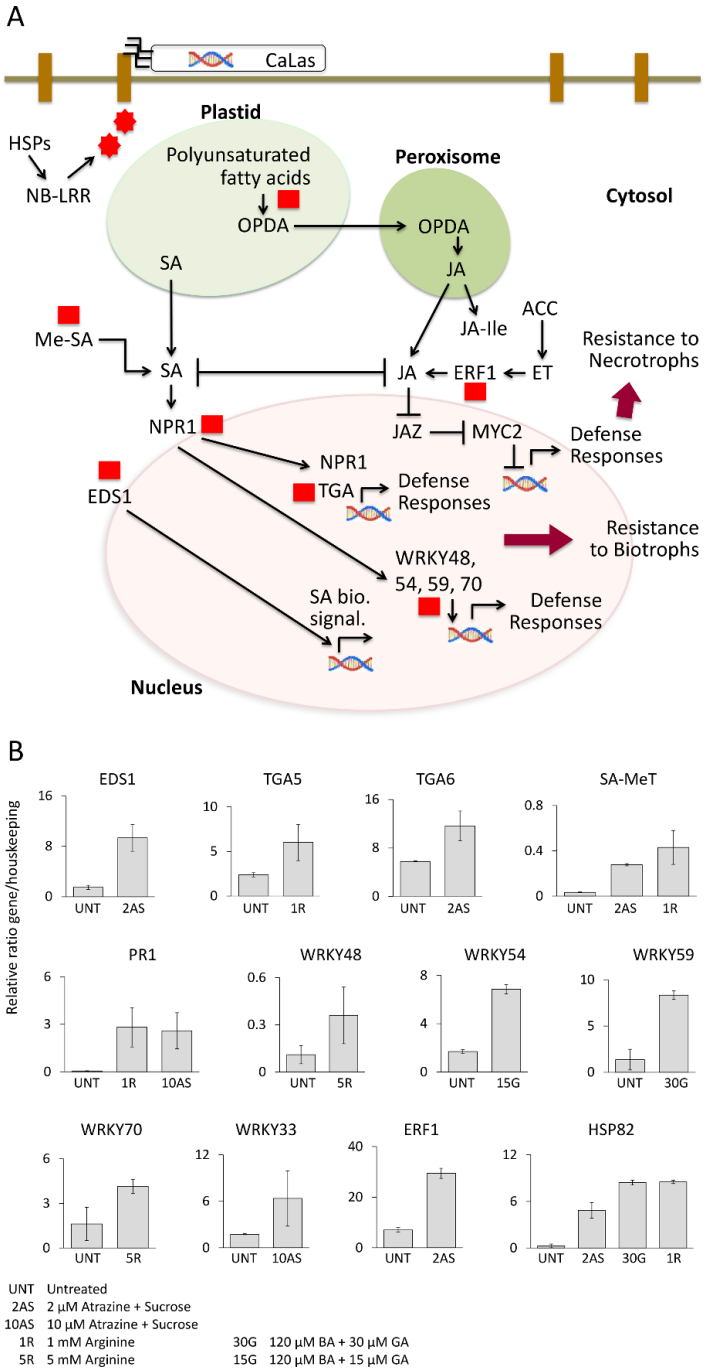

Fig. 4| Key differentially regulated genes in response to treatments involved in biotic stress responses.

5_CONCLUSIONS

Present data confirmed our hypothesis that these small-molecule sprays may affect transcript abundance of key genes involved in HLB carbohydrate metabolic syndrome and innate responses. As expected, there were no phenotypic changes in response to treatments at one to two months after treatment. Treatment sprays did not cause negative effects such as leaf drop or discoloration. As expected, tree measurements showed almost no differences between treated and untreated trees in field conditions. We believe that beneficial effects are likely to be seen only if treatments are applied frequently before or at the onset of visible HLB symptoms. Here, our aim was to analyze the molecular effects of these treatments on gene expression several days after treatment. Future studies should examine long-term molecular and phenotypic improvements associated with ongoing applications to young trees infected with C. Las.

6_REFERENCES

[1] Bove' JM. Huanglongbing: A destructive, newly-emerging, century-old disease of citrus. J Plant Pathol. 2006; 88:7–37.

[2] Jagoueix S, Bové JM, Garnier M. The phloem-limited bacterium of greening disease of citrus is a member of the alpha subdivision of the Proteobacteria. Int J of Syst Bacteriol. 1994; 44:397-86.

[3] Folimonova SY, Robertson CJ, Garnsey SM, Gowda S, Dawson WO. Examination of the responses of different genotypes of Citrus to Huanglongbing (Citrus greening) under different conditions. Phytopathology. 2009; 99:1346–54.

[4] Folimonova SY, Achor D. Early events of citrus greening (Huanglongbing) disease development at the ultrastructural level. Bacteriology. 2010; 100:949–58.

[5] Albrecht U, Bowman KD. Gene expression in *Citrus sinensis* (L.) Osbeck following infection with the bacterial pathogen *Candidatus* Liberibacter asiaticus causing Huanglongbing in Florida. Plant Sci. 2008; 175:291-306.

[6] Kim J-S, Sagaram US, Burns JK, Li J-L, Wang N. Response of sweet orange (*Citrus sinensis*) to '*Candidatus* Liberibacter asiaticus' infection: microscopy and microarray analyses. Phytopathology. 2009; 99:50-57.

[7] Martinelli F, Uratsu SL, Albrecht U, Reagan RL, Phu ML, Britton M, et al. Transcriptome profiling of Citrus fruit response to Huanglongbing disease. PLoS One. 2012; 7:e38039.

[8] Dandekar AM, Martinelli F, Davis CE, Bhushan A, Zhao W, Fiehn O, et al. Analysis of Early Host Responses for Asymptomatic Disease Detection and Management of Specialty Crops. Crit Rev Immunol. 2010; 30:277-89.

[9] Martinelli F, Reagan RL, Uratsu SL, Phu ML, Albrecht U, Zhao W, et al. Gene Regulatory Networks Elucidating Huanglongbing Disease Mechanisms. Plos One. 2013; 8:e74256.

[10] Nwugo CC, Lin H, Duan Y, Civerolo EL. The effect of '*Candidatus* Liberibacter asiaticus' infection on the proteomic profiles and nutritional status of pre-symptomatic and symptomatic grapefruit (*Citrus paradisi*) plants. BMC Plant Biology. 2013; 13:59.

[11] Fan J, Chen C, Yu Q, Brlansky RH, Li Z-G, Gmitter FG. Comparative iTRAQ proteome and transcriptome analyses of sweet orange infected by "Candidatus Liberibacter asiaticus". Physiol Plant. 2011; 143:235–45.

[12] Cong Q, Kinch LN, Kim B-H, Grishin NV. Predictive sequence analysis of the Candidatus liberibacter asiaticu proteome. Plos One. 2012; 7(7):e41071.

[13] Tyler HL, Roesch LFW, Gowda S, Dawson WO, Triplett EW. Confirmation of the sequence of 'Candidatus Liberibacter asiaticus' and assessment of microbial diversity in Huanglongbing-infected Citrus phloem using a metagenomic approach. Mol Plant Microbe Interact. 2009; 22:1624–34.

[14] Khan AA, Afzal M, Qureshi JA. Botanicals, selective insecticides, and predators to control Diaphorina citri (Hemiptera: Liviidae) in citrus orchards. Insect Sci. 2014; 21:717-26.

[15] Zhang M, Powell CA, Zhou L, He Z, Stover E, Duan Y. Chemical compounds effective against the citrus Huanglongbing bacterium 'Candidatus Liberibacter asiaticus' in planta. Phytopathology. 2011; 101:1097–1103.

[16] Zhang M, Powell CA, Guo Y, Doud MS, Duan Y. A graft-based chemotherapy method for screening effective molecules and rescuing huanglongbing-affected citrus plants. Phytopathology. 2012; 102:567-74.

[17] Yang C, Powell CA, Duan Y, Shatters R, Zhang M. Antimicrobial nanoemulsion formulation with improved penetration of foliar spray through citrus leaf cuticles to control citrus huanglongbing. Plos One. 2015; 10(7):e0133826.

[18] Akula N, Trivedi P, Han FQ, Wang N. Identification of small molecule inhibitors against SecA of Candidatus Liberibacter asiaticus by structure based design. Eur J Med Chem. 2012; 54:919-24.

[19] Li W, Hartung JS, Levy L. Quantitative real-time PCR for detection and identification of Candidatus Liberibacter species associated with citrus huanglongbing. J Microbiol Methods. 2006; 66:104–15.

[20] Pieterse CMJ, Leon-Reyes A, Van der Ent S, Van Wees SCM. Networking by small-molecule hormones in plant immunity. Nat Chem Biol. 2009; 5:308-16.

[21] Ramel F, Sulmon C, Cabello-Hurtado F, Tacconat L, Martin-Magniette M-L, Renou J-P, et al. Genome-wide interacting effects of sucrose and herbicide-mediated stress in *Arabidopsis thaliana*: Novel insights into atrazine toxicity and sucrose-induced tolerance. BMC Genomics. 2007; 8:450.

[22] Ramel F, Sulmon C, Gouesbet G, Couee I. Regulatory effects of atrazine differentially override sucrose repression of amino acid catabolism. Acta Physiol Plant. 2013; 35:2329-37.

[23] Zheng Y, Sheng J, Zhao R, Zhang J, Lv S, Liu L, et al. Preharvest l -arginine treatment induced postharvest disease resistance to botrysis cinerea in tomato fruits. J Agric Food Chem. 2011; 59:6543-49.

[24] Navarro L, Bari R, Achard P, Lison P, Nemri A, Harberd N.P, et al. DELLAs control plant immune responses by modulating the balance of jasmonic acid and salicylic acid signaling. Curr Biol. 2008; 18:650–55.

[25] Shen W, Cevallos-Cevallos JM, Nunes da Rocha U, Arevalo HA, Stansly PA, Roberts PD, et al. Relation between plant nutrition, hormones, insecticide applications, bacterial endophytes, and Candidatus Liberibacter Ct values in citrus trees infected with Huanglongbing. Eur J Plant Pathol. 2013; 137:727-42.

[26] Gottwald TR, Graham JH, Irey M, McCollum G, Wood B. Inconsequential effect of nutritional treatments on huanglongbing control, fruit quality, bacterial titer and disease progress. Crop Protection. 2012; 36 :72–82.

[27] Cao J, Cheng C, Yang J, Wang Q. Pathogen infection drives patterns of nutrient resorption in citrus plants. Scientific Reports. 2015; 5:e14675.

[28] Stansly PA, Arevalo HA, Qureshi JA, Jones MM, Hendricks K, Roberts PD, et al. Vector control and foliar nutrition to maintain economic sustainability of bearing citrus in Florida groves affected by huanglongbing. Pest Man Sci. 2014; 70:415-26.

[29] Xu M, Liang M, Chen J, Xia Y, Zheng Z, Zhu Q, et al. Preliminary research on soil conditioner mediated citrus Huanglongbing mitigation in the field in Guangdong, China. Eur J of Plant Pathol. 2013; 137:283-93.

[30] Flores F, Collier CJ, Mercurio P, Negri AP. Phytotoxicity of Four Photosystem II Herbicides to Tropical Seagrasses. PLoS ONE. 2013; 8:e75798.

[31] Aritua V, Achor D, Gmitter FG, Albrigo G, Wang N. Transcriptional and Microscopic Analyses of Citrus Stem and Root Responses to *Candidatus* Liberibacter asiaticus Infection. PLoS ONE. 2013; 8, e73742.

[32] Wang Z, Fang H, Chen Y, Chen K, Li G, Gu S, et al. Overexpression of BnWRKY33 in oilseed rape enhances resistance to *Sclerotinia sclerotiorum*. Mol Plant Pathol. 2014; 15:677-89.

[33] Wang X-M, Gaudet DA, Liu W, Frick M, Puchalski B, Lu Z-X, et al. Defence responses including hypersensitive cell death, oxidative burst and defence gene expression in Moro wheat inoculated with Puccinia striiformis. Can J Plant Pathol. 2014; 36:202-15.

[34] Birkenbihl RP, Diezel C, Somssich IE. Arabidopsis WRKY33 is a key transcriptional regulator of hormonal and metabolic responses toward Botrytis cinerea infection. Plant Physiol. 2012; 159:266–85.

[35] Lorenzo O, Chico JM, Sánchez-Serrano JJ, Solano R. *JASMONATE- INSENSITIVE1* encodes a MYC transcription factor essential to discriminate between different jasmonate-regulated defense responses in Arabidopsis. Plant Cell. 2004; 16:1938–50.

[36] Abe H, Urao T, Ito T, Seki M, Shinozaki K, Yamaguchi-Shinozaki K. Arabidopsis AtMYC2 (bHLH) and AtMYB2 (MYB) function as transcriptional activators in abscisic acid signaling. Plant Cell. 2003; 15:63–78.

[37] Laurie-Berry N, Joardar V, Street IH, Kunkel BN. The *Arabidopsis thaliana JASMONATE INSENSITIVE 1* gene is required for suppression of salicylic acid–dependent defenses during infection by *Pseudomonas syringae*. Mol Plant Microbe Interact. 2006; 19:789–800.

[38] Falk A, Feys BJ, Frost LN, Jones JDG, Daniels MJ, Parker JE. EDS1, an essential component of R gene-mediated disease resistance in Arabidopsis has homology to eukaryotic lipases. Proc Natl Acad Sci USA. 1999; 96:3292–97.

[39] Lipka V, Dittgen J, Bednarek P, Bhat R, Wiermer M, Stein M, et al. Pre- and Postinvasion Defenses Both Contribute to Nonhost Resistance in Arabidopsis. Science. 2005; 310:1180-83.

[40] Feys BJ, Wiermer M, Bhat RA, Moisan LJ, Medina-Escobar N, Neu C, et al. Arabidopsis Senescence-associated gene101 stabilizes and signals within an enhanced disease susceptibility1 complex in plant innate immunity. Plant Cell. 2005; 17:2601–13.

[41] Moreau M, Degrave A, Vedel R, Bitton F, Patrit O, Renou J-P, et al. EDS1 contributes to nonhost resistance of Arabidopsis thaliana against Erwinia amylovora. Mol Plant Microbe In. 2012; 25:421-30.

[42] Besseau S, Li J, Palva ET. WRKY54 and WRKY70 co-operate as negative regulators of leaf senescence in *Arabidopsis thaliana*. J Exp Bot. 2012; 63:2667-679.

[43] Ibanez AM, Martinelli F, Reagan RL, Uratsu SL, Vo A, Tinoco MA, et al. Transcriptome and metabolome analysis of Citrus fruit to elucidate puffing disorder. Plant Science. 2014; 217:87-98.

[44] van Loon LC, Rep M, Pieterse CM. Significance of inducible defense-related proteins in infected plants. Annu Rev Phytopathol. 2006; 44:135–62.

[45] Kiba A, Maimbo M, Kanda A, Tomiyama H, Ohnishi K, Hikichi Y. Isolation and expression analysis of candidate genes related to Ralstonia solanacearum-tobacco interaction. Plant Biotechnol. 2007; 24:409–16.

[46] Martinelli F, Scalenghe R, Giovino A, Pasquale M, Aksenov AA, Pasamontes A, Peirano DJ, Davis CE, Dandekar AM. Proposal of a Citrus translational genomic approach for early and infield detection of Flavescence dorée in Vitis. Plant Biosystems 2016; 150:43–53.

[47] Martinelli F, Scalenghe R, Davino SW, Panno S, Suderi G, Ruisi P, Villa P, Stroppiana D, Boschetti M, Goulart LR, Davis CE, Dandekar AM. Advanced methods of plant disease detection. A Review. Agronomy for Sustainable Development 2015; 35:1–25.

CHAPTER 6

PROTEOMIC ANALYSIS HIGHLIGHTS THE ROLE OF DETOXIFICATION PATHWAYS IN INCREASED TOLERANCE TO HUANGLONGBING DISEASE[4]

Federico Martinelli[1], Russell L. Reagan[2], David Dolan[2], Veronica Fileccia[1], Abhaya M. Dandekar[2*]

[1]Department of Agricultural and Forest Sciences, University of Palermo, viale delle scienze ed. 4, 90128, Palermo, Italy
[2]Plant Sciences Department, University of California, One Shields Avenue, 95616, Davis, CA, USA

*corresponding author; email: amdandekar@ucdavis.edu, Tel: +15307527784

Federico Martinelli: federico.martinelli@unipa.it
Russell L. Reagan: ovoshby@plantsciences.ucdavis.edu
David Dolan: david.dolander@gmail.com
Veronica Fileccia: veronica.fileccia@unipa.it

Background: Huanglongbing (HLB) disease is still the greatest threat to citriculture worldwide. Although there is not any resistance source in the *Citrus* germplasm, a certain level of moderated tolerance is present. A large-scale analysis of proteomic responses of *Citrus* may help: 1) clarifying physiological and molecular effects of disease progression, 2) validating previous data at transcriptomic level, and 3) identifying biomarkers for development of early diagnostics, short-term therapeutics and long-term genetic resistance.

Results: In this work we have conducted a proteomic analysis of mature leaves of two *Citrus* genotypes with well-known differing tolerances to HLB: Navel orange (highly susceptible) and Volkameriana (moderately tolerant). Pathway enrichment analysis showed that amino acid degradation processes occurred to a larger degree in the Navel orange. No clear differences between the two genotypes were observed for primary metabolic pathways. The most important finding was that four glutathione-S-transferases were upregulated in Volkameriana and not in Navel orange. These proteins are involved in radical ion detoxification.

Conclusions: Upregulation of proteins involved in radical ion detoxification should be considered as an important mechanism of increased tolerance to HLB.

[4] Published to BMC Plant Biology, 2016, 16:167. doi: 10.1186/s12870-016-0858-5

1_INTRODUCTION

Huanglongbing disease currently threatens areas where *Citrus* cultivation is important in the agricultural economy such as East Asia, the Middle East, and the Americas. Huanglongbing disease is caused by three species of *Candidatus* liberibacter asiaticus (CaLas), americanus and africanus **[1]**. The pathogen is transmitted by two species of psyllids: Diaphorina citri and Trioza erytreae. Recently, Trioza erytreae was found for the first time in Europe (Galicia, Spain). Typical symptoms of Huanglongbing disease in leaves include shoot yellowing and blotchy, mottled leaves. Although most of the fruits are still of commercial quality, fruits from severely affected branches are unmarketable: small, lopsided, green, and acidic, with many aborted seeds. Leaves accumulate starch, phloem is damaged and cell wall lamellae swell during CaLas infection **[1, 2]**. *Candidatus liberibacter* spp. belong to the alpha subdivision of the proteobacteria based on ribosomal region sequence data **[3]**. The bacterium has not yet been definitively cultured despite attempts to do so **[4]**. Koch's postulates have not been fulfilled for this disease, so possible interactions with other microrganisms cannot be ruled out. The pathogen lives in the insect and in the phloem of *Citrus* trees. Once acquired, it typically persists for the rest of the life of the host. Insecticides can decrease psyllid populations, but since the pathogen remains in the vector, disease spread can occur with the presence of just a few infected psyllids in the orchard. All genotypes within the genus *Citrus* are susceptible to HLB to varying degrees although species of other close-related genera showed some sort of resistance **[5]**. There is variability in disease severity and symptoms among *Citrus* genotypes **[6]**. *Murraya paniculata* (orange jasmine), an ornamental *Citrus* closely-related plant, showed fewer symptoms of the disease **[7]**. A study examining the responses of 30 genotypes to HLB disease grouped them based on phenotypic analysis of induced symptoms **[5]**. Another recent study has evaluated 65 *Citrus* accessions and 33 accessions belonging to other closely related genera. Resistance was reported in accessions not belonging to *Citrus* genera **[8]**. Another work have screened Citrus germplasm susceptibility to HLB analyzing sixteen Citrus genotypes **[9]**. Results showed that *Citrus macrophylla* and *C. medica* were the most susceptible while complex genetic hybrids 'US 1-4-59' and 'Fallglo' were the least susceptible. A metabolomic investigation was conducted comparing five different tolerant hybrids and a highly susceptible cultivar to identify potential metabolites linked with diverse response **[10]**. The causes of the disease have been studied using different "omic" approaches to identify which genes, proteins and metabolites may be targeted by innovative diagnostic and therapeutic methods. The genome of the pathogen was sequenced using a metagenomic approach, both from infected plants **[11]** and the insect vector **[12]**. No toxins or other secreted proteins have been linked to the disease

and the mechanisms of its pathology are still unclear. Large scale microarray analysis revealed significant modulation of genes involved in transport, cell defense and carbohydrate metabolism **[13,14]**. Photosynthesis is diminuished in both young and mature leaves, but it is upregulated in infected fruits **[14]**. Starch accumulation was linked to the upregulation of genes involved in glucose import into the chloroplast and starch biosynthesis **[15,16]**. A modulated Jasmonic (JA)-Salicilic acid (SA) crosstalk of innate responses may lead to a misdirected defence response. An integrated approach of 2-DE and mass spectrometry showed that changes in levels of several proteins involved in photosynthesis and protein synthesis were linked to reduced concentrations of Ca, Mg, Fe, Zn, Mn and Cu in infected grapefruit leaves **[17]**. Proteins upregulated in infected samples were involved in redox stage and cell defense such as Cu/Zn superoxide dismutase, peroxidases, chitinases and lectin-related proteins **[18]**. 'Madam Vinous' sweet orange plants infected by CaLas showed increased miraculin-like proteins, chitinase, Cu/Zn superoxide dismutase and lipoxygenase. Some key metabolites modulated by HLB include proline, β-elemene, (−)-trans-caryophyllene, and α-humulene **[19]**. Increased accumulation of some amino acids (L-proline, L-serine, and L-aspartic acid) and organic acids was linked to greater susceptibility of 'Madam Vinous' sweet orange compared to Carrizo citrange **[20]**. However, it is worthy to notice that these trees were highly infected with many secondary effects so it will be necessary to confirm these results with newly infected trees. An increased amount of most amino acids, involved in plant defense to pathogens was observed in tolerant varieties in such as phenylalanine, tyrosine, tryptophan, lysine, and asparagine **[21]**.

This study examines proteomic changes in fully photosynthesizing leaves to determine how disease mechanisms and susceptibility vary between two *Citrus* genotypes, using an integrated approach of principal component analysis (PCA), gene set and pathway enrichment analysis. The purpose was to characterize key proteins and post-transcriptionally modulated pathways in different *Citrus* genotypes at a late symptomatic stage of HLB.

2_MATERIALS AND METHODS

2.1_Material and experimental design

Citrus plant materials used in this study were propagated from disease free bud wood obtained from the California Citrus Clonal Protection Program (CCPP). Two-year old Volkameriana (V) (*Citrus* × *volkameriana)* and Navel orange (N) (*Citrus* × *sinensis*) trees were grafted on Carrizo citrange rootstocks (*Citrus sinensis* [L.] Osb.× *Poncirus trifoliata* [L.] Raf.). Trees were grown in pots in the greenhouse under natural light at 17 to 25°C in the Contained Research Facility (CRF) at UC Davis. Around 10 trees per genotype were infected with CaLas through graft inoculations using a standard inverted "T" budding technique with infected budwood from Lisbon Lemon (*Citrus limon* Burm.f.), with uninocculated trees maintained as an uninfected control. Starting at 3 months after budding, each plant was tested monthly using quantitative RT-PCR for CaLas species as described **[43]**. Three to four biological replicates of healthy and infected symptomatic trees were chosen for proteomic analysis based on health, phenotype and symptom severity. A pool of five to seven fully expanded leaves at the same developmental stage from each tree was sampled at eight months, constituting a biological replicate. From infected trees, leaves with characteristic yellowing and blotchy mottled appearance were sampled. Healthy leaves at the same developmental stage were harvested from the uninfected control trees. Petioles from four to six leaves sampled from different parts of each tree were tested by PCR for the presence of CaLas at the time of collection. Midribs and petioles were cut, frozen in liquid nitrogen and stored at –80°C for protein extraction and iTRAQ analysis. The other parts of the leaves were used to test for pathogen presence. Ct values of infected trees were < 30 while control trees showed no amplified product.

2.2_Protein extraction

Proteins were extracted using a previously described phenol-based procedure **[44]**. Leaves were ground in a mortar and pestle in liquid nitrogen with 1% (w/w) PVPP. One hundred mg plant material was resuspended in 600 µL extraction buffer (0.7 M Sucrose, 0.1 M KCl, 0.5 M Tris-HCl pH7.5, 0.5 M EDTA, 1 mM PMSF and 2% β-mercaptoethanol). Samples were homogenized twice (one min each) with a MM300 TissueLyser (Qiagen). An equal volume of UltraPure Buffer-Saturated Phenol (Invitrogen) was added and the mixture was rehomogenized as described above. After centrifugation at 12,000 x g for 15 min at 4°C, the upper phenol phase was eliminated and the pellet used for re-extraction in the same buffer. Protein was precipitated from the phenol phase using five volumes saturated ammonium acetate (100 mM) in methanol overnight at -20°C followed by centrifugation at 12,000 x g for 15 min

at 4°C. Pellets were washed four times with four mL saturated ammonium acetate (100 mM) in methanol and dried 10 min. Proteins were dissolved in urea buffer (7 M urea, 2 M thiourea, 40 mM Tris, 2% Chaps and 18 mM DTT). The protein concentration was determined using Bradford's method with BSA as a standard.

2.3_Protein sample preparation and digestion

Samples were precipitated using the ProteoExtract Protein Precipitation Kit (CalBiochem). The resulting protein pellet was solubilized in 400µL of 50mM triethyl ammonium bicarbonate (TEAB) and a 100 µL aliquot was taken for digestion. 500mM tris (2-carboxyethyl)-phosphine (TCEP) (Pierce, Rockford, IL) was added to a final concentration of 10 mM and samples were incubated for 10min at 90 °C to reduce disulfide bonds. Next, 110 mM iodoacetamide (IAA) was added to a final concentration of 15mM and incubated for 1hr at room temperature, followed by the addition of 20 µL DTT to quench the IAA reaction. Trypsin (Promega) was next added in a 1:25 ratio (enzyme: protein) and incubated at 37 °C for overnight. The following day, samples were desalted using C18 Macro Spin columns (Nest Group) and dried down by vacuum centrifugation.

2.4_Tandem mass tag labeling

Desalted and lyophilized samples were resuspended in 50mM TEAB and ~30ug of tryptic digested peptides were taken for TMT labeling. TMT labeling was performed on each aliquot with reporter ions m/z = 126.1, 127.1, 128.1, and 129.1 in 41µL ethanol, and aliquots were incubated for 60 min at room temperature. 8 µL hydroxylamine 5% (v:v) was added to quench the reaction and samples were vacuum-centrifuged prior to desalting using C18 Macro Spin columns (Nest Group). Samples were vacuum-centrifuged once more prior to strong cation exchange fractionation.

2.5_SCX Fractionation of Pooled TMT-Labeled Samples

Strong cation exchange (SCX) was carried out using the SCX SpinTips Sample Prep Kit (ProteaBio). Each aliquot was resuspended in 50µL of the designated buffer and ~10 µg of each sample was pooled prior to SCX fractionation. Samples were fractionated by stepwise addition of 20, 40, 60, 80, 100, 150, 250, and 500 mM ammonium formate in 10% acetonitrile. All eight fractions, including the initial binding flow through, were vacuum-centrifuged to remove any acetonitrile and desalted using C18 Macro Spin columns (Nest Group).

2.6_LC-MS/MS Analysis

LC separation was done on a Waters Nano Acquity UHPLC (Waters Corporation) with a Proxeon nanospray source. Each SCX fraction (9 total) was reconstituted in 2% acetonitrile / 0.1% trifluoroacetic acid and loaded onto a 100 µm x 25 mm Magic C18 100 Å 5U reverse phase trap. Peptides were eluted using a gradient of 0.1 formic acid (A) and 100 % acetonitrile (B) with a flow rate of 300 nL/min. A 60 min gradient was run with 5 to 35 B over 50 min, 35 to 80 B over 3 min, 80 B for 1 min, 80 to 5 B over 1 min, and finally held at 5% B for 5 min.

Mass spectra were collected on an Orbitrap Q Exactive Plus mass spectrometer (Thermo Fisher Scientific). A dynamic exclusion of 15 s was used. MS spectra were acquired with a resolution of 70,000 and a target of 1 × 106 ions or a maximum injection time of 30ms. MS/MS spectra were acquired with a resolution of 17,500 and a target of 5 × 104 ions or a maximum injection time of 50ms, and a fixed first mass of 110 m/z. Peptide fragmentation was performed using higher-energy collision dissociation with a normalized collision energy value of 30. Unassigned charge states as well as +1 and ions > +5 were excluded from MS/MS fragmentation.

2.7_Data Analysis

Tandem mass spectra were extracted and charge states were deconvoluted and deisotoped. All MS/MS samples were analyzed using X! Tandem (The GPM, thegpm.org; version X! Tandem Sledgehammer (2013.09.01.1)). X! Tandem was set up to search the *Citrus sinensis* genome (http://www.ncbi.nlm.nih.gov/protein/?term=txid2706 March 2014) and the NCBInr citrus database (155,237 entries, March 2014) assuming the digestion enzyme trypsin. X! Tandem was searched with a fragment ion mass tolerance of 20 PPM and a parent ion tolerance of 20 PPM. TMT6plex of lysine and the n-terminus was specified in X! Tandem as a fixed modification.

Scaffold Q+ (version Scaffold_4.4.0, Proteome Software Inc., Portland, OR) was used to quantitate Label Based Quantitation (iTRAQ, TMT, SILAC, etc.) peptide and protein identifications. Peptide identifications were accepted if they could be established at a 99.0 % probability by the Scaffold Local FDR algorithm, which corresponded to a 0.20 spectra decoy FDR and a 5.0% protein decoy FDR with 1 identified peptides per protein. Protein probabilities were assigned by the Protein Prophet algorithm **[45]**. Proteins that contained similar peptides and could not be differentiated based on MS/MS analysis alone were grouped to satisfy the principles of parsimony. Proteins sharing significant peptide evidence were grouped into clusters. Proteins sharing significant peptide evidence were grouped into clusters according to

the algorithm described in i-Tracker **[46]**. Individual quantitative samples were normalized within each acquisition run. Intensities for each peptide identification were normalized within the assigned protein. All normalization calculations were performed using medians to multiplicatively normalize data. Differentially expressed proteins were determined using Permutation Test analysis.

2.8_Statistical and functional data mining

Scaffold 4 was used to perform the first functional, annotation and quantitative analysis of the proteomic data. Arabidopsis orthologs, annotations, unique peptides and spectrum counts, and normalized quantitative values were determined for each sequenced and identified peptide. Data were blasted against the *Citrus x sinensis* (L.) and *Candidatus* liberibacter asiaticus (strain psy62) genomes. Arabidopsis orthologs were determined for each sequenced peptide by blastx (e-value < 10–4) to the TAIR database of predicted proteins in Arabidopsis (TAIR10_- pep_20101028; **[47]**). Blastx output was processed using custom scripts to calculate the best correspondence between individual citrus peptide sequences and Arabidopsis proteins, based on alignments over the entire length of each sequence. Lists of significantly differentially expressed proteins ($p < 0.05$, absolute value of log2 fold change > 0.5 or <- 0.5) were determined in pairwise comparison (infected/healthy) for each genotypes. This statistical analysis was performed using MeV software. Functions of differentially regulated proteins (as Arabidopsis orthologs) were visualized using MapMan **[48]**. Gene set enrichment analysis was performed using DAVID Bioinformatics resource 6.7 based on KEGG maps. The corresponding Arabidopsis orthologs of each protein upregulated or downregulated during infection for each genotype was loaded as a gene list in DAVID ($p < 0.05$). Arabidopsis orthologs were determined for each citrus proteins and the gene set enrichment analysis was obtained comparing the list of differentially regulated proteins with all those identified by the proteomic analysis.

The PageMan visualization tool was used for GSEA with the Wilcoxon test (no correction and 1.0 as ORA cutoff). Principal component analysis (PCA) was performed using SAS II (2008) SAS/STAT software (SAS Institute). Principal component analysis was applied to the ratio matrix of gene expression data to examine the contribution of each target gene to the separation of sample classes. A biplot was constructed based on the first two principal components.

3_RESULTS AND DISCUSSION

Navel orange (*Citrus* sinensis (L.)) is an HLB-sensitive cultivar while Volkameriana is moderately tolerant **[5]**. Different techniques (2-DE, mass spectrometry and ICP mass spectroscopy) have been used to identify key proteins differentially regulated by HLB in *Citrus* leaves **[19, 20]**. Over 4000 proteins were analyzed using isobaric tags for relative and absolute quantitation (iTRAQ) for both genotypes (4557 in Volkameriana and 4521 in Navel orange). In Navel orange, 599 proteins were differentially regulated between infected and healthy tissue (P-value < 0.05 and Log_2 FD > 0.5 and < -0.5) (Additional file 1: Table S1). In Volkameriana, 411 differentially regulated proteins were found between infected and healthy tissue (Additional file 2: Table S2).

3.1_PCA analysis

PCA was used to visualize differences between the four analyzed genotypes x disease status, subdividing the entire proteomic profile into three important subcategories: biotic stress responses, overall cell metabolism and transcriptional regulation pathways (**Fig. 1**). All identified proteins belonging to these important functional categories were used for the PCA plots. The four categories of samples (healthy V, healthy N, infected V and infected N) were clearly separated in all three PCA plots, implying significant protein changes in all three gene categories related to species and health status. For biotic stress-related proteins, PC1 and PC2 accounted for 40 and 24% of the data variability, respectively. Important proteins associated with each functional category that contributed to separation between sample types (indicated by directions of vectors) are listed in Fig. 1. Some key proteins involved in redox state significantly contributed in the separation of Infected V from the rest of the other categories. In the general metabolism PCA plot, the PC1 and PC2 accounted for 49 and 24% of the data variability, respectively. Key proteins involved in primary metabolism associated with the separation of Healthy V from the Infected V include malate dehydrogenase and pyruvate dehydrogenase (TCA cycle-glycolysis), sucrose synthase and AGPase (sucrose and starch metabolism). The third PCA plot was generated based on the expression of proteins involved in transcriptional regulation, signaling, hormone and redox state. PC1 and PC2 accounted for 37 and 27% of data variability, respectively. Interestingly, the regulation of few important proteins seems to specifically characterize the infected vs. healthy state of Navel orange. These include MAP kinase 4, UDP-glucosyl transferase, and aspartyl protease. No changes were observed for MAPK6. Proteins that appear in the three PCA plots were highly regulated in the comparison between infected and control in both *Citrus* genotypes. Indeed, they may be

considered as putative candidate biomarkers of a clear symptomatic status in *Citrus* at proteomic level. Their HLB-regulated pattern of expression greatly contributed in distinguishing the four different leaf sample types. Further analysis will need to validate these data and confirm the role in the pathogenesis of HLB disease.

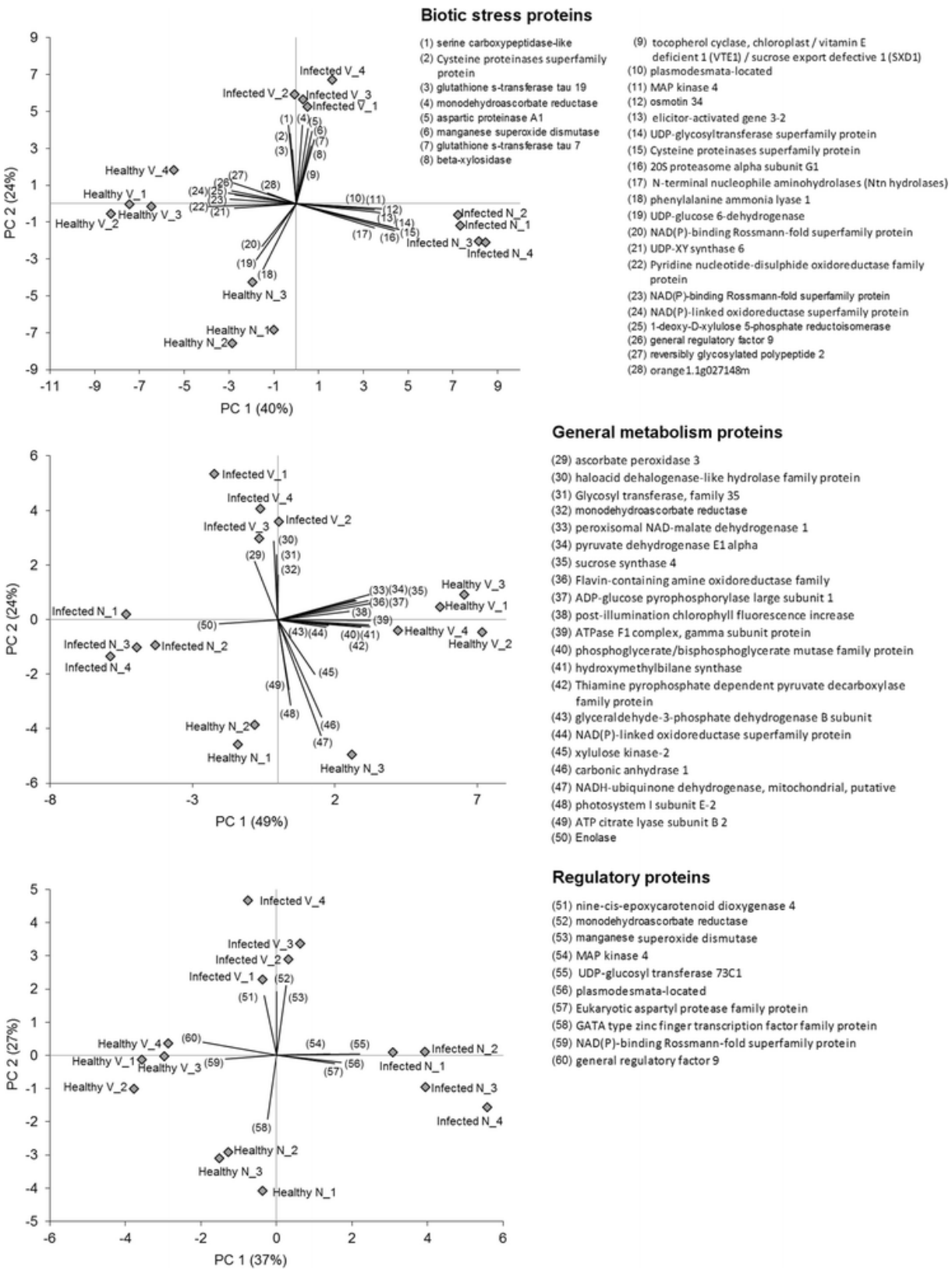

Fig. 1| Principal component analysis of differentially regulated proteins of four types of leaf tissues (Control Navel orange, Control Volkameriana, Infected Volkameriana and Infected Navel orange). Proteins that contribute highly to the separation of the the four samples are numbered and listed next to each graph.

3.2_Gene set and pathway enrichment analysis

The Pageman web tool highlighted which gene categories were up- or down-regulated in each pairwise comparison (**Fig. 2**). Both infected genotypes exhibited repressed amino acid biosynthesis and protein synthesis. In Navel orange, photosynthesis, isoflavone pathways, tetrapyrrole synthesis, and galactose metabolism were significantly inhibited by HLB. In Volkameriana, S-assimilation, isoprenoids, RNA binding and amino acid activation were specifically diminished. In both genotypes, HLB enhanced starch-related pathways, biotic stress-related proteins, beta 1,3 glucan hydrolases, and protein degradation pathways. Some distinct differences were observed between genotypes in HLB response. In Volkameriana, cell wall modifications, galactose metabolism, and heat shock proteins were upregulated. In Navel orange, amino acid degradation, lipid metabolism, jasmonates, and PR-proteins were upregulated.

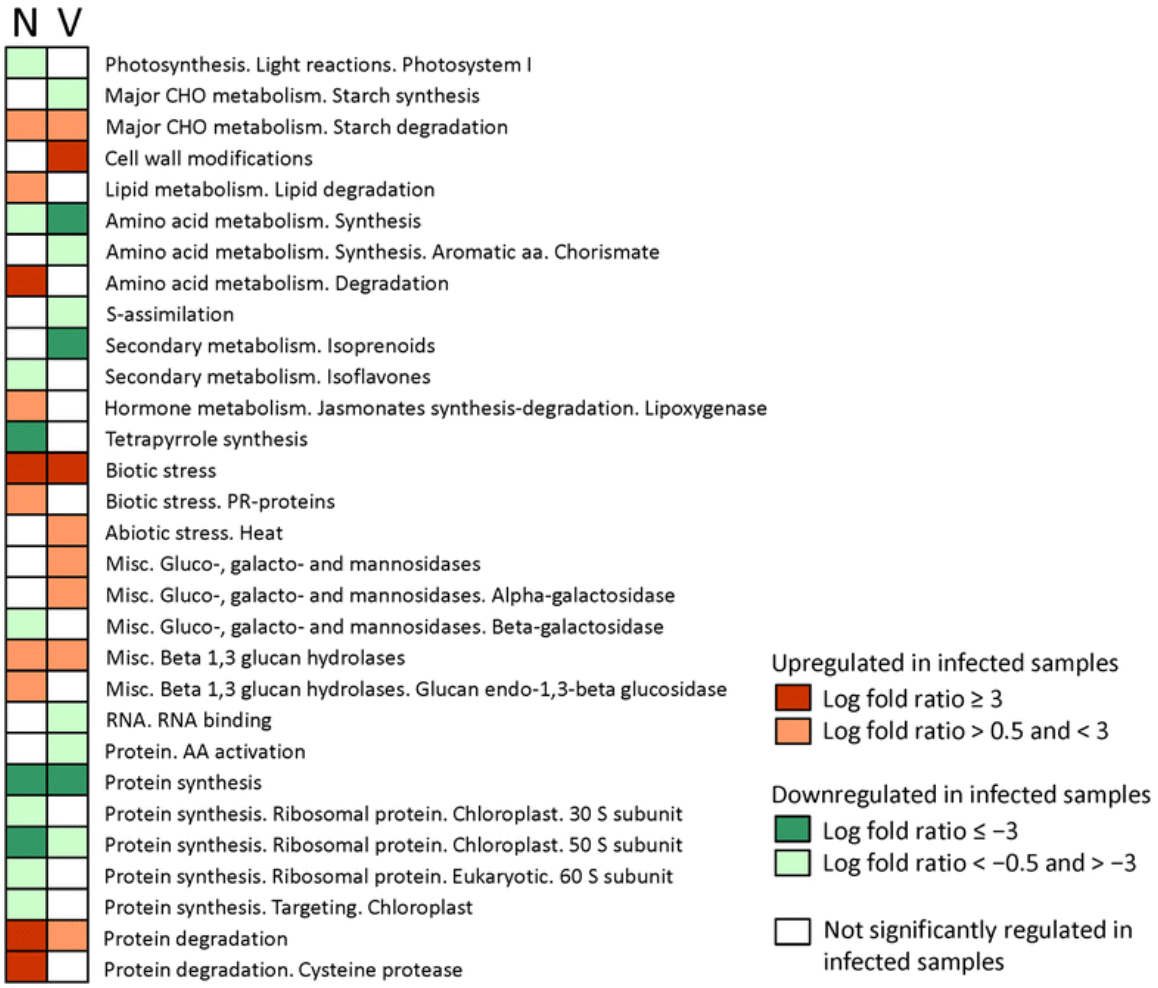

Fig. 2| Gene set enrichment analysis using Pageman web-tool. Upregulated and downregulated pathways at proteomic level in infected Volkameriana (V) and infected Navel orange (N) in comparison to respective healthy controls

A pathway enrichment analysis was performed using the DAVID bioinformatic resource to determine which metabolic pathways were commonly or specifically affected by HLB disease in both genotypes (**Table 1**). Some metabolic pathways were altered by HLB in both species. Amino acid metabolism (glycine, serine, threonine, phenylalanine and tryptophan) was significantly downregulated. Other key inhibited pathways include biosynthesis of plant hormones, terpenoids, and phenylpropanoids. On the other hand, tyrosine metabolism was upregulated in both genotypes. In Navel orange, fatty acid biosynthesis and nitrogen metabolism were diminished while alpha-linolenic acid metabolism was enhanced. In Volkameriana, alkaloids and pyruvate metabolism-related proteins were repressed while galactose metabolism and fatty acid metabolism were upregulated.

Table 1| Pathway enrichment analysis using DAVID Bioinformatics Resources 6.7. Pathways that were upregulated and downregulated for the healthy/infected comparison for each genotype are indicated with the corresponding p-value

Pathway	Navel orange		Volkameriana	
	Up	Down	Up	Down
Fatty acid biosynthesis		$9.2*10^{-3}$		
Glycine, serine and threonine metabolism		$1.3*10^{-2}$		$2.6*10^{-2}$
Biosynthesis of plant hormones		$1.5*10^{-2}$		$1.4*10^{-3}$
Porphyrin and chlorophyll metabolism		$1.6*10^{-2}$		$2.9*10^{-2}$
Phenyalanine, tyrosine and tryptophan biosynthesis		$2.7*10^{-2}$		$3.3*10^{-3}$
Carbon fixation in photosynthetic organisms		$2.9*10^{-2}$		
Terpenoid backbone biosynthesis		$3.0*10^{-2}$		$2.1*10^{-2}$
Nitrogen metabolism		$3.3*10^{-2}$		
Biosynthesis of phenylpropanoids		$4.8*10^{-2}$		$2.3*10^{-2}$
alpha-linolenic acid metabolism	$1.6*10^{-3}$			
Tyrosine metabolism	$8.3*10^{-3}$		$1.8*10^{-2}$	
Biosynthesis of alkaloids from shikimate pathway				$4.4*10^{-3}$
Pyruvate metabolism				$2.5*10^{-2}$
Biosynthesis of alkaloids from terpenoid and polyketide				$4.5*10^{-2}$
Proteasome			$2.7*10^{-3}$	
Galactose metabolism			$8.2*10^{-3}$	
Fatty acid metabolism			$4.3*10^{-2}$	

3.3_Primary metabolism

The integration of the two pairwise comparisons into a unified Mapman visualization allowed us to identify proteins that were commonly or specifically regulated in response to HLB in the two species. Some proteins involved in cell wall modifications were upregulated by HLB only in Volkameriana: expansin A1, expansin A8, expansin-like B1, xyloglucan endotransglycosylase 6, and xyloglucanxyloglucosyltransferase (TCH4) (Additional file 3: Figure S1). In Navel orange, proteins involved in fatty acid biosynthesis and elongation were generally repressed while several key proteins involved in amino acid degradation were upregulated: arginase, pyrroline-5-carboxylase reductase, lactoylglutathione lyase, and 3-hydroxylmethylglutaryl-CoA lyase. The increase of protein degradation indicates that senescence processes may be more highly activated in HLB-diseased Navel orange than in Volkameriana.

Sucrose metabolism was only slightly affected by HLB at the protein level; only sucrose synthase was repressed. Starch metabolism was more altered (**Fig. 3a**). The first enzyme of starch biosynthesis, ADP-glucose pyrophosphorylase, was inhibited by HLB in both genotypes. In Volkameriana, starch synthase was upregulated while 1,4-alpha-glucan starch branching enzyme was slightly downregulated. Among starch degradation enzymes, glucan phosphorylase and heterogycan glucosidase 1 were upregulated in both genotypes. Alpha-amylase was upregulated in Volkameriana while beta-amylase 6 was enhanced in Navel orange. Taken together these findings showed that starch metabolism was highly affected in both genotypes at the protein level. No clear association between differing susceptibility to HLB is evident from starch pathway regulation alone.

A significant downregulation in HLB-infected samples was observed for proteins involved in photosynthetic reactions **[17]**. The altered transcription of sugar and starch metabolism genes caused by HLB **[16]** mostly agreed with the corresponding protein changes presented in the present work. The observed changes in starch-related pathways were consistent with the transcriptomic analysis **[16]**. Increased starch degradation was observed probably due to the increased starch concentrations in infected leaf tissues. ADP glucose-pyrophospholyase (ADPase) was repressed in both infected species. This enzyme is rate-limiting for starch biosynthesis, catalyzing the conversion of glucose-1-phosphate to ADP-glucose that is polymerized into amylopectin or amylose **[22]**. Starch accumulation in infected leaves is a typical symptom of HLB **[1]**. However, the greatest occurrence of this process may occur at an early, asymptomatic stage. Indeed we may speculate that the accumulation of starch may be a secondary effect of the disease instead of being the cause of symptoms. When symptoms are

already evident and yellowing is present, starch biosynthesis may slow down and starch degradation is expected to be activated as a response of the plant to limit damage to cell structures. However, some differences in primary metabolism were observed between transcriptomic and proteomic approaches. Changes in invertase gene expression were observed **[16]**, but not its protein levels. Sucrose, the substrate of invertase, is produced by photosynthesis in leaves and then transported to sink tissues (immature fruits and young leaves) through the phloem. Involvement of sucrose in signaling of innate responses has been described recently **[23]**. Invertase plays an important role in plant stress responses, possibly serving as an extracellular signal of pathogen attacks **[24]**. It is possible that expression of this gene in response to HLB depends on genotype, plant physiological conditions and age, tissue developmental conditions, type of infection (psyllid inoculation or graft-mediated) and/or environmental conditions (field or controlled environment). Taken together all these primary metabolism results concur with previous findings showing significant modification of transcript abundance in minor carbohydrate metabolism **[16]** but do not suggest a clear link to the well-known difference in tolerance between the two genotypes.

GPT2 has been linked with HLB disease: this gene is responsible for glucose import into the chloroplast and consequently for starch accumulation **[13, 16]**. The protein was not found among those extracted and characterized by iTRAQ, therefore no conclusions can be made about changes in protein levels due to HLB. However, the protocol used to analyze the *Citrus* proteome favored detection of soluble cell proteins over membrane proteins such as GPT2.

Expression of key proteins involved in the TCA cycle and PEP metabolism were affected by HLB. ATP-citrate lyase subunit B2 was repressed in both species (**Fig. 3b**). Alcohol dehydrogenase 1 which converts aceltaldehyde to ethanol, was upregulated in both genotypes. In infected Navel orange, isopropyl malate isomerase, which converts citrate to isocitrate and pyruvate decarboxylase involved in fermentation, was more abundant than in healthy tissue. In Volkameriana, pyruvate decarboxylase was repressed while aconitate hydratase involved in TCA cycle was upregulated.

Raffinose metabolism was drastically altered by the disease (**Fig. 3c**). In Navel orange, expression of alpha-galactosidase 1, UDP-glucose-4-epimerase, glucose-6-phosphate isomerase, and alpha-galctosidase 1 were enhanced by HLB. In Volkameriana, raffinose synthase, phosphofructokinase 3 and phosphoglucomutase were upregulated. Sucrose synthase 4 and phosphoglycerate mutase were donwregulated in both genotypes. A transketolase that converts the xylulose-5-P in sedoheptulose-7-P was repressed in infected Navel orange (**Fig. 3d**).

Significant repression of aspartate biosynthesis and serine metabolism was observed in infected Navel orange leaves. This agrees with a previously described downregulation of serine-type peptidases at both asymptomatic and symptomatic stages **[18]**. In infected Navel orange, seventeen proteins involved in amino acid biosynthesis were downregulated. Fewer proteins were downregulated in infected Volkameriana. On the other hand, some upregulated proteins involved in amino acid degradation were identified only in infected Navel orange. Taken together, these findings suggest that amino acid metabolism in Navel orange is more sensitive to degradation during HLB infection than in Volkameriana.

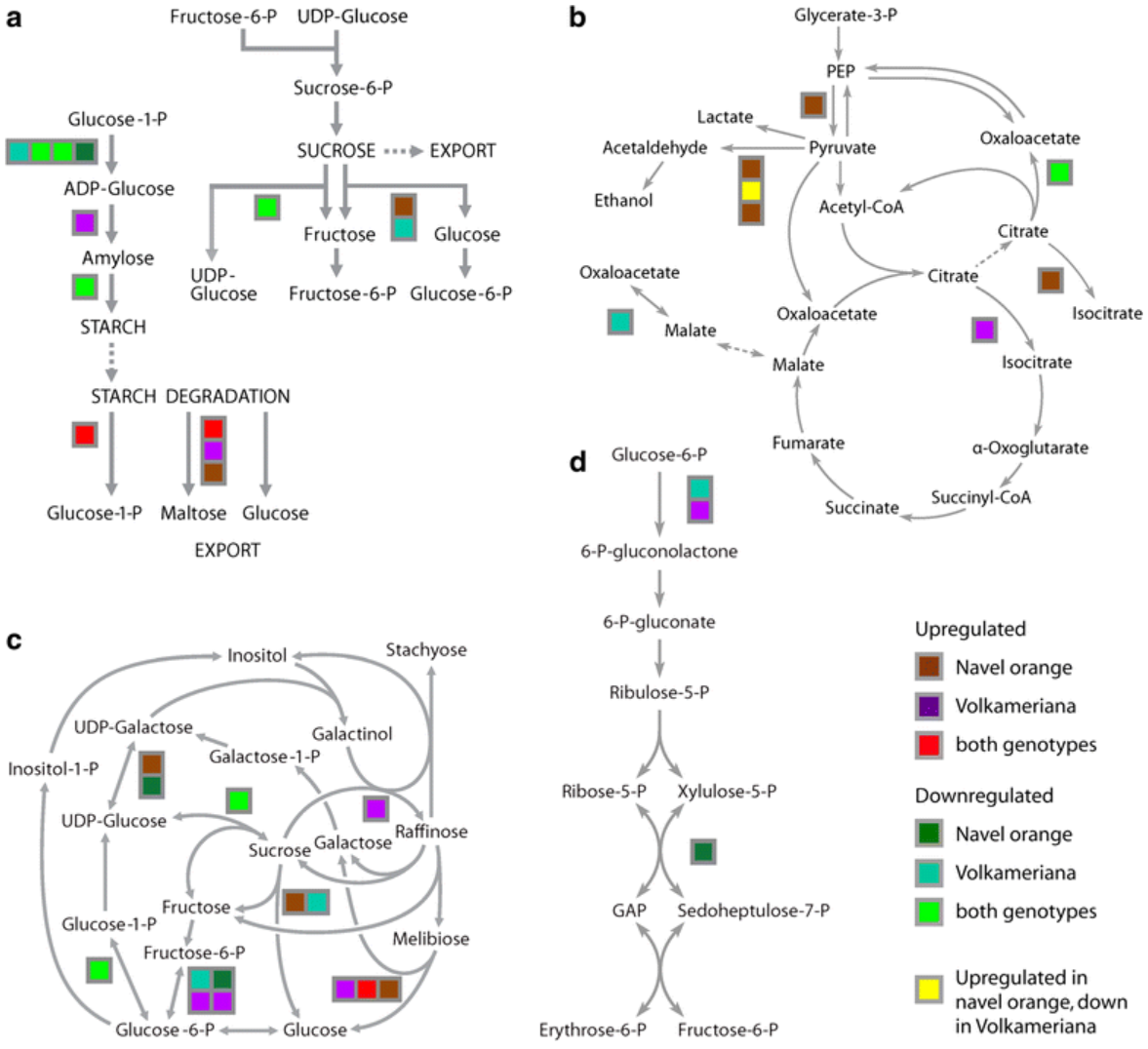

Fig. 3| Proteins involved in primary metabolic responses to HLB. A) Sucrose and starch metabolism; B) Raffinose metabolism; C) TCA cycle; D) Oxidative pentose phosphate. Proteins that were differentially expressed between control and infected trees are indicated by colors, based on their pattern of expression in the two genotypes (see color key). Each colored square represents expression change in a protein catalyzing a step in the pathway. More than one square grouped together indicates different members of the same protein family found to be differentially regulated

3.4_Secondary metabolism

A general repression of key proteins involved in biosynthesis of secondary metabolites was observed in both cultivars in response to CaLas infection (Additional file 4: Figure S2). Geranylgeranyl reductase and 1-deoxy-D-xylulose 5-phosphate reductoisomerase, involved in the non-MVA pathway, were repressed. Other commonly HLB-downregulated proteins involved in the shikimate pathway included 2-dehydro-3-deoxyphosphoheptonate aldolase, 3-dehydroquinate synthase, 3-phosphoshikimate-1-carboxylvinyltransferase and mevalonate diphosphate decarboxylase. Two key proteins involved in phenylpropanoids, phenylalanine ammonia lyase and aryl-alcohol dehydrogenase, were more abundant in both species in response to HLB, while cinnamyl alcohol dehydrogenase 9 was repressed. Two proteins involved in alkaloid biosynthesis, tropinone reductase and strictosidine synthase-like 4, were upregulated in infected Volkameriana.

Findings related to *Citrus* activated defense responses against CaLas infection are shown in **Fig. 4**. Three proteins involved in auxin signal transduction were activated in infected Volkameriana: auxin resistant 1 and two aldo/keto reductases. One aldo/keto reductase was HLB-regulated in both genotypes. Three proteins involved in jasmonic and salicylic acid responses were induced in Navel orange but not in Volkameriana. Lipoxygenase 2 was upregulated in both genotypes. Some key proteins involved in cell wall modifications were commonly regulated by both genotypes: UDP-glucose-6-dehydrogenase, UXS6, UXS2, and RHM1. Proteolytic-related proteins were altered in both genotypes. Taken together these findings do not suggest any clear association between the two genotypes and proteomic changes in hormonal crosstalk, cell wall and proteolytic pathways.

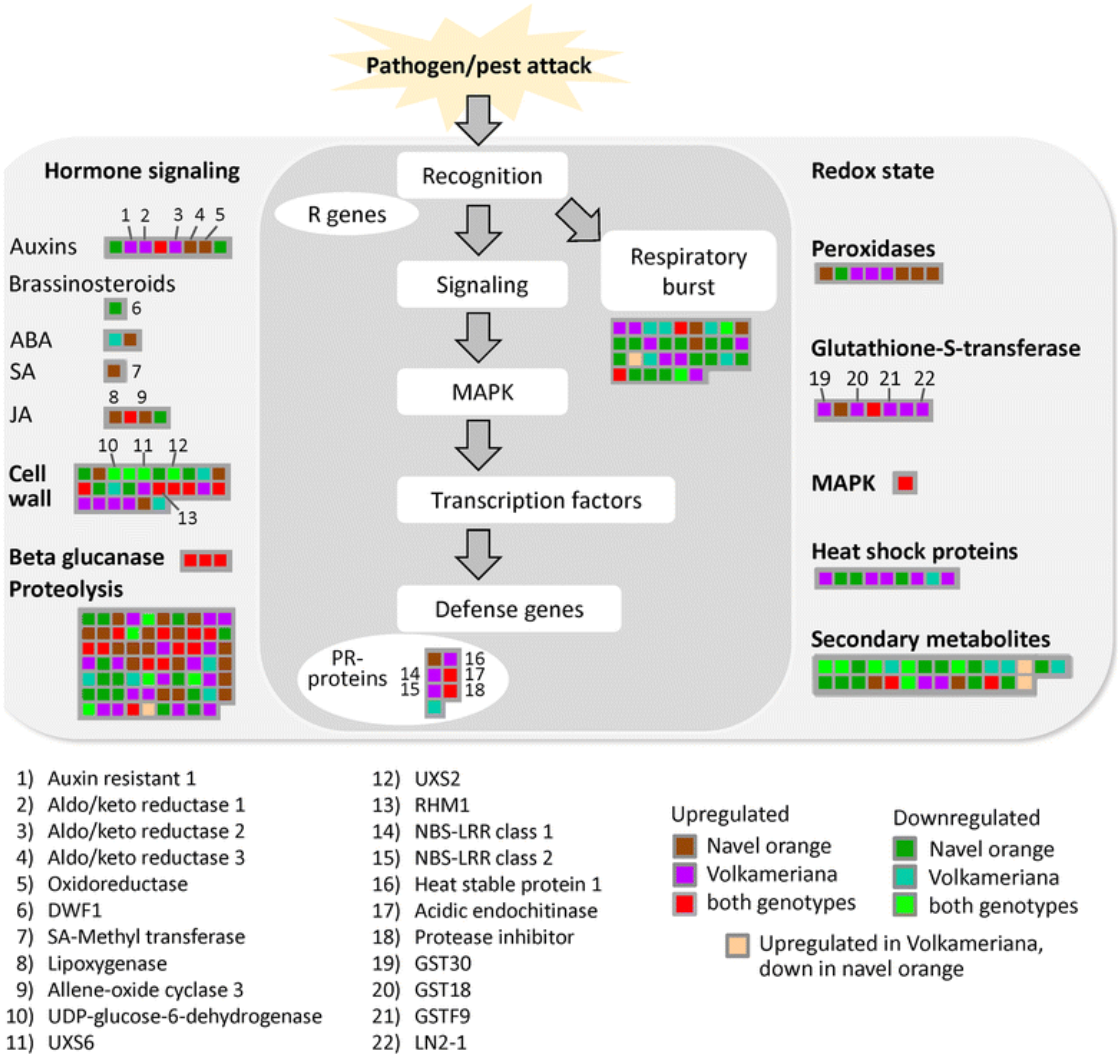

Fig. 4| Biotic stress–related proteins altered in response to HLB disease in both Citrus genotypes. Proteins that were differentially expressed between control and infected trees are indicated by colors, based on their pattern of expression in the two genotypes (see color key). Each colored square represents expression change in a protein associated with regulatory and enzymatic functions

Some proteins synthesizing volatiles via the phenylpropanoid and carotenoid pathways were affected in the present study (**Fig. 5**). The marked differences between the two species suggests that to be effective, any innovative HLB-detection system based on induced volatiles must be cultivar-specific.

Plant phenols not only counteract reactive oxygen species and pathogen-secreted toxins, but also play roles in transport and signal transduction pathways. Polyphenol chemistry is critical to adapting plants to environmental stresses, including pathogens **[25]**. Phenylalanine ammonia-lyase (PAL) was downregulated by HLB infection in both species (Additional file 4: Fig. S2). This enzyme is a key regulatory point for the entire phenylpropanoid pathway. Enhancement of its transcript abundance is linked to phytopathogen attacks **[26]**. Another

important protein encoding isoflavone reductase and involved in antioxidant reactions was repressed in both the infected species, consistent with previous proteomic analysis **[18]**. In general, RNA-seq analysis showed that phenylpropanoid pathways were transcriptionally affected by HLB in both young and mature infected leaves in field grown mature trees **[16]**. These previous findings are not completely consistent with the present proteomic data. Gene set enrichment analysis showed a general downregulation of secondary metabolism in both genotypes, although some key proteins were upregulated in response to the disease. These contrasting findings may reflect differences in developmental and physiological stages of the plants analyzed in the two studies or differences in environmental and agronomic conditions. Although phenylpropanoids may be activated at early stages of infection, their repression when symptoms are severe is expected. The large number and complexity of metabolites belonging to phenylpropanoid pathways makes the clarification of their many roles in the host-pathogen battle difficult.

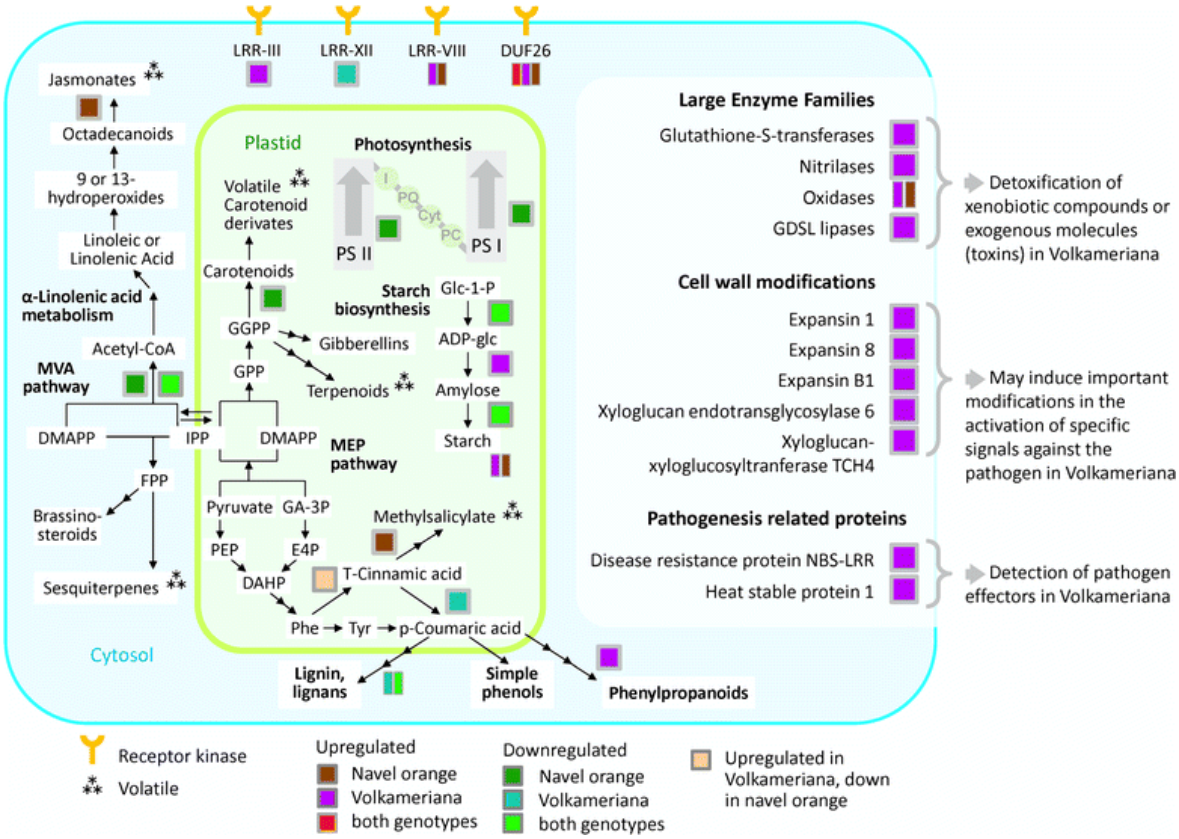

Fig. 5| Global view of proteomic changes in Citrus leaves (Volkameriana and Navel orange) in response to CaLas infections. Proteins, pathways, and cell functions that were differentially expressed are indicated by colors, based on their pattern of expression in the two genotypes. Each colored square represents expression change in a protein associated with regulatory and enzymatic functions. More than one rectangle grouped together indicates different members of the same protein family were found to be differentially regulated

3.5_Hormonal crosstalk

Plant innate responses are finely controlled by hormonal crosstalk, particularly between JA and SA signaling. The induction of allene oxide cyclase in infected Navel orange (**Fig. 4**) is intriguing because jasmonic acid signal transduction is a key pathway activated in response to necrotroph and herbivore attacks. JA-responsive proteins, gibberellin signaling (GASA1 and gibberellin-2-oxydase), and auxin signaling (CYP711A1 and SAUR-like proteins) were upregulated in mature infected leaves of Valencia orange **[16]**. Because CaLas is a biotroph, the activation of JA may be deleterious for the host as previously suggested **[16]**. Brassinosteroids affect disease resistance in plants **[27]** probably due to the induction of BAK1, which interacts with PAMP receptors such as bacterial flagellin to activate immune responses **[28]**. The ST1 gene was repressed in HLB-infected leaves **[16]**. However, the connections of brassinosteroids with the SA-ET-JA crosstalk and plant immunity remain elusive. On the other hand, auxin-related proteins were upregulated by HLB in both *Citrus* genotypes. Because of the antagonist role of auxins toward SA response **[29]**, we may speculate that these effects are deleterious to the infected host.

Proteomic studies have revealed post-transcriptional regulation of genes involved in key pathways which may be responsible for variations in phenotypic responses to HLB. The regulation of carbohydrate metabolism (sucrose, starch, and raffinose metabolism) is clearly altered at symptomatic stage at both transcript and protein levels. Differences in signaling mechanisms and hormone-mediated defense responses may also contribute to the range of tolerance to HLB within the *Citrus* germplasm. The most compelling finding was that proteins involved in redox pathways and defense against xenobiotics (especially GSTS) were more abundant in Volkameriana than in Navel orange, and this may be linked with the former's greater tolerance. Four GSTs were significantly upregulated in infected Volkameriana and not in infected Navel orange: GST18, GST19, GHST30, LN2-1. These effects on the proteome may explain the greater susceptibility of Navel orange compared to Volkameriana. While these findings regarding *Citrus* responses are valuable in the ongoing efforts to combat this deadly disease, further studies are still needed to validate these findings and deliver effective targets to develop new therapeutic strategies.

3.6_Signaling and defense response pathways

Some proteins encoding receptor kinases of the LRR type were HLB-regulated: one was upregulated in Volkameriana, one was repressed in Navel orange and two different proteins of LRR-VIII were upregulated (one in Volkameriana and one in Navel orange). Leucine-rich

repeat receptor kinases are the largest category of receptor kinases and mediate signaling of defense responses in plants. Other receptor kinases (VIII and DUF26) were upregulated in both *Citrus* genotypes. The proteins belonging to Domain of Unknown Function 26 were upregulated in response to HLB: one in Volkameriana, one in Navel orange and one commonly regulated. DUF26 is one of the largest classes of receptor-like kinases (RLKs). These proteins play important roles in regulating pathogen defense and programmed cell death **[30]**. Based on the proteomic results in this study, we speculate that diverse signaling mechanisms occur depending on the *Citrus* genotype. It is possible that variability in susceptibility of *Citrus* may result from pathogen perception due to activation of different receptors which in turn activate defense responses which vary in speed and intensity. Much remains to be learned regarding which receptor family is involved in susceptible or resistant responses to HLB.

Several proteins involved in calcium regulation were less abundant in infected leaves of Navel orange: calmodulin-binding and calcium-transporting ATPase. This is consistent with the significant drop in calcium concentration observed in symptomatic leaves **[17]**. Three 14-3-3 proteins were also HLB-downregulated in Navel orange and not in Volkameriana. These are a large family of proteins present in all eukaryotic organisms that aid signaling by binding other proteins such as kinases, phosphatases, and receptors (i.e. the P-type H+ ATPases) **[31]**.

Volkameriana showed significant stimulation of respiratory burst and consequent redox state, a prerequisite of the upregulation of pathogenesis-related proteins. Enzymes involved in the control of reactive oxygen species were generally enhanced in response to CaLas infection in both genotypes although Volkameriana showed a higher activation of glutathione-S-transferases (GST30, GST18, GSTF9, LN2-1). The upregulation of these important detoxification proteins may be linked with the increased tolerance of Volkameriana in comparison to Navel orange. An upregulation of enzymes involved in the biosynthesis of peroxiredoxins, Cu/Zn superoxide dismutase and 2Fe-2S ferredoxin-like protein, occurred at both asymptomatic and symptomatic stages **[18]**. Glutathione S-transferase family proteins include several isozymes that help detoxify xenobiotic compounds **[32]**. Plant GSTs add glutathione to electrophilic xenobiotic molecules pushing them into the cell vacuole. Regulation of these proteins by environmental stress stimuli suggests a role in protection against any harmful event **[33]**. GSTs have been linked with hormone homeostasis and their high affinity for auxins suggests their upregulation is a general signal of responses to stress **[34]**. Stress-inducible GSTs conjugate deleterious metabolites caused by oxidative damage. Inducible GSTs may play the important role of detoxifying exogenous molecules such as phytotoxins produced by pathogen attacks. Higher levels of GSTs in Volkameriana strengthens the hypothesis that they protect against dangerous molecules generated by CaLas attack. Indeed, differential

activation of GSTs may explain some of the variability of *Citrus* responses to HLB. Some peroxidases were also upregulated in both genotypes. These enzymes detoxify excess H_2O_2 **[35]** and they are grouped based on their subcellular localization **[36]**. As previously suggested **[37]**, greater *Citrus* susceptibility to HLB may be linked to a failure to rapidly induce antioxidant components to alleviate the devastating effects of ROS produced by CaLas. It has been suggested **[38]** that this category of proteins may be considered candidate markers in field-grown for the detection of the devastating disease "Esca" in grapevine. In the same way high expression of GSTs are potential candidate markers for genotypes with useful tolerance to HLB. Further investigations will need to be conducted for a large number of genotypes.

Pathogenesis-related (PR) proteins are plant defensive proteins against biotic attacks **[39]**. More PR-proteins were induced in Volkameriana than in Navel orange, consistent with the differing tolerance. Resistance (R) genes specifically activate a resistance reaction to a particular pathogen. NBS-LRR proteins are the most numerous R-gene class. NBS-LRR genes are finely controlled by regulatory mechanisms that allow their expression only when a biotic attack occurs, and limiting their metabolic cost when they are not required **[40]**. It is possible that the two NBS-LRR proteins upregulated in Volkameriana may contribute to enhanced tolerance of HLB disease. Heat shock proteins (HSP) are molecular chaperones with important functions in non-covalent protein folding or unfolding, assembly, and modifications. Genes encoding HSP70, HSP82 and other small heat shock proteins were expressed at lower levels in HLB disease in both fruit and leaf tissues **[16, 41]**. Down-regulation of HSP70, chaperon-60kD and chaperonin-60alpha was also seen in infected grapefruit **[17]**. In the present study, HSP81, HSP21 and HSP23 were induced in Volkameriana while several HSP proteins were inhibited in Navel orange. Taken together, we conclude that the observed upregulation of some HSPs in Volkameriana may contribute to increased tolerance to HLB disease.

3.7_Overall metabolism

The repression of key proteins involved in photosynthetic light reactions was linked with the upregulation of starch-related pathways. Infected Volkameriana exhibited up-regulated nitrilases, oxydases, glutathione-S-transferases and other proteins involved in redox state. Infected Volkameriana also exhibited enhanced production of expansins and xyloglucan endotransglycosylases.

Proteins commonly altered by HLB in both genotypes strengthen the data at proteomic level. The WD40 repeat-like protein was upregulated along with some enzymes involved in protein targeting, degradation, and glycosylation such as cysteine peptidase 3, proteinase A1,

and cysteine protease. Additional file 5: Figure S3 presents a complete list of commonly regulated proteins and their abundance in the four examined *Citrus* sample categories.

4_CONCLUSIONS

Forty-six of the 71 proteins were encoded by genes that were found to be transcriptionally regulated by HLB by previous studies in field conditions. Any comparison between transcriptomic and proteomic studies should take into consideration that experiments were performed with different plant material grown under differing environmental, developmental and physiological conditions. We have applied an integrated approach using principal component analysis (PCA), gene set enrichment analysis and functional data mining to identify specific key proteomic changes in response to Huanglongbing disease in these two *Citrus* genotypes. The analysis of post-transcriptional mechanisms is an essential step to link molecular regulatory networks to observed phenotypic changes. Interestingly, the clearest differences between the two genotypes were observed for proteins involved in redox state and detoxification pathways such as glutathione-S-tranferases. HLB disease strongly affected genes and metabolites of the terpenoid, carotenoid, and jasmonic acid pathways **[16, 42]**.

5_REFERENCES

1. Bové JM. Huanglongbing: a destructive, newly-emerging, century-old disease of Citrus. J Plant Pathol. 2006; 88:7-37.

2. Folimonova SY, Achor D. Early events of Citrus greening (Huanglongbing) disease development at the ultrastructural level. Bacteriology. 2010; 100:949-58.

3. Jagoueix S, Bové JM, Garnier M. The phloem-limited bacterium of greening disease of Citrus is a member of the alpha subdivision of the Proteobacteria. Int J of Syst Bacteriol. 1994; 44:397-86.

4. Sechler A, Schuenzel EL, Cooke P, Donnua S, Thaveechai N, Postnikova E, Stone AL, Schneider WL, Damsteegt VD, Schaad NW. Cultivation of "Candidatus Liberibacter asiaticus", "Ca. L. africanus", and "Ca. L. americanus" associated with huanglongbing. Phytopathology. 2009; 99:480-86.

5. Folimonova SY, Robertson CJ, Garnsey SM, Gowda S, Dawson WO. Examination of the responses of different genotypes of Citrus to Huanglongbing (Citrus greening) under different conditions. Phytopathology. 2009; 99:1346-54.

6. Fraser LR, Singh D. Reaction of Indian citrus varieties to greening virus. In: H.D. Chapman (Editor), Proc. 1st Int. Citrus Symp. Vol. I, Univ. Calif., Riverside; 1969. p. 365-366.

7. Manjunath KL, Halbert SE, Ramadugu C, Webb S, Lee RF. Detection of 'Candidatus Liberibacter asiaticus' in Diaphorina citriand its importance in the management of Citrus huanglongbing in Florida. Phytopathology. 2008; 98:387-396.

8. Ramadugu C, Keremane ML, Halbert SE, Duan Y, Roose M, Stover E, Lee RF. Long term field evaluation reveals HLB resistance in *Citrus* relatives. Plant Disease. doi: http://dx.doi.org/10.1094/PDIS-03-16-0271-RE.

9. McCollum G, Hilf M. Susceptibility of Sixteen Citrus Genotypes to '*Candidatus* Liberibacter asiaticus'. Plant Disease 2016; 100:1080-1086.

10. Albrecht U, Fiehn O, Bowman KD. Metabolic variations in different citrus rootstock cultivars associated with different responses to Huanglongbing 2016; 107:33-44.

11. Tyler HL, Roesch LFW, Gowda S, Dawson WO, Triplett EW. Confirmation of the sequence of 'Candidatus liberibacter asiaticus' and assessment of microbial diversity in huanglongbing-infected Citrus phloem using a metagenomic approach. Mol Plant Microbe In. 2009; 22:1624-34.

12. Duan Y, Zhou L, Hall DG, Li W, Doddapaneni H, Lin H, Liu L, Vahling CM, Gabriel DW, Williams KP, Dickerman A, Sun Y, Gottwald T. Complete genome sequence of Citrus huanglongbing bacterium, 'Candidatus Liberibacter asiaticus' obtained through metagenomics. MPMI. 2009; 22:1011–20.

13. Albrecht U, Bowman KD. Gene expression in Citrus sinensis (L.) Osbeck following infection with the bacterial pathogen Candidatus Liberibacter asiaticus causing Huanglongbing in Florida. Plant Sci. 2008; 175:291-306.

14. Kim J-S, Sagaram US, Burns JK, Li J-L, Wang N. Response of sweet orange (Citrus sinensis) to 'Candidatus Liberibacter asiaticus' infection: microscopy and microarray analyses. Phytopathology. 2009; 99:50-57.

15. Martinelli F, Uratsu SL, Albrecht U, Reagan RL, Phu ML, Britton M, Buffalo V, Fass J, Leicht E, Zhao W, Lin D, D'Souza R, Davis CE, Bowman KD, Dandekar AM. Transcriptome profiling of Citrus fruit response to Huanglongbing disease. PLoS One. 2012; 7:e38039.

16. Martinelli F, Reagan RL, Uratsu SL, Phu ML, Albrecht U, Zhao W, Davis CE, Bowman KD, Dandekar AM. Gene Regulatory Networks Elucidating Huanglongbing Disease Mechanisms. Plos One. 2013; 8:e74256.

17. Nwugo CC, Lin H, Duan Y, Civerolo EL. The effect of 'Candidatus Liberibacter asiaticus'infection on the proteomic profiles and nutritional status of pre-symptomatic and symptomatic grapefruit (Citrus paradisi) plants. BMC Plant Biology. 2013; 13:59.

18. Fan J, Chen C, Yu Q, Brlansky RH, Li Z-G, Gmitter FG. Comparative iTRAQ proteome and transcriptome analyses of sweet orange infected by "Candidatus Liberibacter asiaticus". Physiol Plant. 2011; 143:235-45.

19. Cevallos-Cevallos JM, García-Torres R, Etxeberria E, Reyes-De-Corcuera JI. GC-MS Analysis of Headspace and Liquid Extracts for Metabolomic Differentiation of Citrus Huanglongbing and Zinc Deficiency in Leaves of 'Valencia' Sweet Orange from Commercial Groves. Phytochem Anal. 2011; 22:236-46.

20. Cevallos-Cevallos JM, Futch DB, Shilts T, Folimonova SY, Reyes-De-Corcuera JI. GC-MS metabolomic differentiation of selected Citrus varieties with different sensitivity to citrus huanglongbing. Plant Physiol Biochem. 2012; 53:69-76.

21. Killiny N, Hijaz F. Amino acids implicated in plant defense are higher in Candidatus Liberibacter asiaticus-tolerant citrus varieties. Plant Signaling & Behavior 2016; 4: e1171449.

22. Nakamura T, Yamamori M, Hirano H, Hidaka S, Nagamine T. Production of waxy (amylose-free) wheats. MGG Mol Gen Gen. 1995; 248:253-59.

23. Tauzin AS, Giardina T. Sucrose and invertases, a part of the plant defense response to the biotic stresses. Front Plant Sci. 2014; 5:293.

24. Herbers K, Takahata Y, Melzer M, Mock HP, Hajirezaei M, Sonnewald U. Regulation of carbohydrate partitioning during the interaction of potato virus Y with tobacco. Mol Plant Pathol. 2000; 1:51-59.

25. Cheynier V, Comte G, Davies KM, Lattanzio V, Martens S. Plant phenolics: recent advances on their biosynthesis, genetics, and ecophysiology. Plant Physiol Biochem. 2013; 72:1-20.

26. Tonelli ML, Ibanez F, Taurian T, Argüello J, Fabra A. Analysis of a phenylalanine ammonia-lyase gene sequence from Arachis hypogaea L. and its transcript abundance in induced systemic resistance against Sclerotium rolfsii. J Plant Pathol. 2013; 95:191-95.

27. Nakashita H, Yasuda M, Nitta T, Asami T, Fujioka S, Arai Y, Sekimata K, Takatsuto S, Yamaguchi I, Yoshida S. Brassinosteroid functions in a broad range of disease resistance in

tobacco and rice. Plant J. 2003; 33:887-98.

28. Chinchilla D, Zipfel C, Robatzek S, Kemmerling B, Nürnberger T, Jones JDG, Felix G, Bolle T. A flagellin-induced complex of the receptor FLS2 and BAK1 initiates plant defence. Nature. 2007; 448:497-500.

29. Pieterse CMJ, Leon-Reyes A, Van der Ent S, Van Wees SCM. Networking by small-molecules hormones in plant immunity. Nat Chem Biol. 2009; 5:308-16.

30. Feuillet C, Schachermayr G, Keller B. Molecular cloning of a new receptor-like kinase gene encoded at the Lr10 disease resistance locus of wheat. Plant J. 1997; 11:45-52.

31. Jahn T, Fuglsang AT, Olsson A, Brüntrup IM, Collinge DB, Volkmann D, Sommarin M, Palmgren MG, Larsson C. The 14-3-3 protein interacts directly with the C-terminal region of the plant plasma membrane HC-ATPase. Plant Cell. 1997; 9:1805–14.

32. Sheehan D, Meade G, Foley VM, Dowd CA. Structure, function and evolution of glutathione transferases: implications for classification of non-mammalian members of an ancient enzyme superfamily. Biochem J. 2001; 360:1-16.

33. Edwards R, Dixon DP, Walbot V. Plant glutathione S-transferases: enzymes with multiple functions in sickness and in health. Trends Plant Sci. 2000; 5:193-98.

34. Marrs KA. The functions and regulation of glutathione S-transferases in plants. Annu Rev Plant Physiol Plant Mol Biol. 1996; 47:127-58.

35. Shigeoka S, Ishikawa T, Tamoi M, Miyagawa Y, Takeda T, Yabuta Y, Yoshimura K. Regulation and function of ascorbate peroxidase isoenzymes. J Exp Bot 2002; 53:1305-19.

36. Teixeira FK, Menezes-Benavente L, Galvão VC, Margis R, Margis-Pinheiro M. Rice ascorbate peroxidase gene family encodes functionally diverse isoforms localized in different subcellular compartments. Planta. 2006; 224:300-14.

37. Albrecht U, Bowman KD. Transcriptional response of susceptible and tolerant citrus to infection with 'Candidatus Liberibacter asiaticus'. Plant Sci. 2012; 185–186:118-130.

38. Valtaud C, Larignon P, Roblin G, Fleurat-Lessard P. Developmental and ultrastructural features of Phaeomoniella chlamydospora and Phaeoacremonium aleophilum in relation to xylem degradation in esca disease of the grapevine. J Plant Pathol. 2009; 91:37-51.

39. Lionetti V. PECTOPLATE: The simultaneous phenotyping of pectin methylesterases, pectinases, and oligogalacturonides in plants during biotic stresses. Front Plant Sci. 2015; 6:1-8.

40. Marone D, Russo MA, Laidò G, De Leonardis AM, Mastrangelo AM. Plant Nucleotide Binding Site–Leucine-Rich Repeat (NBS-LRR) Genes: Active Guardians in Host Defense Responses. Int J Mol Sci. 2013; 14:7302-26.

41. Martinelli F, Ibanez AM, Reagan RL, Phu M, Dandekar AM. Stress responses in citrus peel: Comparative analysis of host responses to Huanglongbing disease and puffing disorder. Sci Hortic. 2015b; 192:409-20.

42. Dandekar AM, Martinelli F, Davis CE, Bhushan A, Zhao W, Fiehn O, Skogerson K,

Wohlgemuth G, D'Souza R, Roy S, Reagan RL, Lin D, Cary RB, Pardington P, Gupta G. Analysis of Early Host Responses for Asymptomatic Disease Detection and Management of Specialty Crops. Crit Rev Immunol. 2010; 30:277-89.

43. Li W, Hartung JS, Levy L. Quantitative real-time PCR for detection and identification of Candidatus Liberibacter species associated with citrus huanglongbing. J Microbiol Methods. 2006; 66:104-15.

44. Schuster AM, Davies E. Ribonucleic Acid and Protein Metabolism in Pea Epicotyls. Plant Physiol. 1983; 73:817-21.

45. Shadforth IP, Dunkley TP, Lilley KS, Bessant C. i-Tracker: For quantitative proteomics using iTRAQTM. BMC Genomics. 2005; 6:145.

46. Nesvizhskii A, Keller A, Kolker E, Aebersold R. A statistical model for identifying proteins by tandem mass spectrometry. Anal Chem. 2003; 75: 4646-58.

47. Lamesch P, Berardini TZ, Li D, Swarbreck D, Wilks C, Sasidharan R, Muller R, Dreher K, Alexander DL, Garcia-Hernandez M, Karthikeyan AS, Lee CH, Nelson WD, Ploetz L, Singh S, Wensel A, Huala E. 2012. The Arabidopsis Information Resource (TAIR): improved gene annotation and new tools. Nucleic Acids Research, 2012; 40(Database issue): D1202–D1210.

48. Thimm O, Bläsing O, Gibon Y, Nagel A, Meyer S, Krüger P, Selbig J, Müller LA, Rhee SY, Stitt M. MAPMAN: a user-driven tool to display genomics data sets onto diagrams of metabolic pathways and other biological processes. Plant J. 2004; 37:914-939.

CHAPTER 7

IDENTIFICATION AND CHARACTERIZATION OF DURUM WHEAT MICRORNAS IN LEAF AND ROOT TISSUES[5]

Veronica Fileccia[1§], Edoardo Bertolini[3§], Paolo Ruisi[1], Dario Giambalvo[1,2], Alfonso Salvatore Frenda[1,2], Gina Cannarozzi[4], Zerihun Tadele[4], Cristina Crosatti[5], Federico Martinelli[1,2*]

[1]Dipartimento di Scienze Agrarie e Forestali, Università degli Studi di Palermo, Palermo, Italy, [2]Fondazione A. e S. Lima Mancuso, Università degli Studi di Palermo, Palermo, Italy, [3]Institute of Life Sciences, Scuola Superiore Sant'Anna, Piazza Martiri della Libertà 33, 56127 Pisa, Italy, [4]University of Bern, Institute of Plant Sciences, Bern, Switzerland, [5]Consiglio per la Ricerca in Agricoltura e l'Analisi dell'Economia Agraria, Genomics Research Centre, Fiorenzuola d'Arda (PC), Italy

*****Correspondence: Dr Federico Martinelli; Email: federico.martinelli@unipa.it;
[§]These authors should be considered as first authors.

MicroRNAs are a class of post-transcriptional regulators of plant developmental and physiological processes and responses to environmental stresses. Here, we present the study regarding the annotation and characterization of *MIR* genes conducted in durum wheat. We characterized the miRNAome of leaf and root tissues at tillering stage under two environmental conditions: irrigated with 100 % (control) and 55 % of evapotranspiration (early water stress). In total, 90 microRNAs were identified, of which 32 classified as putative novel and species-specific miRNAs. In addition 7 microRNA homeologous groups were identified in each of the two genomes of the tetraploid durum wheat. Differential expression analysis highlighted a total of 45 microRNAs significantly differentially regulated in the pairwise comparisons leaf versus root. The miRNA families, miR530, miR395, miR393, miR5168, miR396 and miR166, miR171, miR319, miR167 were the most expressed in leaves in comparison to roots. Putative microRNA targets were predicted for both five and three prime sequences derived from the stem-loop of the *MIR* gene. Gene ontology analysis showed significant over-represented gene categories in microRNA targets belonging to transcription factors, phenylpropanoids, oxydases and lipid binding-protein. This work represents one of the first genome wide characterization of *MIR* genes in durum wheat, identifying leaf and root tissue-specific microRNAs. This genomic identification of microRNAs together with the analysis of their expression profiles is a well-accepted starting point leading to a better comprehension of the role of *MIR* genes in the genus *Triticum*.

[5] Accepted to Functional & Integrative Genomics (in press)

1_INTRODUCTION

Durum wheat (*Triticum turgidum* L. ssp. *durum*) is a tetraploid wheat cultivated around the world. This cereal is characterized by a high resistance to semiarid climates and presents advantages compared to bread wheat under water deficit conditions. As stated by the International Grains Council, the global durum wheat production is around 35 million metric tons per year. In developing countries, durum wheat is usually cultivated in challenging environments especially on poor soil and semiarid conditions. In these harsh environments, production is usually characterized by high variability due to fluctuations in annual rainfall. Tolerance to water stress is a key aspect of the improvement of durum wheat for Mediterranean environments, where a reduced water supply greatly limits the production from a quantitative and qualitative point of view (Peng et al. 2011).

Since the discovery of small RNAs, increased attention has been given to the importance of their function in post-transcriptional gene regulation in response to environmental stresses. MiRNAs are a class of small non-coding RNAs that are between 21 and 24 nucleotides (nt) long. Mature miRNAs are produced from longer noncoding pre-miRNAs, and they are processed by multiple cleavage steps, involving a complex system of different enzymes (Kurihara and Watanabe 2004). They are mostly involved in silencing the expression of genes through hybridization with their targets, with whom they share a complementary sequence (Jeong et al. 2001). They are present in all plant genomes in large families with 1–32 loci. Interestingly, among members of the same family, miRNAs potentially encode identical or nearly identical mature sequences. Approximately 20 families are present in the plant kingdom. Among them, some members have been shown to be present in primitive land plants while others seem to be linked with more recent evolutionary events (Sunkar et al. 2008). These small RNAs have been associated with responses to different environmental stresses including drought (Cheah et al. 2015; Shui et al. 2013). The identification of those involved in the regulation of key genes in secondary metabolism will be highly desirable (Martinelli and Tonutti, 2012). The number of newly discovered miRNAs is continually increasing, especially in Arabidopsis (Kozomara and Griffiths-Jones 2014). Although many of the new microRNAs have not been analyzed in response to environmental changes, the role of some has been clarified. For example, miR169 is one of the most conserved miRNAs and it has been associated with plant responses to abiotic stress (Li et al. 2008; Zhao et al. 2011). Several cereal miRNAomes have been characterized, although knowledge of the complex networks in which these miRNAs are involved is far from completely understood (Budak et al. 2015).

Specifically in wheat, several studies have been conducted with the aim to characterize the miRNAome of wheat species and identify key miRNA involved in tolerance and resistance to abiotic stresses (Pandey et al. 2014; Liu et al. 2015; Zhao et al. 2014; Ma et al. 2015; Akpinar et al. 2015; Alptekin and Budak 2016; Alptekin et al. 2016; Liu et al. 2016a). However, no studies have been conducted which include the annotation and chromosome mapping of tissue-specific miRNAs. Here we propose the first attempt to accurately annotate and map miRNA in relation to their expression in leaf and root tissues under two conditions: irrigated to 100% and 55% of evapotranspiration (early water stress).

2_MATERIALS AND METHODS

2.1_Plant Material and Experimental Design

The experiment was conducted at Pietranera Farm (Sicily, Italy; 37°30′ N, 13°31′ E) using durum wheat (*Triticum durum* Desf.) plants grown outdoors in pots under the shade. In order to characterize the miRNAome under two conditions (i.e., irrigated and water stress), a complete randomized factorial design replicated six times was adopted. Each pot (diameter 150 mm, height 130 mm) was filled with a vermiculite: soil mixture (1:1). Soil properties were as follows: 273 g kg^{-1} clay, 249 g kg^{-1} silt, and 488 g kg^{-1} sand; pH 8.0; 7.4 g kg^{-1} total C and 0.86 g kg^{-1} total N. All pots were weighed, fully wetted, and, after allowing them to drain freely, weighed again to determine the soil water content (SWC) at the retention capacity.

Eighteen seeds of durum wheat (cv. Simeto), previously surface-sterilized with hydrogen peroxide at 4% for 3 minutes, were sown in each pot. Simeto, released in 1988, is the most widely grown variety in southern Italy; it is an early, short, high-yielding cultivar with excellent grain quality, and it is sensitive to drought (Bresta et al. 2011). One week after emergence, plants were thinned to six seedlings per pot. From emergence to tillering stage, plants were grown under well-watered conditions. Starting from the advanced tillering stage (stages 22-24 of Zadoks scale, Zadoks et al. 1974), plants were subjected to four different water regimes: Contr100 which consisted of total replenishment of lost water daily; STR55, STR70, and STR85 which consisted in replenishing of 55%, 70%, and 85% of the daily evapotranspiration, respectively, as measured on Contr100. The pots were weighed daily and the water amounts were regulated by weight. The SWC during the period of application of the different water regimes was calculated for each pot as difference between the pot weight at retention capacity and the pot weight measured daily. All the experimental treatments were watered at the same time as the Contr100 treatment.

All pots were harvested after ten days from the start of water stress. Plant biomass was immediately separated into roots and shoots, and fresh weights were recorded. One pool of leaves and one of roots (primary and secondary), both equal to approximately one third of the respective total fresh weights, have been sampled, immediately frozen in liquid nitrogen (N), grinded and weighed out 1 g for the analysis. At the same time, a sample of fresh full expanded leaves (about 1 g) was taken from each pot to determine the leaf relative water content (RWC). The leaves were weighed immediately (to determine fresh mass, FM), cut into several sections, and soon soaked in deionized water for 12 h, and then weighed again to determine the fully turgid mass (TM). Finally, the leaves were dried at 65 °C to determine the dry mass (DM). The leaf RWC was calculated as follows (Salisbury and Ross 1992):

$$RWC = (FM-DM)/(TM-DM)$$

For each pot, the remaining plant roots and shoots (both always greater than the 50% of the total fresh weight of each pot) were separately dried at 65 °C to determine the dry matter content and calculate the belowground and aboveground dry masses.

Among the three levels of water stress, we chose the extreme water stress treatment (STR55) and Contr100 for the characterization of the durum wheat miRNAome. 10 days after that stress was applied, leaf and root tissues were harvested followed by miRNA extraction and sequencing.

2.2._RNA extraction, library preparation and microRNA profiling

RNA was extracted using the Spectrum Plant Total RNA kit (Sigma-Aldrich) from a total of 12 samples, composed by 6 leaves and 6 roots, grown in water stress and control condition were collected. For each sample, a pool of leaves and roots were used for the analysis and three biological replicates were considered for both conditions.. RNA quantity and quality was measured using the Nanodrop (Thermo Fisher Scientific, Massachussetts, USA) and the integrity was checked using electrophoresis by loading 1 µl of sample on 2 % agarose gel. RNA samples were processed to generate small RNA-seq libraries containing short inserts according to the TruSeq Small RNA Library Preparation Kit (Illumina, San Diego, CA), following manufacturer's instruction.

Once quality control was passed, Next-Generation sequencing (NGS) was performed using an Illumina Hiseq2500 sequencer at IGA Technology Services (Udine, Italy).

Raw reads were uploaded to the National Center for Biotechnology Information (NCBI) Sequence Read Archive (SRA) (Accession number: SUB2309521 N).

2.3_Small RNA Annotation

Raw sequencing data were of good quality (mean sequence quality score: Phred > 30) and no quality filters were applied. Three prime sequencing adapters were trimmed using the program Cutadapt (Martin 2011) version 1.8.3 with the settings: --trim-n –a TGGAATTCTCGGGTGCCAAGG –m 15 –M 35; resulting in trimmed reads ranged from 15-35 nucleotides in length.

For each sample, trimmed reads were mapped independently against the hexaploid *Triticum aestivum* cv. *Chinese Spring* reference genome version IWGSC2 downloaded from Ensembl Genomes (ftp://ftp.ensemblgenomes.org/pub/plants/release-26). Since the official tetraploid wheat genome is not yet available, only chromosomes belonging to genomes A and B were considered as reference sequences to create a synthetic *Triticum durum* reference. Moreover, mitochondrial and plastid genome were not considered in this analysis.

Bowtie (Langmead 2009) version 1.0.1 was used to align trimmed reads to the reference genome allowing 2 mismatches. The mapping results of each sample were analyzed with ShortStack (Axtell 2013) version v.2.0.9 with default settings, annotating a total of 66,795 clusters corresponding to significant genomic regions harboring small RNA accumulation. This initial annotation was restricted to 90 high confidence miRNA loci based on the current criteria for the annotation of plant mircoRNA (Meyers et al. 2008).

To identify conserved miRNA loci BLASTn (McGinnis and Madden 2004) with Evalue < e-10 was applied using as subject all the hairpin sequences belonging to monocotyledonous species present in miRBase (Kozomara and Griffiths-Jones 2014) version 21.

Finally, homeologous miRNA loci were identified based on sequence similarity along the entire stem-loop sequence using the clustering program CD-HIT (Fu et al. 2012) with sequence identity of 0.95.

2.4_miRNA target identification and annotation

The non-redundant set of 5 and 3 prime miRNA sequences was used to predict targets in the full set of cDNA transcripts annotated in the *Triticum aestivum* cv. *Chinese Spring* version IWGSC2 downloaded from Ensembl Genomes (ftp://ftp.ensemblgenomes.org/pub/plants/release-26).

The program TargetFinder (Fahlgren et al. 2007) with default parameters was applied and only results with a score cutoff of 3 or less were considered as putative miRNA targets.

The resulted list of unique *T. durum* miRNA targets was annotated using TRAPID (Van Bel et al. 2013), an online tool for functional and comparative transcriptome analysis. Similarity searches were conducted against the model grass species *Brachypodium distachyion* based on the data source contained in the PLAZA 2.5 database (Proost et al. 2009).

2.5_Differential Expression analysis

The detection of differentially expressed miRNAs was identified using the Bioconductor R package DESeq2 (Love et al. 2014) with Wald hypothesis test. For each miRNA locus the total number of sequencing read counts mapped unambiguously to the hairpin sequence in each condition was used as the input to the expression analysis. No normalization methods were applied to the raw data before performing the test since DESeq2 uses an internal method to normalize the raw data (Love et al. 2014). MicroRNAs with FDR ≤ 0.05 were considered differentially expressed.

2.6_Statistical analysis

Data on soil water content, plant biomass, and leaf RWC were subjected to analysis of variance (ANOVA) according to the experimental design. Variables corresponding to proportions were arcsine transformed before analysis to assure a better fit with the Gaussian law distribution. Normality was confirmed using a Kolmogorov-Smirnov test. Treatment means were compared using Fisher's protected least significant differences test at the 5% probability level.

3_RESULTS

3.1_Soil water content, plant biomass, and leaf RWC

In the Contr100 treatment, the soil water content never dropped below 23% during the experiment, whereas in all other treatments soil water content decreased more or less rapidly as a function of the level of the applied water stress (**Fig. 1**). At harvest, the soil water content ranged from 11.6% (STR55) to 23.5% (Contr100).

Water regime significantly affected the aboveground plant biomass and the leaf RWC but not the belowground plant biomass (**Table 1**). In particular, decreases in shoot biomass were

observed when the intensity of water stress increased. Leaf RWC ranged from a high of approximately 90% for the well-watered treatment (Contr100) to a low of 82% for the most highly water-stressed treatment (STR55).

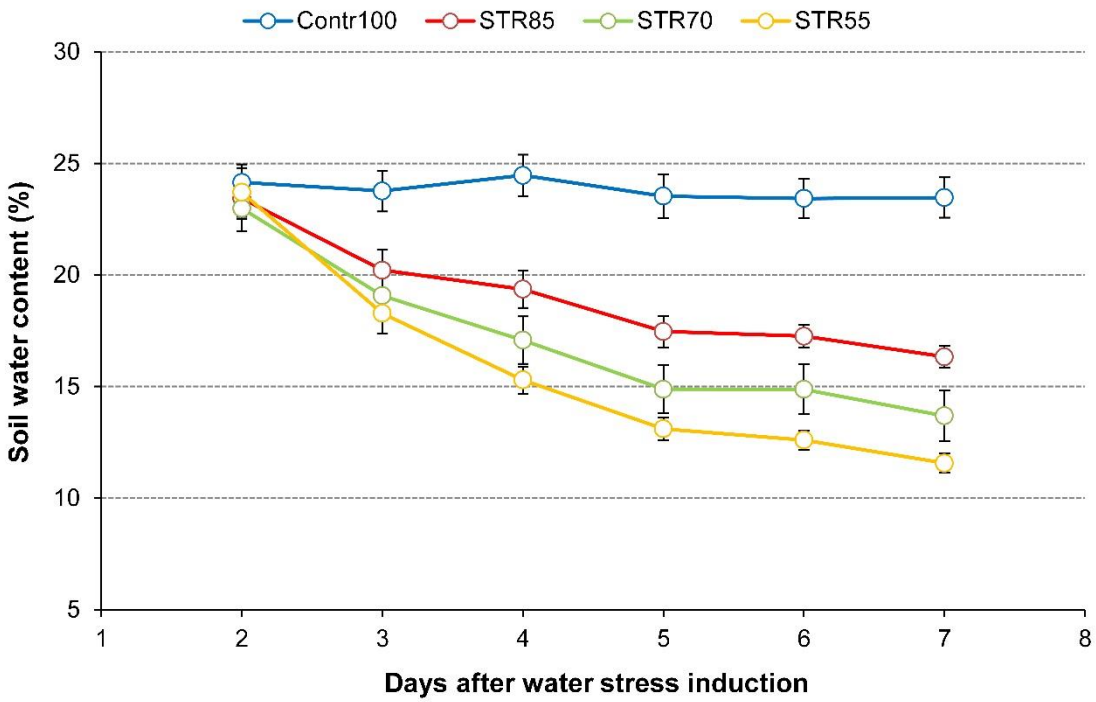

Fig. 1| Changes in soil water content (±S.D.. n = 6) (%) in the days after the water stress induction. Contr100 = total replenishing of the amount of water lost daily from the pots; STR85. STR70. and STR55 = replenishing of 85%. 70%. and 55% of the daily evapotranspiration measured on Contr100.

Table 1| Below- and above-ground biomass (as grams of dry matter per pot) and leaf relative water content (leaf RWC) under different water regimes.

Water regime	Belowground biomass	Aboveground biomass		Leaf RWC	
	g DM pot^{-1}	g DM pot^{-1}		—	
Contr100	2.13	5.07	a	0.92	a
STR85	2.05	4.91	a	0.89	a
STR70	2.09	4.51	ab	0.86	ab
STR55	2.14	4.12	b	0.82	b

Contr100 = total replenishing of the amount of water lost daily from the pots; STR85, STR70, and STR55 = replenishing of 85%, 70%, and 55% of the daily evapotranspiration measured on Contr100. Within each column, different letters denote significant differences at 5% probability level.

3.2_Overview of microRNA profiling data

In this study, Illumina sequencing platform was used to identify and characterize at genomic level miRNAs in durum wheat, focusing on leaf and root tissues subjected to drought stress. In total, twelve small RNA (sRNA) libraries were constructed using total RNAs isolated from four conditions (namely, leaf-control (leaf-N), root-control (root-N), leaf-drought (leaf-S), root-drought (root-S). sRNA sequencing yielded a total of 189,135,623 high-quality raw sequences with an average number of raw reads over the 3 replicates of at least 30 million (**Table 2**).

Table 2| Data set summary of miRNA sequencing data.

	Roots		**Leaves**	
	Control	**Drought**	**Control**	**Drought**
Total raw reads	58,677,892	50,893,655	30,665,332	48,898,744
Uniquely mapped reads	6,789,788	4,963,645	2,404,013	3,487,512
Multi mapped reads	20,549,748	16,102,052	21,173,031	37,276,683
Total mapped reads	27,339,536 (46%)	21065697 (41%)	23577044 (76%)	40764195 (83%)

The average number of reads for the three biological replicates in each condition and tissue are shown.

After removing sequencing adapters, sRNA sequencing reads were mapped against the reference genome of bread wheat produced by the International Wheat Genome Sequencing Consortium (IWGSC) (A chromosome-based draft sequence of the hexaploid bread wheat (Triticum aestivum) genome) considering only chromosomes belonging to A and B genome to *de-novo* identify *MIR* genes in *T. turgidum durum*. Between 40% and 83% (**Table 2**) of the reads generated from root and leaf were mapped respectively to bread wheat genome allowed us to perform a miRNA identification at genome level using the pipeline ShortStack as proposed by Axtell (2013). This approach resulted in 66,795 small RNA clusters corresponding to significant genomic regions harboring small RNA sequences. Of these, 90 high confidence miRNA loci were retained since passed all the current criteria for the plant microRNA annotation (**Table 3**) (Meyers et al. 2008). A Plot Diagram of the differential analysis between roots and leaves was performed (**Fig. 2**).

Table 3| List of conserved miRNA in durum wheat tissues.

Cluster name	Known pre-miRNA	%	5P Cluster Sequence	Known type	3P Cluster Sequence	Known type
Cluster_513	tae-MIR5384	100.00	UUCGCCGGUCGCGCGUUCCCC		UGAGCGCGCCGCCGUCGAAUG	tae-miR5384-3p
Cluster_1282	tae-MIR9664	93.86	ACGGCAUAGAGGCACUGCAAA		UGCAGUCCUCGAUGUCGUAG	tae-miR9664-3p
Cluster_6065	ata-MIR9863b	95.12	UGAGAAGGUAGAUCAUAAUAGC	ata-miR9863b-3p	UGUUAUGAUCUGCUUCUCAUU	ata-miR9863b-5p
Cluster_6404	tae-MIR9664	98.31	ACGGCAUAGAGGCACUGCAAA		UGCAGUCCUCGAUGUCGUAG	tae-miR9664-3p
Cluster_8073	tae-MIR399	84.33	GGGCGCUUCUCCCUUGGCACG	ata-miR399a-5p	UGCCAAAGGAGAAUUGCCCUG	ata-miR399a-3p
Cluster_10104	tae-MIR530	98.76	CUGCAUUUGCACCUGCACCUA	osa-miR530-5p	GGUGCAGUGGCAUAUGCAACU	tae-miR530
Cluster_10719	ata-MIR156c	99.09	UGACAGAAGAGAGUGAGCAC	ata-miR156c-5p	GCUCACUGCUCUAUCUGUCACC	ata-miR156c-3p
Cluster_11634	ata-MIR1432	90.65	CUCAGGAGAGAUGACACCGAC	ata-miR1432-5p	UGGUGUCACCUCGCCUGAACA	ata-miR1432-3p
Cluster_11636	ata-MIR1432	97.27	AUCAGGAGAGAUGACACCGAC		UGGUGUCACCUCGCCUGAACA	ata-miR1432-3p
Cluster_12802	bdi-MIR827	95.24	UUUUGCUGGUUGUCAUCUAACC	bdi-miR827-5p	UUAGAUGACCAUCAGCAAACA	bdi-miR827-3p
Cluster_13147	ata-MIR9776	86.90	UGGACGAGGAUGUGCAGCUGC	ata-miR9776-5p	AGCUGCACAUCCACUUCCAAG	ata-miR9776-3p
Cluster_13262	ata-MIR395a	95.24	AGUUCCCUUCAAGCACUUCAGG	ata-miR395a-5p	UGAAGUGUUUGGGGAACUCU	ata-miR395a-3p
Cluster_14263	ata-MIR166c	89.77	GGAACGUUGGCUGGCUCGAGG	ata-miR166c-5p	UCGGACCAUGCUUCAUUCCUC	ata-miR166c-3p
Cluster_14872	ata-MIR164c	94.78	UGGAGAAGCAGGGCACGUGCA	ata-miR164c-5p	CACGUGUUCUUCUCCUCCAUC	ata-miR164c-3p
Cluster_16065	ata-MIR1432	99.09	AUCAGGAGAGAUGACACCGA	ata-miR1432-5p	GGUGUCACCUCGCCUGAACA	ata-miR1432-3p
Cluster_18140	tae-MIR530	95.12	CUGCAUUUGCACCUGCACCUA		GGUGCAGUGGCAUAUGCAACU	tae-miR530
Cluster_18283	bdi-MIR827	97.83	UUUUGUUGGUUGUCAUCUAACC	bdi-miR827-5p	UUAGAUGACCAUCAGCAAACA	bdi-miR827-3p
Cluster_18506	ata-MIR156c	94.55	UGACAGAAGAGAGUGAGCAC	ata-miR156c-5p	GCUCACUGCUCUAUCUGUCACC	ata-miR156c-3p
Cluster_18775	ata-MIR171a	98.86	UGGUAUUGUUUCGGCUCAUA	ata-miR171a-5p	UGAGCCGAACCAAUAUCACU	ata-miR171a-3p

Cluster_20349	ata-MIR396d	87.50	UCCACAGGCUUUCUUGAACU	ata-miR396d-5p	UUCAAGAAAGCCCAUGGAAA	ata-miR396d-3p
Cluster_20589	ata-MIR393	89.13	UUCCAAAGGGAUCGCAUUGAU	ata-miR393-5p	CAGUGCAAUCCCUCUGGAAUU	ata-miR393-3p
Cluster_20808	hvu-MIR159a	94.94	GAGCUCCUAUCAUUCCAAUGA	hvu-miR159a	UUUGGAUUGAAGGGAGCUCUG	hvu-miR159a
Cluster_25388	bdi-MIR156f	93.94	UGACAGAAGAGAGUGAGCAC	bdi-miR156f-5p	GCUCACUGCUCUAUCUGUCAGC	bdi-miR156f-3p
Cluster_26451	tae-MIR9676	100.00	UGGAUGUCAUCGUGGCCGUACA	tae-miR9676-5p	UACGGCCUGAUGACAUCCACG	
Cluster_28135	zma-MIR319b	87.70	AGAGCGUCCUUCAGUCCACUC	zma-miR319b-5p	UUGGACUGAAGGGUGCUCCCU	zma-miR319b-3p
Cluster_33098	ata-MIR167d	88.24	UGAAGCUGCCAGCAUGAUCUGA	ata-miR167d-5p	AGGUCAUGUGGCAGCUUCAUU	ata-miR167d-3p
Cluster_41670	ata-MIR167d	90.44	UGAAGCUGCCAGCAUGAUCUGA	ata-miR167d-5p	AGGUCAUGUGGCAGCUUCAUU	ata-miR167d-3p
Cluster_41943	ata-MIR166e	89.91	GGAAUGUUGUCUGGUUGGAGA	ata-miR166e-5p	UCGGACCAGGCUUCAUUCCCC	ata-miR166e-3p
Cluster_42520	tae-MIR9674a	93.10	AUAGCAUCAUCCAUUCUACCA	ata-miR9674a-5p	GUAGGAUGGCUGGUGCUAUGG	ata-miR9674a-3p
Cluster_43339	tae-MIR9666b	98.98	GCCAUCAUACGUCCAACCGU	tae-miR9666b-5p	GGUUGGGCUGUAUGAUGGCGA	tae-miR9666b-3p
Cluster_43357	tae-MIR156	99.15	UGACAGAAGAGAGUGAGCAC		GCUCACCCUCUCUCUGUCAGC	
Cluster_43534	ata-MIR5168	97.58	GGGUUGUUGUCUGGUUCAAG	ata-miR5168-5p	CGGACCAGGCUUCAAUCCCU	ata-miR5168-3p
Cluster_44265	ata-MIR167a	83.67	UGAAGCUGCCAGCAUGAUCUA	ata-miR167a-5p	GAUCGUGCUGUGACAGUUUCACU	ata-miR167a-3p
Cluster_47002	ata-MIR167c	98.96	UGAAGCUGCCAGCAUGAUCUA	ata-miR167c-5p	GAUCAUGACUGACAGCCUCAUU	ata-miR167c-3p
Cluster_47003	ata-MIR167b	97.94	UGAAGCUGCCAGCAUGAUCUGA	ata-miR167b-5p	AGGUCAUGCUGGAGUUUCAUC	ata-miR167b-3p
Cluster_48327	ata-MIR5168	96.77	GGGUUGUUGUCUGGUUCAAG	ata-miR5168-5p	CGGACCAGGCUUCAAUCCCU	ata-miR5168-3p
Cluster_48425	tae-MIR156	98.29	UGACAGAAGAGAGUGAGCAC		GCUCACCCUCUCUCUGUCAGC	
Cluster_49696	ata-MIR166b	99.00	GAAUGACGCCGGGUCCGAAAG	ata-miR166b-5p	UUCGGACCAGGCUUCAUUCCC	ata-miR166b-3p
Cluster_52794	tae-MIR9670	97.47	UUCUUCAAGUACUCCACUUUU		AGGUGGAAUACUUGAAGAAGA	tae-miR9670-3p
Cluster_53245	bdi-MIR156c	92.70	UUGACAGAAGAGAGUGAGCAC	bdi-miR156c	GCUCACUCCUCUUUCUGUCAGCC	
Cluster_53705	tae-MIR397	95.74	UUGAGUGCAGCGUUGAUGAAC		UCACCGGCGCUGCACACAAUG	tae-miR397-5p

Cluster_55297	bdi-MIR396c	100.00	UUCCACAGCUUUCUUGAACUG	bdi-miR396c-5p	GUUCAAUAAAGCUGUGGGAAG	bdi-miR396c-3p
Cluster_55342	ata-MIR396c	96.57	UUCCACAGCUUUCUUGAACUU	ata-miR396c-5p	GGUCAAGAAAGCUGUGGGAAG	ata-miR396c-3p
Cluster_55558	ata-MIR172b	96.33	GCAGCACCACCAAGAUUCACA	ata-miR172b-5p	AGAAUCUUGAUGAUGCUGCAU	ata-miR172b-3p
Cluster_55636	ata-MIR396b	83.91	UCCACAGGCUUUCUUGAACUG	ata-miR396b-5p	GUUCAAGAAAGUCCUUGGAAA	ata-miR396b-3p
Cluster_57238	bdi-MIR156c	94.16	UUGACAGAAGAGAGUGAGCAC	bdi-miR156c	GCUCACUCCUCUUUCUGUCAGCC	
Cluster_57508	tae-MIR167c	91.10	UGAAGCUGCCAGCAUGAUCUGC	tae-miR167c-5p	AGAUCAUGCUGCAGCUUCAUU	
Cluster_58599	tae-MIR9660	100.00	UUGCGAGCAACGGAUGAAUCAGCC	tae-miR9660-5p	CUGAUUUCUCCUUUGCUCGAGUAGA	
Cluster_58886	ata-MIR396b	86.89	UCCACAGGCUUUCUUGAACUG	ata-miR396b-5p	GUUCAAGAAAGUCCUUGGAAA	ata-miR396b-3p
Cluster_59780	ata-MIR396e	97.17	UUCCACAGCUUUCUUGAACUG	ata-miR396e-5p	GUUCAAUAAAGCUGUGGGAAA	ata-miR396e-3p
Cluster_63022	tae-MIR5200	100.00	AAGCCUUAGUGAAUAUCUACA	tae-miR5200	UAGAUACUCCCUAAGGCUUGG	tae-miR5200-3p
Cluster_63134	ata-MIR396e	97.17	UUCCACAGCUUUCUUGAACUG	ata-miR396e-5p	GUUCAAUAAAGCUGUGGGAAA	ata-miR396e-3p
Cluster_65040	bdi-MIR399a	93.75	GUGCAGUUCUCCUCUGGCAUG		UGCCAAAGGAGAAUUGCCCUG	bdi-miR399a-3p
Cluster_65295	ata-MIR166d	95.45	GGAAUGUUGUCUGGCUCGGGG	ata-miR166d-5p	UCGGACCAGGCUUCAUUCCCC	ata-miR166d-3p
Cluster_65537	hvu-MIR5048a	82.59	UAUAUUUGCAGGUUUUAGGUCU	hvu-miR5048a	ACCUAGACAUGCAAGUAUAUU	
Cluster_12754	ata-MIR171a	100.00			UGAGCCGAACCAAUAUCACUC	ata-miR171a-3p
Cluster_16064	ata-MIR1432	90.91	AUCAGGAGAGAUGACACCGAC	ata-miR1432-5p		
Cluster_42519	ata-MIR9674c	89.81	UGAAUUUGUCCAUAGCAUCAG	ata-miR9674c-5p		
Cluster_59780	ata-MIR396e	94.38	UUCCACAGCUUUCUUGAACUG	ata-miR396e-5p	GUUCAAUAAAGCUGUGGGAAA	ata-miR396e-3p

Cluster name, Known pre-miRNA, Percentage of identity with Known pre-miRNA, 5P sequence, Known type, 5P Cluster Sequence and 3P Cluster Sequence are indicated.

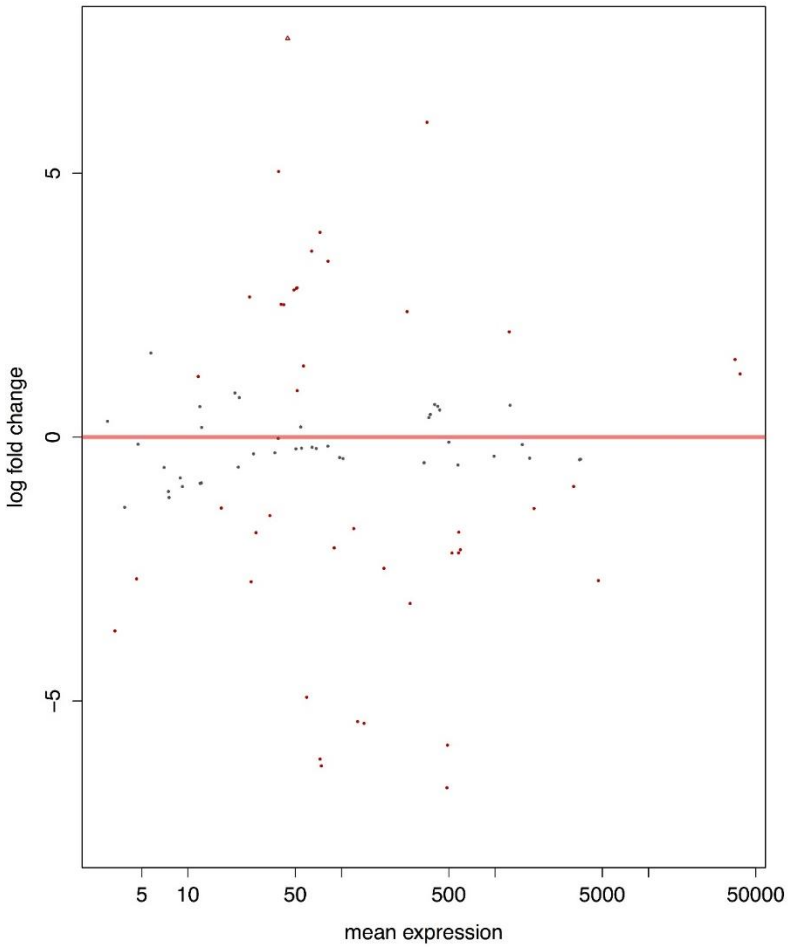

Fig. 2| Plot Diagram of the differential analysis between roots and leaves. In red miRNAs differentially expressed with padj < 0.05; triangle indicates that the microRNA has a FoldChange value exceeds the scale in Y.

3.3_Identification of conserved and novel miRNAs in durum wheat

Among the 90 high confidence miRNA loci found, 59 were found to be conserved with a sequence identity greater to 82% with miRNAs representing 41 families (**Table 3**). In particular, the conserved miRNAs belonged to families identified in *Agilops tauschii* (33 miRNAs), *Triticum aestivum* (16 miRNAs), *Brachypodium distachyon* (7 miRNAs), *Hordeum vulgare* (2 miRNAs) and *Zea mays* (1 miRNAs) and in most of them the 5 and 3 prime sequences were found to be conserved with 100% of identity. Well-represented miRNA families were MIR156, MIR167 and MIR396. About one third of the total *MIR* loci found were classified as novel miRNAs since no hit against the deposited miRNAs were found (**Table 4**). Unlike conserved miRNAs, which were absent in three chromosomes, the novel miRNAs were distributed amongst the seven chromosomes of durum wheat. BlastN results of known miRNA was shown in S1.

Table 4| Complete list of miRNA identified in durum wheat.

Cluster Name	Chromosome	Coordinates (Start-End)	Strand
Cluster_513	1A	15633872-15633951	-
Cluster_1282	1A	79918253-79918380	-
Cluster_6065	1B	112783112-112783726	-
Cluster_6206	1B	122612157-122612269	-
Cluster_6404	1B	141665387-141665516	-
Cluster_6749	1B	170059132-170059244	-
Cluster_8073	1B	260670499-260670644	+
Cluster_10104	2A	45376842-45377015	+
Cluster_10719	2A	84081359-84081605	-
Cluster_11634	2A	143411184-143411299	-
Cluster_11636	2A	143414592-143414715	-
Cluster_12802	2A	213324183-213324354	-
Cluster_13143	2A	226019236-226019319	-
Cluster_13147	2A	226139343-226139454	-
Cluster_13262	2A	230308678-230308772	-
Cluster_13639	2A	240081115-240081289	-
Cluster_14263	2B	2222883-2222985	-
Cluster_14872	2B	23833127-23833288	+
Cluster_15646	2B	58576789-58577076	+
Cluster_15688	2B	60519240-60519467	+
Cluster_16065	2B	84759598-84759722	-
Cluster_18140	2B	217777285-217777488	+
Cluster_18283	2B	227895401-227895646	+
Cluster_18506	2B	243201566-243201809	-
Cluster_18775	2B	259602537-259602631	+
Cluster_20349	2B	335036178-335036300	-
Cluster_20589	2B	342233257-342233339	+
Cluster_20808	3A	2080433-2080633	-
Cluster_25388	3B	110274755-110274947	+
Cluster_25487	3B	119184659-119184775	+
Cluster_26451	3B	200808871-200809000	+
Cluster_27040	3B	269731006-269731167	-
Cluster_28135	3B	397138896-397139082	+
Cluster_33098	4A	2957490-2957630	-
Cluster_33442	4A	20971211-20971293	-
Cluster_34476	4A	78276500-78276742	+
Cluster_34518	4A	80581584-80581770	-
Cluster_37179	4A	201734016-201734186	+
Cluster_38047	4B	14197219-14197444	+
Cluster_39268	4B	111421293-111421546	+
Cluster_41670	4B	277748474-277748655	-

Cluster_41943	4B	289870488-289870595	+
Cluster_42520	4B	313527214-313527308	+
Cluster_43339	5A	59439291-59439409	+
Cluster_43357	5A	61589422-61589539	+
Cluster_43534	5A	73069415-73069551	-
Cluster_43663	5A	80552389-80552564	+
Cluster_44265	5A	109129156-109129252	+
Cluster_44683	5A	124245876-124246107	+
Cluster_46325	5B	53725031-53725280	+
Cluster_47002	5B	89505892-89506004	+
Cluster_47003	5B	89508484-89508593	+
Cluster_47293	5B	105883615-105883794	+
Cluster_48327	5B	163330209-163330340	+
Cluster_48425	5B	168674312-168674427	-
Cluster_49696	5B	217147284-217147387	+
Cluster_50473	5B	243482443-243482634	-
Cluster_50615	5B	248077388-248077474	+
Cluster_52794	6A	54567623-54567714	+
Cluster_53245	6A	87949906-87950062	+
Cluster_53705	6A	120354259-120354366	-
Cluster_55297	6A	198934069-198934223	+
Cluster_55342	6A	199645078-199645263	-
Cluster_55558	6A	203905899-203906020	+
Cluster_55636	6A	205704194-205704363	-
Cluster_57238	6B	96378404-96378579	+
Cluster_57508	6B	117919946-117920091	-
Cluster_58599	6B	190032396-190032500	-
Cluster_58886	6B	201394961-201395149	-
Cluster_59228	7A	5577146-5577252	+
Cluster_59780	7A	20932743-20932904	+
Cluster_60668	7A	67722401-67722565	+
Cluster_62182	7A	158762241-158762338	-
Cluster_63022	7B	3426764-3426925	+
Cluster_63023	7B	3427326-3427561	+
Cluster_63134	7B	8739076-8739320	-
Cluster_64950	7B	152744447-152744540	+
Cluster_65040	7B	162293419-162293567	-
Cluster_65295	7B	177711980-177712189	-
Cluster_65537	7B	193135466-193135860	-
Cluster_66590	7B	244136062-244136291	-
Cluster_9890	2A	30340652-30340876	-
Cluster_11382	2A	128544212-128544409	-
Cluster_12754	2A	210529750-210529991	-
Cluster_16064	2B	84756262-84756383	-

Cluster_35124	4A	121123343-121123572	+
Cluster_42519	4B	313526045-313526385	+
Cluster_45124	5A	144036512-144036609	-
Cluster_53303	6A	92088615-92088860	-
Cluster_66669	7B	247337007-247337127	-

Cluster name, Chromosome (Chr), Coordinates, Strand, Type and 5P and 3P sequence are indicated. Loci with both 5P and 3P sequences are defined MIRNA. HP are miRNA loci with no evidence of star sequence but have passed all the criteria for the annotation.

3.4_Differential expression analysis

Differential miRNA expression profiles were observed between leaf and root tissue but not between the condition drought versus control. This was particularly due to the high variance observed between the three biological replicates where biological replications of control leaf were found more similar to the water stressed treatment. Moreover, miRNA expression patterns in root samples were even more variable and this situation did not allow us to identify any significantly regulated miRNA in either leaf or root tissue in response to drought. Therefore, we focused our differential expression analysis on the comparison between the two tissues using the full set of six samples as biological replicates in each tissue, increasing the power of the statistical test. A total of 45 miRNAs were differentially expressed (DE) between root and leaf with FDR = 0.05 (**Table 5**). In particular we noticed an equal distribution of the miRNAs expression pattern in which 23 miRNA were induced in the root tissue whereas 22 miRNA were induced in leaf tissue. Interestingly, among the most DE we found the homeologous miRNAs which showed a conservation also in the pattern of expression. miR530, miR1432 and miR5168 were drastically down-regulated in root compared to miR171 and miR396 that viceversa were found up-regulated in root (**Fig. 3**).

Table 5| MicroRNAs differentially expressed between roots and leaves.

Cluster name	Base Mean	log2 Fold Change	pvalue	Annotation name
Cluster_10104	73.842	-6.231	5.91E-40	tae-MIR530
Cluster_11382	44.531	8.683	3.77E-14	Unknown
Cluster_11634	89.553	-2.097	1.20E-10	ata-MIR1432
Cluster_11636	578.675	-2.193	1.91E-08	ata-MIR1432
Cluster_12754	41.992	2.509	1.27E-10	ata-MIR171a
Cluster_13147	267.452	2.377	1.23E-18	ata-MIR9776
Cluster_13262	3.337	-3.671	1.00E-03	ata-MIR395a

Cluster_14263	63.869	3.522	4.31E-05	ata-MIR166c
Cluster_16064	524.537	-2.197	4.62E-08	ata-MIR1432
Cluster_16065	594.784	-2.133	1.51E-08	ata-MIR1432
Cluster_18140	72.432	-6.100	1.68E-39	tae-MIR530
Cluster_18775	40.373	2.518	2.64E-10	ata-MIR171a
Cluster_20589	279.681	-3.153	7.94E-16	ata-MIR393
Cluster_20808	3250.971	-0.937	1.22E-03	hvu-MIR159a
Cluster_26451	27.742	-1.812	1.00E-04	tae-MIR9676
Cluster_28135	360.330	5.964	6.42E-62	zma-MIR319b
Cluster_33442	56.529	1.347	2.03E-03	Unknown
Cluster_34518	59.294	-4.930	4.99E-28	Unknown
Cluster_35124	72.293	3.879	4.88E-14	Unknown
Cluster_38047	11.644	1.147	1.98E-02	Unknown
Cluster_41943	39522.440	1.196	9.35E-06	ata-MIR166e
Cluster_42519	120.106	-1.734	2.36E-06	ata-MIR9674c
Cluster_43534	485.938	-6.642	6.78E-80	ata-MIR5168
Cluster_44265	25.156	2.656	6.93E-10	ata-MIR167a
Cluster_45124	51.401	0.878	9.26E-03	Unknown
Cluster_48327	490.112	-5.837	2.81E-56	ata-MIR5168
Cluster_49696	39546.873	1.196	9.18E-06	ata-MIR166b
Cluster_50615	1238.103	1.994	8.41E-07	Unknown
Cluster_53303	4721.973	-2.719	1.71E-04	Unknown
Cluster_55297	48.980	2.787	7.26E-12	bdi-MIR396c
Cluster_55342	188.782	-2.487	9.44E-07	ata-MIR396c
Cluster_57508	580.931	-1.802	5.62E-11	tae-MIR167c
Cluster_59228	81.647	3.331	2.22E-12	Unknown
Cluster_59780	51.272	2.830	5.45E-13	ata-MIR396e
Cluster_59780	51.272	2.830	5.45E-13	ata-MIR396e
Cluster_62182	25.762	-2.739	1.88E-08	Unknown
Cluster_63022	140.125	-5.423	4.68E-33	tae-MIR5200
Cluster_63023	127.093	-5.388	5.96E-31	Unknown
Cluster_63134	50.893	2.820	8.48E-13	ata-MIR396e
Cluster_65295	36643.371	1.470	8.16E-08	ata-MIR166d
Cluster_65537	1796.238	-1.353	4.27E-08	hvu-MIR5048a
Cluster_66590	34.121	-1.488	3.18E-04	Unknown
Cluster_66669	38.841	5.031	1.42E-21	Unknown
Cluster_6749	4.620	-2.687	7.24E-04	Unknown
Cluster_9890	16.453	-1.344	3.71E-03	Unknown

Cluster name. base means. Log fold change. P value and annotation name. A positive fold change means more expression in leaves/roots.

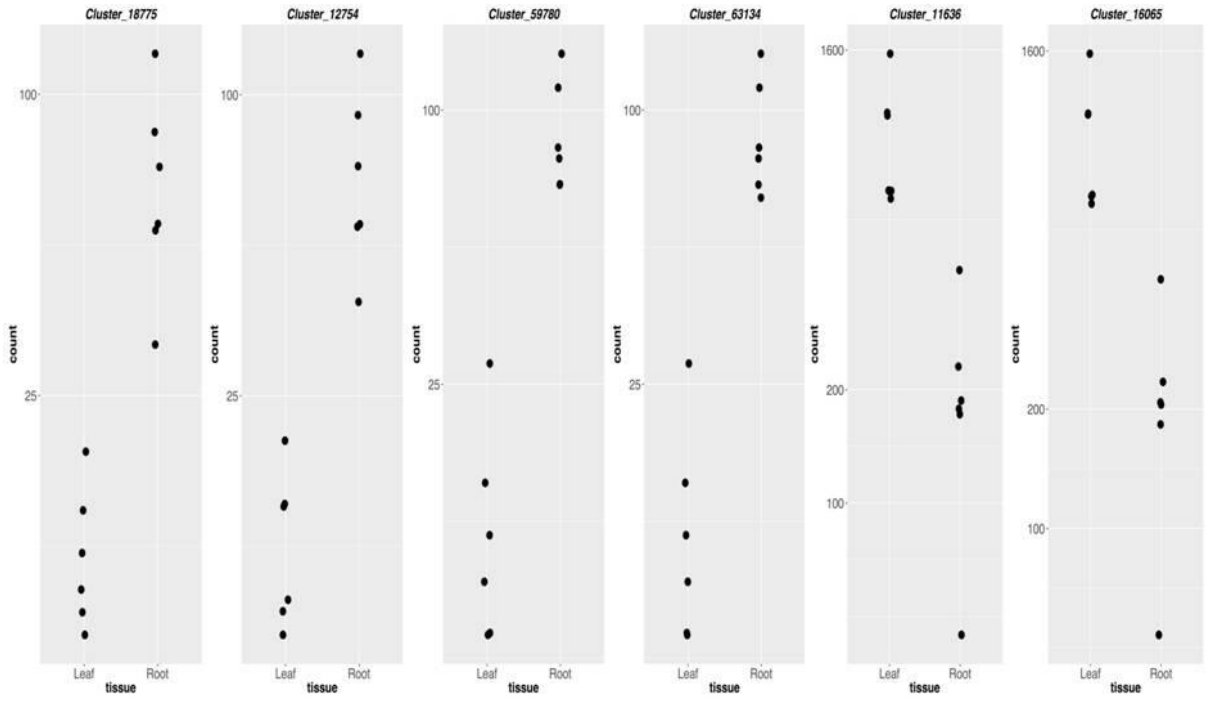

Fig. 3| Particular miRNA homologous genes differentially expressed between roots and leaves. (a) miRNA530; (b) miRNA5168; (c) miRNA1432; (d) miRNA171; (e) miRNA396.

3.5_miRNA mapping and homeologous identification

To better investigate the genomic organization of MIR genes in durum wheat we have performed a cluster analysis of the 90 hairpin miRNA structures here found, using a sequence identity cut-off of 95%. All the miRNAs (known and unknown) were mapped on wheat chromosomes (**Fig. 4**). This analysis allowed us to highlight for the first time 7 miRNA syntenic groups within homeologus chromosomes. We defined paralog homeologous miRNAs all the pre-miRNA structures belonging to the same family which mapped on a couple of homeolog chromosomes (**Table 6**). Three MIR genes were found on chromosomes 2 (miR530, miR1432, miR171a), two (miR156, miR5168) on chromosome five and one (miR156c and miR396e) respectively on chromosome 6 and 7. Interestingly, two inversions were found on chromosomes two and five respectively between miR530 - miR1432 and miR156 - miR5168. To better investigate the chromosomal miRNA distribution and organization, we plotted miRNAs based on their coordinates on the bread wheat genome (**Fig. 5**). Interestingly, miRNAs were found randomly distributed along the seven chromosomes and accumulation of miRNAs appear on chromosomes 2, 5, 6 and 7 while some chromosomes such as 3A had very few miRNAs.

Table 6| List of homeologous known miRNA in durum wheat.

Cluster name	Chromosome	Coordinates(Start-End)	Strand	miRNA type
Cluster_59780	7A	20932743-20932904	+	ata-MIR396e
Cluster_63134	7B	8739076-8739320	-	ata-MIR396e
Cluster_18775	2B	259602537-259602631	+	ata-MIR171a
Cluster_12754	2A	210529750-210529991	-	ata-MIR171a
Cluster_10104	2A	45376842-45377015	+	tae-MIR530
Cluster_18140	2B	217777285-217777488	+	tae-MIR530
Cluster_53245	6A	87949906-87950062	+	bdi-MIR156c
Cluster_57238	6B	96378404-96378579	+	bdi-MIR156c
Cluster_43534	5A	73069415-73069551	-	ata-MIR5168
Cluster_48327	5B	163330209-163330340	+	ata-MIR5168
Cluster_11636	2A	143414592-143414715	-	ata-MIR1432
Cluster_16065	2B	84759598-84759722	-	ata-MIR1432
Cluster_43357	5A	61589422-61589539	+	tae-MIR156
Cluster_48425	5B	168674312-168674427	-	tae-MIR156

Cluster name, chromosomal location, coordinates, strand and miRNA type name are indicated.

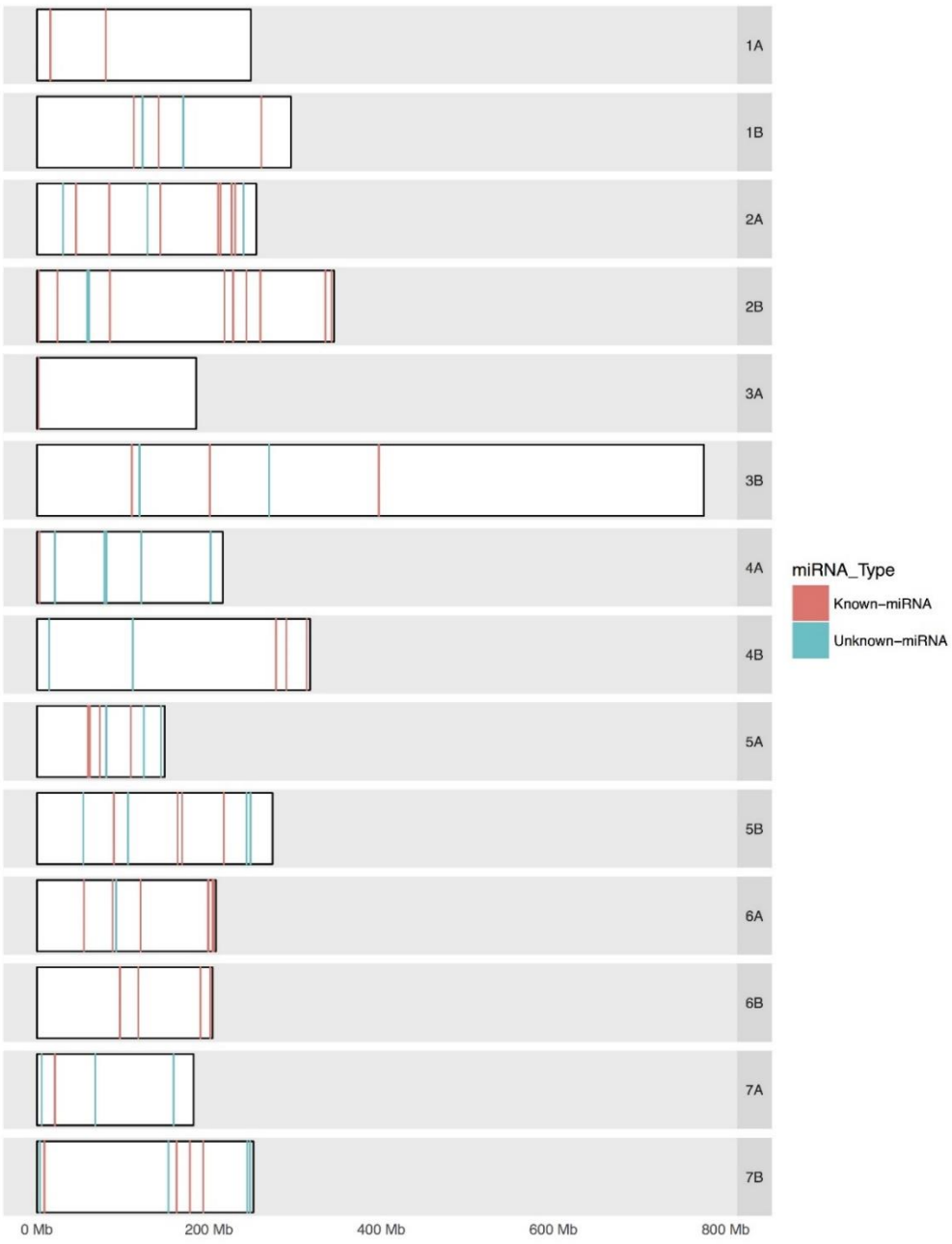

Fig. 4| Chromosome mapping of all identified miRNA.

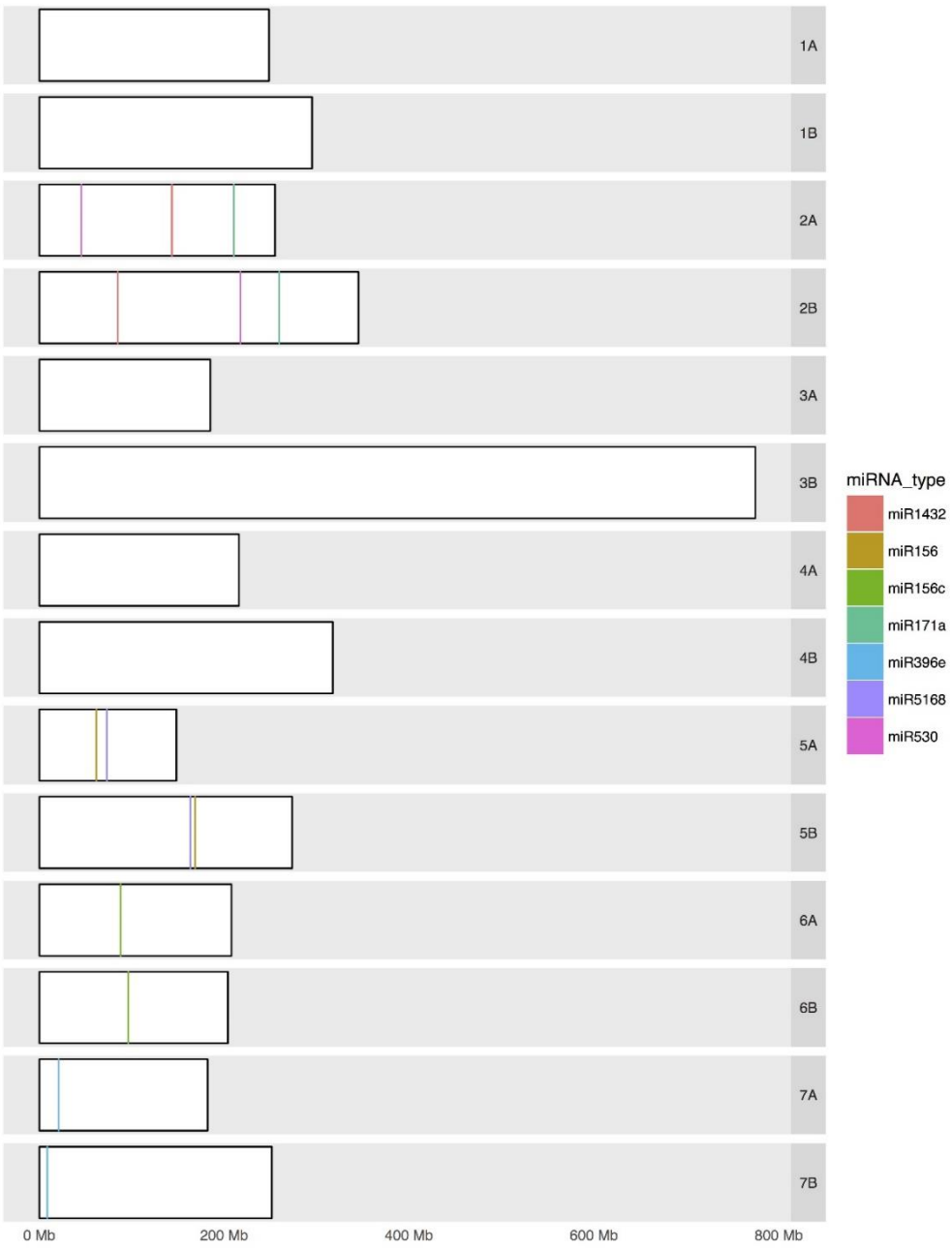

Fig. 5| Chromosome mapping of homeologous identified miRNA.

3.6_Potential targets of conserved and novel miRNAs

To understand better the biological functions of both known and novel miRNAs in durum wheat, putative miRNA targets were identified using the computational tool TargetFinder using as reference transcript database the cDNA transcripts annotated in the *Triticum aestivum* (version IWGSC2). Five and three prime sequences of both known and novel miRNAs were used as query sequences database to search for targets (Table S2a S2b). Secondary structures of all the MIR

loci identified in this work were shown in Table S3. Putative miRNA target transcripts genes with score cut-off not higher than 3 were identified (Supplemental S4). Their GO terms, interpro description and gene families were identified (Table S5-S7). Interestingly the 5 homeologous miRNA differentially expressed between root/leaf were found to have conserved putative targets. This feature together with the conservation of the miRNA expression pattern could be related to a mechanism associated to miRNA biology in polyploidy species.

Moreover, the GO enrichment analysis showed a high number of target genes annotated as having the function of nucleoside phosphate, purine nucleotide, ion and carbohydrate binding. A clear enrichment of gene target ontologies was related to lignin metabolism, phenylpropanoids, and oxidoreductases.

4_DISCUSSION

Durum wheat is an important cereal widely grown in the Mediterranean basin and is an ancestral progenitor of bread wheat, contributing genomes A and B to the bread wheat genome. Its tetraploid nature offers a valid alternative to hexaploid bread wheat as a model for investigation of the role of miRNA in the regulation of key phenomenon in cereal physiology. With the purpose of clarifying the roles of miRNAs in durum wheat physiology and development, we present the annotation and mapping of tissue-specific miRNAs in durum wheat as well as the analysis of miRNA expression in leaf and root tissues. We identified 90 known and 32 novel miRNAs and additionally, we predicted all the potential targets for both novel and known miRNAs.

Previous studies with the aim of identifying miRNAs and their target genes have already been conducted in different species including aestivum wheat (Xin et al. 2010; Tang et al. 2012; Wang et al. 2013). Several studies have been conducted to analyze tissue-specific expression of miRNAs in wheat (Agharbaoui et al. 2015; Liu et al. 2015; Ma et al. 2015). Previous articles have dealt with the identification of the cis-element RHE in the promoters of genes (Won et al. 2009; Bruex et al. 2012). Other important leaf cis-acting regulatory elements (motifs) were found in the promoters of genes that were predominantly expressed in leaves (Xu et al. 2011; Zhang et al. 2012). An interesting work has been conducted by Lucas and Budak (2012) on *Triticum aestivum* chromosome 1AL. They demonstrated that a number of miRNA sequences were closely related to transposable elements and they proposed a strategy for annotation to minimize the risk of mis-identifying TE sequences as miRNAs. The nature of polyploidy of *Triticum species*

renders more difficult the correct discrimination of homologous copies of miRNA thorugh *in silico* methods and experimental validation. Recently two new scripts, "SUmirPredictor" and "SUmirLocator" have been developed to improve previous methods of miRNA prediction and identification, especially for species with highly repetitive genomic sequences (Alptekin et al., 2017). These freely available tools furnish comprehensive understanding of how miRNA precursors are located in the genome and transcriptome and their association with transposons.

Based on the miRBase registry (miRBase release 20), around 42 miRNA sequences have been identified in wheat.

4.1_Mapping miRNA in durum wheat

Our analysis was focused on mapping the identified tissue-specific miRNA and we delivered the first map of miRNA distribution in the two genomes of durum wheat. Although the genome sequence for *Triticum turgidum* ssp. *durum* has not yet been completed, we mapped the miRNA to the durum wheat chromosomes that are present in the bread wheat genome. Mapping the miRNAs will allow the targeting of them through genetic improvement schemes assisted by molecular markers. In additions, our work can further the development of new molecular markers of important agronomic traits linked with key miRNA actions. For example, 13 conserved miRNA (including miR166, miR172 and miR393) have been associated with genotypic diversity in relation to drought tolerance (Li et al. 2013). The mapping of these key miRNAs will be extremely important in the development of molecular markers useful for breeding purposes. We mapped miR156 in the wheat genome. Previous findings showed that miR156 members were modulated by drought in both wild and domesticated wheat implying that this miRNA family is highly conserved between cereals. The function of this miRNA is to modulate the expression of *SQUAMOSA PROMOTER-BINDING LIKE* proteins. However, clear differences have been observed between the patterns of expression of members of this family implying that they may have contributed to evolution of wheat species (Kantar et al. 2011, 2012; Kurtoglu et al. 2013, 2014). Previous studies have shown that the effect on drought tolerance might be dose-dependent and their regulation might be due to the regulation of target genes using post-transcriptional or translation repression mechanisms. Seven conserved miRNAs and three novel miRNAs were analyzed in flag leaf and developing head tissues of different durum genotypes (Liu et al. 2015). These authors inferred their role in water stress tolerance arising from the physiological modulation triggered by their target genes. These miRNAs are close relatives of wheat miRNAs mapped in the present work.

4.2_Leaves vs roots

In the present work, we identified 58 miRNAs that were expressed in both leaves and root tissues and mapped to the A and B genomes. Of these, seven were homeologous gene pairs, present in both of the two genomes. Differential expression analysis highlighted 45 miRNAs significantly regulated in the leaf/root pairwise comparisons. miR530, miR395, miR393, miR5168, miR396 were more expressed in leaves while miR166, miR171, miR319, miR167 had higher expression in roots than in leaves.

Ma et al. (2015) characterized the miRNA in two different wheat genotypes Three hundred and sixty seven differentially expressed miRNAs were reported and among them, there were members of miR156, miR166, miR167, miR168, miR444. We observed significantly higher expression of miR166 in roots while miR167c was more expressed in leaves. Interestingly miR166 and miR396 had opposite trends of expression patterns between tolerant and susceptible wheat genotypes. It is noteworthy that these two genes were also differentially regulated between leaf and root tissues. Both miRNAs were upregulated in root tissues compared to leaves implying that they may have a key role in root physiological processes related to water stress conditions. miR166h targets HD-ZIP4 while miR396 targets GRFs (Ma et al. 2015). Indeed these transcription factors might be involved in the modulation of genes involved in root architecture, development and growth in response to drought.

Kantar et al. (2011) identified other miRNAs that were repressed in response to drought that showed to have a clear differential tissue-specific expression such as miR396 and miR166. MiR159a that targets a MYB3 transcription factor might play a role in cold-stress responses (Liu et al. 2013). Interestingly we showed that this miRNA was more expressed in leaves than in roots. MYB genes have also been shown to be involved in plant tolerance to abiotic stresses through their action in hormone-related signaling networks (Phillips et al. 2007).

4.3_Functional analysis of miRNA targets

A high number of targets has been shown to have nucleic acid binding activities encoding proteins involved in signaling and defense responses. Several auxin-specific transcription factors and auxin-related genes have been identified as potential targets of abiotic stress-related miRNA (Liu et al. 2016b; Sun et al. 2016). It has been hypothesized that a miRNA-driven modulation of auxin genes might affect the lateral root development due to an altered auxin:cytokinin ratio (Su et al. 2011). Genes encoding lipid-transfer proteins have been shown to be targeted by miRNA regulated under drought conditions (Liu et al. 2015). The regulation of these genes have been

linked with genotypic differences in maintaining osmotic pressure. Lipid transfer proteins (LTPs) aid to prevent or adjust stress-induced damage in membranes related to changes in lipid composition (Jung et al. 2003). Interestingly our data showed that a significant higher number of potential targets were related to lipid binding. We identified members of the miR164 family that target NAC transcription factors, which are known to have roles in various abiotic stress responses (Nakashima et al. 2012). Liu et al. (2015) found that several miRNA were drought responsive such as miR1136, miR1432, miR5048, miR5054, miR5071, miR5200 and miR6300. Most of them were successfully mapped to diverse chromosome in the genome A and B in wheat.

5_CONCLUSIONS

We have analyzed the miRNAome of these two tissues under two conditions: watered and drought to determine if some of these tissue-specific miRNA might be regulated under drought conditions. This work confirms the difficulties of analyzing the miRNAome under field conditions and suggests a need to perform studies under artificial conditions such as hydroponics. We have mapped and assigned key miRNAs involved in the response to each wheat chromosome. This will allow the targeting of them through genetic improvement schemes assisted by molecular markers. The specific expression of them in leaves or roots will also help to define their role in important plant developmental and physiological processes. The identification of different homeologous and the analysis of their expression trends are also essential to clarify the role of these miRNAs in the evolution of cereal species as well as their key agronomic aspects. The determination of expression patterns in different tissues is essential for the clarification of the role of key miRNAs in affecting the phenotype of important agronomic traits.

6_REFERENCES

Agharbaoui Z, Leclercq M, Remita MA, Badawi MA, Lord E, Houde M, Danyluk J, Diallo AB, Sarhan F (2015) An integrative approach to identify hexaploid wheat miRNAome associated with development and tolerance to abiotic stress. BMC Genomics 16:339. doi: 10.1186/s12864-015-1490-8

Alptekin B, Akpinar B, Buda H (2017) A comprehensive prediction for plant miRNA identification. Front Plant Sci 7:2058. doi: 10.3389/fpls.2016.02058

Alptekin B, Budak H (2016) Wheat miRNA ancestors: evident by transcriptome analysis of A, B, and D genome donors. Funct Integr Genomics 1-17. doi: 10.1007/s10142-016-0487-y

Alptekin B, Langridge P, Budak H (2016) Abiotic stress miRNomes in the Triticeae. Funct Integr Genomics 1-26. doi: 10.1007/s10142-016-0525-9

Akpinar BA, Kantar M, Budak H (2015) Root precursors of microRNAs in wild emmer and modern wheats show major differences in response to drought stress. Funct Integr Genomics 15(5):587-598. doi: 10.1007/s10142-015-0453-0

Axtell MJ (2013) ShortStack: Comprehensive Annotation and Quantification of Small RNA Genes. RNA 19(6):740–51. doi: 10.1261/rna.035279.112

Bresta P, Nikolopoulos D, Economou G, Vahamidis P, Lyra D, Karamanos A, Karabourniotis G (2011) Modification of water entry (xylem vessels) and water exit (stomata) orchestrates long term drought acclimation of wheat leaves. Plant Soil 349:179–193. doi: 10.1007/s11104-011-0837-4

Bruex A, Kainkaryam RM, Wieckowski Y, Kang YH, Bernhardt C, Xia Y, Zheng X, Wang JY, Lee MM, Benfey P, Woolf PJ, Schiefelbein J (2012) A gene regulatory network for root epidermis cell differentiation in Arabidopsis. PLoS Genet 8:e1002446. doi: 10.1371/journal.pgen.1002446

Budak H, Kantar M, Bulut R, Akpinar BA (2015) Stress responsive miRNAs and isomiRs in cereals. Plant Sci 235:1-13. doi: 10.1016/j.plantsci.2015.02.008

Cheah BH, Nadarajah K, Divate MD, Wickneswari R (2015) Identification of four functionally important microRNA families with contrasting differential expression profiles between drought-tolerant and susceptible rice leaf at vegetative stage. BMC Genomics 16:692. doi 10.1186/s12864-015-1851-3

Fahlgren N, Howell MD, Kasschau KD, Chapman EJ, Sullivan CM, Cumbie JS, Givan SA, Law TF, Grant SR, Dangl JL, Carrington JC (2007) High-Throughput Sequencing of Arabidopsis microRNAs: Evidence for Frequent Birth and Death of MIRNA Genes. PloS One 2(2):e219. doi:10.1371/journal.pone.0000219

Fu L, Niu B, Zhu Z, Wu S, Li W (2012) CD-HIT: Accelerated for Clustering the next-generation Sequencing Data. Bioinformatics 28(23):3150-52. doi: 10.1093/bioinformatics/bts565

Jeong H, Mason SP, Barabási A-L, Oltvai ZN (2001) Lethality and centrality in protein networks. Nature 41:41-42. doi: 10.1038/35075138

Jung HW, Kim W, Hwang BK (2003) Three pathogen-inducible genes encoding lipid transfer protein from pepper are differentially activated by pathogens, abiotic, and environmental stresses. Plant Cell Environ 26:915-928. doi: 10.1046/j.1365-3040.2003.01024.x

Kantar M, Lucas SJ, Budak H (2011) miRNA expression patterns of Triticum dicoccoides in response to shock drought stress. Planta 233:471-484. doi: 10.1007/s00425-010-1309-4

Kantar M, Akpinar BA, Valarik M, Lucas SJ, Dolezel J, Hernandez P, Budak H (2012) Subgenomic analysis of microRNAs in polyploid wheat. Funct & Integr Genomics 12 (3): 465-479. doi: 10.1007/s10142-012-0285-0

Kozomara A, Griffiths-Jones S (2014) miRBase: annotating high confidence microRNAs using deep sequencing data. Nucl Acids Res 42(D1):D68-D73. doi: 10.1093/nar/gkt1181

Kurihara Y, Watanabe Y (2004) Arabidopsis micro-RNA biogenesis through Dicer-like 1 protein functions. PNAS 101(34):12753-12758. doi: 10.1073/pnas.0403115101

Kurtoglu KY, Kantar M, Lucas SJ, Budak H (2013) Unique and conserved microRNAs in wheat chromosome 5D revealed by next-generation sequencing. PLoS One. doi: 10.1371/journal.pone.0069801

Kurtoglu KY, Kantar M, Budak H (2014) New wheat microRNA using whole-genome sequence. Funct Integr Genomics 14(2): 363-379. doi:10.1007/s10142-013-0357-9

International Wheat Genome Sequencing Consortium (2014) A chromosome-based draft sequence of the hexaploid bread wheat (Triticum aestivum) genome. Science 345:6194. doi: 10.1126/science.1251788

Langmead B, Trapnell C, Pop M, Salzberg SL (2009) Ultrafast and Memory-Efficient Alignment of Short DNA Sequences to the Human Genome. Genome Biol 10(3):R25. doi: 10.1186/gb-2009-10-3-r25

Li JS, Fu FL, An M, Zhou SF, She YH, Li WC (2013) Differential expression of microRNAs in response to drought stress in maize. Journal of Integrative Agriculture 12: 1414 –1422. doi: 10.1016/s2095-3119(13)60311-1

Li W-X, Oono Y, Zhu J, He XJ, Wu JM, Iida K, Lu XY, Cui X, Jin H, Zhu JK (2008) The Arabidopsis NFYA5 transcription factor is regulated transcriptionally and posttranscriptionally to promote drought resistance. Plant Cell 20:2238–51. doi:10.1105/tpc.108.059444

Liu H, Able AJ, Able JA (2016a) SMARTER de-stressed cereal breeding. Trends Plant Sci. doi: 10.1016/j.tplants.2016.07.006

Liu H, Able AJ, Able JA (2016b) Water-deficit stress-responsive microRNAs and their targets in four durum wheat genotypes. Functional & Integrative Genomics 1-15. doi:10.1007/s10142-016-0515-y

Liu H, Searle IR, Watson-Haigh NS, Baumann U, Mather DE, Able AJ, Able JA (2015) Genome-wide identification of microRNAs in leaves and the developing head of four durum genotypes during water deficit stress. PLoS ONE 10(11):e0142799. doi:10.1371/journal.pone.0142799

Liu SH, Wang NF, Zhang PY, Cong B, Lin X, Wang S, Xia G, Huang X (2013) Next-generation sequencing-based transcriptome profiling analysis of Pohlia nutans reveals insight into the stress-relevant genes in antarctic moss. Extremophiles 17:391-403. doi: 10.1007/s00792-013-0528-6

Love MI, Huber W, Anders S (2014) Moderated Estimation of Fold Change and Dispersion for RNA-Seq Data with DESeq2. Genome Biol 15(12):550. doi: 10.1186/s13059-014-0550-8

Lucas SJ, Budak H (2012) Sorting the Wheat from the Chaff: Identifying miRNAs in Genomic Survey Sequences of Triticum aestivum Chromosome 1AL. PLoS ONE 7(7): e40859. doi:10.1371/journal.pone.0040859

Ma X, Xin Z, Wang Z, Yang Q, Guo S, Guo X, Cao L, Lin T (2015) Identification and comparative analysis of differentially expressed miRNAs in leaves of two wheat (Triticum aestivum L.) genotypes during dehydration stress. BMC Plant Biol 15:21. doi: 10.1186/s12870-015-0413-9

Martin M (2011) Cutadapt Removes Adapter Sequences from High-Throughput Sequencing Reads. EMBnet.journal 17(1):10-12. doi: http://dx.doi.org/10.14806/ej.17.1.200

Martinelli F, Tonutti P (2012) Flavonoid metabolism and gene expression in developing olive (*Olea europaea L.*) fruit. Plant Biosyst 146 (1):164-170. doi: 10.1080/11263504.2012.681320

McGinnis Scott, Madden TL (2004) BLAST: At the Core of a Powerful and Diverse Set of Sequence Analysis Tools. Nucleic Acids Res 32(Web Server issue):W20–25. doi: 10.1093/nar/gkh435

Meyers BC, Axtell MJ, Bartel B, Bartel DP, Baulcombe D, Bowman JL, Cao X, Carrington JC, Chen X, Green PJ, Griffiths-Jones S, Jacobsen SE, Mallory AC, Martienssen RA, Poethig RS, Qi Y, Vaucheret H, Voinnet O, Watanabe Y, Weigel D, Zhu JK (2008) Criteria for Annotation of Plant MicroRNAs. Plant Cell 20(12):3186-90. doi: 10.1105/tpc.108.064311

Nakashima K, Takasaki H, Mizoi J, Shinozaki K, Shinozaki KY (2012) NAC transcription factors in plant abiotic stress responses. BBA-Gene Regul Mech. 1819:97-103. doi: 10.1016/j.bbagrm.2011.10.005

Pandey R, Joshi G, Bhardwaj AR, Agarwal M, Katiyar-Agarwal S (2014) A comprehensive genome-wide study on tissue-specific and abiotic stress-specific miRNAs in Triticum aestivum. PLoS One. doi: 10.1371/journal.pone.0095800

Peng JH, Sun D, Nevo E (2011) Domestication evolution, genetics and genomics in wheat. Mol Breed 28 (3): 281-301. doi: 10.1007/s11032-011-9608-4

Phillips JR, Dalmay T, Bartels D (2007) The role of small RNAs in abiotic stress. Febs Letters 581:3592-7.

Proost S, Van Bel M, Sterck L, Billiau K, Van Parys T, Van de Peer Y, Vandepoele K (2009) PLAZA: A Comparative Genomics Resource to Study Gene and Genome Evolution in Plants. Plant Cell 21(12):3718-31. doi: 10.1105/tpc.109.071506

Salisbury FB, Ross CW (1992) Photosynthesis: environmental and agricultural aspects. Plant physiology. Wadsworth Publishing Company, Belmont, CA, 286, 249-265.

Su YH, Liu YB, Zhang XS (2011) Auxin-cytokinin interaction regulates meristem development. Mol Plant 4:616-625. doi: 10.1093/mp/ssr007

Shui X-R, Chen Z-W, Li J-X (2013) MicroRNA prediction and its function in regulating drought-related genes in cowpea. Plant Sci 210:25-35. doi: 10.1016/j.plantsci.2013.05.002

Sun Z, Wang Y, Mou F, Tian Y, Chen L, Zhang S, Jiang Q, Li X (2016) Genome-Wide Small RNA Analysis of Soybean Reveals Auxin Responsive microRNAs that are Differentially Expressed in Response to Salt Stress in Root Apex. Front Plant Sci 6:1273. doi: 10.3389/fpls.2015.01273

Sunkar R, Zhou X, Zheng Y, Zhang W, Zhu JK (2008) Identification of novel and candidate miRNAs in rice by high throughput sequencing. BMC Plant Biol 8:25. doi: 10.1186/1471-2229-8-25

Tang Z, Zhang L, Xu C, Yuan S, Zhang F, Zheng Y, Zhao C (2012) Uncovering small RNA-mediated responses to cold stress in a wheat thermosensitive genic male-sterile line by deep sequencing. Plant Physiol 159:71-738. doi: 10.1104/pp.112.196048

Van Bel M, Proost S, Van Neste C, Deforce D, Van de Peer Y, Vandepoele K (2013) TRAPID: An Efficient Online Tool for the Functional and Comparative Analysis of de Novo RNA-Seq Transcriptomes. Genome Biol 14(12):R134. doi: 10.1186/gb-2013-14-12-r134

Wang Y, Zhang C, Hao Q, Sha A, Zhou R, Zhou X, Yuan L (2013) Elucidation of miRNAs-mediated responses to low nitrogen stress by deep sequencing of two soybean genotypes. PLoS One 8:e67423. doi: 10.1371/journal.pone.0067423

Won SK, Lee Y, Lee HY, Heo YK, Cho M, Cho HT (2009) cis-element- and transcriptome-based screening of root hair-specific genes and their functional characterization in Arabidopsis. Plant Physiol 150:1459-1473. doi: http://dx.doi.org/10.1104/pp.109.140905

Xin M, Wang Y, Yao Y, Xie C, Peng H, Ni Z, Sun Q (2010) Diverse set of microRNAs are responsive to powdery mildew infection and heat stress in wheat (Triticum aestivum L.). BMC Plant Biol 10:123-133. doi: 10.1186/1471-2229-10-123

Xu Z, Zhong S, Li X, Li W, Rothstein SJ, Zhang S, Bi Y, Xie C (2011) Genome-wide identification of microRNAs in response to low nitrate availability in maize leaves and roots. PLoS One 6:e28009. doi: 10.1371/journal.pone.0028009

Zhang L, Yu S, Zuo K, Luo L, Tang K (2012) Identification of gene modules associated with drought response in rice by network-based analysis. - PLoS One 7: e33748. doi: 10.1371/journal.pone.0033748

Zhao M, Ding H, Zhu J-K, Zhang F, Li W-X (2011) Involvement of miR169 in the nitrogen-starvation responses in Arabidopsis. New Phytol 190:906-915. doi: 10.1111/j.1469-8137.2011.03647.x

Zhao YY, Guo CJ, Li XJ, Duan WW, Ma CY, Chan HM, Wen YL, Lu WJ, Xiao K (2014) Characterization and expression pattern analysis of microRNAs in wheat under drought stress. Biol Plantarum 59:37-46. doi: 10.1007/s10535-014-0463-0

CHAPTER 8

WHEAT MOLECULAR RESPONSES TO SALINITY AND MYCORRHIZAL INOCULATIONS

Veronica Fileccia[1,2§], Paolo Ruisi[1,2], Rosolino Ingraffia[1,2], Dario Giambalvo[1,2], Federico Martinelli[1,2*]

[1]Dipartimento di Scienze Agrarie e Forestali, Università degli Studi di Palermo, Palermo, Italy
[2]Fondazione A. e S. Lima Mancuso, Università degli Studi di Palermo, Palermo, Italy
*Correspondence: Dr Federico Martinelli, Dipartimento di Scienze Agrarie e Forestali, Università degli Studi di Palermo, Viale delle Scienze Ed.4, Palermo, 90128, Italy. Email: federico.martinelli@unipa.it; Tel: +393318039998
§These authors should be considered as first authors.

Salt stress is one of the most serious problem to the plant growth and their production because of the toxic effect of ions, drought stress and nutrition imbalance. It has also effect to the growth of arbuscular mycorrhizal fungi reducing their colonization. The goal of this work is to determine how some key genes of durum wheat (cv. Anco Marzio) involved in stress responses and nutrient transport are regulated by AMF inoculations in a high salinity environment. For this reason plants grown outdoors in pots under four conditions: absence and presence of salinity stress with or without AM fungi inoculation (No-stress +AM, No-stress -AM, Saline-stress -AM, Saline-stress +AM). We analyzed, through Real-Time PCR, eleven genes involved into nitrate and ammonium transporters (NRT1.1, NAR2.2, AMT1.1, AMT1.2) and drought stress responses (AQP1, AQP4, DHN15.3, PIP1, NAC8, DREB5, DREB6). The results of the present study showed an induction of NAC8, DREB6 and DHN15.3 wheat genes in response to salt stress condition. Our data confirmed agronomic benefits from AM symbiosis. Under salinity conditions, they had a favorable impact on N acquisition and N concentration, aboveground and root biomass, and membrane stability.

1_INTRODUCTION

Soil salinity is one of the most serious environmental stresses that limit crop production; more than 6% of the world's total land area is indeed affected by salinity and sodicity (Munns and Tester 2008). High concentrations in soil of cations such as sodium (Na^+) or anions such as chloride (Cl^-) make it difficult for plant roots to extract water (due to the reduction of soil osmotic potential) and nutrients, and high concentrations of salts inside the plant can have toxic effects (Munns and Tester 2008), with inhibition of protein synthesis, disruption of enzymes, damage of membrane integrity and cell organelles (Ruíz-Lozano et al. 2012). To avoid damages from salinity, plants have evolved several mechanisms that are implicated in ionic and water/osmotic homeostasis through the regulation of genes involved in the transport and compartmentation of nutrients (Munns 2005), the accumulation of solutes (Talaat and Shawky 2013), and the expression of aquaporins (Ouziad et al. 2006), the latter being a group of water-channel proteins that promote and regulate the passive movement of water molecules through a water potential gradient (Kruse et al. 2006; Heinen et al. 2009). However, although it is well established that aquaporins play an important role in regulating the transcellular transport of water in plant tissues, the comprehension of the relationship between expression of aquaporin genes and plant response to water deficit caused by osmotic stress still remains quite limited. Besides these mechanisms, plants have also evolved systems to repair the cellular damages caused by salinity. For instance, changes in the expression of dehydrin (DHN) genes in plants grown under water-related stresses have been reported (Brini et al. 2007; Hanin et al. 2016). Dehydrins are considered as stress proteins involved in formation of plant protective reactions against dehydration, but their specific function has not been well understood so far (Allagulova et al. 2003; Kumar et al. 2014). Drira et al. (2016) showed that *Arabidopsis thaliana* (L.) Heynh overexpressing wheat (*Triticum aestivum* L.) DHN-5 maintained higher reactive oxygen species (ROS)-scavenging enzymatic activity and accumulated lower levels of H_2O_2, thus improving their resistance to water-related stress.

In addition to these intrinsic mechanisms of adaptation, plants growing under adverse environmental conditions, such as saline soils, can improve their performance indirectly, by establishing associative relationships with a number of soil microorganisms, such as bacteria and/or fungi. Among the latter, arbuscular-mycorrhizal (AM) fungi are able to activate symbiotic relationships with the majority of land plants. AM symbiosis has a positive influence on plant growth, which is mainly attributable to the ability of AM fungi to take up from the soil both water (Jayne and Quigley 2014; Saia et al. 2014a) and nutrients—especially phosphorus, P (Barea et al. 2008; Lambers et al. 2008), and to a lesser extent nitrogen, N (Azcón et al. 2001; Saia et al.

2014b) and deliver them to the roots of its host, and also to enhance the health of its host by protecting it from pathogens, pests, and parasitic plants (Jung et al. 2012). AM fungi occur naturally in saline soils and they can be present even under severe salinity (Yamato et al. 2008; Wilde et al. 2009). Many studies have shown that AM symbiosis can improve the tolerance of plants in growing under salt-stress conditions, reducing their yield losses (Cantrell and Linderman 2001; Feng et al. 2002; Colla et al. 2008; Hajiboland et al. 2010; Talaat and Shawky 2011). Several mechanisms have been suggested to be involved in the increased salinity tolerance of mycorrhizal plants compared to non-mycorrhizal plants, including enhanced capacity in the uptake of both water and nutrients (mainly P, N, calcium, and potassium, K) (Mohammad et al. 2003; Giri et al. 2007; Hajiboland et al. 2010), better maintenance of membrane integrity (which facilitates compartmentation of Na^+ and Cl^- within vacuoles and selective ion intake and translocation; Cramer 2004), maintenance of proper K^+/Na^+ ratios in plant tissues (thus helping to prevent the disruption of K-mediated enzymatic processes and the inhibition of protein synthesis; Wu et al. 2010), enhanced osmoregulation due to a higher accumulation of osmoprotectant solutes (such as proline and glycine betaine) and soluble sugars in plant tissues (Sharifi et al. 2007; Sheng et al. 2011; Talaat and Shawky 2011). However, according to Ruíz-Lozano et al. (2012), the understanding of the deeper mechanisms that allow mycorrhizal plants to exhibit higher tolerance to salinity is far from being complete. In particular, the molecular mechanisms involved in this beneficial effect are still poorly investigated. Consequently, to improve the comprehension of the mechanisms implicated in salinity stress alleviation by AM symbiosis, it is important to study how the expression of the genes involved in the regulation of functions such as the uptake and transport of water and nutrients varies in mycorrhizal plants grown under salt-stress conditions. Hence, an experiment was conducted growing durum wheat (*Triticum durum* Desf.) plants under salt-stress conditions to evaluate the influence of AM symbiosis on the expression of a number of genes (nitrate and ammonium transporters and drought stress-related genes) most likely of relevance in plant response to salinity stress. Moreover, the agronomic response to salinity of durum wheat mycorrhizal plants was also evaluated to find relationships with the variation in gene expression. Durum wheat was chosen as model plant for this investigation due to its importance as crop plant in the arid and semiarid areas of the Mediterranean basin.

2_MATERIALS AND METHODS

2.1_Plant Material and Experimental Design

The experiment was conducted at the Department of Agricultural and Forest Sciences of the University of Palermo, Italy, using durum wheat (*Triticum durum* Desf.) plants grown outdoors in pots under four conditions: absence of salinity stress with or without AM fungi inoculation (No-stress +AM and No-stress -AM, respectively); presence of salinity stress with or without AM fungi inoculation (Saline-stress +AM and Saline-stress -AM, respectively). A complete randomized factorial design was adopted considering seven replicates. Each pot (diameter 150 mm, height 130 mm) was filled with 2000 g of a quartz sand:soil mixture (1:1). Soil properties were as follows: 267 g kg^{-1} clay, 247 g kg^{-1} silt, and 486 g kg^{-1} sand; pH 8.0; 6.3 g kg^{-1} total C; 0.86 g kg^{-1} total N; 1.70 dS m^{-1} saturated electrical conductivity (EC) (25 °C). Both soil and sand were sieved through a 2 mm mesh and autoclaved at 121 °C for 20 min in order to completely impair soil biological (both fungal and bacterial) activity. The bacterial microflora was extracted by suspending 500 g soil in 1.5 l distilled water. After shaking and decanting, the suspension was filtered (11 μm mesh) to discard natural AM fungi. Before starting the experiment, each pot received 30 ml of soil suspension filtrate to reintroduce the natural microbial community. Inoculation with AM fungi involved the application of a commercial AM inoculum at a rate of 10 g per pot. The inoculum consisted of a mixture of spores of *Rhizophagus irregularis* (formerly *Glomus intraradices*) and *Funneliformis mosseae* (formerly *G. mosseae*), each of which was present at a rate of 700 spores g^{-1} of inoculum. Each pot received 60 mg of N in the form of $[NH_4]_2SO_4$.

Sixteen seeds of durum wheat (cv Anco Marzio), previously surface-sterilized with hydrogen peroxide at 4% for 3 minutes, were sown in each pot. Ten days after emergence, plants were thinned to six seedlings per pot. To avoid the negative effect of salinity on both the thin seedlings and the establishment of the AM symbiosis, wheat plants were grown for 15 days before the application of the salinity treatment. The latter was obtained by adding NaCl in irrigation water (0 and 10 g l^{-1}). To prevent osmotic shock, salt was added gradually by distributing in total 1 l of the NaCl solution in each pot during the 7 days starting from the beginning of the salinity treatment. This led the EC of saturated soil extract to 1.50 and to 13.00 dS m^{-1} in the non-stressed and salt-stressed treatments, respectively. From this moment, plants were watered with tap water (0.58 dS m^{-1}) until harvest. Leaching was avoided by maintaining soil water always below field capacity. During the experiment, irrigation was done every two days and, for each pot, the amount of irrigation water consisted of total replenishment of water

lost though evapotranspiration. Evapotranspiration losses were determined considering the variations in pot weight measured daily.

All pots were harvested after 45 days from sowing. On the harvest day, before biomass was sampled, the chlorophyll contents of leaves were determined using a hand-held chlorophyll meter (SPAD-502, Minolta, UK), averaging readings from ten full expanded leaves of plants randomly selected in each pot. After this, plant biomass was immediately separated into roots, stems, green leaves, and senescent and dry leaves, and fresh weights were recorded. About 1 g of green leaves and 1 g of roots from each pot were immediately frozen in liquid nitrogen (N), stored at −80 °C, and subsequently pulverized without thawing. At the same time, a sample of green full expanded leaves (about 400 mg) was taken from each pot to determine the membrane stability index (MSI). The leaf material was divided in two sets of 200 mg each. The first set was heated at 40 °C for 30 min in a water bath (10 cm^3); then the electrical conductivity bridge (*C*1) was measured. The second set was boiled at 100 °C for 10 min (in 10 cm^3 of water) before measuring the electrical conductivity bridge (*C*2). MSI was calculated according to the formula by Sairam et al. (1997):

$$MSI = \left[1 - \frac{C1}{C2}\right] \times 100$$

Moreover a representative root sample (about 1 g) was taken from each pot to determine the overall colonization of roots by AM fungi. To this end, root samples were cleared with 100 g/l potassium hydroxide (KOH) and stained with 50 mg/l trypan blue following the method described by Phillips and Hayman (1970). Root colonization by AM fungi was then measured with the grid intersect method according to Giovannetti and Mosse (1980).

For each pot, the remaining plant biomass was dried at 65 °C for 36 h (separately for each botanical fraction) to determine the dry matter content and calculate the belowground and aboveground dry masses. Moreover, plant N content was determined separately for each botanical fraction using the combustion method of Dumas (DuMaster D-480, Büchi Labortechnik AG, Switzerland).

2.2_RNA extraction and cDNA preparation

RNA was extracted using the Spectrum Plant Total RNA kit (Sigma). RNA quantity was measured with the Nanodrop and the quality was analyzed using electrophoresis by loading 1 µl of sample on 2 % agarose gel. DNase treatment and cDNA synthesis were performed in a combined protocol following Quantitect Reverse Transcription Kit (Qiagen) instructions.

2.3_Gene expression analysis

Quantitative RT-PCR was used to analyze the expression of durum wheat genes. Three biological replicates were considered for each condition. Eleven genes were analyzed belonging to nitrate transporters and ammonium transporters (NRT1.1, NAR2.2, AMT1.1, AMT1.2) and drought stress responses (AQP1, AQP4, DHN15.3, PIP1, NAC8, DREB5, DREB6). For each target gene, PCR primers were designed basing on *T. aestivum* sequences deposited in NCBI (**Table 1**). Real Time PCR was performed with iTaq Universal SYBR Green Supermix (BioRad). Amplifications were conducted using 25 ng cDNA in a 15 µL final volume with a Biorad iQ5 PCR system (Biorad) with standard conditions: 3 min at 95°C, 40 cycles of 15 s at 95°C, and 45 sec at 60°C. All PCR reactions were performed in duplicates and 18S of *T. aestivum* was used as an endogenous reference. Fluorescent signals were determined during the annealing temperature and CT values extracted with an auto-calculated threshold followed by baseline subtraction. ΔΔCT was determined by subtracting the average of 18S from the average CT of the analyzed gene.

2.4_Statistical data analysis

Data collected on plants were subjected to analysis of variance (ANOVA) according to the experimental design. Variables corresponding to proportions were arcsine transformed before analysis to assure a better fit with the Gaussian law distribution. Treatment means were compared using Fisher's protected least significant differences test at the 5% probability level.

Table 1| List of primers used in qRT-PCR analysis

Gene	GenBank Accession number	Primer sequences
NRT1.1	AY587265.1	F: CACAGCGAATAGGGATTGGT
		R: CGCCTAGCAGGAAGTACTGG
NAR2.2	AY763795.1	F: CCTCTCCAAGCTTCCTGTGA
		R: CGTAGCAGAGGCTGACCTT
AMT1.1	AY390355.1	F: CCAAGAACACCATGAACATC
		R: GGAAGAGGAAGAAGCTGTAG
AMT1.2	AY525638.1	F: CGGCTTCGACTACAGCTTCT
		R: AGTGGGACACCACAGGGTAG
AQP1	DQ867075.1	F: AGCGAACAAGTACTCGGAG
		R: TAGAGGAAGAGGGAGGTG
AQP4	DQ867078.1	F: CGGATGTGGTCCTTCTAC
		R: ACGAGGACGAAGATCATG
DHN15.3	AM180931.1	F: CGTCGACGAGTACGGTAAC
		R: CCATGCCATCATCCTCAGAC
PIP1	AF366564.1	F: CACCTTCGGGCTGTTTTTG
		R: GTCTGGAACCCCTTGACC
NAC8	HM027573.1	F: CGCATGGGATGATGTCAAG
		R: CATAGGGAAGTTCACCGTC
DREB5	AY781358.1	F: GAGGAACTTGTGGAGCAGAG
		R: ATCTCCGAGGTCGCTTTTTC
DREB6	AY781361.1	F: AAAACCAGAAGCTCCTGC
		R: TGCTCTGAGAAGTTGACAC
18S	AB778770.1	F: CAACGGATATCTCGGCTCTC
		R: TTGCGTTCAAAGACTCGATG

3_RESULTS

Salinity significantly affected all the traits measured in plants (**Tables 2** and **3**). On average, compared to the control (non-stressed condition), salt stress reduced the number of stems per plant (–47%), the aboveground biomass (–33%), and, particularly, the root biomass (–64%; **Table 2**). On the contrary, plants grown under salt stress conditions had chlorophyll meter readings (SPAD values) higher than non-stressed plants. Similarly, the N concentrations of both the root and the aboveground biomass (the latter including green leaves, senescent and dry leaves, and stems) were all significantly higher under salt stress compared to the control (**Table 3**). On the contrary, the total N uptake was on average markedly lower in salt stressed plants (–30%).

Uninoculated plants showed insignificant mycorrhizal colonization levels (always <1% of root length colonized; **Table 2**). Characteristic structures of AM fungi were observed in the roots after inoculation, with mycorrhizal colonization levels >30% both in non-stressed and salt stressed conditions. On average, compared to the non-mycorrhizal treatment, AM plants showed higher aboveground and root biomass (+5% and +14%, respectively), whereas no effect of AM symbiosis was observed on the number of stems per plant and the proportion of leaves on the aboveground biomass. Mycorrhizal plants showed SPAD values slightly higher than uninoculated plants under both salt stressed and non-stressed conditions. Moreover, AM plants, compared to non-AM plants, had a higher total N uptake (+18% on average) and a higher N concentration in the total aboveground biomass (+13% on average; **Table 3**). This evidence was confirmed for all the botanical fractions except for the roots. The effects of both the treatments applied ('Salinity stress' and 'Mycorrhizal inoculum') on SPAD values were similar to those observed for total aboveground biomass N concentration. These two traits were strictly and positively correlated.

Soil salinization significantly decreased MSI values compared to the non-stressed condition (–18% on average; **Table 2**). The interaction 'Salinity stress × Mycorrhizal' inoculum was significant at the 5% probability level; in fact, while under non-stressed conditions no effect was observed by AM symbiosis, under salinity stress the MSI values were significantly higher in +AM compared to –AM treatment.

Table 2| Number of stems per plant, aboveground and root biomass (as grams of dry matter per pot), proportion of green leaves, SPAD value, membrane stability index (MSI), and levels of mycorrhizal infection in durum wheat grown under no- and saline-stress regimes and in the presence or absence of arbuscular mycorrhizal symbiosis. +AM = inoculation with arbuscular mycorrhizal spores; –AM, suppression of arbuscular mycorrhizal symbiosis.

Trait		No-stress		Saline-stress		Significance		
		+AM	–AM	+AM	–AM	Stress	Inoc.	Stress × Inoc.
No. stems per plant	n°	4.6	5.0	2.7	2.4	***	ns	ns
Aboveground biomass (AB)	g per pot	2.19	2.15	1.51	1.39	***	*	ns
Root biomass	g per pot	2.33	2.14	0.93	0.70	***	*	ns
Proportion of green leaves	% on AB	50.1	46.2	34.3	34.1	***	ns	ns
SPAD value	—	50.5	49.3	53.1	52.1	***	*	ns
MSI	—	86.1	86.0	75.0	66.6	***	ns	*
Mycorrhizal infection	%	36.4	0.8	31.2	0.5	*	***	ns

****, **, * denote significant differences at 0.001, 0.01, and 0.05 probability levels, respectively; ns indicate differences not significant*

Table 3| Nitrogen concentration in the aboveground (total and separately for each botanical fraction) and root biomasses, and total N uptake in durum wheat grown under no- and saline-stress regimes and in the presence or absence of arbuscular mycorrhizal symbiosis. +AM = inoculation with arbuscular mycorrhizal spores; –AM, suppression of arbuscular mycorrhizal symbiosis.

Trait		No-stress		Saline-stress		Significance		
		+AM	–AM	+AM	–AM	Stress	Inoc.	Stress × Inoc.
N concentration of:								
Total aboveground biomass	g kg^{-1}	0.309	0.265	0.365	0.331	***	***	*
Green leaves	g kg^{-1}	0.385	0.343	0.409	0.389	***	***	*
Senescent and dry leaves	g kg^{-1}	0.204	0.209	0.338	0.359	***	ns	*
Stems	g kg^{-1}	0.251	0.212	0.274	0.232	*	***	ns
Root biomass	g kg^{-1}	0.124	0.122	0.143	0.150	**	ns	ns
Total N uptake	mg N per pot	95.1	82.6	68.5	56.3	***	***	ns

****, **, * denote significant differences at 0.001, 0.01, and 0.05 probability levels, respectively; ns indicate differences not significant*

3.1_Nitrogen transporter genes

The expression of both ammonium transporters was not significantly regulated by both salinity stress and mycorrhizal inoculation. Salt stress condition induced NAR2.2 expression while the presence of mycorrhizae upregulated the expression of NRT1.1 (**Fig. 1**).

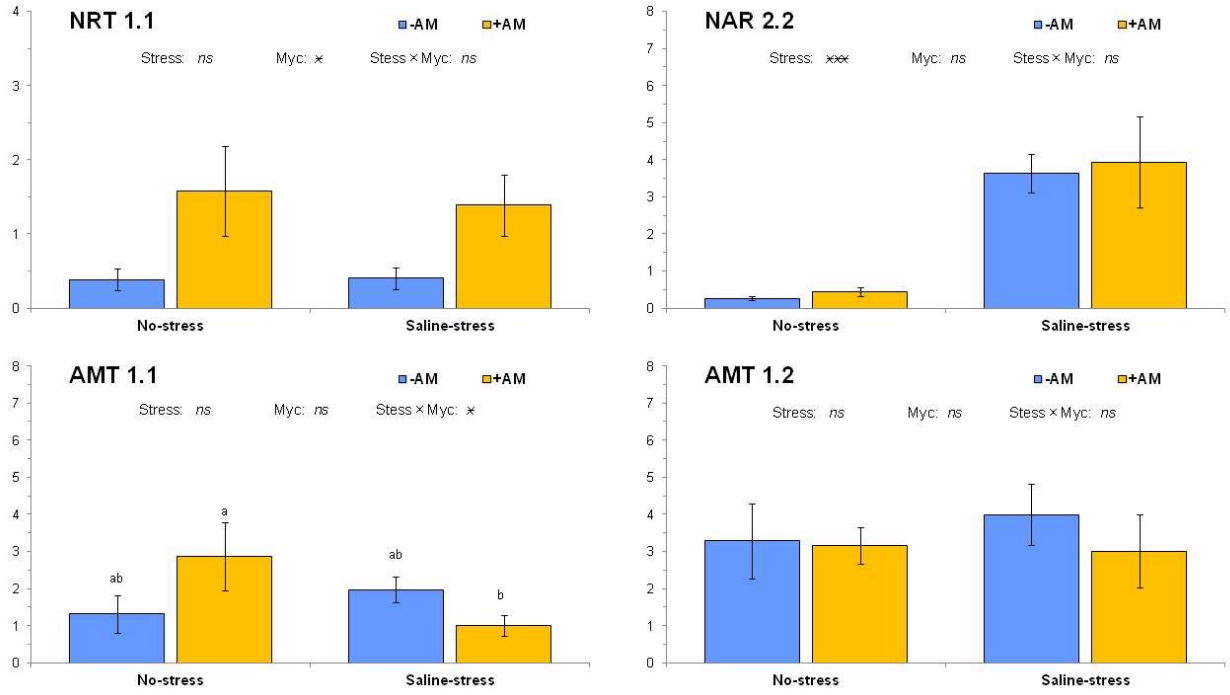

Fig. 1| Expression of nitrogen transport-related genes (NRT1.1, NAR2.2, AMT1.1 and AMT1.2) in response to salt stress and mycorrhizae inoculation. Means and standard deviation were indicated. Different letters means significant differences among the four treatments using post-hoc test. ns = not significant; † = p value 0,1; x = p value 0,05; xx = p value 0,01; xxx = p value 0,001.

3.2_Stress related genes

Seven genes involved in abiotic stress responses (AQP1, AQP4, DREB5, DREB6, DHN15.3, PIP1 and NAC8) were analyzed in relation to salt stress and mycorrhizal inoculation (**Fig. 2**). An upregulation effect of mycorrhizae of NAC8 was clearly observed by stress salinity. This gene was also significantly induced by mycorrhizal inoculation under no stress conditions. Most of the genes are induced in salt stress condition. NAC8, DREB5, DHN15 were significantly induced by salinity and absence of mycorrhizal inoculation. Although differences were not significant, mycorrhizae seemed to mitigate the salt-induction of AQP1, AQP4, PIP1, DREB5, DHN15 (**Fig. 2**).

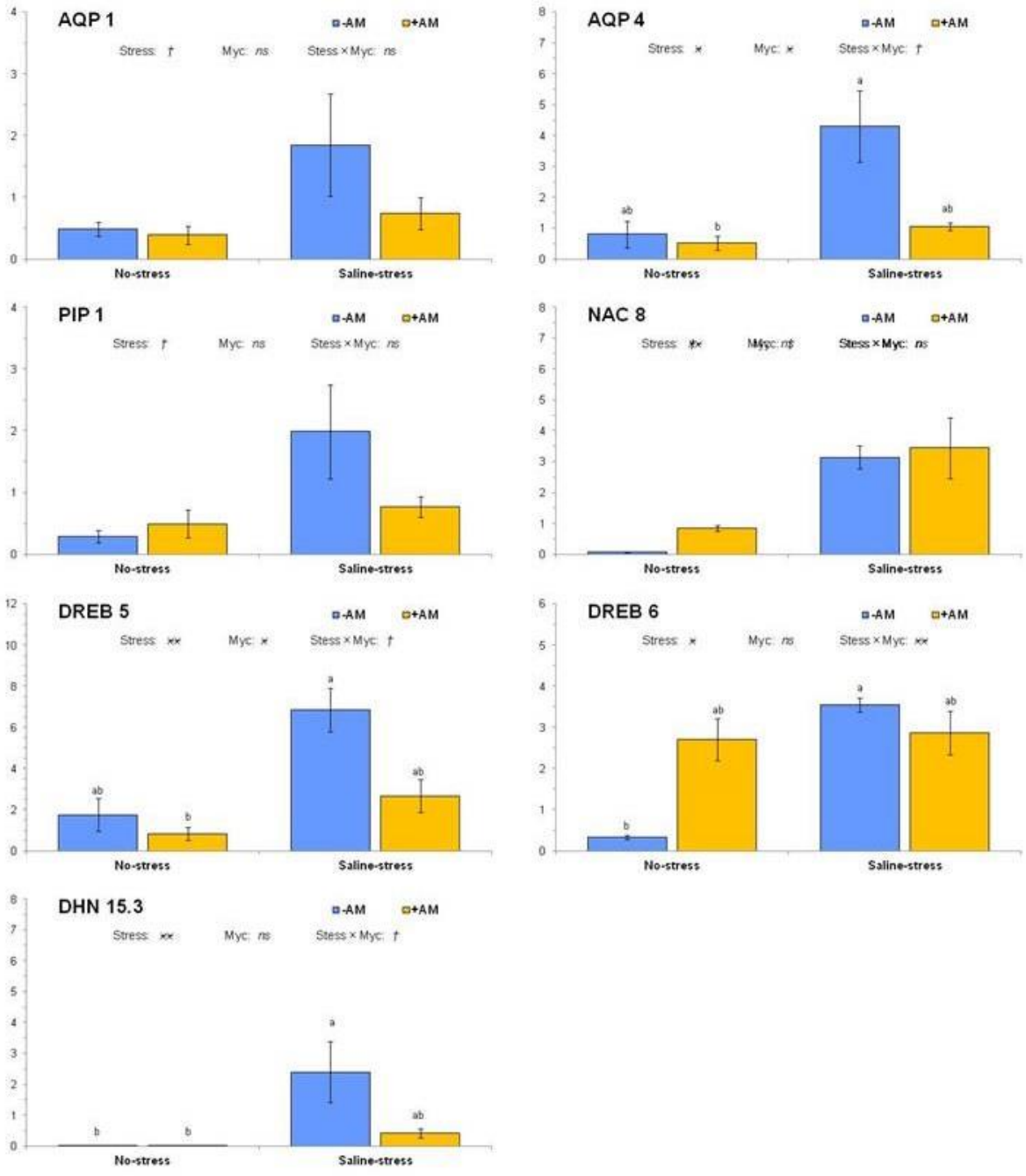

Fig. 2| Expression of drought stress response genes (AQP1, AQP4, DREB5, DREB6, DHN15.3, PIP1 and NAC8) in response to salt stress and mycorrhizae inoculation. Means and standard deviation were indicated. Different letters means significant differences among the four treatments using post-hoc test. ns = not significant; † = p value 0,1; x = p value 0,05; xx = p value 0,01; xxx = p value 0,001.

3.3_Principal component analysis

Principal component analysis (PCA) was performed to determine how the four conditions globally affect expression of the 11 analyzed genes (**Fig. 3**). The PC component 1 accounted for 43% of the total variation and separated all two salt stress condition (Saline-stress -AM and Saline-stress +AM) from no stress conditions (No-stress -AM and No-stress +AM). Ten of the eleven analyzed genes contributed to this distinctive profile although at different extent. PC component 2 accounted for 14% of the total variability and separated mycorrhizae-salt stress condition (Saline-stress +AM) from the others. NAR2.2, DREB6, DHN15.3 and NAC8 greatly contributed to this separation.

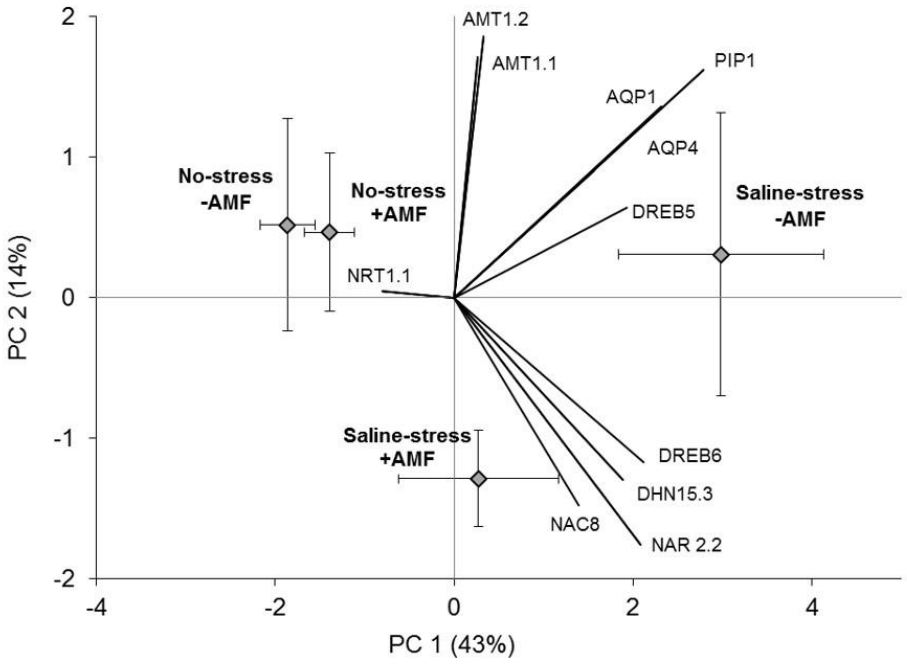

Fig. 3| Principal component analysis of the four salt stress conditions of durum wheat in presence and absence of both salinity and mycorrhizal inoculation. Components of the eleven analyzed genes were also indicated. No-stress +AM and No-stress -AM means absence of salt stress with or without AMF inoculations, respectively; Saline-stress +AM and Saline-stress -AM means presence of salt stress with or without AMF inoculations, respectively.

4_DISCUSSION

Soil salinity is an environmental stress that drastically affects crop growth and productivity. Many studies have demonstrated that salinity can inhibits plant growth through several mechanisms including damage of enzymes and plasma membranes (Hasegawa et al. 2000), reduction in plant water availability (due to the lower soil water potential; Munns and Tester 2008), accumulation of toxic elements (i.e., Na^+ and Cl^-), inhibition of chlorophyll and protein synthesis, reduction in nutrient uptake, transport and/or partitioning within the plant (Grattan and Grieve 1999). In the present study, a severe reduction in both shoot and root biomass was observed in plants of durum wheat when salinity stress was imposed at tillering stage. This reduction was associated to decreases in the stability of membranes (< MSI values in salt stressed plants) and the total N uptake. Many studies showed that salinity can reduces N accumulation in crop plants and that this decrease is generally accompanied by an increase in Cl^- uptake. Therefore, the decrease in plant N uptake is probably to be partially related to the antagonism of nitrate metabolism from chloride (Abdul-Kadir and Paulsen 1982). However, in the present study, while the total N accumulated by plants decreased under salt stress conditions, the N concentrations in all plant tissues (leaves, stems, roots) increased. This result may seem surprising, as much research reports decreases in plant tissues N concentrations due to the negative effects of salt stress on plant N uptake (Talaat and Shawky 2014). Nevertheless, other studies have shown that the plant N concentration increases or remains unchanged when plants are grown under optimal N conditions (Munns and Termaat 1986; Hu and Schmidhalter 2005). The latter condition certainly occurred in the present research in which N was not a limiting factor thanks to the substrate chemical characteristics and the amount of N-fertilizer applied. Therefore, our findings suggest that the negative effects of salinity observed on plant growth cannot be attributed to difficulties in N absorption. At the same time, it is interesting to highlight how the effects of salt stress affected the efficiency of N transport within plant tissues. The high N concentration values observed in the senescent and dry leaves of plants grown under salt stress conditions (which were close to those of green leaves) demonstrate that salt stress prevented the translocation of this element from the senescent leaves to the other plant organs (differently from what observed in plants not subjected to salt stress). On the other hand, salinity may have a negative effect on membrane proteins and change their integrity (Kohler and Raschke 2000), thus compromising nutrient absorption and translocation to the different organs.

Under non-stressed conditions, wheat plants inoculated with AM fungi accumulated more N than non-mycorrhizal plants. This result could be attributable to both the facilitation in host N uptake by AM fungi through the extensive extraradical hyphal network that increases the volume

of soil explored by mycorrhizal plants compared to non-mycorrhizal plants (Bonfante and Genre 2010), and the enhanced effectiveness of AM plants than roots alone in competing with soil microorganisms for inorganic N (Hodge et al. 2000). The increased N accumulation in leaf tissues may be also partially due to the AMF-upregulation of nitrogen transport genes in both stressed and unstressed conditions such as NRT1.1. This gene leads to the import of nitrate in leaf tissues from the apoplast (xylem) and the induction of this gene may contribute to the increase of N uptake observed in leaf tissues.

Moreover, data from the present study revealed that AM symbiosis can mitigates the negative effects of salt stress on plant growth. In particular, under salt stress conditions AM symbiosis had a favorable impact on N acquisition and N concentration, and aboveground and root biomass, in line with the findings of many studies (as reviewed by Porcel et al. 2012). Although the concentration of such osmoprotectant compounds was not measured, we detected a clear positive effect of AM symbiosis on the alleviation of the damaging effect of salinity on the stability of plasma membranes.

4.1_Nutrient transporter genes

Maathuis et al. (2003) and Wang et al. (2012b) showed how under salt stress, the transcripts of nutrient transporter genes were significantly changed. These observations have suggested that, changes in the concentration of a specific nutrient are strictly modulated to preserve a stable nutrient status in salt stress conditions (Maathuis et al. 2003).

A critical role of nitrogen (N) for the growth of plants in numerous agricultural systems is well-known (Yang et al. 2015). NRTs (nitrate transporter genes) are implicated in $NO3^-$ transport at high affinity regulating lateral root development (Remans et al. 2006). The expression of some key nitrogen transport genes have been already investigated in durum wheat roots in response to mycorrhizae inoculations. Different effects of mycorrhizae has been observed depending on the specific genes (Saia et al. 2015a). Although the importance of analyze them on root tissues is widely accepted, their analysis in leaf tissues is also very important to determine how N is translocated between leaf tissues and how it is assimilated in leaf cells from the xylem. Indeed, these genes regulated the import of nitrogen (both nitrate and ammonium) in leaf cells from apoplastic and vascular xylematic solutions (Hsu and Tsay 2013; Hu et al. 2014; Nielsen and Schjoerring 1998; Husted and Schjoerring 1995). The N transport from apoplastic spaces to leaf cells is essential to provide nitrogen for leaf growth, and enhance those pathways directly linked to photosynthetic production.

The nitrate transporter NRT1.1 was the first identified in Arabidopsis thaliana (Alvarez et al. 2012). This gene was shown to be expressed in roots and shoots. The highest expression was observed in the tip epidermis of the primary roots. However the gene was also expressed in the endodermis and mature parts of root tissues (Nazoa et al. 2003). The role of this gene is essential not only in root tissues but also in leaves. Considering that, only one nitrate transport gene was analyzed it is not possible to conclude that the higher leaf concentration of N in mycorrhized plants might be due mycorrhizal-driven transcriptional activation of genes encoding N transport. A different pattern of expression of different genes involved N transport is expected since these genes belong to a large family. The presence of different members in the genome is a typical characteristic in plants because it allows modulate the expression of the same type of protein in different organs and tissues depending on the needs (changes in the apoplast conditions: soil solution or xylem). This does not deny the existence of other AM-driven mechanisms that increase N uptake in leaves such as increased root architecture and growth. This AM-upregulation was not observed for NAR2.2 that is an interactive protein that makes functional the high-affinity transport system for N transport (Saia et al. 2015a). On the contrary NAR2.2 expression is induced by salt stress condition. This diverse regulation of different types of genes involved in N transport may allow the plant to distinguish the two different factors and finely modulate the expression of the genes basing on presence/absence of different environmental factors. Indeed NAR2.2 is not an N transporter but it is a functional interactive protein. So it is possible that mycorrhizal inoculation may regulate N transport by activating directly N transport genes while salinity may regulates plant responses through the induction of genes involved in the interaction with N transporters. This hypothesis will need to be confirmed with next experiments once more genes involved in N transport and uptake will be isolated in durum wheat.

AMT genes were not be altered by mycorrhizal inoculations. These genes belong to a large family of genes that may be differentially modulated by mycorrhizae as previously found in roots (Saia et al. 2015b). The literature on the effect of mycorrhizae on these genes in other plants is scarce. In *Oryza sativa*, the high salinity conditions has induced a greater expression of OsAMT1;1 than other AMT genes. Wang et al. (2012a) have found different salt stress responses in OsAMT genes comparing young leaves, where OsAMT1 was more expressed, and old leaves in which OsAMT1;2, OsAMT2;3, OsAMT3;1 OsAMT3;3 expression level was decreased (Wang et al. 2012a). As stated by Goel and Singh (2015), the differential expression of these genes may be due to the fact that an early response to abiotic stresses can determine cell survival.

4.2_Stress-related genes

Salinity stress has similar effects of a water-deficit condition (Mahajan and Tuteja 2005) forcing plants to increase the water acquiring (Ouziad et al. 2006).

In the present experiment, most of the drought-regulated genes are induced in salt stress condition. Our results confirmed a great variety of studies conducted on varieties or cultivars of economically important crops that showed how salinity drastically affects expression of salt-responsive genes. These studies showed that salt-treatment induced a higher expression of aquaporin genes, DREBs (dehydration responsive element binding) and NAC transcription factors (Zhao et al. 2012; Chen et al. 2007; Zheng et al. 2009; Hu et al. 2006). Furthermore, other researches provide evidence for a positive correlation between DHN gene expression and plant abiotic stress tolerance (Hanin et al. 2011; Pelah et al. 1997; Park et al. 2006) including durum wheat (*T. turgidum* ssp. *durum*) (Labhilili et al. 1995). It is generally accepted that the higher expression of these drought stress-responsive genes plays a critical role in improving salt stress tolerance in plants.

Several studies conducted in a variety of cultivated plants show how AM symbiosis improves salt stress resistance in these plants (Rosendahl and Rosendahl 1991; Ruiz-Lozano and Azcón 1996; Al-Karaki et al. 2001; Feng et al. 2002). Although not significantly regulated, a trend of downregulation by mycorrhizae seems to occur in our work when high salinity is present. Results by Ouziad et al. (2006), Aroca et al. (2007) and Jahromi et al. (2008) suggest that aquaporin gene responds differently to AM colonization. This result may be depend on various factors such as the type of aquaporins family and their different complexity of expression patterns, the characteristics of plant and AM species studied, the mode, concentration and time of exposure of salinity stress application (Sarda et al. 1999).

Interestingly mycorrhizae showed a positive regulation of key drought-responsive transcription factors in unstressed conditions such as NAC8 and DREB6. Aroca et al. (2007) studied four aquaporin genes from in mycorrhizal and non mycorrhizal bean plants and they showed that salt-stress increase the expression level of three PIP genes in both conditions but especially in AM plants. Data from Ouziad et al. (2006) showed that salt treatment in AM tomato repressed the amount of TIP and PIP1 but not PIP2 transcripts. DREBs are important transcription factors that control in plants the expression of many stress-responsive genes thus improving the abiotic stress tolerance (Lata and Prasad 2011) and their role is confirmed by different studies in which the expression of DREB genes were induced under diverse abiotic stress treatments (Zhao et al. 2012; Chen et al. 2007). NACs, one of the largest families of transcriptional factors, play critical roles in the regulation of plant abiotic stress–responsive genes

(Nuruzzaman et al. 2013) as it is shown by several studies on rice in which the expression of NAC045 and NAC1 genes was positively improved by diverse abiotic stresses and ABA treatment (Zheng et al. 2009; Hu et al. 2006). The AM-upregulation of NAC8 is interesting because it allows speculate that mycorrhizae may be involved in changes of plant responses to salt stress through an induction of key transcription factors involved in the activation of plant responses to abiotic stress.

5_CONCLUSIONS

Data from the present study confirmed agronomic benefits from AM symbiosis. Under salt stress conditions, they had a favorable impact on N acquisition and N concentration, aboveground and root biomass, and membrane stability. This effect may be partially linked with the upregulation of nitrate transporters in leaves such as NRT1.1 The induction of NAC8, DREB6, DHN15.3 in response to salt stress confirmed previous studies. The upregulation of NAC8 by mycorhizal inoculation is intriguing and needs further investigation.

6_REFERENCES

Abdul-Kadir SM, Paulsen GM (1982) Effect of salinity on nitrogen metabolism in wheat. J Plant Nutr 5:1141–1151. doi: http://dx.doi.org/10.1080/01904168209363047

Adiku G, Renger M, Wessolek G, Facklam M, Hech-Bischoltz C (2001) Simulation of dry matter production and seed yield of common beans under varying soil water and salinity conditions. Agric Water Manage 47:55-68. doi: 10.1016/S0378-3774(00)00094-9

Al-Karaki GN, Hammad R, Rusan M (2001) Response of two tomato cultivars differing in salt tolerance to inoculation with mycorrhizal fungi under salt stress. Mycorrhiza 11:43–47. doi: 10.1007/s005720100098

Allagulova ChR, Gilamov FR, Shakirova FM, Vakhitov VA (2003) The plant dehydrins: structure and functions. Biochemistry (Moscow) 68:945−951. doi: 10.1023/A:1026077825584

Alvarez JM, Vidal EA, Gutiérrez RA (2012) Integration of local and systemic signaling pathways for plant N responses. Curr Opin Plant Biol 15:185–191. doi: 10.1016/j.pbi.2012.03.009

Aroca R, Porcel R, Ruiz-Lozano JM (2007) How does arbuscular mycorrhizal symbiosis regulate root hydraulic properties and plasma membrane aquaporins in Phaseolus vulgaris under drought, cold or salinity stresses?. New Phytol 173:808-816. doi: 10.1111/j.1469-8137.2006.01961.x

Barea JM, Ferrol N, Azcón-Aguilar C, Azcón R (2008) Mycorrhizal symbioses. In: White PJ, Hammond JP, editors. The Ecophysiology of Plant-Phosphorus Interactions. Dordrecht: Springer Netherlands, Vol. 7, pp:143–163.

Bonfante P, Genre A (2010) Mechanisms underlying beneficial plant–fungus interactions in mycorrhizal symbiosis. Nat Commun 1:48. doi:10.1038/ncomms1046

Bravo LA, Gallardo J, Navarrete A, Olave N, Martínez J et al (2003) Cryoprotective activity of a cold-induced dehydrin purified from barley. Physiol Plant 118:262−269. doi: 10.1034/j.1399-3054.2003.00060.x

Brini F, Hanin M, Lumbreras V, Amara I, Khoudi H et al (2007) Overexpression of wheat dehydrin DHN-5 enhances tolerance to salt and osmotic stress in Arabidopsis thaliana. Plant Cell Rep 26:2017−2026. doi: 10.1007/s00299-007-0412-x

Cantrell IC, Linderman RG (2001) Preinoculation of lettuce and onion with VA mycorrhizal fungi reduces deleterious effects of soil salinity. Plant and Soil 233:269–281.

Chaumont F, Barrieu F, Wojcik E, Chrispeels MJ, Jung R (2001) Aquaporins constitute a large and highly divergent protein family in maize. Plant Physiol 125:1206-15.

Chen M, Wang QY, Cheng XG, Xu ZS, Li LC et al (2007) GmDREB2, a soybean DRE-binding transcription factor, conferred drought and high-salt tolerance in transgenic plants. Biochem Biophys Res Commun 353:299–305. doi: 10.1016/j.bbrc.2006.12.027

Colla G, Rouphael Y, Cardarelli M, Tullio M, Rivera CM, Rea E (2008) Alleviation of salt stress by arbuscular mycorrhizal in zucchini plants grown at low and high phosphorus concentration. Biol Fert Soils 44:501–509.

Cutler SR, Rodriguez PL, Finkelstein RR, Abrams SR (2010) Abscisic Acid: Emergence of a Core Signaling Network. Annu. Rev. Plant Biol 61:651–79. doi: 10.1146/annurev-arplant-042809-112122

Drira M, Hanin M, Masmoudi K, Brini F (2016) Comparison of full-length and conserved segments of wheat dehydrin DHN-5 overexpressed in Arabidopsis thaliana showed different responses to abiotic and biotic stress. Funct Plant Biol 43(11):1048-1060.

Feng G, Zhang FS, Li Xl, Tian CY, Tang C, Rengel Z (2002) Improved tolerance of maize plants to salt stress by arbuscular mycorrhiza is related to higher accumulation of soluble sugars in roots. Mycorrhiza 12:185-190. doi: 10.1007/s00572-002-0170-0

Giovannetti M, Mosse B (1980) An evaluation of techniques for measuring vesicular arbuscular mycorrhizal infection in roots. New Phytol 84:489–500. doi: 10.1111/j.1469-8137.1980.tb04556.x

Giri B, Kapoor R, Mukerji KG (2007) Improved tolerance of Acacia nilotica to salt stress by arbuscular mycorrhiza, Glomus fasciculatum, maybe partly related to elevated K+/Na+ ratio in root and shoot tissues. Microb Ecol 54:753–760. doi: 10.1007/s00248-007-9239-9

Goel P, Singh AK (2015) Abiotic Stresses Downregulate Key Genes Involved in Nitrogen Uptake and Assimilation in Brassica juncea L. PLoS ONE 10:e0143645. doi:10.1371/journal.pone.0143645

Grattan SR, Grieve CM (1999) Salinity-mineral nutrient relations in horticultural crops. Sci Hort 78:127–157. doi: http://dx.doi.org/10.1016/S0304-4238(98)00192-7

Hajiboland R, Aliasgharzadeh N, Laiegh SF, Poschenrieder C (2010) Colonization with arbuscular mycorrhizal fungi improves salinity tolerance of tomato (Solanum lycopersicum L.) plants. Plant and Soil 331:313–327.

Hanin M, Brini F, Ebel C, Toda Y, Takeda S, Masmoudi K (2011) Plant dehydrins and stress tolerance: versatile proteins for complex mechanisms. Plant Signal Behav 6:1503-1509. doi: 10.4161/psb.6.10.17088

Hanin M, Ebel C, Ngom M, Laplaze L, Masmoudi K (2016) New Insights on plant salt tolerance mechanisms and their potential use for breeding. Front Plant Sci 7.

Hasegawa PM, Bressan RA, Zhu JK, Bohnert HJ (2000) Plant cellular and molecular responses to high salinity. Annu Rev Plant Physiol Plant Mol Biol 51:463–499. doi: 10.1146/annurev.arplant.51.1.463

Heinen RB, Ye Q, Chaumont F (2009) Role of aquaporins in leaf physiology. J Exp Bot 60(11):2971-2985.

Hodge A (2000) Microbial ecology of the arbuscular mycorrhiza. Microbiol Ecol 32:91-96. doi: 10.1111/j.1574-6941.2000.tb00702.x

Houde M, Dallaire S, N'Dong D, Sarhan F (2004) Overexpression of the acidic dehydrin WCOR410 improves freezing tolerance in transgenic strawberry leaves. Plant Biotechnol J 2:381−387. doi: 10.1111/j.1467-7652.2004.00082.x

Hsu Pk, Tsay YF (2013) Two Phloem Nitrate Transporters, NRT1.11 and NRT1.12, are Important for Redistributing Xylem-Borne Nitrate to Enhance Plant Growth. Plant Physiol 163:844-856. doi: 10.1104/pp.113.226563

Hu Y, Fernández V, Ma L (2014) Nitrate transporters in leaves and their potential roles in foliar uptake of nitrogen dioxide. Front Plant Sci 30:5-360. doi:10.3389/fpls.2014.00360

Hu H, Dai M, Yao J, Xiao B, Li X et al (2006) Overexpressing a NAM, ATAF, and CUC (NAC) transcription factor enhances drought resistance and salt tolerance in rice. Proc Natl Acad Sci USA 103:12987-12992. doi: 10.1073/pnas.0604882103

Hu YC, Schmidhalter U (2005) Drought and salinity: a comparison of their effects on mineral nutrition of plants. J Plant Nutr Soil Sci 168:541–549. DOI: 10.1002/jpln.200420516

Hubbard KE, Nishimura N, Hitomi K, Getzoff ED, Schroeder JI (2010) Early abscisic acid signal transduction mechanisms: newly discovered components and newly emerging questions. Genes Dev 24:1695–1708. doi: 10.1101/gad.1953910

Husted S, Schjoerring JK (1995) Apoplastic pH and ammonium concentration in leaves of Brassica napus L.. Plant Physiol 109:1453-1460.

Ingram J, Bartels D (1996) The molecular basis of dehydration tolerance in plants. Annu Rev Plant Physiol Plant Mol Biol 47:377–403. doi: 10.1146/annurev.arplant.47.1.377

Jahromi F, Aroca R, Porcel R, Ruiz-Lozano JM (2008) Influence of salinity on the in vitro development of Glomus intraradices and on the in vivo physiological and molecular responses of mycorrhizal lettuce plants. Microb Ecol 55:45-53. doi: 10.1007/s00248-007-9249-7

Jayne B, Quigley M (2014) Influence of arbuscular mycorrhiza on growth and reproductive response of plants under water deficit: a meta-analysis. Mycorrhiza 24(2):109-119.

Johanson U, Karlsson M, Johansson I, Gustavsson S, Sjovall S et al (2001) The complete set of genes encoding major intrinsic proteins in Arabidopsis provides a framework for a new nomenclature for major intrinsic proteins in plants. Plant Physiol 126:1358–1369.

Jung SC, Martinez-Medina A, Lopez-Raez JA, Pozo MJ (2012) Mycorrhiza induced resistance and priming of plant defenses. J Chem Ecol 38: 651–664.

Juniper S, Abbott LK (1993) Vesicular-arbuscular mycorrhizas and soil salinity. Mycorrhiza 4:45-57. doi: 10.1007/BF00204058

Kobae Y, Tamura Y, Takai S, Banba M, Hata S (2010) Localized expression of arbuscular mycorrhiza-inducible ammonium transporters in soybean. Plant Cell Physiol 51:1411–1415. doi: 10.1093/pcp/pcq099

Kohler B, Raschke K (2000) The delivery of salts to the xylem. Three types of anion conductance in the plasma membrane of the xylem parenchyma of roots of barley. Plant Physiol 122:243–254.

Kruse E, Uehlein N, Kaldenhoff R (2006) The aquaporins. Genome Biol 7:206. doi:10.1186/gb-2006-7-2-206

Kumar M, Lee SC, Kim JY, Kim SJ, Aye SS, Kim SR (2014) Over-expression of dehydrin gene, *OsDhn1*, improves drought and salt stress tolerance through scavenging of reactive oxygen species in rice (*Oryza sativa* L.). J Plant Biol 57:383. doi:10.1007/s12374-014-0487-1

Labhilili M, Joudrier P, Gautier MF (1995) Characterization of cDNAs encoding Triticum durum dehydrins and their expression patterns in cultivars that differ in drought tolerance. Plant Sci 112:219-30. doi: http://dx.doi.org/10.1016/0168-9452(95)04267-9

Lambers H, Raven JA, Shaver GR, Smith SE (2008) Plant nutrient-acquisition strategies change with soil age. Trends Ecol Evol 23: 95–103.

Lata C, Prasad M (2011) Role of DREBs in regulation of abiotic stress responses in plants. J Exp Bot 62:4731–4748. doi:10.1093/jxb/err210

Léran S, Varala K, Boyer JC, Chiurazzi M, Crawford N et al (2014) A unified nomenclature of Nitrate Transporter 1/Peptide Transporter family members in plants. Trends Plant Sci 19:5-9. doi: 10.1016/j.tplants.2013.08.008

Luu DT, Maurel C (2005) Aquaporins in a challenging environment: molecular gears for adjusting plant water status. Plant Cell Environ 28:85-96. doi: 10.1111/j.1365-3040.2004.01295.x

Maathuis FJM, Filatov V, Herzyk P, Krijger GC, Axelsen KB et al (2003) Transcriptome analysis of root transporters reveals participation of multiple gene families in the response to cation stress. Plant J 35:675–692. doi: 10.1046/j.1365-313X.2003.01839.x

Mahajan S, Tuteja N (2005) Cold, salinity and drought stresses: an overview. Arch Biochem Biophys 444:139-158. doi: 10.1016/j.abb.2005.10.018

Malagoli P, Lainé P, Le Deunff E, Rossato L, Ney B, Ourry A (2004) Modeling nitrogen uptake in oilseed rape cv Capitol during a growth cycle using influx kinetics of root nitrate transport systems and field experimental data. Plant Physiol 134:388–400. doi: 10.1104/pp.103.029538

Marschner H (1995) Mineral nutrition of higher plants. 2nd Edition. Academic Press, San Diego.

Mohammad MJ, Malkawi HI, Shibli R (2003) Effects of arbuscular mycorrhizal fungi and phosphorus fertilization on growth and nutrient uptake of barley grown on soils with different levels of salts. J Plant Nutr 26:125–137.

Munns R, Termaat A (1986) Whole-plant responses to salinity. Aust J Plant Physiol 13:143–160.

Munns R (2005) Genes and salt tolerance: bringing them together. New Phytol 167:645–663.

Munns R, Tester M (2008) Mechanisms of salinity tolerance. Annu Rev Plant Biol 59:651–681. doi: 10.1146/annurev.arplant.59.032607.092911

Nazoa P, Vidmar JJ, Tranbarger TJ, Mouline K, Damiani I et al (2003) Regulation of the nitrate transporter gene AtNRT2.1 in Arabidopsis thaliana: responses to nitrate, amino acids and developmental stage. Plant Mol Biol 52:689–703. doi: 10.1023/A:1024899808018

Nielsen KH, Schjoerring JK (1998) Regulation of apoplastic NH4+ concentration in leaves of oilseed rape. Plant Physiol 118:1361-1368.

Nuruzzaman M, Sharoni AM, Kikuchi S (2013) Roles of NAC transcription factors in the regulation of biotic and abiotic stress responses in plants. Frontiers Microbiol 4:248. doi: 10.3389/fmicb.2013.00248

Orsel M, Chopin F, Leleu O, Smith SJ, Krapp A, Daniel-Vedele F, Miller AJ (2006) Characterization of a two-component high-affinity nitrate uptake system in Arabidopsis. Physiology and protein-protein interaction. Plant Physiol 142:1304-17. doi: 10.1104/pp.106.085209

Ouziad F, Wilde P, Schmelzer E, Hildebrandt U, Bothe H (2006) Analysis of expression of aquaporins and Na^+/H^+ transporters in tomato colonized by arbuscular mycorrhizal fungi and affected by salt stress. Environ Exp Bot 57:177-186. doi: http://dx.doi.org/10.1016/j.envexpbot.2005.05.011

Park SY, Noh KJ, Yoo JH, Yu JW, Lee BW, Kim JG et al (2006) Rapid upregulation of dehydrin3 and dehydrin4 in response to dehydration is a characteristic of drought tolerant genotypes in barley. J Plant Biol 49:455-62. doi: http://dx.doi.org/10.1007/BF03031126

Pelah D, Wang W, Altman A, Shoseyov O, Bartels D (1997) Differential accumulation of water stressrelated proteins, sucrose synthase and soluble sugars in Populus species that differ in their water stress response. Physiol Plant 99:153-9. doi: http://dx.doi.org/10.1111/j.1399-3054.1997.tb03443.x.

Phillips JM, Hayman DS (1970) Improved procedures for clearing roots and staining parasitic and vesicular-arbuscular mycorrhizal fungi for rapid assessment of infection. Transactions of the British Mycological Society 55:158–161.

Pitman MG, Lauchli A (2002) Global impact of salinity and agricultural ecosystems. In: Lauchli A, Luttge U (eds) Salinity: environment plants molecules. Kluwer, Dordrecht, pp 3–20.

Porcel R, Aroca R, Ruiz-Lozano JM (2012) Salinity stress alleviation using arbuscular mycorrhizal fungi. A review. Agron Sustain Dev 32:181–200. doi: 10.1007/s13593-011-0029-x

Remans T, Nacry P, Pervent M, Girin T, Tillard P, Lepetit M et al (2006) A central role for the nitrate transporter NRT2.1 in the integrated morphological and physiological responses of the root system to nitrogen limitation in Arabidopsis. Plant Physiol 140:909–21.

Rosendahl CN, Rosendahl S (1991) Influence of vesicular-arbuscular mycorrhizal fungi (Glomus spp.) on the response of cucumber (Cucumis sativus L.) to salt stress. Environ Exp Bot 31:313-318. doi:10.1016/0098-8472(91)90055-S

Ruiz-Lozano JM, Azcón R, Goméz M (1996) Alleviation of salt stress by arbuscular-mycorrhizal Glomus species in Lactuca sativa plants. Physiol Plantarum 98:767-772. doi: 10.1111/j.1399-3054.1996.tb06683.x

Saia S, Amato G, Frenda AS, Giambalvo D, Ruisi P (2014a) Influence of arbuscular mycorrhizae on biomass production and nitrogen fixation of berseem clover plants subjected to water stress. PloS ONE 9(3):e90738.

Saia S, Benítez E, García-Garrido JM, Settanni L, Amato G, Giambalvo D (2014b) The effect of arbuscular mycorrhizal fungi on total plant nitrogen uptake and nitrogen recovery from soil organic material. J Agric Sci 152(03):370-378.

Saia S, Rappa V, Ruisi P, Amato G, Frenda AS, Martinelli F (2015a) Soil inoculation with symbiotic microorganisms promotes plant growth and nutrient transporter genes expression in durum wheat. Front Plant Sci 6:815. doi: 10.3389/fpls.2015.00815

Saia S, Ruisi P, Fileccia V, Di Miceli G, Amato G, Martinelli F (2015b) Metabolomics suggests that soil inoculation with arbuscular mycorrhizal fungi decreased free amino acid content in roots of durum wheat grown under N-limited. P-Rich Field Conditions. PLoS ONE 10:e0129591. doi: 10.1371/journal.pone.0129591

Saibo NJM, Lourenco T, Oliveira MM (2009) Transcription factors and regulation of photosynthetic and related metabolism under environmental stresses. Ann Bot 103:609–623. doi: 10.1093/aob/mcn227

Sairam RK, Deshmukh PS, Shukla DS (1997) Tolerance to drought and temperature stress in relation to increased antioxidant enzyme activity in wheat. J Agron Crop Sci 178:171–177.

Sakurai J, Ishikawa F, Yamaguchi T, Uemura M, Maeshima M (2005) Identification of 33 rice aquaporin genes and analysis of their expression and function. Plant Cell Physiol 46:1568–1577. doi: 10.1093/pcp/pci172

Sarda X, Tousch D, Ferrare K, Cellier F, Alcon C et al (1999) Characterization of closely related δ-TIP genes encoding aquaporins which are differentially expressed in sunflower roots upon water deprivation through exposure to air. Plant Mol Biol 40(1):179-191. doi: 10.1023/a:1026488605778

Sharifi M, Ghorbanli M, Ebrahimzadeh H (2007) Improved growth of salinity-stressed soybean after inoculation with salt pre-treated mycorrhizal fungi. J Plant Physiol 164:1144–1151.

Talaat NB, Shawky BT (2011) Influence of arbuscular mycorrhizae on yield, nutrients, organic solutes, and antioxidant enzymes of two wheat cultivars under salt stress. J Plant Nutr Soil Sci 174:283–291.

Talaat NB, Shawky BT (2013) 24-Epibrassinolide alleviates salt-induced inhibition of productivity by increasing nutrients and compatible solutes accumulation and enhancing antioxidant system in wheat (*Triticum aestivum* L.). Acta Physiol Plant 35:729–740.

Talaat NB, Shawky BT (2014) Protective effects of arbuscular mycorrhizal fungi on wheat (Triticum aestivum L.) plants exposed to salinity. Environ Exp Bot 98:20–31.

Tanaka Y, Yano K (2005) Nitrogen delivery to maize via mycorrhizal hyphae depends on the form of N supplied. Plant Cell Environ 28:1247–1254. doi: 10.1111/j.1365-3040.2005.01360.x

Tong Y, Zhou JJ, Li Z, Miller AJ (2006) A two-component high-affinity nitrate uptake system in barley. Plant J 41:442-50. doi: 10.1111/j.1365-313X.2004.02310.x

Wang H, Zhang M, Guo R, Shi D, Liu B, Lin X, Yang C (2012a) Effects of salt stress on ion balance and nitrogen metabolism of old and young leaves in rice (Oryza sativa L.). BMC Plant Biol 12:194. doi: 10.1186/1471-2229-12-194

Wang H, Wu Z, Han J, Zheng W, Yang C (2012b) Comparison of Ion Balance and Nitrogen Metabolism in Old and Young Leaves of Alkali-Stressed Rice Plants. PloS One 7(5):e37817. doi: 10.1371/journal.pone.0037817

Wilde P, Manal A, Stodden M, Sieverding E, Hilderbrandt U, Bothe H(2009) Biodiversity of arbuscular mycorrhizal fungi in roots and soils of two salt marshes. Environ Microbiol 11:1548–1561.

Yang W, Yoon J, Choi H, Fan Y, Chen R, An G (2015) Transcriptome analysis of nitrogen-starvation-responsive genes in rice. BMC Plant Biol 15:31. doi: 10.1186/s12870-015-0425-5

Yamaguchi-Shinozaki K, Shinozaki K (2005) Organization of cis-acting regulatory elements in osmotic- and cold stress-responsive promoters. Trends Plant Sci 10:88–94. doi: 10.1016/j.tplants.2004.12.012

Yamato M, Ikeda S, Iwase K (2008) Community of arbuscular mycorrhizal fungi in coastal vegetation on Okinawa Island and effect of the isolated fungi on growth of sorghum under salt-treated conditions. Mycorrhiza 18:241-249. doi: 10.1007/s00572-008-0177-2

Zhao T, Liang D, Wang P, Liu J, Ma F (2012) Genome-wide analysis and expression profiling of the DREB transcription factor gene family in Malus under abiotic stress. Mol Genet Genom 287:423–436. doi 10.1007/s00438-012-0687-7

Zheng X, Chen B, Lu G, Han B (2009) Overexpression of a NAC transcription factor enhances rice drought and salt tolerance. Biochem Biophys Res Commun 379:985-989. doi: 10.1016/j.bbrc.2008.12.163

CHAPTER 9

CONCLUDING REMARKS

Functional genomics is a general approach to understand how the genes of an organism work together by assigning new functions to unknown genes (Holtorf et al., 2002). Unlike DNA, which is largely independent of the environment, the "omics" technologies are extremely stress-responsive. Through collecting the molecular information, they are able to provide a total view of the physiology in cell (Witzel et al., 2015).

In this thesis, functional genomics technologies were used to better clarify plant biotic stress-resistance (Chapters 3-6) and to study abiotic stress responses in durum wheat (Chapter 7 and 8). The use of integrated omic approaches to dissect gene regulatory networks involved in plant responses to stress has been previously shown to be useful to help diagnosis and management of plant diseases (Dandekar et al., 2010; Martinelli et al., 2016). Although these approaches are not able to substitute the detection analysis of pathogen, they may help in defing a general status of plant stress and improve the diagnosis of the stress at early stages, especially for pathogens characterized by long incubation times and unevenly distributed in the plant. The outcome of molecular detection of plant pathogen through qPCR or ELISA-based methods is often unreliable at asymptomatic and early symptomatic stage. Indeed, it is necessary to complement pathogen detection with molecular methods that deeply analysis host responses in order to identify possible genes involved in early-induced stress conditions.

Through the comparative analysis of all the four biotic stress studies (Chapters 3-6) several common findings may be observed. Carbohydrate metabolism has been linked by Huanglongbing disease in Citrus. This pathway has been observed to be highly modulated by the pathogen in both leaf and fruit tissues (Martinelli et al., 2012, 2013). Interestingly several genes belonging to this pathway were repressed by flavescence doree such as alpha-amylase and starch synthase (Chapter 4). These genes were upregulated by small molecule treatments in Citrus (Chapter 5) and the increase of biosynthesis of the corresponding proteins was linked to increased Citrus resistance to Huanglongbing disease (Chapter 6). Starch and sucrose metabolism was also significantly regulated by red plam weevil attacks in palm (Chapter 3). Taken together all these findings let us to speculate that biotic stresses drastically affect carbohydrate-related pathways and this modulation might be considered a general indication of a plant biotic stress status.

Phenylpropanoids were induced by both red palm weevil attacks in palm (Chapter 3) and stolbur disease in vitis (Chapter 4). Their involvement in both abiotic and biotic stress responses

is well-known. The secondary metabolites are often produced by plants attacked by pathogens since they directly counteract intruders through not completely clear mechanisms.

Interestingly a DUF26 receptor, involved stress signaling, was upregulated by both RPW attacks in palms (Chapter 3) and Huanglongbing disease in citrus (Chapter 6). On the contrary, a gene encoding a leucine rich repeat III was downregulated in response to RPW attacks and phytoplasma infections in Vitis. These findings confirmed that plants perceive pathogen attacks through a different signaling mechanism.

As expected hormonal pathways and crosstalk was severely affected in all four studies. Pathways enrichment analysis showed that ethylene, salicylic acid and ABA pathways were enhanced by RPW attacks and in stolbur disease. A gene encoding an allene oxide synthase, involved in jasmonic acid responses, was upregulated by these two studies.

WRKYs are well-known transcription factors involved in the transcriptional activation of both abiotic and biotic stress pathways. Interestingly WRKY40, WRKY47, WRKY75 were significantly upregulated by both RPW attacks and stolbur disease. Although it is extremely difficult to find one WRKY member that may serve a highly specific disease biomarker, the simultaneous analysis of a subset of these genes may help the diagnosis of pathogen attacks. Studies in controlled conditions are ongoing to determine how the analysis of WRKYs may allow distinguish different stages of RPW infestations in palms (Martinelli et al., unpublished).

The durum wheat miRNAome analyzed in Chapter 7 provides a greater global understanding of tissue-specific miRNAs expression in leaf and root tissues and will help to define their role in important plant developmental and physiological processes. Data from the article reported in Chapter 8 confirmed agronomic benefits deriving from AM symbiosis in plants under salt stress condition and showed an induction of some analyzed wheat genes in response to salinity. Further analyses are ongoing to determine how miRNAs are modulated by mycorrhizal inoculation in order to gain insight into the biological regulatory networks between plants-mycorrhizae interactions. The aim is to identify which miRNAs play a key role in the well-known agronomic improvements due to mycorrhizal symbiosis. Data analysis of RNA-seq studies in durum wheat are ongoing. Plants were cultivated in both drought and salinity stress conditions in order to match transcriptome and miRNAome data and identify agreeing findings that could deliver possible genes and miRNAs candidates eventually exploitable as molecular markers of these quantitative crop traits.

All these scientific works contribute to better understand the complex molecular network that generate stress responses in plants. Future studies are however necessary to complement these approaches in order to develop plants with increased resistance to environmental stress conditions.

REFERENCES

Dandekar AM, Martinelli F, Davis CE, et al (2010) Analysis of Early Host Responses for Asymptomatic Disease Detection and Management of Specialty Crops. Crit Rev Immunol 30:277-89.

Holtorf H, Guitton MC, Reski R (2002) Plant functional genomics. Naturwissenschaften 89:235-249. doi:10.1007/s00114-002-0321-3

Martinelli F, Reagan RL, Uratsu SL, Phu ML, Albrecht U, Zhao W, et al (2013). Gene regulatory networks elucidating huanglongbing disease mechanisms. PLoS ONE 8:e74256. doi: 10.1371/journal.pone. 0074256

Martinelli F, Scalenghe R, Giovino A, Pasquale M, Aksenov AA, Pasamontes A, Peirano DJ, Davis CE, Dandekar AM (2016) Proposal of a Citrus translational genomic approach for early and infield detection of Flavescence dorée in Vitis. Plant Biosyst 150:43–53. doi: 10.1080/11263504.2014.908976

Martinelli F, Uratsu SL, Albrecht U, Reagan RL, Phu ML, Britton M, et al (2012). Transcriptome profiling of citrus fruit response to huanglongbing disease. PLoS ONE 7:e38039. doi:10.1371/journal.pone. 0038039

Witzel K, Neugart S, Ruppel S, et al (2015) Recent progress in the use of “omics” technologies in brassicaceous vegetables. Front Plant Sci 6:244. doi: 10.3389/fpls.2015.00244

CHAPTER 10

AKNOWLEDGEMENTS

Fisrt of all, I wish to thank Dr. Federico Martinelli for his leadership, his teachings, his answers to all my doubts and his support over the years and especially for having given me the opportunity to carry out research both in Italy and abroad in accordance to my wishes.

Special thanks to Prof. Dario Giambalvo for his great availability, for his valuable teachings, advice sincere and his undisputed aid not only in science but also moral.

My thanks to "Fondazione Lima Mancuso". Without the funds of PON project "Sviluppo tecnologico e innovazione per la sostenibilità e competitività della cerealicoltura meridionale (PON01_01145/5-ISCOCEM)" of the Ministry of Education, University and Research (MIUR), I would not have been able to start, go forward and conclude my research during these years.

A heartfelt thanks to Prof. Amato and Prof. Frenda for their closeness, the interest in my work, and friendliness, to Dr. Paolo Ruisi for the advice and cooperation during the course of the tests and the processing of the results, and to Mario Dominici for technical support and help shown to me whenever I needed it.

Veronica